LUÍS MIGUEL SIMÃO MADEIRA

INDUSTRIAL WASTEWATER TREATMENT USING ECO-INNOVATIVE TECHNOLOGIES

UAlg FCT
UNIVERSIDADE DO ALGARVE
FACULDADE DE CIÊNCIAS E TECNOLOGIA

2023

LUÍS MIGUEL SIMÃO MADEIRA

INDUSTRIAL WASTEWATER TREATMENT USING ECO-INNOVATIVE TECHNOLOGIES

Doutoramento em Ciências do Mar, da Terra e do Ambiente
Ramo Ciências e Tecnologias do Ambiente
Especialidade de Tecnologias do Ambiente

Trabalho realizado sob a orientação da
Professora Doutora Maria Margarida da Cruz Godinho Ribau Teixeira
Professora Doutora Maria de Fátima Nunes de Carvalho

2023

Declaração de autoria de trabalho

INDUSTRIAL WASTEWATER TREATMENT USING ECO-INNOVATIVE TECHNOLOGIES

Declaro ser o autor deste trabalho, que é original e inédito. Autores e trabalhos consultados estão devidamente citados no texto e constam da listagem de referências incluída.

_____

This thesis was supported by

PhD scholarship (SFRH/BD/137209/2018) from the Portuguese Foundation of Science and Technology, trough the *European Social Found* from European Union.

Acknowledgments

This work would not have been possible without the support of some people and institutions, for which it is essential to thank:

To supervisor Professor Margarida Ribau Teixeira and co-supervisor Professor Fátima Carvalho, for their friendliness, encouragement, availability, guidance provided, transmitted knowledge, corrections and suggestions, and opportunities created to improve my skills.

To Professor Adelaide Almeida, for the support, encouragement and guidance provided in the phytoremediation trials.

To Professor Ana Costa, for her help in obtaining modified activated carbons, analysis of adsorption kinetics and isotherms, and contributions in the revision of the manuscript.

To Professor Teresa Santos, for her help in carrying out the microbiological analyses.

To Professor Ana Sofia Mestre, for the characterization analyzes of activated carbons.

To Professor Teresa Carvalhos, for providing the equipment to measure air quality.

To Professor Humberto Chaves, Professor Carlos Ribeiro, and Ana Rita Prazeres, for their contributions to the manuscripts.

To Professor Luís Nunes, for his help in statistics.

To Vânia Sousa, Maria José Imaginário, Isabel, Ivone, Mariana, Filomena, and Paulo Santana, for their availability and support provided in the laboratory.

To the University of Algarve and the Polytechnic Institute of Beja, for the opportunity they gave me to carry out this research work.

To slaughterhouse and international industry of ANFO and emulsion explosives manufacture, for providing the effluent and help during effluent sample collection.

To my parents and siblings, for their unconditional support, encouragement, and affection throughout these years.

ABSTRACT

The aim of this thesis is the development of a circular treatment sequence for (i) poorly biodegradable effluents with low C/N ratio and (ii) biodegradable effluents with high C/N ratio, using explosives wastewater and slaughterhouse wastewater as case studies, respectively. The proposed integrated treatment system comprises an immediate one-step lime precipitation (IOSLM) and atmospheric carbonation (AC), followed by constructed wetlands (CW) or adsorption, to allow reuse or disposal of the treated wastewater and the reuse of the sludge produced by the IOSLM process.

High removals of chemical oxygen demand (COD) (92%), oils and fats (98%), organic nitrogen (100%) and NH_4^+ (63%) from explosives wastewater were achieved under optimized conditions of IOSLM (7.76 g L^{-1} of hydrated lime) and atmospheric carbonation (10 days and in the presence of sludge). Later, higher removals of nitrates (55%), COD (90%) and NH_4^+ (75%) were achieved in CW with 25% flooding rate, an external carbon source (ratio C/N of 1.3), nitrate load of 12 g m^{-2} d^{-1} and hydraulic load of 83 L m^{-2} d^{-1}.

For slaughterhouse wastewater, high removals of COD (7 to 91%), Kjeldahl nitrogen (71 to 97%), biological oxygen demand (BOD_5) (80 to 86%), NH_4^+ (52 to 88%), total phosphorus (98 to 99%), and pH 7.8 were obtained under optimized conditions (pH 12 and 10 to 15 days of carbonation). Shorter atmospheric carbonation times and ammonia capture are possible when atmospheric carbonation occurs in a closed system with air injection. High COD removals (89.9 to 95.0%) in deeper beds (0.7 m) and with lower organic loads (3.2 g m^{-2} d^{-1}) were obtained. The adsorption by activated carbon was less efficient than CW.

The successive reuse of lime sludge from the IOSLM process, previously treated by heat treatment and reused as an adjuvant coagulant, proved to be efficient in the slaughterhouse wastewater treatment.

Keywords: Explosives wastewater, slaughterhouse wastewater, immediate one-step lime precipitation, atmospheric carbonation, constructed wetlands, adsorption.

Resumo alargado

A transição do paradigma economia linear para economia circular em sistemas de tratamento de águas residuais industriais está na agenda mundial. A procura de novos processos simples, eco inovativos e de baixo custo para o tratamento de águas residuais industriais, que possam ser também usados por pequenas e médias indústrias, tem sido um desafio constante, para garantir a sustentabilidade ambiental em todos os tipos de indústrias.

O objetivo da presente tese é o de desenvolver uma sequência de tratamento integrado e circular para: (i) efluentes pouco biodegradáveis com baixo rácio C/N, utilizando as águas residuais dos explosivos como caso de estudo e (ii) efluentes biodegradáveis com alto rácio C/N, utilizando as águas residuais do matadouro como caso de estudo. O sistema de tratamento integrado proposto é composto pelo processo de precipitação química imediata de etapa única com cal hidratada (IOSLM) com reutilização das lamas produzidas no próprio processo IOSLM (como coagulante ou coagulante adjuvante no tratamento, testado para águas residuais do matadouro) e carbonatação atmosférica (AC), seguida de zonas húmidas construídas (CW) ou adsorção por carvão ativado.

O processo IOSLM foi aplicado com o objetivo de remover grande parte da contaminação presente nos efluentes industriais, designadamente, em termos de matéria orgânica, sólidos suspensos totais, óleos e gorduras, e nutrientes (como o azoto orgânico e fósforo), avaliando o efeito da dose/pH de reação. Posteriormente, o processo AC foi utilizado para diminuir o pH do efluente obtido no processo IOSLM, bem como para reduzir a condutividade e as concentrações de cálcio e de azoto amoniacal, através das reações de carbonatação atmosférica. O processo AC foi desenvolvido em sistema aberto ou em sistema fechado. No sistema aberto, foi estudado o efeito do tempo de carbonatação, rácio área/volume, pH de reação e a presença/ausência de precipitado na neutralização do efluente. No sistema fechado, foram desenvolvidos dois modos de carbonatação atmosférica: reator de borbulhamento com agitação (SBC) e reator capilar de fluxo continuo e escalonado (SCFCR, estudando-se o efeito de diferentes variáveis operatórias através da metodologia de superfície de resposta. Foram ainda testados dois processos de afinação, para ambas as águas, após o processo combinado IOSLM + AC, nomeadamente as zonas húmidas construídas e adsorção. Na afinação de águas residuais de explosivos

através da utilização de zonas húmidas construídas plantadas com *Vetiveria zizanioides* sob escoamento subsuperficial vertical, avaliou-se o efeito da taxa de inundação do leito, da variação do rácio carbono/azoto e da carga de azoto aplicada na remoção de azoto amoniacal e de nitratos. Por outro lado, na afinação de águas residuais de matadouro avaliou-se o efeito da profundidade do leito e da variação da carga orgânica aplicada na remoção da matéria orgânica. O estudo do processo de afinação por adsorção com carvão ativado teve por objetivo principal a remoção da matéria orgânica da água residual do matadouro, utilizando diferentes carvões ativados em pó (PAC) e carvão ativado granular (GAC) e carvões ativados modificados (PACMAG e GACMAG) obtidos pela incorporação de nanopartículas de óxido de ferro em PAC e GAC. O efeito da dosagem de carvão ativado aplicado, do tempo de contacto, e dos métodos de separação do adsorvente da solução (filtração, sedimentação e separação magnética) também foram avaliados.

Os resultados do processo de tratamento integrado composto por IOSLM + AC, mostraram que a dose e o pH de reação influenciam a remoção de contaminantes em ambas as águas residuais industriais estudadas.

Relativamente ao tratamento da água residual dos explosivos por IOSLM + AC, os resultados obtidos indicam altas remoções de CQO (92%), óleos e gorduras (98%), azoto orgânico (100%) e azoto amoniacal (63%), alcançadas sob condições otimizadas de IOSLM (de 7.76 g L^{-1}) e carbonatação atmosférica (de 10 dias e na presença de lamas). A presença de lamas durante o processo de carbonatação contribuiu para um maior tempo de carbonatação e consequentemente uma maior remoção da amónia. A água residual obtida apresenta qualidade compatível com a reutilização para rega de culturas, mas não possui qualidade para ser descarregada no meio hídrico dadas as elevadas concentrações de azoto (nitratos e azoto amoniacal). No processo combinado de IOSLM + AC+ zonas húmidas construídas, os resultados obtidos indicaram uma maior remoção de nitratos (55%), CQO (90%) e azoto amoniacal (75%) quando foi aplicada uma taxa de inundação de 25% e adicionada uma fonte de carbono externa (relação C/N de 1,3), carga de nitrato de 12 g m^{-2} d^{-1} e carga hidráulica de 83 L m^{-2} d^{-1}. Apesar das remoções observadas, ainda assim as águas residuais dos explosivos apresentaram elevadas concentrações de azoto amoniacal e de nitratos para poderem ser descarregadas em meio hídrico.

Em relação às águas residuais do matadouro, foram obtidas altas remoções de CQO (7 a 91%), azoto Kjeldahl (71 a 97%), CBO_5 (80 a 86%), azoto amoniacal (52 a 88%), fósforo total (98 a 99%), sólidos suspensos totais (52 a 99%), turvação (62 a 97%) e óleos e gorduras (47 a 92%), e um pH em torno de 7.8, quando IOSLM e AC foram aplicadas sob condições ótimas de pH de reação de 12, tempo de carbonatação a variar entre os 10 e 15 dias e na ausência de lamas. As remoções dos contaminantes variaram conforme as características das águas residuais a tratar. Quando a carbonatação atmosférica foi realizada em sistema aberto, foi observado que o aumento do rácio área/volume contribuiu para uma redução drástica do pH da água residual, resultando num menor tempo de carbonatação. No entanto, quando a carbonatação atmosférica foi realizada em sistema fechado e com injeção de ar observou-se uma maior redução do tempo de carbonatação, a captura da amónia (≈99%) em solução ácida, bem como uma disponibilização imediata do efluente a pH próximo da neutralidade com o decorrer do funcionamento do SCFCR. Apesar das remoções observadas pelo pré-tratamento IOSLM +AC, as águas residuais do matadouro ainda apresentavam concentrações de matéria orgânica consideráveis, o que indica que o pré-tratamento não permite a descarga em meio hídrico. Apenas só é possível a sua reutilização agrícola quando este pré-tratamento é complementado com o sistema de pré-tratamento existente no matadouro. No entanto, no processo combinado de IOSLM + AC+ zonas húmidas construídas, observou-se elevadas remoções de CQO (89.9 a 95.0%) em leitos mais profundos (0,7 m) e com menores cargas orgânicas (i.e., 3.2 g m^{-2} d^{-1}), o que já permite a sua descarga em meio hídrico ou a sua reutilização agrícola. Não foram detetados sinais de toxicidade e nem sintomas de deficiência de micronutrientes na planta *Vetiveria zizanioides*. Por fim, o processo de adsorção foi avaliado como alternativa às zonas húmidas construídas, no tratamento das águas residuais do matadouro. Verificou-se que sob condições otimizadas (dose de 60 g L^{-1} e tempo de contato de 60 min.) foram alcançadas remoções de CQO de 76% e 74%, correspondendo a uma capacidade de adsorção de CQO de 5,78 mg g^{-1} e 5,61 mg g^{-1} para GAC e GACMAG, respetivamente. Para PAC e PACMAG, sob condições otimizadas (dose 70 g L^{-1} e um tempo de contacto de 5 min.), foram obtidas menores eficiências de remoção de CQO, ou seja, de 60 e 59%, correspondendo a uma capacidade de adsorção de 3,90 mg g^{-1} e 3,86 mg g^{-1}, respetivamente. Apesar das remoções de CQO observadas, o efluente obtido não apresenta qualidade para ser descarregado em meio hídrico ou reutilizado na agricultura, uma vez que os valores de CBO se encontram acima do limite permitido. Ficou demonstrado que o processo de adsorção de CQO não é afetado

com a incorporação de nanopartículas de óxido de ferro no PAC ou GAC, e que a separação magnética do adsorvente pode ser uma alternativa à filtração e sedimentação.

Por fim, as eficiências de remoção obtidas pelo reúso de lamas de cal do processo IOSLM no tratamento de águas residuais do matadouro, variaram conforme as características das águas residuais do matadouro a tratar e as formas de reúso de lamas. Maiores de remoções de CQO (3 a 95%), fósforo total (98 a 99%), turvação (99 a 100%), *E. coli* (100%) e azoto Kjeldahl (3 a 62%) foram obtidas com a reutilização das lamas como coagulante adjuvante e com tratamento térmico prévio. Por outro lado, a reutilização sucessiva das lamas não alterou a qualidade da água residual tratada (exceto para o fósforo) e contribuiu para uma poupança de cal hidratada adicionada bem como para obtenção de lamas cada vez mais estabilizadas e compactadas.

Palavras-chave: águas residuais dos explosivos, água residual do matadouro, precipitação química imediata de etapa única com cal hidratada, carbonatação atmosférica, zonas húmidas construídas, adsorção.

Table of contents

List of Figures

List of Tables

List of abbreviations and symbols

A	Surface area.
AARD	Average absolute relative deviation percent
A_{BET}	Apparent surface area
Abs 254	Absorbance at 254 nm
Abs 410	Absorbance at 410 nm
AC	Atmospheric CO_2 carbonation
AHC	Agglomerative hierarchical clustering
AN	Ammonium nitrate
ANFO	Ammonium nitrate-fuel oil
AOP	Advanced oxidation process
AOX	Adsorbable organic halides
AS	Activated sludge
A/V	Area/Volume
BET	Brunauer–Emmett–Teller
BOD	Biological oxygen demand
BPA	Bisphenol A
b_T	Temkin constant
C	Final concentration of absorbate
C_0	Initial concentration of absorbate
C_e	Concentration of adsorbate in solution at equilibrium (for adsorption) or Concentration of a parameter at outlet of the bed (for constructed wetlands).
CF	Coagulation-Flocculation
CF/DAF SWW	SWW collected after coagulation-flocculation/dissolved air flotation
C_i	Concentrations of a parameter at the inlet of the bed
C/N ratio	Carbon/nitrogen ratio
COD	Chemical oxygen demand
Cond.	Conductivity
CSC	Calcined sludge as coagulant
CSCA	Calcined sludge as coagulant aid
CV	Coefficient of variation
CW	Constructed wetlands
DAF	Dissolved air flotation
df	Degrees of freedom
DO	Dissolved oxygen
DOC	Dissolved organic carbon
E	Root-mean-square error
EC	Electrical conductivity
Eh	Redox potential
Effl.	Effluent
EN	European Norm
EU	European Union
EW	Explosives wastewater
FMBO	Ferric and manganese binary metal oxide
FOG	Oils and greases
FWSCW	Free water flow constructed wetland

GAC	Granular activated carbons
GACMAG	GAC incorporated with iron oxide nanoparticles
HFCW	Horizontal flow constructed wetland
HL	Hydraulic load
H_{Le}	Hydraulic loads at outlet of the bed
H_{Li}	Hydraulic loads at the inlet of the bed
HMX	High Melting Explosive
HRT	Hydraulic retention time
Infl.	Influent
IONP	Iron oxide nanoparticles
IONPAC	Powdered activated carbons impregnated with iron oxide nanoparticles
IOSLM	Immediate one-step lime precipitation
k	Bangham constant
k_1	Rate constant of the pseudo-first order kinetics
k_2	Rate constant of the pseudo-second order kinetics or pseudo-order n kinetics (g mg^{-1} min^{-1});
K_a	Langmuir model isotherm constant
K_F	Freundlich model isotherm constant
k_{ip}	Intra-particle rate constant
K_L	Equilibrium constant of adsorption for upper layers in BET isotherm
K_T	Toch or Temkin model isotherm constant
Leca	Light expanded clay aggregates
L/G ratio	Liquid-to-gas ratio
LSD	Least significance difference
m	Adsorbent mass
MACs	Magnetic-activated carbons
MPAC	Magnetic powdered activated carbons
MPN	Most probable number
MSTP	Municipal sewage treatment plant
n	Heterogeneity factor or Order of reaction to the adsorbent in the pseudo-order n model
N	Number of experiments
NOM	Natural organic matter
NPs	Nanoparticles
NR	Not reported.
p	Porosity of the bed
P. Alkalinity	Phenolphthalein Alkalinity
PAC	Powdered activated carbons
PACl	Polyaluminum chloride
PACMAG	PAC incorporated with iron oxide nanoparticles
PCA	Principal component analysis
PEW	Pretreated explosives wastewaters
pH	Potential hydrogen
pH_{PZC}	pH at the point of zero charge
Pre-aerated SWW	Slaughterhouse wastewater collected in the aeration and homogenization tank
q	Adsorption capacity of absorbate
$q_{cal.i}$	Adsorption capacity of the absorbate obtained by calculation,

q_e	Amount of substance adsorbed per mass of adsorbent at equilibrium
$q_{e.i}$	Adsorption capacity of the absorbate obtained by the experimental method
Q_i	Influent flow rate
q_m	Maximum adsorption capacity
q_{mean}	Average of the $q_{e.}$ values
q_t	Amount of substance adsorbed per mass of adsorbent at time t
R	Universal gas constant
RDX	Research Department Explosive
RSM	Response Surface Methodology
SBC	Stirrer bubble column
SBR	Sequencing batch reactor
SCFCR	Stepped continuous flow capillary column
SCOD	Soluble chemical oxygen demand
SD	Standard deviation
SEM	Scanning electron microscope
SFCW	Subsurface flow constructed wetlands
Sieved SWW	SWW collected at the exit of the sieve
Sludge V.	Sludge volume
S. Turbidity	Soluble turbidity
SWPP	On-Site Pretreatment Plant
SWW	Slaughterhouse wastewater
SWW1	SWW collected in the aeration and homogenization tank
SWW2	SWW collected at the exit of the sieve
SWW3	SWW collected after coagulation-flocculation/dissolved air flotation
t	Time
T	Absolute temperature
T. Alkalinity	Total alkalinity
TDS	Total dissolved solids
TKN	Total Kjeldahl nitrogen
TN	Total nitrogen
TNT	2,4,6-trinitrotoluene
TOC	Total organic carbon
TP	Total phosphorus
TS	Total solids
TSS	Total suspended solids
Turb.	Turbidity
UASB	Upflow Anaerobic Sludge Blanket
UV	Ultraviolet radiation
UV/Vis	Ultraviolet-Visible radiation
V	Wastewater volume or Volume of the bed (for constructed wetlands)
VFCW	Vertical flow constructed wetland
V_{meso}	Mesopore volume
V_{micro}	Micropore volume
V_{total}	Total pore volume
WSC	Wetted sludges as coagulant

WSCA	Wetted sludges as coagulant aid
WTP	Water treatment plants
y	Depth of the bed

%R	Percentage of removal of the absorbate
α	Elovich constant
β	Elovich exponent
ν	Parameter in the Bangham model
η	Removal efficiency of each parameter

Chapter 1

Introduction

ABSTRACT

This chapter deals with the problem of industrial wastewater treatment, especially industrial wastewater from the explosives industry and slaughterhouses. The main emphasis goes to the description of the technologies studied in this thesis, namely, the lime precipitation process (and its reuse of lime sludge), atmospheric carbonation process, phytoremediation process, and adsorption process. A background on functionality, applicability, advantages and disadvantages, operating variables that affect the process, contaminant removal mechanisms, main challenges, and recent advances are carried out for each of these processes. This section also presents the objectives and outline of this thesis.

1.1. Industrial wastewater characteristics

Industries are of great importance in society as they meet the daily needs of consumers. However, due to cleaning operations, cooling water, and manufacturing in industry, wastewaters are generated. The produced wastewater volume and the industrial wastewater characteristics are different from industry to industry as different raw materials are used (Table 1.1). Furthermore, the industry can produce several industrial effluents with different characteristics, depending on the industrial processes used, as well as variable wastewater characteristics as a result of changes in the industrial process (e.g., production volume, changes in the manufacturing process, and degree of cleaning performed).

Generally, the contaminant levels in industrial effluents are quite high compared with contaminant levels in domestic wastewater. Meanwhile, domestic wastewater has a pH around neutrality, and some industrial wastewaters such as winery wastewater and brewery wastewater have a wide pH range of around 3 and 12 (Mosse et al., 2011; Rao et al., 2007). Furthermore, other effluents such as rubber processing wastewater (pH 3.7 to 5.5) (Mohammadi et al., 2010), distillery industry wastewater (pH 3.8 to 4.4) (Saha et al., 2005), and olive mill wastewater (pH 4 to 6) (Khdair and Abu-Rumman, 2020) are acidic. According to Metcalf and Eddy (2003), a typical untreated domestic wastewater can have a chemical oxygen demand (COD) of 250 to 800 mg O_2 L^{-1}, biochemical oxygen demand (BOD) of 110 to 350 mg O_2 L^{-1}, total suspended solids (TSS) of 120 to 400 mg L^{-1}, total nitrogen (TN) of 20 to 70 mg N L^{-1}, absence of nitrates, trace concentrations of heavy metals, ammonia of 12 to 45 mg N L^{-1}, and total phosphorus (TP) of 4 to 12 mg P L^{-1}, depending on the wastewater flowrate. These values are much lower than those found in many industrial wastewaters.

Table 1.1 - Major characteristics of industrial wastewaters.

Type of industrial effluent	Major characteristics	Reference
Rubber processing wastewater	High COD, BOD, TSS, and TN.	Mohammadi et al. (2010)
Dairy wastewater	High TSS, BOD, COD, TN, TP, and FOG.	Kolev Slavov (2017)
Textile industry wastewater	High COD, pH, color, turbidity, BOD, and TS.	Raj et al. (2023)
Seafood processing wastewater	High salinity, COD, BOD, and TN.	Anh et al. (2021)
Brewery wastewater	High COD, BOD, nitrogen, and phosphorus.	Alayu and Yirgu (2018)
Battery manufacture wastewater	High amounts of Fe^{3+}, Pb^{2+}, and Cu^{2+}.	Paulino et al. (2008)
Swine wastewater	High COD, TP, TSS, ammonium nitrogen, and some heavy metals (Cu and Zn).	Wang et al. (2023)
Pulp and paper mill wastewater	High color, BOD, COD, AOX, TSS, TDS, phenolics, heavy metals, and plant components like lignin, tannin, resin acids, and extractives.	Haq and Raj (2020)
Slaughterhouse wastewater	High BOD, COD, TSS, nitrogen, phosphorus, pathogenic bacteria, grease, and fats.	Cruz et al. (2019)
Distillery industry wastewater	High conductivity, inorganic total dissolved solids, TDS, TSS, COD, acidity, BOD, sulfate, ammoniacal nitrogen, chlorides, phenols, phosphate, and total nitrogen.	Dinesh Kumar et al. (2022)
Tannery wastewater	High COD, BOD, salinity, and chromium level.	Ghorab et al. (2022)
Olive mill wastewater	High COD and BOD, low biodegradability, and high content of polyphenols.	Mechnou et al. (2022)
Winery wastewater	High COD, BOD, acidity, electrical conductivity, and phenolic compounds.	Ioannou et al. (2015)
Ammonium nitrate-based explosive wastewater	High nitrate, ammonium, nitroglycerin, nitroglycol, and COD.	Cyplik et al. (2012)
HMX explosive wastewater	High COD, BOD, acetate, TN, nitrates, HMX, and low pH.	Zhang et al. (2013)
RDX explosive wastewater	High COD, BOD, RDX, TKN, TSS. Low pH and biodegradability.	Chen et al. (2011)
TNT explosive wastewater	High COD, TN, TSS, and TNT. Low pH.	Bhanot et al. (2020)
Pharmaceutical wastewater	High COD, BOD, TN, TP, TSS, biological toxicity, and chromaticity.	Guo et al. (2017)
Petroleum refinery wastewater	High COD and oil and grease. Low biodegradability.	Ishak and Malakahmad (2013)
Metallurgical industry wastewater	High COD and metal ions (e.g., Al., Cr, Zn, and others).	Kuokkanen et al. (2021)
Nuclear industry wastewater	High COD, ammonium, nitrate, and uranium.	Venturini et al. (2021)
Laundry wastewater	High COD, BOD, and TSS.	Sheth et al. (2017)

Note: FOG (oils and greases), AOX (adsorbable organic halides), TDS (total dissolved solids), TS (total solids), HMX (High Melting Explosive), RDX (Research Department Explosive), and TNT (trinitrotoluene).

For example, high values of COD, BOD, and TSS have been found in some industrial effluents (Table 1.2), such as dairy wastewater (Deshannavar et al., 2012), brewery wastewater (Rao et al., 2007), distillery industry wastewater (Saha et al., 2005), winery wastewater (Mosse et al., 2011), and among others. Regarding total nitrogen, rubber processing, and distillery industry wastewaters have higher concentrations (Table 1.2). For ammonia, higher values were found for seafood processing wastewater, swine wastewater, and tannery wastewater (Table 1.2). Greater phosphorus concentrations have been found for swine wastewater and slaughterhouse (Table 1.2). On the other hand, higher concentrations of heavy metals (e.g., Fe^{3+}, Pb^{2+}, and Cu^{2+}) are expected to find in battery manufacture wastewater (Paulino et al., 2008).

Thus, compared to domestic wastewater, industrial wastewater presents a greater challenge in its treatment, given the high concentration of pollutants present, the high variability of its composition, and consequently the high damage that it can cause to the environment if there is no treatment or if the treatment is inappropriate.

Unfortunately, the lack of treatment or inappropriate treatment of industrial wastewater has been a source of pollution of groundwater, lakes, and rivers (Edokpayi et al., 2017; Singh et al., 2021). For example, eutrophication is one of the problems associated with the discharge of nutrients (especially nitrogen and phosphorus) and organic matter into the receiving watercourse, which leads to a marked oxygen depletion due to bacterial decomposition of organic matter and high turbidity, with severe consequences for the natural fauna and flora (Fabricius, 2011; Heredia et al., 2022). On the other hand, the presence of toxic products in industrial effluents is another factor that, in addition to being lethal for many organisms, can, in some cases, lead to the accumulation of these compounds in the food chain, making them unfit for consumption (Sukmana et al., 2021). In addition, industrial effluents (rich in organic matter) are often released into public sewage networks without prior treatment, which causes problems in urban wastewater treatment systems since these systems have a limited treatment capacity. Therefore, the installation of industrial wastewater treatment plants in industries is essential to produce effluents with characteristics that can be discharged into water or the domestic sewage system.

Table 1.2 – Typical characteristics of different industrial wastewaters.

Type of industrial effluent	pH	COD (mg O_2 L^{-1})	BOD (mg O_2 L^{-1})	TSS (mg L^{-1})	TN (mg N L^{-1})	NH_3 (mg N L^{-1})	TKN (mg N L^{-1})	TP (mg P L^{-1})	Reference
Rubber processing wastewater	3.7 – 5.5	3,500 – 14,000	1,500 – 7,000	200 – 700	200 – 1,800	NR	NR	NR	Mohammadi et al. (2010)
Dairy wastewater	7.2 – 8.8	1,900 – 2,700	1,200 – 1,800	500 – 740	NR	NR	NR	NR	Deshannavar et al. (2012)
Textile industry wastewater	5.5 – 10.5	350 – 700	150 – 350	200 – 1,100	NR	NR	NR	NR	Sanmuga and Senthamil (2017)
Seafood processing wastewater	6.1 – 7.1	1,147 – 8,313	463 – 4,569	324 – 3,150	21 – 471	3.2 – 1,059	NR	13 – 47	Cristóvão et al. (2014)
Brewery wastewater	3 – 12	2000 – 6000	1,200 – 3,600	2,901 – 3,000	NR	NR	25 – 80	NR	Rao et al. (2007)
Swine wastewater	7.4 – 7.9	2,050 – 33,860	287 – 5,820	1,000 – 27,800	NR	321 – 1,129	483 – 2,502	148 – 1,039	Hunt et al. (2012)
Pulp and paper mill wastewater	3.9 – 8.2	1,314 – 4,100	480 – 1,353	83 – 605	NR	NR	NR	NR	Amor et al. (2019)
Slaughterhouse wastewater	4.9 – 8.1	1,250 – 15,900	610 – 4,635	300 – 2,800	50 – 841	NR	NR	25 – 200	Bustillo-Lecompte et al. (2016)
Distillery industry wastewater	3.8 – 4.4	70,000 – 98,000	45,000 – 60,000	2,000 – 14,000	1,000 – 1,200	NR	NR	NR	Saha et al. (2005)
Tannery wastewater	7 – 8.5	3,000 – 6,000	1,200 – 2,700	2,000 – 3,000	NR	100 – 300	250 – 400	NR	Sabumon (2016)
Olive mill wastewater	4 – 6	40,000 – 220,000	35,000 – 110,000	NR	NR	NR	NR	NR	Khdair and Abu-Rumman (2020)
Winery wastewater	3 – 12	320 – 296,119	125 – 130,000	0 – 30,300	NR	NR	NR	NR	Mosse et al. (2011)
Pharmaceutical wastewater	6.7 – 7.2	616 – 4,750	322 – 2,440	120 – 354	NR	NR	24.6 – 82.7	1.2 – 3.4	Fawzy et al. (2018)
Petroleum refinery wastewater	7.5 – 9.4	744 –1,673	205 – 448	280 – 340	NR	40 – 45	82 – 95	1.67-1.73	Ishak and Malakahmad (2013)

Note: NR - not reported.

1.2. Industrial wastewater treatment strategies

1.2.1. General

Different physical, chemical, and biological methods have been reported in the literature to remove/reduce nutrients (e.g., ammonium, nitrate, and phosphorus) and organic matter from industrial wastewater.

Physical-chemical treatments include membrane filtration, coagulation-flocculation, adsorption, ion-exchange, air stripping, breakpoint chlorination, dissolved air flotation, chemical precipitation, and other processes. Some of these processes are simple, fast, and flexible in their ability to handle fluctuations in temperature, load, and flow. However, they present some disadvantages such as the use of chemicals (which increases the operating cost), the high energy consumption, and/or the cost of disposing of the sludge generated (Singh et al., 2021).

Biological treatments such as aerobic treatment (e.g., activated sludge process), anaerobic treatment (e.g., anaerobic baffled reactor, anaerobic lagoon), microalgal-bacterial process, and constructed wetlands are effective processes in the removal of nutrients, organic matter, and some metals. Anaerobic treatments have the possibility of producing energy from biogas. However, these treatments have some disadvantages: a possible inhibition due to the presence of toxic compounds (such as resistant pathogens, heavy metals, and other organic compounds) and sensitivity to environmental conditions (pH, temperature, organic load) which require high hydraulic retention times and maintenance (Folino et al., 2020).

A typical industrial wastewater treatment plant includes a set of treatment stages (Figure 1.1) (Crini and Lichtfouse, 2019; Singh et al., 2021; Wun Jern, 2006), namely:

- Preliminary treatment or pretreatment, which includes physical and mechanical methods such as screening and grit removal, to remove coarse suspended solids;
- Primary treatment, which includes physical-chemical methods, for suspended solids and particulate BOD settle as sludge while the lighter materials float to the

top and are skimmed off. Coagulation-flocculation/dissolved air flotation processes can also be used to remove precipitable organic matter;

- Secondary treatment, which includes chemical and biological methods, the microorganisms are used to break down the remaining organic matter in the wastewater (particulate and soluble BOD), using for example stabilization ponds, aerated lagoons, activated sludge, trickling filters, or rotating biological contactors;
- Tertiary or final treatment, which includes some physical and chemical methods to remove trace contaminants or organic matter that may not be removed by other methods. For example, nitrogen removal can be reached by ion-exchange, gas stripping, or other processes; phosphorus can be removed by chemical precipitation; TSS removal can be reached by chemical coagulation and filtration (e.g., sand filters and microfiltration); organics and metal can be removed by carbon adsorption; organic matter can be removed by advanced oxidation processes (AOP), and the dissolved solids by reverse osmosis, electrodialysis or distillation;
- Treatment of the sludge produced.

In all stages, the removal of organic matter may occur. Not all industrial wastewater treatment plants have all these stages, as they may have only a minimum treatment to discharge at urban collectors. Since each effluent has its characteristics, the combined treatments will have to be specific for that wastewater.

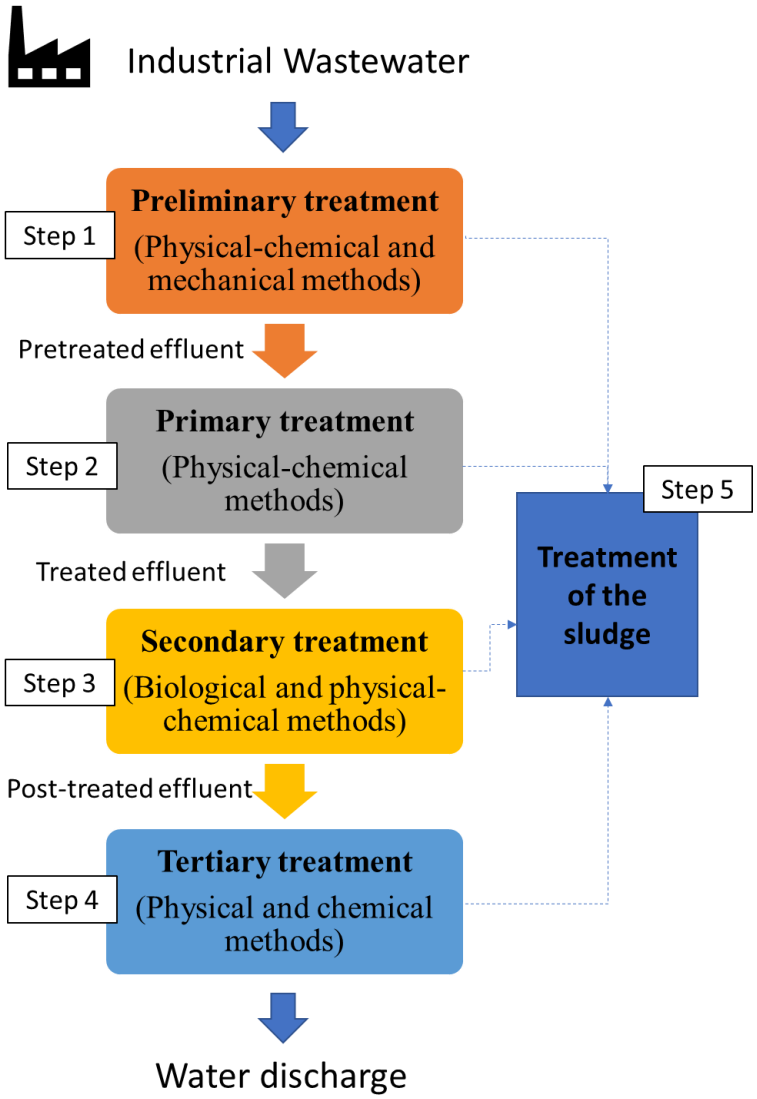

Figure 1.1 – Typical industrial wastewater treatment strategy (adapted from Crini and Lichtfouse (2019)).

No process is better than all the others, as each process has its advantages and disadvantages (Table 1.3) in terms of cost, efficiency, complexity, environmental impact, or need for skilled labor (Keerthana and Thivyatharsan, 2018; Mahmood et al., 2022).

Table 1.3 – Advantages and disadvantages of different industrial wastewater treatment processes.

Process	Advantages	Disadvantages	References
Adsorption	• High performance in removing organic and inorganic pollutants. • Low-cost. • Wide pH range. • Easy operation.	• Waste product. • Weak selectivity. • Regeneration is expensive.	Rashed (2013) Sadegh and Ali (2018)
Air stripping	• Simple in removing volatile pollutants (e.g., ammonia). • Cost-effective process.	• Fouling of stripping tower (e.g. calcium carbonate). • Emission of the stripped ammonia to the atmosphere if it is not captured. • Low ammonia concentration (less than 2 g L^{-1}) is not economically sustainable.	Folino et al. (2020) Kinidi et al. (2018)
Breakpoint chlorination	• High effectiveness in removing ammonia. • High efficiency. • Less investment.	• High operation cost. • High acidity generated. • Formation of disinfection by-products (e.g., chloramine and chlorinated organics). • Ineffective against some types of microbes.	Qi (2018) Al-Abri et al. (2019)
Electrodialysis	• An effective technique in removing cations (e.g., NH_4^+) and anions (e.g., NO_3^-). • No chemicals are required. • Works under a wide pH range. • High separation selectivity.	• Higher power consumption. • Skilled labors require. • Membrane fouling.	Singh et al. (2013)
Dissolved air flotation (DAF)	• Fast system start-up. • High separation efficiency in removing organic matter, algae, fats, oils and grease (FOG), microparticles, and microorganisms. • Operational versatility. • Low construction and operation costs. • High loading rates.	• High energy consumption and increased operating costs. • DAF foam generation.	Muñoz-Alegría et al. (2021)

Table 1.3 – (continued) Advantages and disadvantages of different industrial wastewater treatment processes.

Process	Advantages	Disadvantages	References
Chemical precipitation	• Effective in removing ionic compounds, organic molecules, phosphorus, metals, FOG, and suspended solids. • Well-established technology with ready availability of equipment and many chemicals. • Low capital cost. • Simple operation. • Some treatment chemicals, especially lime, are very inexpensive.	• Large volumes of relatively low-density sludge are produced. • Overdosing can decrease the effectiveness of the treatment. • Large amounts of chemicals may need to be transported to the treatment location. • Frequent jar tests are necessary for confirmation of optimal treatment conditions. • Operating costs (reagents). • Costs of disposal of produced sludge.	Wang et al. (2005)
Evaporation	• Zero discharge of wastewater treatment. • Effective in desalination, separation of mixtures, and concentration of solutions.	• High energy consumption. • Easy to scale. • Large equipment investment.	Wang (2016)
Coagulation/ flocculation	• The flexibility of the operational process in removing organic matter and other inorganic compounds. • Low capital cost.	• Sludge production. • Sludge/concentrate contains undesired by-products of the chemical process or toxic compounds. • Possible inhibitory effects in the following biological treatment. • Low nutrient availability and agronomic utilization, particularly with aluminum and iron coagulation.	Folino et al. (2020) Tetteh and Rathilal (2020)
Ion-exchange	• Effective in removing inorganic ions. • Can regenerate the resin that's used.	• Adsorption of organic matter and calcium sulfate fouling. • Long-term costs are high. • The brine is discharged into the environment. • It is nonselective. • Highly sensitive to pH change.	Pandey and Keshavkant (2021)

Table 1.3 – (continued) Advantages and disadvantages of different industrial wastewater treatment processes.

Process	Advantages	Disadvantages	References
Membrane filtration	• Selective separation of the constituents from waste streams based on the membrane used.	• High investment costs • High energy consumption. • High cost for membrane replacement due to fouling. • Pre-treatment is needed to prevent membrane fouling.	Folino et al. (2020) Elkarrach et al. (2022)
Activated sludge process	• Low installation cost. • Good-quality effluent. • Need for less space. • Without odor nuisance.	• Inflexible method. • High operating cost. • Need for large space to dispose of sludge. • Need for skilled supervision. • Sensitive process.	Sivapragasam et al. (2021)
Rotary biological contactor	• Effective. • Simple to operate and maintain. • Low operating costs. • Little skill is required in the operation of the plant. • Short retention time. • Low operating power requirements. • Low output of sludge. • Excellent process control.	• Need protection against freezing in the northern climate. • Frequent maintenance.	Mohameda et al. (2022)
Aerobic sequencing batch reactor (ASBR)	• Easy to modify cycles. • Small footprint. • Cost-effective. • High removal efficiency. • Wide operation flexibility.	• High energy consumption. • Frequent sludge disposal.	Goli et al. (2019)

Table 1.3 – (continued) Advantages and disadvantages of different industrial wastewater treatment processes.

Process	Advantages	Disadvantages	References
Biological treatment under anaerobic conditions (Stirred tank anaerobic filter, UASB, movie bed, fixed bed)	• Simple techniques. • Low cost. • Reduced hydraulic holding times. • Low sludge generation.	• Ammonia can be an inhibitor of anaerobic degradation.	Lippi et al. (2018)
Constructed Wetlands	• Low operation and maintenance (required supplies and energy) cost. • Periodic and non-continuous operation and maintenance. • Tolerate fluctuations in flow. • Esthetic benefits.	• Take up space on the surface of the ground. • Variable efficiency in case of changing environmental conditions. • Limited by regional climatic features, especially in cold regions.	Omondi and Navalia (2021) Xu et al. (2022)
Advanced oxidation processes (AOP)	• Effective in removing toxins, chemicals of emerging concern, pesticides, and other deleterious substances. • No energy input is necessary to activate hydrogen peroxide. • No hazardous end product materials with high chemical stability and/or low biodegradability.	• Sludge generation. • Technology complexity. • Requires a qualified technical operator. • Hydrogen peroxide is a costly chemical.	Viktoryová et al. (2022) Lippi et al. (2018)
Electrochemical treatment	• Rapid process and is effective for certain metal ions. • No chemicals are needed. • Low sludge production. • Cost-effectiveness. • Ease of automation and adaptability. • Environmental compatibility. • Selectivity. • Minimal maintenance costs.	• High energy costs. • Formation of large particles.	Viktoryová et al. (2022) Asaithambi et al. (2022)

Although biological treatments seem to be more interesting processes in ecological terms than physicochemical treatments, some characteristics of industrial wastewater, such as the carbon and nitrogen (C/N) ratio and the low biodegradability of the effluent may condition their use (Hamza et al., 2019; Saha et al., 2022; Wang et al., 2018; Wu et al., 2012).

A high C/N ratio means there is more carbon than nitrogen. Phanwilai et al. (2020) define wastewater with a COD/N ratio lower than 4.3 as a low C/N ratio wastewater and higher than 4.3 as a high C/N ratio wastewater. High C/N ratios have been found in breweries wastewater (Rao et al., 2007), distillery industry wastewater (Saha et al., 2005), tannery wastewater (Sabumon, 2016), and other types of wastewater. In biological treatment, high C/N ratios may not only reduce nitrification efficiency but also increase denitrification (Navada et al., 2020). Carrera et al. (2004) found that as the C/N ratio increased, the population of heterotrophic bacteria increased, leading to a reduction in the dissolved oxygen levels in the reactor. As a result, nitrifying bacteria faced increased competition for the limited available oxygen, which resulted in a decrease in their growth and activity. On the other hand, the authors also observed that the denitrification rate was favored with an increase in the C/N ratio. Thus, maintaining a balanced C/N ratio is crucial for the optimal performance of nitrifying bacteria in wastewater treatment systems. For efficient removal of nitrogen from effluent by biological treatment, the reduction of high C/N ratios can go through a physical-chemical pre-treatment (e.g., coagulation-flocculation, chemical precipitation, membrane processes, or AOP) that first removes the organic matter, or an alternating set of aerobic and anaerobic phases in biological treatment (Hande Gursoy-Haksevenler and Arslan-Alaton, 2020).

If the C/N ratio in wastewater is too low (i.e., it has more nitrogen (nitrate and/or ammonium nitrogen) than carbon), in the biological treatment the microorganisms may have not enough carbon to use the available nitrogen, resulting in incomplete nitrogen removal and potential release of nitrogen compounds into the environment (Liu et al., 2021; J. Shen et al., 2009; Thakur and Medhi, 2019). Some wastewaters such as ammonia and/or nitrate-rich industrial wastewaters (e.g., the effluent of a fertilizer industry (Zala et al., 2004), effluent from initiating explosive factory (Shen et al., 2009), wastewater produced during the frosting process of bottles in a winery (Carrera et al., 2004), and among others), have low C/N ratios. Therefore, optimizing the C/N ratio in wastewater

treatment is important for achieving efficient and effective treatment. The treatment of wastewater with a low C/N ratio can involve the use of physical-chemical processes that remove nitrates (e.g., ion-exchange (Yaragal and Mutnuri, 2023), reverse osmosis (Shelly et al., 2021) and electrochemical (Chauhan and Srivastava, 2020)) or ammonium nitrogen (e.g., chemical precipitation (by struvite recover) (Li et al., 2012), membrane filtration (reverse osmosis and nanofiltration) (Kurama et al., 2002), ion-exchange (Jorgensen and Weatherley, 2003), activated carbon adsorption (Han et al., 2021) and air stripping (Ulu and Kobya, 2020)), if present. Some advantages and disadvantages of these processes are identified in Table 1.3. Biological treatment (e.g., nitrification-denitrification (Thakur and Medhi, 2019)) could also be a solution in the treatment of wastewater with a low C/N ratio if an addition of an external organic carbon source is made, however, this solution is considered a cost burden (Zhu et al., 2019). On the other hand, the anammox biological process could be useful to remove ammonium nitrogen, but it is a treatment that requires very controlled conditions to occur (Li et al., 2021).

The biodegradability index is defined as the ratio between BOD and COD. Low BOD_5/COD ratio (less than 0.25) indicates that the inert (non-biodegradable) fraction is high, so possible indication of physical-chemical treatment. An intermediate BOD_5/COD ratio (0.25 to 0.4) indicates that the inert (non-biodegradable) fraction is not high, therefore, treatability studies to verify the feasibility of the biological treatment must be carried out. On the other hand, a high BOD_5/COD ratio (greater than 0.4) indicates that the biodegradable fraction is high, which is a good indication for biological treatment (von Sperling, 2007). Some industrial wastewaters such as textile industry wastewater (Ghoreishi and Haghighi, 2003), paper mill wastewater (Zodi et al., 2011), tannery wastewater (Mariliz et al., 2015), explosives wastewater (e.g., TNT, RDX, and HMX) (Chitra and Lakshmanaperumalsamy, 2006), petrochemical wastewaters (Derakhshan and Fazeli, 2018) and others, are poorly biodegradable. Poor biodegradability may be due to the presence of non-biodegradable organic matter or toxic substances that inhibit microbial activity (Mangkoedihardjo, 2006). For this reason, activated sludge is not viable for treating poorly biodegradable wastewater (Derakhshan and Fazeli, 2018). Mixing low biodegradability effluents with highly biodegradable effluents, or adding biodegradable organic matter to the effluent could be examples of solutions to improve the biodegradability of wastewater to use in biological treatment, however, the latter solution entails costs Mangkoedihardjo (2006).

Recently, several pretreatment technologies have been evaluated to treat and improve the biodegradability of industrial wastewater for suitable biological treatment. Some examples of wastewater treatment technologies that improve the biodegradability of wastewater include AOP and electrochemical treatments (Cheng et al., 2022; Devda et al., 2021; Ma et al., 2019; Saravanathamizhan and Perarasu, 2021), and constructed wetlands (Mangkoedihardjo, 2006). AOP (e.g., ozonation, UV/O_3, ozonation coupled with H_2O_2, O_3/UV/H_2O_2, sonification, photocatalytic oxidation, Fenton, and other processes) are effective in the treatment of various wastes. However, they have the disadvantages of generating sludge, are a complex technology, and some reagents (e.g., hydrogen peroxide) are costly (Kokkinos et al., 2021). Electrochemical treatments (e.g., electrocoagulation, electrodialysis, electrochemical oxidation, among others) are fast and effective processes for certain metals, do not need chemicals, and have low sludge production. However, these processes have high energy consumption costs (Ding et al., 2019; Pandey and Keshavkant, 2021). Compared to these processes, the adsorption process and constructed wetlands are recognized for their low-cost wastewater treatment (Waly et al., 2022), eco-friendly treatment, and treatment of various types of industrial wastewaters, including low biodegradable wastewater (e.g., pulp and paper wastewater, petrochemical wastewater, pharmaceutical wastewater, and others) (Almazán-Sánchez et al., 2016; Álvarez-Torrellas et al., 2017; Rodríguez et al., 2004; Skrzypiec and Gajewska, 2017). However, the adsorption process can be less efficient than constructed wetlands (Keerthana and Thivyatharsan, 2018). Constructed Wetlands can also improve the biodegradability of effluents, since in these systems, the exudates produced by plants are highly biodegradable and can stimulate cometabolism of contaminants in the rhizosphere (Mangkoedihardjo, 2006). Mangkoedihardjo (2006) investigated the performance of low-biodegradable wastewater using phytotreatment before the biological oxidation process. The author observed that hyacinths plants were able to increase the BOD/COD ratio of industrial wastewater from 0.05-0.11 to 0.30-0.52, with simultaneous high significant COD removals. For better efficiency of constructed wetlands, pretreatment of wastewater is necessary to remove various contaminants (e.g. TSS) and thus reduce the potential risk of system clogging (Achak et al., 2023). The precipitation of nondegradable pollutants on the substrate surface reason is also one of the reasons for clogging (Wang et al., 2021). According to Karungamye (2021), the effluents to treat in constructed wetlands should not exceed a suspended solids concentration of 100 mg L^{-1}. Thus, the effluent must

undergo a primary treatment to reduce the solid load. Primary decanters and coagulation-flocculation processes have been used as pretreatment methods to reduce the contaminant load of constructed wetlands (Ying et al., 2011). Recently, a combined process consisting of lime precipitation followed by atmospheric carbonation has been considered an efficient pretreatment of industrial wastewaters (Luz et al., 2021), leachate (Ramalho et al., 2022), and urban wastewaters for the production of hydroponic nutrient solutions (Correia et al., 2020), in the removal of COD, TSS, oils and fats, phosphorus and ammonium nitrogen. This process is also called immediate one-step lime precipitation process (IOSLM). Some eco-innovative aspects have been found in this integrated process, namely (Correia et al., 2020; Prazeres et al., 2016; Ramalho et al., 2022):

- A single reagent (hydrated lime) of low cost and high availability is used;
- The sludge produced is stabilized, is rich in nutrients, has the potential to be used in acid soils, and is less harmful than iron/alum sludge obtained by conventional coagulation-flocculation processes;
- The atmospheric carbonation process contributes to atmospheric CO_2 mitigation since in this process atmospheric CO_2 is used to neutralize alkaline effluent to values around neutrality. In this way, no consumption of acids and the problems associated with them occurs.

Eco-innovative wastewater treatment technologies refer to the application of environmentally sustainable technologies and approaches in treating wastewater to minimize their negative impacts (e.g., minimizing greenhouse gas emissions) on the environment while also maximizing their potential benefits. These technologies typically are energy-efficient and resource-efficient processes that minimize the use of chemicals and other inputs and may incorporate renewable energy sources and closed-loop systems to reduce the overall environmental footprint (de Jesus et al., 2022).

However, a decrease in the biodegradability index has also been observed with the application of lime precipitation, making the wastewater non-biodegradable, as observed by Luz et al. (2021) and Ramalho et al. (2022). Therefore, the optimization needs further investigation, mainly in the treatment of industrial wastewater that is not very biodegradable and has a low C/N ratio. The potentialities of each of these treatment processes in wastewater treatment are described in the following sections.

1.2.2. Lime precipitation

Lime precipitation aims to change the solubility of the substances, converting the soluble substances into insoluble substances, by adding lime to the wastewater. A scheme of the process is presented in Figure 1.2. It is a process, where rapid and slow mixing take place. Rapid mixing for a good mixture between the precipitating agent and the wastewater to form precipitates. Slow mixing for the agglomeration of particles to increase their sedimentation (Figure 1.2). In immediate one-step lime precipitation, the flocculation step does not exist since it uses high lime dosages to produce immediately large amounts of precipitates that settle in the mantle, dragging many particles with it (Prazeres et al., 2016).

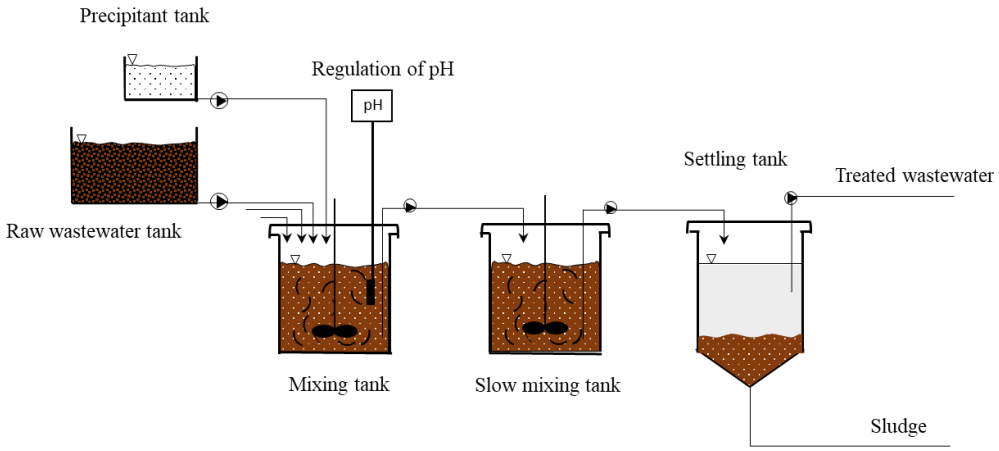

Figure 1.2 – Lime precipitation process.

Quicklime (CaO) and hydrated lime ($Ca(OH)_2$) are the two forms of lime mostly used in wastewater treatment. CaO is the result of the calcination of $CaCO_3$ at high temperatures (Eq. 1). Hydrated lime results from the hydration of CaO with water (Eq. 2). The solubility of $Ca(OH)_2$ decreases with increasing temperature (Zhao et al., 2018).

$$CaCO_3\,(s) \rightarrow CaO + CO_2\,(g) \quad (1)$$

$$CaO + H_2O \rightarrow Ca(OH)_2 \quad (2)$$

Lime has been used for Ph control (An et al., 2023; Niaounakis and Halvadakis, 2006) and treatment of industrial wastewaters, such as plywood industries wastewater (Prasad et al., 2019), cotton textile wastewater (Georgiou et al., 2003), tannery wastewater (Ayoub

et al., 2011; Reyes-Serrano et al., 2020), olive mill wastewater (Boukhoubza et al., 2009) and others) and stabilized leachates (Renou et al., 2009) (Table 1.4).

High removals of COD, BOD, color, total phosphorus, total coliforms, heavy metals, turbidity, and organic nitrogen have been observed in the lime treatment of various types of wastewaters (Table 1.4). The amount of hydrated lime required for optimal effluent clarification varies with the type of wastewater to be treated (more specifically with the composition of the water, for example, alkalinity, total hardness, and ammonium concentration, (Folkman and Wachs, 1973). Sometimes the dosages used are higher than theoretically foreseeable since hydrated lime partially dissolves (Semerjian and Ayoub, 2003). Boukhoubza et al. (2009) tested different concentrations of hydrated lime (10 to 150 g L^{-1}) to treat 1 L of olive mill wastewater at pH 12. The authors observed that small concentrations of hydrated lime contributed to a greater effluent dilution effect than the effect of coagulation. Increasing concentrations of lime decreased the volume of solution added and, in this case, the recorded reductions could be related to the coagulation effect rather than dilution. High concentrations of hydrated lime or CaO solution (e.g., 200 g L^{-1}) have been used in the literature (Luz et al., 2021; Prazeres et al., 2019b; Ramalho et al., 2022; Renou et al., 2009). Ramalho et al. (2022) observed that stirring time in the immediate one-step lime precipitation process has a small influence on organic load and NH_4^+ removal.

Table 1.4 - Application of lime precipitation/IOSLM in the treatment of industrial wastewater, landfill leachate, and urban wastewater.

Type of wastewater	Reagent and applied dose/pH	Operation mode	Optimum removal efficiency	Reference
Landfill leachates	Lime (4g L^{-1}), pH 11.85	Rapid mixing (300 rpm) for 5 min, slow mixing (30 rpm) for 30 min followed by settling for 30 min.	COD (25.5%), Ca^{2+} (93.5%), Mg^{2+} (98.5%), NH_4^+ (56.2%), total alkalinity (87.7%), and Fe (75.4%).	Renou et al. (2009)
	Lime (2.0 g L^{-1}), pH = 11.20		COD (18.0%), Ca^{2+} (65.0%), Mg^{2+} (65.0%), NH_4^+ (29.7%), and total alkalinity (80.0%).	
	Lime (6.0 g L^{-1}), pH 10,40		COD (0.4%), Ca^{2+} (91.5%), Mg^{2+} (95.5%), NH_4^+ (24.7%), and total alkalinity (90.9%).	
	CaO (27.6 g L^{-1})	300 rpm stirring speed for 2–60 min followed by settling for 2 h.	Stirring time has a small influence on organic load and NH_4^+ removal.	Ramalho et al. (2022)
	CaO (18.2–33.3 g L^{-1})	300 rpm stirring speed for 40 min followed by settling for 2 h.	COD (64%) at 27.6 g L^{-1} of CaO.	
Plywood industry wastewater	Lime (1.5 g L^{-1})	Rapid mixing and settling for 2 h.	COD (40%), TSS (36.8%), phenol (41%), and TKN (48.1%).	Prasad et al. (2019)
Olive mill wastewater	Lime (10 g L^{-1}), pH 12	Rapid mixing (200 rpm) for 5 min, slow mixing (60 rpm) for 10 min, and filtration (11 μm) after a resting period.	COD (72%), TSS (73%), and Phenol (60%).	Boukhoubza et al. (2009)
Textile wastewater	Lime (0.8 g L^{-1}), pH 13-13.5	Rapid mixing for 1-2 min, slow mixing for 15-20 min, followed by settling for 45 min.	COD (50-60%) and color (70-90%).	Georgiou et al. (2003)
Cheese whey wastewater	Lime, pH 6 to 13	700–800 rpm for 1 min, 300–400 rpm for 1 min, followed by settling for 24 h.	The highest COD removal (29.7%) was obtained at pH 11.0. Total phosphorus (61.9–95.6%) only occurred for pH ≥ 8.0. Highest total phenols removals (63.2–65.5%) at pH 12.0 and 13.0.	Prazeres et al. (2020)
	$Ca(OH)_2$, pH 8.57 to 12.37	Vigorous agitation. Then the agitation system was switched off.	Under optimum conditions: COD (90%), turbidity (99.8%), TSS (98–99%), oils and fats (82–96%), phosphorus (98–99%), potassium (96–97%), and total coliforms (100%) for 80% cheese whey recovery and lime application.	Prazeres et al. (2016)
Tannery wastewater	CaO and $Ca(OH)_2$ (0.3 to 3.2 g alkali/g Cr^{3+})	10 min of vigorous stirring, 200 rpm, and a settling time of 24 h.	Cr (99.8%), SO_4^{2-} (66.9%), $ZnSO_4$ (99.6%), $FeSO_4$ (21.4%), CN^{-1} (70.9%), $NiSO_4$ (52.8%) and $Fe_2[Fe(CN)_6]$ (76.4%) for CaO, Cr (99.8%), SO_4^{2-} (61.6%), $ZnSO_4$ (99.9%), $FeSO_4$ (7.1%), CN^{-1} (84.0%), $NiSO_4$ (54.4%) and $Fe_2[Fe(CN)_6]$ (90.5%) for $Ca(OH)_2$	Reyes-Serrano et al. (2020)

Table 1.4 – (continued) Application of lime precipitation/IOSLM in the treatment of industrial wastewater, landfill leachate, and urban wastewater.

Type of wastewater	Reagent and applied dose/pH	Operation mode	Optimum removal efficiency	Reference
Vinasse wastewater	$Ca(OH)_2$ (12–100 g L^{-1}), pH 10.14-12.49.	Rapid agitation.	COD (51%), absorbances, magnesium, nitrogen, and phosphorus had depletions (≥70%) at pH 12.13 and 12.49.	Prazeres et al. (2019b)
Olive oil mill wastewater	$Ca(OH)_2$, pH 11.0 to 12.75.	Rapid agitation followed a settling time of 24 h.	COD (11.4–17.8%), total phosphorus (23.6–42.2%), turbidity (60.9–100%), total phenols (25.9–48.0%), and absorbances at 220 nm (10.3–33.5%), 254 nm (18.5–45.9%), 410 nm (34.2–81.6%) and 600 nm (22.1–77.3%).	Prazeres et al. (2021)
Winery wastewater	Quicklime, slaked lime, Calcium hydroxide, using 1–50 mL L^{-1} for slaked lime and calcium hydroxide, and 5–40 mL L^{-1} for the quicklime.	Vigorous stirring for 2 min followed by the settling time of 1 h.	High removal levels of BOD_5 (77.9%), turbidity (98.7%), total phosphorus (87.1%), total phenols (99.9%), fecal coliforms, and Enterococcus (100%) at 25 ml L^{-1} of slaked lime.	Luz et al. (2021)
Urban wastewater	Hydrated lime, reagent grade $Ca(OH)_2$ and quick lime, pH 9.5 to 12.5.	Vigorous mechanical stirring (magnetically agitated, rotation speed of 300 rpm) followed by a settling time of 120 min.	COD (88%), BOD_5 (86%), TP (89%), N-organic (75%), and total coliform count (100%) at 0.7 g L^{-1} (reaction pH of 11.5) of hydrated lime.	Correia et al. (2020)
Slaughterhouse wastewater	Lime (100-600 mg L^{-1})	Stirring at 100 rpm for 1 min, slow mixing at 40 rpm for 30 min, followed by a settling time of 30 min.	TSS (41.9%), BOD (38.9%), and COD (36.1%) at 400 mg L^{-1} of lime.	Satyanarayan et al. (2005)

The effect of the effluent composition buoyancy on the effectiveness of the lime precipitation process has been very scarcely documented in the literature (Wang et al., 2016). Prazeres et al. (2016) applied IOSLM to treat different high-strength cheese whey wastewaters (without cheese whey recovery, 60% cheese whey recovery, and 80% cheese whey recovery). The authors observed that cheese whey recovery significantly influenced the characteristics of the wastewater to be treated and consequently the removal of various parameters.

Some reaction mechanisms of the lime precipitation process in wastewater treatment have been observed, namely:

- Effluent pH increase since the dissolution of hydrated lime in wastewater provides the hydroxyl ions (OH^-) (Eq. 3) (Georgiou et al., 2003; Renou et al., 2009).

$$Ca(OH)_2 \rightarrow Ca^{2+} + 2OH^- \quad (3)$$

- Carbonate and hydroxide anions can react with a wide range of cations, leading to the formation of highly insoluble sediments (Forouzesh et al., 2023). For example, the instantaneous conversion of calcium bicarbonates and magnesium bicarbonates into precipitated calcium carbonates (Eq. 4) and magnesium carbonates (Eq. 5), as well as the transformation of magnesium carbonates into precipitated magnesium hydroxides (Eq. 6) (Renou et al., 2009; Semerjian and Ayoub, 2003). In fact, these compounds have low solubility product values (i.e., 4.7×10^{-9} for $CaCO_3$ and 8.9×10^{-12} for $Mg(OH)_2$, respectively), and the minimum solubility of calcium carbonate and magnesium hydroxide occurs at pH 9.1–9.5 and around 11, respectively (Spellman, 2020).

$$Ca(OH)_2 + Ca(HCO_3)_2 \leftrightarrow 2CaCO_3\,(s) + 2H_2O \quad (4)$$

$$Ca(OH)_2 + Mg(HCO_3)_2 \leftrightarrow MgCO_3 + CaCO_3\,(s) + 2H_2O \quad (5)$$

$$Ca(OH)_2 + MgCO_3 \leftrightarrow Mg(OH)_2\,(s) + CaCO_3\,(s) \quad (6)$$

- Neutralization of suspended impurities, results in the destabilization of charged particles and their aggregation (Prasad et al., 2019). The formed calcium carbonate and magnesium hydroxide can act as coagulants (Ayoub and Merhebi,

2002). Furthermore, colloidal particles can be trapped during the formation of calcium carbonate precipitates (Ayeche, 2012).

- Total phosphorus removal (Eqs. 7 and 8) occurs in the pH range of 8-12 (Ayeche, 2012). The degree of phosphorus removal by lime precipitation is a function of the following factors: initial phosphorus concentration, lime concentration, the concentration of other anions competing with phosphorus for precipitating cations, and wastewater pH (Liu and Lipták, 2000). The phosphate precipitation rate is influenced by the presence of carbonates, as the latter compete with the phosphate ions for calcium ions (Li et al., 2021; Prazeres et al., 2020).

$$3Ca(OH)_2 + 2PO_4^{3-} \rightarrow Ca_3(PO_4)_2 \downarrow + 6\ OH^- \quad (7)$$

$$4Ca(OH)_2 + 3PO_4^{3-} + H_2O \rightarrow Ca_4H(PO_4)_3 \downarrow + 9\ OH^- \quad (8)$$

- Disinfection of the effluent due to the exposure of microorganisms/viruses to high pH under a certain contact time, as well as the occurrence of adsorption of microorganisms to the formed precipitates (Luz et al., 2021; Semerjian and Ayoub, 2003).
- Organic matter removal by surface adsorption, co-precipitation, precipitation, coagulation-flocculation, or chemical reaction (Renou et al., 2009).
- Removal of heavy metals (e.g., Ni, Zn, Fe, Cr, and others) in the form of precipitated hydroxides (Eqs. 9 to 12) or carbonates, as well as their adsorption on calcium carbonate. Metal hydroxide precipitation is highly dependent on pH (Forouzesh et al., 2023; Habte et al., 2020; Reyes-Serrano et al., 2020; Wang et al., 2016).

$$C_r(SO_4)_3 + 3Ca(OH)_2 \rightarrow 2Cr(OH)_3\downarrow + 3CaSO_4 \downarrow \quad (9)$$

$$NiSO_4 + Ca(OH)_2 \rightarrow Ni(OH)_2\downarrow + CaSO_4 \downarrow \quad (10)$$

$$ZnSO_4 + Ca(OH)_2 \rightarrow Zn(OH)_2\downarrow + CaSO_4 \downarrow \quad (11)$$

$$FeSO_4 + Ca(OH)_2 \rightarrow Fe(OH)_2\downarrow + CaSO_4 \downarrow \quad (12)$$

The main advantages of using hydrated lime are:

- It is a simple operation, fast (i.e., high precipitation speed) and low-cost (chemical cost and energy requirements) (Chen et al., 2009; Mirbagheri and Hosseini, 2005),

- Lime is cheaper than other chemicals and can easily be purchased anywhere (Semerjian and Ayoub, 2003; Wang et al., 2016),
- Does not contribute to an increase in salinity, unlike some salts used such as iron and alum (Semerjian and Ayoub, 2003),
- No formation of toxic secondary pollutants (Forouzesh et al., 2023),
- The sludges possess superior thickening and dewatering characteristics and are suitable for filter pressing at a lower cost than sludges generated from ferric chloride or alum (Prazeres et al., 2016; Semerjian and Ayoub, 2003),
- The sludge does not need the addition of polymers or more lime to dewater it, which results in savings in chemical reagents, unlike the iron and alum sludge obtained by the coagulation process which still needs to be conditioned (Semerjian and Ayoub, 2003),
- The sludge is chemically stabilized due to the high pH applied, does not decompose quickly, causes few odor problems, and has recycling potential (Ayoub and Merhebi, 2002; Semerjian and Ayoub, 2003).

The disadvantages of using hydrated lime are:

- Leaves the effluent with high pH, making it unsuitable for some sequence treatment processes within a wastewater treatment plant, and calcium carbonate precipitation may occur in the distribution pipelines (Habte et al., 2020),
- The removal rate of some pollutants like NH_4^+ is limited (Cheng et al., 2021),
- Production of large amounts of sludge, when compared to coagulation processes using ferric chloride or alum chloride as coagulants (Semerjian and Ayoub, 2003).

The first two disadvantages can be minimized by the atmospheric carbonation process (See section 1.2.3). Finding economically viable and ecological solutions is important to minimize the impact of increased sludge production. The reuse of lime sludge from landfill leachate treatment by lime precipitation to cover landfills has been considered an eco-innovative solution (Martínez-Cruz et al., 2021). Some sludge resulting from the treatment of cheese whey wastewater by lime precipitation has potential application in agriculture as a fertilizer since it contains many nutrients such as calcium, phosphorus, potassium, magnesium, and others, although with some limitations due to its saline nature (i.e., high NaCl content) (Prazeres et al., 2016). On the other hand, the reuse of lime

sludge from the lime precipitation process to treat wastewater is rarely reported. Ayeche (2012) used hydrated lime sludge (with a purity of 67.03%) produced in the manufacture of acetylene to treat dairy wastewater, and the author observed substantial removals of suspended solids, organic matter, nitrogen, and phosphorus. The use of thermal treatment (calcination process) can also be a solution to recover the hydrated lime from the sludge and use it again as a reagent. Bal Krishna et al. (2017) investigate the effectiveness of pre-treated lime sludge from a groundwater treatment plant through heat treatment in removing phosphorus from an aqueous solution. The authors observed that calcination of the sludge at 700 °C greatly improved the phosphorus removal from the aqueous solution than if it were applied to dry lime sludge at 105ºC. Information regarding the reuse of lime sludge in the treatment of industrial wastewater is scarce and necessary.

1.2.3. Atmospheric carbonation

Atmospheric carbonation (or atmospheric CO_2 sequestration) is a process that aims to reduce the pH of an alkaline effluent using atmospheric CO_2. Basically, this process consists of leaving the alkaline effluent exposed to the atmosphere over time, at rest, and at room temperature (Figure 1.3).

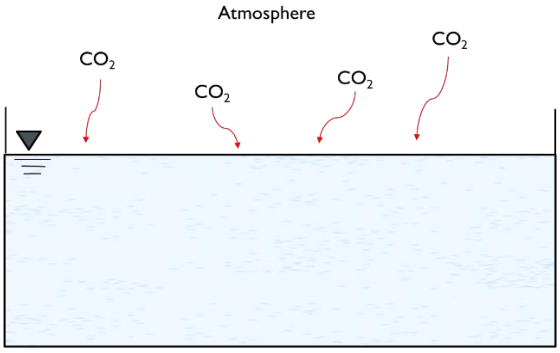

Figure 1.3 - Atmospheric carbonation process.

The atmospheric carbonation process has recently been used to neutralize industrial wastewater (e.g., vinasse from the sugarcane ethanol industry (Prazeres et al., 2019b), winery wastewater (Luz et al., 2021) and cheese whey wastewater (Prazeres et al., 2016)), urban wastewater (Correia et al., 2020), and landfill leachate (Ramalho et al., 2022), resulting from lime precipitation process.

Reductions in pH, conductivity, calcium concentration, magnesium concentration, ammonia concentration, phenolphthalein alkalinity, and total alkalinity have been observed over the carbonation time for most wastewater treated by lime precipitation (Table 1.5).

Time, the absence/presence of precipitates from lime precipitation, and the injection of atmospheric air have been the factors analyzed in the carbonation process. Time has been the main factor analyzed by the authors, as it is the factor that regulates the continuity of carbonation reactions between the supernatant and the atmosphere. This factor is dependent on the operational variables applied (e.g., air injection or absence/presence of sludge) (Correia et al., 2020; Prazeres et al., 2019b) and on the initial characteristics of the alkaline wastewater (e.g. pH, temperature, and others) (Viswanaathan et al., 2022). Correia et al. (2020) observed that the injection of atmospheric air contributes to a shorter carbonation time. On the other hand, Prazeres et al. (2019b) found that the presence of sludge from lime precipitation contributes to an increase in the carbonation time to reach a pH around neutrality. The minimum and maximum atmospheric carbonation times reported in the literature were 4.2 (Correia et al., 2020) to 20 days (Prazeres et al., 2019b) to reach pH ≈ 8. On the other hand, a non-completion of the carbonation process at pH 8 has been observed by some authors, such as the authors Ramalho et al. (2022) who observed that the effluent still had a pH of 10.10 after 32 days of carbonation (Table 1.5). Prazeres et al. (2016) also found that the time required for natural carbonation depends on effluent characteristics.

The decrease in pH of the effluent during the atmospheric carbonation process follows the same reaction mechanisms (Eqs. 13 to 16) that lead to ocean acidification caused by increased CO_2 emissions into the atmosphere from anthropogenic sources (Mollica et al., 2018).

$$CO_2\ (g) \rightleftarrows CO_2\ (aq) \quad (13)$$

$$CO_2\ (aq) + H_2O\ (l) \rightleftarrows H_2CO_3\ (aq) \quad (14)$$

$$H_2CO_3 \rightleftarrows H^+ + HCO_3^- \quad (15)$$

$$HCO_3^- \rightleftarrows H^+ + CO_3^{2-} \quad (16)$$

Table 1.5 - Summary of literature review about the neutralization of alkaline wastewater treated by lime precipitation, through carbonation of atmospheric CO_2.

Type of effluent	Operating conditions	Initial physicochemical characteristics	Final physicochemical characteristics	References
Vinasse from the sugarcane ethanol industry	V = 2.6 L A = 162 cm^2 Room temperature = 16.8±2.3 ºC Without agitation, air injection, and reagent addition With or without precipitate	Without precipitate: pH =10.6 Conductivity ≈ 10 mS cm^{-1} Ca ≈ 2400 mg L^{-1}	After 15 days: pH ≈ 8 Conductivity ≈ 10.8 mS cm^{-1} Ca ≈ 2400 mg L^{-1}	Prazeres et al. (2019b)
		With precipitate: pH =12.34	After 20 days: pH ≈ 8	
		Without precipitate: pH =12.05	After 9.2 days: pH ≈ 8	
Winery wastewater	V = 1 L Without agitation, air injection, and reagent addition Without precipitate	pH =12.4 Conductivity = 6.5 mS cm^{-1} Ca = 499.8 mg L^{-1} Mg = 179.9 mg L^{-1}	After 15 days: pH = 7.46 Conductivity = 1.805 mS cm^{-1} Ca= 426.5 mg L^{-1} Mg = 6.6 mg L^{-1}	Luz et al. (2021)
Cheese whey wastewater	V = 3.5 L A = 162 cm^2 Without agitation, air injection, and reagent addition Without precipitate	pH ≈ 12 Conductivity ≈ 4.75 mS cm^{-1} Ca ≈ 300 mg L^{-1} Mg ≈ 13 mg L^{-1}	After 7.3 days: pH ≈ 8 Conductivity ≈ 4 mS cm^{-1} Ca ≈ 200 mg L^{-1} Mg ≈ 2 mg L^{-1}	Prazeres et al. (2016)
Landfill leachate	V = 3 to 4 L A = 200 cm^2 Without agitation, air injection, and reagent addition Without precipitate	pH = 12.5 NH_4^+ = 889 mg N L^{-1} Conductivity = 23.1 mS cm^{-1} Ca = 490 mg L^{-1} Phenolphthalein alkalinity = 6600 mg $CaCO_3$ L^{-1} Total alkalinity = 7530 mg $CaCO_3$ L^{-1} COD = 460 mg O_2 L^{-1}	After 32 days: pH = 10.10 NH_4^+ < 0.1 mg N L^{-1} Conductivity = 15.0 mS cm^{-1} Ca < 0.1 mg L^{-1} Phenolphthalein alkalinity = 2350 mg $CaCO_3$ L^{-1} Total alkalinity = 4480 mg $CaCO_3$ L^{-1} COD = 474 mg O_2 L^{-1}	Ramalho et al. (2022)
Urban wastewater	V = 4 L A = 200 cm^2 Without agitation and reagent addition With precipitate With or without air injection	Without air injection: pH ≈ 11.5 Conductivity = 1.144 mS cm^{-1}	After 9.2 days: pH = 8.4 Conductivity ≈ 1.050 mS cm^{-1}	Correia et al. (2020)
		With air injection (85 L h^{-1}): pH ≈ 11.5 Conductivity ≈ 1.300 mS cm^{-1}	After 4.2 days: pH ≈ 8 Conductivity ≈ 1.170 mS cm^{-1}	

Note: V – wastewater volume; A - surface area.

In fact, the effluents from lime precipitation are quite alkaline and consequently, the free CO_2 in the effluent is unavailable, which causes a chemical imbalance of CO_2 between the effluent and the atmosphere with considerable concentrations of CO_2. As a way of counteracting this imbalance, the CO_2 present in the atmosphere tends to dissolve in the water through the water-air interface until it reaches equilibrium (Eq. 13). After dissolution in the water, the dissolved CO_2 is subjected to a hydration reaction through reaction with water to form H_2CO_3 (Eq. 14). As H_2CO_3 is a weak acid, it dissociates in two steps, the first step (Eq. 15) the formation of HCO_3^- and H^+ ions, and the second step (Eq. 16) the formation of CO_3^{2-} and H^+ ions, from HCO_3^-. The production of H^+ ions leads to a decrease in the pH of the effluent. During atmospheric CO_2 sequestration, H^+ ions are attracted by opposite charges, namely by hydroxide ions forming water molecules. CO_3^{2-} ions are attracted by positive charges, namely calcium or magnesium ions, to form precipitated calcium carbonate and magnesium carbonate. In addition to the decrease in pH, water stabilization also occurs during atmospheric CO_2 sequestration, since carbonates tend to be converted into bicarbonates (HCO_3^-), reaching a maximum in the pH range of 8.4 to 8.6. At this pH range, precipitation of carbonates (CO_3^{2-}) does not occur, since the fraction of carbonates in this pH range is practically zero (Mihelcic et al., 2002).

During atmospheric carbonation, ammonia can be released into the atmosphere (Ramalho et al., 2022). However, as the pH decreases ammonia removal becomes more difficult as ammonia is converted to ammonium ions (Eq. 17), reaching 50% ammonia and 50% ammonium ion at pH 9.25 (Lin et al., 2009; Wang et al., 2005). Since air stripping of wastewater with low ammonia concentration (less than 2 g L^{-1}) is not economically sustainable (Folino et al., 2020), the atmospheric carbonation process could be an alternative solution.

$$NH_3 + H_2O \leftrightarrow NH_4^+ + OH^- \quad (17)$$

COD removal is not expected during the atmospheric carbonation process (Ramalho et al., 2022).

The use of atmospheric CO_2 as a neutralizing agent in wastewater treatment has some advantages and disadvantages. The advantages are the following (Prazeres et al., 2016):

- It is an innovative, low-cost, and environmentally friendly technology,
- It is easy to apply and does not require reagents or energy (if not using atmospheric air injection),
- Contributes to the mitigation of greenhouse gases,
- Avoids the use of acids (e.g., H_2SO_4 or HCl) or CO_2 injection, and consequently reduces costs of reagents, corrosion of equipment by acids, and costs of transport/storage of CO_2 to the treatment site,
- Produces stable wastewater concerning $CaCO_3$, preventing precipitation of $CaCO_3$ in distribution systems.

As disadvantages, the atmospheric carbonation process:

- It has a high carbonation time,
- Contributes to the release of ammonia into the atmosphere if it is present in the effluent.

New approaches to atmospheric carbonation will need to be investigated to minimize the current disadvantages found.

1.2.4. Constructed wetlands

In recent years, constructed wetlands have gained in popularity, as an emerging green technology for the treatment of industrial wastewaters (Dinesh Kumar et al., 2020; Hota et al., 2023).

Constructed wetlands are artificial wetlands that mimic a set of biological, physicochemical, and chemical processes that occur in natural wetlands to treat industrial wastewater, urban wastewater, and landfill leachate. These processes result from the interaction between the different elements that make up the system, namely: water, plants, microorganisms, and substrate (Lajayer et al., 2022). Plant roots and the substrate act as a barrier to intercept coarse particles that the effluent may contain, while the microorganisms and plants break down and absorb pollutants from the effluent, which makes the constructed wetlands a filtration and purification system for effluents (Kadlec

and Wallace, 2008). Generally, the resulting effluents can be discharged into surface waterways or reused for different purposes.

Constructed wetlands have been used as secondary treatment (on a small scale, in isolated areas) for BOD removal, or as a tertiary treatment (on a large scale, in developed countries) for wastewater refinement (BOD, solids and nutrients) (Fitch, 2013). The advantages of these systems are numerous (Avellan et al., 2017; García-Ávila et al., 2023; Rahman et al., 2020; Stefanakis et al., 2014), such as:

- Ease of operation and maintenance;
- Lower maintenance and capital construction costs than conventional systems;
- Consistent compliance with the permit requirements;
- Aesthetically pleasing and can provide wildlife habitat;
- Require little external energy input;
- Low carbon footprint;
- Provide effective and reliable wastewater treatment under fluctuating hydraulic and contaminant loading rates;
- The biomass produced can be valued;
- Facilitate wastewater reuse and recycling.

However, some limitations can be observed in these systems (García-Ávila et al., 2023; Gorgoglione and Torretta, 2018; Makopondo et al., 2020; Milani et al., 2019), such as:

- High land area requirements compared to conventional systems;
- The need for a preliminary treatment to avoid clogging the filter medium;
- The need for higher (than a conventional system) retention time;
- Efficiency may be reduced in cold climates;
- Require mosquito control (in free water surface systems);
- Require a period of vegetation stabilization to be effective in removing pollutants;
- The applied hydraulic load can be compromised in dry climates due to evapotranspiration.

Substantial removals of pollutants have been observed in the treatment of different industrial wastewaters by constructed wetlands (Table 1.6).

Table 1.6 – Pollutant removal efficiencies obtained in constructed wetlands for different industrial wastewaters.

Wastewater types	Removals	Reference
Seafood wastewater	BOD (91–99%), TSS (52–90%), TN (72–92%) and TP (72–77%)	Sohsalam et al. (2008)
Winery wastewater	BOD (70%), COD (71%), TSS (87%), TKN (52%), and PO_4^{3-} (17%)	Serrano et al. (2011)
Tannery wastewater	BOD (98%), COD (98%), TSS (55%), TP (87%), and NH_4^+ (86%)	Saeed et al. (2012)
Steel industry wastewater	COD (77%), NH_4^+ (77%), Fe (94%), and Mn (81%)	Huang et al. (2011)
Refinery wastewater	COD (80%), oil (93%), BOD (88%), and TKN (86%)	Ji et al. (2007)
Aquaculture wastewater	COD (27%), TSS (66%), TN (67%), TP (24%), and NO_3^- (59%)	Shi et al. (2011)
Textile wastewater	Cr (40–50%)	Fibbi et al. (2011)
Abattoir wastewater	BOD (97%), COD (97%), TSS (94%), TN (74%), and NH_4^+ (99%)	Soroko (2007)
Distillery wastewater	BOD (85%), COD (80%), TKN (75%), NO_3^- (57%), NH_4^+ (2–10%), and SO_4^{2-} (69%)	Olguín et al. (2008)
Brewery wastewater	TSS (89%), COD (92%), TN (83.6%), NH_4^+ (92.9%), TP (74.4%), and PO_4^{3-} (79.5%)	Alayu and Leta (2021)
Cheese wastewater	BOD (55%), COD (72%), TSS (60%), TP (30%), and TN (50%)	Comino et al. (2011)
Olive mill wastewater	COD (85%), TSS (90%), TP (83%), TKN (83%), Phenol (80%), NH_4^+ (54%), and NO_3^- (46%)	Kapellakis et al. (2012)
Pulp and paper wastewater	COD (88%), color (96%), BOD (93%), and chlorophenols (90%)	Kumar and Choudhary (2018)
Mixed industrial wastewater	BOD (66%), COD (67%), NH_4^+ (24%), organic-N (83%), and PO_4^{3-} (62%)	Justin et al. (2009)

Different types and combinations of plants, substrates, and constructed wetlands configurations have been reported in the literature for various types of industrial wastewater, to find the higher efficiency of removal of pollutants from wastewater.

Biological media (e.g., bagasse, biochar, coal, and oyster shell), construction materials media (e.g., recycled brick, mortar, gravel, and sand), artificial media (e.g., activated carbon, compost, and lightweight aggregates), and industrial by-product (e.g., slag and fly ash) have been used as adhesion materials for biofilms or external sources of organic matter (in the case of biological media) (Saeed and Khan, 2019; Wu et al., 2015). Light-expanded clay aggregates (LECA) have also been widely used as a substrate as they can remove phosphates, have good mechanical strength and hydraulic conductivity, and are a good support structure for the growth of biofilms and plant roots (Mlih et al., 2020).

In terms of wastewater flow regime, different designs have been used, namely, the traditionally constructed wetlands (e.g., free water flow constructed wetlands (FWSCW)

and subsurface flow constructed wetlands (SFCW) (i.e., horizontal flow constructed wetlands (HFCW) and vertical flow constructed wetlands (VFCW)), hybrid constructed wetlands (e.g., two-stage constructed wetlands and multi-stage constructed wetlands), and innovative constructed wetlands (e.g. aerated CW, circular flow corridor CW, baffled flow CW, and others) (Masoud et al., 2022). Each of these systems has its advantages and disadvantages, and applications. FWSCW has lower construction and operating costs than SFCW, however, odor issues may occur and feature lower contaminant removal ratios per unit area (which requires a larger area of land) than SFCW (Stefanakis, 2020). Compared to FWSCW, SFCW tolerate cold weather, have fewer odor problems, and have greater sorption and exchange sites, however, they have higher costs, are subject to clogging of the media, and use small flows (Hassan et al., 2021). VFCW has been applied to promote greater aerobic degradation of pollutants since they have a good oxygen supply, and require a smaller land area compared to HFCW, however, the flow distances are short, and they present poor denitrification (Gorgoglione and Torretta, 2018). HFCW has long flow distances that allow for more complete degradation of pollutants and enables nitrification and denitrification, however, they require larger land areas and therefore higher capital cost (Pundlik et al., 2022). To overcome each other's disadvantages in removing pollutants, hybrid constructed wetlands (e.g., VFCW-HFCW, VFCW-HFCW-VFCW, and other combinations) have also been applied to reach higher treatment efficiency (Singh et al., 2022; Waly et al., 2022). The denitrification capacity in VFCW has also been studied with the application of flood levels (Almeida et al., 2019). Different types of constructed wetlands have been applied to treat different types of industrial wastewater, however, most of the cases reviewed by Vymazal (2014) used FWSCW or HFCW to treat industrial wastewater. There are few cases reported with the use of VFCW and for wastewater from explosives and slaughterhouses.

Many studies have indicated that pollutant removal efficiencies depend on the type of plant species used in the constructed wetland (Ky et al., 2020). Therefore, the choice of the appropriate plant is an important factor in phytoremediation processes (Vymazal et al., 2021). Plants have been classified as emergent, submerged, or floating, and their use depends on the constructed wetlands type (García-Ávila et al., 2023). Plants that have been applied in constructed wetlands for industrial wastewater treatment, include: *Typha latifólia* e.g., for distillery wastewater (Billore et al., 2001), slaughterhouse wastewater (Gutiérrez-Sarabia et al., 2004), petroleum refinery wastewater (Mustapha et al., 2018)

and floriculture wastewater (Engida et al., 2020); *Phragmites karka* e.g., for distillery wastewater (Billore et al., 2001); *Juncus effusus* e.g., for winery wastewater (Serrano et al., 2011); *Cyperus immensus* e.g., for paper and pulp wastewater (Abira et al., 2005); *Phragmites australis* e.g., for slaughterhouse wastewater (Gutiérrez-Sarabia et al., 2004), dye wastewater (Hussein and Scholz, 2018), textile wastewater (Bulc and Ojstršek, 2008), cork boiling wastewater (Gomes et al., 2018), fish farm wastewater (Schulz et al., 2003) and olive mil wastewater (Kapellakis et al., 2012); *Brachiaria mútica* e.g., for textile wastewater (Hussain et al., 2018); *Typha domingensis* e.g., for paper and pulp wastewater (Abira et al., 2005); *Canna indica* e.g., for mixed wastewater from steel mill, paper and dyeing factory (Saeed et al., 2018); *Pampas grass* e.g., for glass industry wastewater (Gholipour et al., 2020); *Eichhornia crassipes* e.g., for petrochemical wastewater (Agarry et al., 2020); *Typha augustifolia* e.g., for seafood processing wastewater (Yirong and Puetpaiboon, 2004); *Canna lilies* e.g., for floriculture wastewater (Engida et al., 2020); *Pennisetum purpureum* e.g., for swine wastewater (Klomjek, 2016); *Cyperus papyrus* e.g., for sugar mill wastewater (Bojcevska and Tonderski, 2007); *Phalaris arundinácea* e.g., for tile drainage (Vymazal et al., 2020) and among others.

In recent years, *Chrysopogon zizanioides* (L.) Roberty (formerly known as *Vetiveria zizanioides* (Linn.) Nash) has instigated the interest of several researchers in the phytoremediation process due to its characteristics, namely its strong resistance and survival to extreme climatic and edaphic conditions (e.g. drought and flooding, high concentration of pollutants (i.e., nutrients, heavy metals, and persistent organic matter), pH 3 to 10.5, salinity until 47.5 dS m^{-1}, temperatures ranging from -9 to 55°C), as well as its roots quite long that allow greater absorption of pollutants and a greater supply of oxygen for aerobic bacteria to develop (Ramos-Arcos et al., 2022; Danh et al., 2009; Fasani et al., 2019; Goren et al., 2021; Seroja et al., 2018). In addition, this plant also has an economic value since it serves as a raw material for the production of perfumes and cosmetics (Burger et al., 2017). This plant has shown similar potential and sometimes more effectiveness in removing contaminants from industrial wastewater than some commonly used plant species such as Cyperus species, Phragmites species, and Typha species (Darajeh et al., 2019).

Vetiveria zizanioides has been applied to remove organic matter from contaminated surface water (Ky et al., 2020; Nguyen et al., 2023), treat landfill leachate (Ramalho et

al., 2022) and urban wastewater (Badejo et al., 2017; Hemalatha et al., 2020; Mudhiriza et al., 2015), rehabilitation and soil stabilization of sites contaminated with high levels of heavy metals (Banerjee et al., 2019; Chintani et al., 2021; Kriti et al., 2021), and industrial wastewater, e.g. aquaculture wastewater (Raharjo et al., 2018), piggery effluent (Liao et al., 2003; Pongthornpruek, 2017), pinora effluent, palm oil mill effluent, biogas effluent (Yeboah et al., 2015), textile wastewater (Njau and Mlay, 2003), olive mill wastewater (Goren et al., 2021), milk factory wastewater (Roongtanakiat et al., 2007), tofu wastewater (Seroja et al., 2018), paperboard mill wastewater (Davamani et al., 2021), high explosives from munition industry wastewater (Panja et al., 2018) and others.

High COD, BOD, and TSS removal efficiencies have been observed in some poorly biodegradable water from industrial wastewater (e.g., biogas wastewater (Yeboah et al., 2015) and tofu wastewater (Seroja et al., 2018)) when *Vetiveria zizanioides* is used (Table 1.7), however, the same did not occur for some wastewater that was not very biodegradable, such as palm oil mill wastewater (Yeboah et al., 2015) and textile wastewater (Njau and Mlay, 2003). The use of constructed wetlands to treat poorly biodegradable industrial wastewater is a challenge since the effluent can influence the growth of microorganisms as well as the associated removal mechanisms (Saeed et al., 2018). Most investigations have been carried out with FWSCW, requiring a long hydraulic retention time (1 to 120 days), when using *Vetiveria zizanioides* (Table 1.7).

Table 1.7 – Application cases of phytoremediation of industrial wastewater using *Vetiveria zizanioides*.

Wastewater types	CW type	Media	HRT (d)	HL (m^3 d^{-1})	Initial concentrations	Removal performance (%)	Country	References
Aquaculture Wastewater	FWSCW (2 m x 1 m x 0.5 m)	Coarse sand and corals	1	0.576	NH_3 (0.1 – 0.2 mg L^{-1}), PO_4^{3-} (6 – 10 mg L^{-1})	NH_3 (2 - 67%), PO_4^{3-} (0 - 75%)	Indonesia	Raharjo et al. (2018)
Piggery Wastewater	FWSCW (1 m x 3 m x 1 m)	Soil	5	0.18	BOD (767.90 mg L^{-1}), COD (1,330.25 mg L^{-1}), TKN (158.67 mg L^{-1}), TP (69.90 mg L^{-1})	BOD (74%), COD (70%), TKN (88%), TP (83%)	Thailand	Pongthornpruek (2017)
Pinora Wastewater	FWSCW	-	120	-	TSS (385 mg L^{-1}), BOD (4,836 mg L^{-1}), COD (6,296 mg L^{-1}), NO_3^- (0.721 mg L^{-1}), NH_3 (9.69 mg L^{-1})	TSS (82%), BOD (94%), COD (86%), NO_3^- (10%), NH_3 (41%)	Ghana	Yeboah et al. (2015)
Palm Oil Mill Wastewater	FWSCW	-	120	-	TSS (278,600 mg L^{-1}), BOD (44,520 mg L^{-1}), COD (128,911 mg L^{-1}), NO_3^- (0.80 mg L^{-1}), NH_3 (20.40 mg L^{-1})	TSS (71%), BOD (51%), COD (10%), NO_3^- (6%), NH_3 (40%)	Ghana	Yeboah et al. (2015)
Biogas Wastewater	FWSCW	-	120	-	TSS (330 mg L^{-1}), BOD (492 mg L^{-1}), COD (1,952 mg L^{-1}), NO_3^- (0.122 mg L^{-1}), NH_3 (17.3 mg L^{-1})	TSS (95%), BOD (91%), COD (82%), NO_3^- (99%), NH_3 (42%)	Ghana	Yeboah et al. (2015)
Pig farm Wastewater	FWSCW (50 cm x 38.5 cm x 23 cm)	-	4	-	COD (825 mg L^{-1}), BOD_5 (500 mg L^{-1}), NH_3 (130 mg N L^{-1}), TP (23 mg L^{-1})	COD (64%), BOD (69%), NH_3 (20%), TP (27%)	China	Liao et al. (2003)
Textile wastewater	HFCW (1 m x 0.6 m x 0.3 m)	Limestone soil	25	-	TSS (100-120 mg L^{-1}), COD (820-1,200 mg L^{-1}), BOD (226-282 mg L^{-1})	TSS (81%), COD (46.2%), Cu (73.6%), color (78.2%)	Tanzania	Njau and Mlay (2003)

Note: HRT - Hydraulic Residence Time; HL - Hydraulic Load.

Table 1.7 – (continued) Application cases of phytoremediation of industrial wastewater using *Vetiveria zizanioides*.

Wastewater types	CW type	Media	HRT (d)	HL (m^3 d^{-1})	Initial concentrations	Removal performance (%)	Country	References
Olive mill wastewater	FWSCW	-	67	-	TOC (1,132 mg L^{-1}), TN (26.6 mg L^{-1})	TOC (85%), TN (93%), TP (39%)	Turkey	Goren et al. (2021)
					TOC (3,168 mg L^{-1}), TN (72.6 mg L^{-1})	TOC (89%), TN (24%), TP (92%)		
Milk factory wastewater	FWSCW	-	120	-	Mn (0.49 mg L^{-1}), Fe (16.15 mg L^{-1}), Zn (4.09 mg L^{-1}) Pb (0.05 mg L^{-1})	Mn (34%), Fe (28%), Zn (53%), Pb (9%)	Thailand	Roongtanakiat et al. (2007)
Tofu wastewater	FWSCW	Zeliac	15	-	COD (5,759 mg L^{-1}), BOD (580 mg L^{-1}), TSS (552 mg L^{-1})	COD (76%), BOD (72%), TSS (75%)	Indonesia	Seroja et al. (2018)
Paperboard mill wastewater (raw and treated)	FWSCW	-	40	-	TSS (1,000 mg L^{-1}), BOD (156 mg L^{-1}), COD (512 mg L^{-1}), TN (39 mg L^{-1}), TP (9.25 mg L^{-1}), Lead (2.01 mg L^{-1}), cadmium (1.90 mg L^{-1})	TSS (60%), BOD (96%), COD (50%), TN (64%), TP (65%), Lead (51%), cadmium (27%)	India	Davamani et al. (2021)
					TSS (200 mg L^{-1}), BOD (44 mg L^{-1}), COD (256 mg L^{-1}), TN (25 mg L^{-1}) TP (8.50 mg L^{-1}), Lead (0.96 mg L^{-1}), cadmium (0.42 mg L^{-1})	TSS (75%), BOD (72%), COD (56%), TN (70%), TP (43%), Lead (91%), cadmium (81%)		
Munition industry wastewater	FWSCW	-	100 100 100 20	-	Nitroguanidine (3,996 mg L^{-1}) NO_3^- (352,734 mg N L^{-1}) Dinitroanisole (120 mg L^{-1}) RDX (7.8 mg L^{-1}), HMX (12 mg L^{-1})	Nitroguanidine (79%) NO_3^- (95%) Dinitroanisole (96%) RDX (100%), HMX (100%)	United States of America	Panja et al. (2018)

Although several investigations have been registered on the potential of vetiver in wastewater treatment, studies on its efficacy in treating industrial effluents with high nitrate content are limited. Panja et al. (2018) evaluate the phytoremediation potential of *Vetiveria zizanioides* in removing explosive compounds and nitrates from wastewater effluents generated in an industrial munition facility. The authors observed high removal efficiencies of nitroguanidine (79%), nitrates (95%), dinitroanisole (96%), RDX (100%), and HMX (100%), however, this was only possible with the use of four successive batches (except for RDX and HMX which was one batch) once the vetiver plants started to show visible symptoms of stress, such as chlorosis and fallen leaves, and died within the first few days, returning to be replaced by a new batch of vetiver plants. These results show that further research is needed.

Almeida et al. (2019) evaluate the potential of phytoremediation of *Vetiveria zizanioides* to nitrate and organic matter removal from synthetic wastewater, in subsurface vertical flow constructed wetland systems. The authors observed that the ratio of COD/NO_3^--N in wastewater affected the efficiency of NO_3^--N removal, and that low hydraulic load and high COD/NO_3^--N ratio ensure good effects of nitrate and organic matter removal. The authors did not observe obvious symptoms of toxicity signals during the experimental tests. Thus, *Vetiveria zizanioides* have good phytoremediation potential in the field of nitrate nitrogen and organic substance removal.

For the heterotrophic denitrification process to occur, high concentrated nitrate wastewaters require a certain amount of organic matter, which sometimes they do not have (Krishna Mohan et al., 2016). Studies related to the effect of the C/N ratio in the denitrification of effluents with high concentrated nitrate are still limited. Low nitrogen removals (28 to 58%) in constructed wetlands have been reported when effluents with low biodegradability (i.e. 0.16 to 0.36) are used (Saeed and Khan, 2019). When poor biodegradability is due to a lack of biodegradable carbon in the effluent, some authors have added an external carbon source (e.g., methanol) (Laber et al., 1997) or used organic substrates (Tee et al., 2012), to supply carbon to the system, and thus increase the biodegradability of the effluent and consequently improve heterotrophic denitrification in constructed wetlands. Saeed and Sun (2013) evaluated the constructed wetlands with sugarcane bagasse and sand media for the treatment of textile wastewater. The authors observed that the organic carbon content of sugarcane bagasse facilitated denitrification

in the vertical flow constructed wetlands. Saeed and Khan (2019) evaluated the removal of pollutants from a low biodegradable mixed industrial wastewater using two parallel hybrid constructed wetlands composed of two VFCW (with different combinations of biological (i.e., bagasse, biochar, coal, and oyster shell) and construction (recycled brick, mortar, gravel, and sand) media materials) followed by surface flow constructed wetland, planted by *Phragmites australis*. The authors concluded that higher organics and nitrogen removal percentages were obtained with biological materials than with construction materials, due to carbon leaching. However, high removals of NH_4-N (≥ 90%), TN (≥ 86%), P (≥ 91%), BOD (≥ 92%), COD (≥ 85%), and color (≥ 87%) removal percentages across both systems were obtained, which reveals that the combination of VFCW (packed with biological and construction materials) and FWSCW, can be a solution for the treatment of hardly degradable industrial wastewater.

The removal of pollutants from constructed wetlands is quite complex and involves a set of removal mechanisms, from physical (sedimentation and filtration), chemical (e.g., sorption, complexation, and precipitation), and biological (biodegradation, microbial transformation, and microbial/plant assimilation) processes, which can occur simultaneously (Biswal and Balasubramanian, 2022). According to Vymazal (2007), the nitrogen transformation mechanisms involved in constructed wetlands are ammonia volatilization, ammonification, nitrification, denitrification, fixation, absorption and assimilation by plants, ammonium ion adsorption, and anammox. Removal of organic matter in constructed wetlands is associated with both aerobic and anaerobic degradation (Cooper et al., 1996). The plant also plays an important role in the phytoremediation of industrial effluents, and many mechanisms may occur, namely: degradation (rhizodegradation, phytodegradation), accumulation (phytoextraction, rhizofiltration), dissipation (phytovolatilization), and immobilization (phytostabilization) to degrade, remove, or immobilize contaminants (Kafle et al., 2022).

Several environmental factors and operational conditions can affect nitrogen and organics removal, such as pH, temperature, availability of oxygen, availability of organic carbon source, hydraulic load and retention time, the mode of influent feed (i.e., continuous, intermittent, batch, tidal, and step feed modes), nitrogen and organics loading, recirculation, bed depth, and plant harvesting (Almeida et al., 2020; Saeed and Sun, 2012). In addition, the removal of nutrients and organic matter in constructed wetlands

can be inhibited by the harmful effect of the presence of heavy metals on plants and microorganisms. Removal of metals in constructed wetlands can occur by precipitation, plant uptake, and microbial metabolism, but depend on substrate type, plant species, and wastewater composition (Vymazal and Březinová, 2016). Removal of heavy metals (e.g., Pb, Cd, Cu, and Zn) (>85%) present in mixed domestic-industrial wastewater has been observed using recirculating standing hybrid constructed wetlands planted by *Canna indica L.* and filled with lava rock and gravel (Zhang et al., 2020). According to Zhang et al. (2020), these systems require a smaller land, allow a rapid co-precipitation of heavy metals, and consequently a decrease in toxicity in plants and microorganisms, and a consistent and effective removal of total nitrogen, total phosphorus, and organic matter.

1.2.5. Adsorption

Adsorption is a process that has been widely used to remove organic matter from industrial wastewater. This process has the advantages of high performance, low-cost, simple operation, and application in a wide pH range. However, low selectivity and generation of a residue are some of the disadvantages (Sadegh and Ali, 2018).

In the adsorption process occurs an accumulation of adsorbates (e.g., organic, or inorganic pollutants) on the surface of the adsorbent using intermolecular forces of attraction. This happens when the adsorbent with a highly porous surface structure comes into contact with a solution containing absorbates (Nageeb, 2013). Then, the adsorbent is removed from the solution by sedimentation or filtration.

Different conventional and nonconventional adsorbents have been used for the removal of pollutants from wastewater. Conventional adsorbents include commercial activated carbons, inorganic materials, and ion-exchange resins. On the other hand, nonconventional adsorbents include natural materials, agricultural wastes, industrial by-products, activated carbons from solid wastes, biosorbents, and miscellaneous adsorbents (Crini, 2006, 2005; Crini et al., 2019).

Commercial activated carbons are the most prevalent and extensively used adsorbents for wastewater treatment (Ali et al., 2020). These are produced from the carbonization process of carbon-rich organic materials such as wood, peat, coconut shells, and coals

(anthracite, bituminous, lignite, and others). This process occurs under slow heating in the absence of air below 600 °C to remove volatile impurities such as oxygen, hydrogen, nitrogen, and sulfur. Then, a physical activation (using agents such as O_2, CO_2, or steam at high temperatures) or chemical activation (using agents such as H_2SO_4, H_3PO_4, KOH, K_2S, and $ZnCl_2$) is carried out (Dlamini et al., 2020; Renu et al., 2017). As a result, the activated carbon produced has a porous structure, large specific surface area, and high surface reactivity (Phothong et al., 2021). These properties are important in the removal of various types of contaminants such as heavy metals (Vasiraja et al., 2023), organic matter (Hatt et al., 2013; Lakdawala MM and Lakdawala JM, 2013; Subki et al., 2020), phosphorus (Almanassra et al., 2021), and nitrogen (Zhao et al., 2013). Activated carbon is usually used as a tertiary treatment for persistent pollutants removal after biological treatment (Ani et al., 2019). The pore structure is composed of micropores (pore diameter < 2 nm), mesopores (2 nm < pore diameter < 50 nm), and macropores (pore diameter > 50 nm) (Kuptajit et al., 2021).

Powdered activated carbon (PAC) and granular activated carbon (GAC) are the two forms of activated carbon applied in wastewater treatment, being able to remove pesticides, aromatic and phenolic derivatives, pharmaceutics, volatile organic compounds, hydrocarbons and surfactants, metals, dyes and among others (Crini et al., 2019). PAC and GAC differ essentially in terms of the origin of production, grain size, type of equipment used, mode of use, the possibility of regeneration, and production costs (Radhi, 2020). PAC is mainly made from wood, while GAC is from coconut shells or coal. GAC has a larger particle size than PAC (Newcombe, 2006). PAC is used in rapid mix units by batch treatment processes, while the adsorption for GAC is usually done continuously on a packed bed (Hatt et al., 2013). Granular active carbon can be used several times before going through the regeneration process, while PAC is not regenerated, but rather, usually disposed of (Upadhyayula and Chaudhary, 2021). The production of powdered activated carbon is less costly than the GAC, however, when used frequently, it has higher operating costs than the GAC (Soni et al., 2020). So, GAC is a cost-friendly option for large treatment plants. Contrary to the PAC, which is soon discarded, there is the possibility of bacteria growing in the GAC (Wilcox et al., 1983).

The adsorption process is complex and it is influenced by several factors, namely the dosage and characteristics of the adsorbent (i.e., specific area, porosity, pore diameter and

structure, and granulometry), characteristics of the solution (i.e., pH, the concentration of adsorbate, presence of others species and temperature), characteristics of the adsorbate (i.e., polarity, ionic nature, functional groups, solubility, and diameter), and the contact time (Marczewski et al., 2016; Sukmana et al., 2021). For example, the pH of the solution plays a very important role in the adsorption process since it can influence the degree of ionization of the substances present in it, as well as the surface charge of the adsorbent, which affects the reaction kinetics (Nizam et al., 2021). Lee et al. (2003) observed that an accumulation of calcium (in the form of calcium carbonate) over time on activated carbon deteriorates synthetic organic chemical's adsorption. It is not expected that the removal of ammonia by adsorption occurs in very alkaline effluents since the ammonia molecule is in neutral form (unlike the NH_4^+ ion) to be adsorbed to carbon (Soltani et al., 2015).

The adsorption capacity of adsorbent materials has been evaluated through adsorption isotherms, which is the ratio between the amount of adsorbate adsorbed per unit mass of adsorbent and the concentration of adsorbate in solution at equilibrium, at constant temperature (Mokhatab et al., 2019). From the equilibrium models, it is possible to obtain useful information about the surface properties of the adsorbent, the mechanism of adsorption, and the interaction between the adsorbent and the adsorbate (Kalam et al., 2021). Thus, different isothermal models have been used to evaluate and interpret experimental adsorption data, namely the Langmuir isotherms (which assumes, for example, that the surfaces are homogeneous and that the adsorption occurs chemically in a monolayer), Freundlich isotherms (which assumes, for example, that the surfaces are heterogeneous and that the adsorption occurs in multilayers) and among other models (Ribas et al., 2014). On the other hand, the speed with which the adsorbate is retained on the surface of the adsorbent material has been evaluated through adsorption kinetics studies. Kinetics is important as it controls the efficiency of the process. Different models can be fitted to the adsorption process data concerning time, among the most used are pseudo-first-order kinetics and pseudo-second-order kinetics (Yagub et al., 2014). Other kinetic models such as Weber and Morris model, Bangham model, and Pseudo n order model have also been used (Largitte and Pasquier, 2016). The adsorption mechanism can involve four steps (Kajjumba et al., 2019; Patel, 2018):

1. The transport of the adsorbate from the bulk of the solution to the boundary layer surrounding the adsorbent particles,

2. Transport of the adsorbate by diffusion along the boundary layer to the entrance of the adsorbent pores,
3. The transport of the adsorbate inside the pores of the particle to the adsorption sites, by a combination of molecular diffusion through the liquid contained inside the pores and diffusion along the surface of the adsorbent,
4. Attachment of the adsorbate to an available site of the adsorbent involves several mechanisms, such as physical adsorption, chemical adsorption, ion exchange, precipitation, and complexation.

Small particle size means faster adsorption kinetics. A large volume of micropores generally corresponds to a high surface area and good adsorption capacity for small molecules, while a large volume of mesopores or macropores may indicate a good adsorption capacity for larger molecules (Hsieh and Teng, 2000).

One of the challenges of using conventional adsorbents is separating the adsorbent from the treated wastewater. The use of GAC in a packed bed does not require an additional step to remove the adsorbent from the water, however, the same does not happen with PAC. In most studies, the adsorbent separation is carried out by filtration and centrifugation methods (Yegane Badi et al., 2018). Separation of the adsorbent by filtration and sedimentation represents an extra cost and time for wastewater purification. Conventional separation processes such as centrifugation, precipitation, filtration, and chromatography are not economically viable (Ali et al., 2020). Furthermore, as the PAC has a small particle size, the blockage of filters or the loss of the solid particles could occur (Do et al., 2011). Magnetic separation of the adsorbent is not possible since activated carbon has no magnetic properties. However, the combination of activated carbon with iron oxide nanoparticles (e.g., Fe_3O_4 (magnetite) or Fe_2O_3 (maghemite)) has been studied to achieve a separation of the combined using a magnetic field (Borghi and Fabbri, 2014), since magnetic iron oxide nanoparticles have superparamagnetic properties (Khajeh et al., 2013). Borghi and Fabbri (2014) compared the percentage of magnetic-activated carbons (MACs) residues obtained using magnetic separation, sedimentation, and filtration. The authors noted that the magnetic separation of MACs would result in a lower percentage of MAC residues in the treated water. Since iron is one of the most abundant metals on Earth, and the production of iron oxide nanoparticles (using co-precipitation) is low cost and easy to synthesize, its incorporation into activated

carbon is popular (Aragaw et al., 2021; Besenhard et al., 2020; Kumari et al., 2019; Y. F. Shen et al., 2009). On the other hand, the synthesis of magnetic carbon nanocomposites is considerably cheap and requires low operational energy (Barasarathi et al., 2022; Vinayagam et al., 2022). Moreover, magnetic carbon nanocomposites can be used several times after desorption, making it an environmentally friendly water-purification process.

MAC has been extensively applied to remove organic (water-soluble organic dyes, phenolic compounds, humic substances, pharmaceuticals, and others) and inorganic (mercury (II), arsenic (V), gold, phosphate, and others) compounds (Abdullah et al., 2019; Jain et al., 2018; Safarik et al., 2012). However, despite the advantages in terms of magnetic separation, some limitations have been observed in terms of the efficiency of contaminant removal in the MAC adsorption process. Lompe et al. (2017) evaluated the influence of iron oxide nanoparticles (IONP) upon the adsorption of organic matter on magnetic powdered activated carbon, using three magnetic powdered activated carbons (MPAC) with mass fractions of 10%, 38%, and 54% maghemite nanoparticles. The authors observed that maghemite IONP does not contribute significantly to the adsorption of natural organic matter itself and reduces the adsorption capacity of MPAC by blocking the mesopores of the carbon matrix when mass fractions above 38% of maghemite nanoparticles were used. However, improvements in the adsorption capacity with the incorporation of iron oxide nanoparticles in PAC have also been observed by other authors. Park et al. (2015) evaluated the simultaneous removal of bisphenol A (BPA) and natural organic matter (NOM) by applying powdered activated carbons impregnated with iron oxide nanoparticles (IONPACs). The authors observed that IONPAC adsorbents had considerably greater sorption capabilities for BPA and NOM compared to native, bare PAC particles. Vargues et al. (2021) used PAC and PAC combined with iron oxide nanoparticles (PACMAG) as adsorbents to remove common pharmaceuticals (ibuprofen and amoxicillin). These authors observed that the kinetic models and the isothermal models were different between PAC and PACMAG, for both drugs, which means that the incorporation of iron oxide nanoparticles can influence the adsorption mechanism.

1.3. Cases studies

Two case studies are proposed and described in this work, namely ammonium nitrate-based explosive wastewater and slaughterhouse wastewater.

1.3.1. Ammonium nitrate-based explosive wastewater

In this work, ammonium nitrate-based explosive wastewater was collected from an international explosives industry. This effluent results from the washing of equipment, floors, and tank trucks (which transport explosives), which are collected in retention basins in the battery of tanks and the tank truck parking area. Currently, these effluents are subject to a simple treatment (i.e., the addition of a special liquid detergent) to break down amounts of residual emulsion. The oil residues obtained at the top are burned in the burning field, while the effluent (characterized for being poorly biodegradable and containing high amounts of nitrates and ammonium) is collected in reservoirs and sent periodically (monthly) to an authorized waste operator. This transport and disposal method constitute a high cost for the company.

Contrary to other types of explosive wastewater (e.g., HMX and RDX wastewater or TNT wastewater, Bhanot et al., 2020), information regarding the treatment of ammonium nitrate-based explosive wastewater in the literature is quite limited.

Reverse osmosis and ion-exchange are treatment technologies that have been evaluated to recover ammonium nitrate and purify the condensate from ammonium nitrate production for environmental discharge (Duong et al., 2021; Noworyta et al., 2003). However, the disadvantages of these technologies are well known (as shown in Table 1.3). These condensates can reach 659 to 2,460 mg L^{-1} as ammonia and 2,360 to 6,590 mg L^{-1} as nitrate (Duong et al., 2021). Nitrate-rich wastewater treatment from explosives production plants is a challenging task, but the phytoremediation process has been reported as a low-cost alternative for nitrate removal (Marecik et al., 2013).

1.3.2. Slaughterhouse wastewater

Wastewater from the slaughterhouse under study was collected at different stages of a pre-treatment plant for wastewater from the slaughterhouse, located in the Alentejo region, southern Portugal. This pre-treatment system consists of screening, rotary filtration, aeration/homogenization, flocculation, and flotation. Then, it is discharged into the municipal wastewater collection system. Slaughterhouse wastewater results from the slaughter of animals and the washing, and disinfection of facilities and equipment. The effluents from the slaughterhouse to be treated are characterized by being biodegradable and containing a high organic and microbiological load, oils and fats, total suspended solids, and nutrients (phosphorus and nitrogen). The current pretreatment system has some drawbacks, such as the production of pretreated effluents containing recalcitrant and residual organic content that cannot be degraded biologically and through conventional processes (Bahadur and Bhargava, 2022; Bustillo-Lecompte and Mehrvar, 2015), as well as the production of metal-contaminated sludge. Although these sludges are rich in nutrients they need to be stabilized and have low potential to be used in agriculture. These sludges contain metallic residues from coagulants applied in the coagulation-flocculation processes (e.g. ferric sulfate, ferric chloride, aluminum sulfate, or aluminum chloride Bustillo-Lecompte and Mehrvar, 2015), whose presence is associated with human and environmental health concerns (Rahman et al., 2018; Tetteh and Rathilal, 2020). Moreover, these sludges can contaminate groundwater by leaching iron and aluminum salts in acidic soils (Aguilar et al., 2005) and limit plant growth due to lower nutrient availability (Mahedi et al., 2019; Serra et al., 2018). The destination of these sludges is landfilling disposal. Thus, in terms of environmental sustainability, new treatments of effluents from slaughterhouses should be rethought. Different slaughterhouse treatment processes have been reviewed (Bustillo-Lecompte and Mehrvar, 2017, 2015; Ng et al., 2022; Philipp et al., 2021; Shende and Pophali, 2021), namely: i) physical-chemical treatments, e.g., coagulation and flocculation (Amuda and Alade, 2006; Satyanarayan et al., 2005; Tariq et al., 2012), dissolved air flotation (de Nardi et al., 2008), electrocoagulation (Martínez-Cruz et al., 2020), adsorption (Agarry and Owabor, 2012; del Real-Olvera et al., 2016; K. Keerthana and Thivyatharsan, 2018), acid precipitation (Prazeres et al., 2019a), and membranes (Almandoz et al., 2015); ii) biological treatments, e.g., activated sludge (Carvalho et al., 2013), anaerobic filters (Martinez et al., 2014), and constructed wetlands (Carreau et al., 2012; K. Keerthana and

Thivyatharsan, 2018; Odong et al., 2013; Soroko, 2007); iii) chemical oxidation processes, e.g., ozonation (Wu and Doan, 2005); iv) advanced oxidation processes, e.g., UV-H_2O_2 (Bustillo-Lecompte et al., 2014), gamma radiation (Melo et al., 2008), Fenton (Fe^{2+}/H_2O_2), photo-Fenton (UV-Fe^{2+}/H_2O_2), and electro-Fenton (Paramo-Vargas et al., 2015)), and v) combined processes, e.g., coagulation/adsorption (Mahtab et al., 2009), activated sludge/reverse osmosis (Bohdziewicz and Sroka, 2005), anaerobic baffled reactor/UV/H_2O_2 (Cao and Mehrvar, 2011), anaerobic baffled reactor/aerobic activated sludge/UV/H_2O_2 (Bustillo-Lecompte et al., 2016), anaerobic lagoon/constructed wetlands (Gutiérrez-Sarabia et al., 2004), anaerobic digestion/wetlands (Manh et al., 2014), and chemical coagulation/electro-Fenton (Bazrafshan et al., 2022)). Despite the high efficiencies found in some individual and/or combined processes, drawbacks of these processes are identified, such as treatment complexity, high energy consumption, and no recovery nutrients (as can be seen in Table 1.3).

1.4. Guidelines and Regulations

Different regulations have been established around the world to control the impact of industrial wastewater on the environment. Some jurisdictions have specific regulations for certain industries.

The specific regulations for the discharge of explosive effluents are very limited. The limit values of the different parameters established for discharge have been based on the number of explosives produced in the industry (Table 1.8) (US Environmental Protection Agency, 1976).

Table 1.8 - Standard limits for explosive wastewater discharge.

Parameter	USA[a)]
pH	6 - 9
BOD*	0.24 – 0.72
COD *	2.59 – 7.77
Oil and grease*	0.035 – 0.11
TSS *	0.084 – 0.25

Note: *kg/kkg of the product; a) US Environmental Protection Agency (1976).

This sparse regulation at an international level may indicate that the discharge of this effluent into surface waters will have to respect the discharge standards applied to treated urban wastewater.

For slaughterhouse wastewater, the World Bank Group (2007), the Council of the European Communities (1991), and the US Environmental Protection Agency (2004) have defined discharge limits (Table 1.9). In general, the established limit values are quite similar to each other (Table 1.9). On the other hand, rules and recommendations have also been made available to the slaughterhouse sector, as is the case of the document entitled "Best Available Techniques in the Slaughterhouses and Animal By-products Industries", which summarizes the wastewater treatment technologies that are available in the literature to reach discharge limits (European Commission, 2005).

Table 1.9 - Standard limits for slaughterhouse wastewater discharge from different regulations.

Parameter	World Bank[a)]	EU[b)]	USA[c)]
pH	6 – 9	-	6 - 9
BOD (mg L^{-1})	50	25	16 - 26
COD (mg L^{-1})	250	125	-
TN (mg N L^{-1})	10	10 - 15	4 - 8
TP (mg L^{-1})	2	1 - 2	-
Oil and grease (mg L^{-1})	10	-	8 - 14
TSS (mg L^{-1})	50	35 - 60	20 - 30
Total coliform bacteria (MPN/100 mL)	400	-	400

Note: MPN – Most Probable Number; a) World Bank Group (2007); b) Council of the European Communities (1991); c) US Environmental Protection Agency (2004).

In terms of international standards for irrigation with reclaimed water, legislation varies from country to country (Zhao et al., 2022). In Portugal, the legal regime for producing water to be reused, obtained from wastewater treatment, is established by Decree-Law No. 119/2019 (Portuguese Government, 2019), according to Table 1.10.

Table 1.10 – Reclaimed water quality requirements for agricultural irrigation.

Reclaimed water quality class	BOD_5 (mg L^{-1})	TSS (mg L^{-1})	Turbidity (NTU)	*E. coli* (number/100 mL)	Intestinal parasite eggs (Nº/L)
A	≤ 10	≤ 10	≤ 5	≤ 10	-
B	≤ 25	≤ 35	-	≤ 100	-
C	≤ 25	≤ 35	-	≤ 1000	≤ 1
D	≤ 25	≤ 35	-	≤ 10000	≤ 1
E	≤ 40	≤ 60	-	≤ 10000	-

Thus, the assessment of compliance with the discharge and irrigation requirements of the different processes studied in this work was based on the limits established by the Council of the European Communities (1991) and the Portuguese Government (2019), respectively, for both effluents under study.

1.5. Objective and structure of the thesis

Some industries still see wastewater as a residue or a problem, which they seek to solve by applying an industrial wastewater treatment system that results in wastewater disposal and often with the formation of by-products that are difficult to recover. This solution is not environmentally sustainable. It is necessary to change the linear paradigm to the circular one, that is, to propose solutions capable of boosting the circular economy (reduce, reuse, recover) making wastewater treatment plants self-sustainable using low-energy processes and capable of generating marketable products instead of waste.

Given the challenges encountered in the treatment of industrial effluents (as observed in the previous sections), the need to look for new, simple, eco-innovative, and low-cost strategies in the treatment of industrial effluents, especially in effluents from explosives and slaughterhouses, becomes evident.

The objective of this thesis is to develop a circular treatment sequence for (i) poorly biodegradable effluents with low C/N and (ii) biodegradable effluents with a high C/N ratio. Therefore, this work proposes an integrated treatment composed of immediate one-step lime precipitation (IOSLM) and atmospheric carbonation (AC) followed by constructed wetland or adsorption process to allow the reuse or disposal of the referred treated wastewaters and the reuse of sludges produced in IOSLM. Two case studies were used, namely wastewaters from the explosive industry for (i) effluents, and from slaughterhouse wastewater for (ii) effluents.

The objective of IOSLM and AC is to reduce effluent contamination, for organic matter, TSS, oils and fats, and nutrients (e.g., organic nitrogen and phosphorus), as well as reduce pH and concentrations of ammonia, calcium, and conductivity. The constructed wetlands and adsorption process are used as an effluent refining process to remove contaminants

(e.g., organic matter, ammoniacal nitrogen, and nitrates) that were not possible to be removed by the previous processes.

It is expected that the proposed system can contribute to the circular economy, through the creation of by-products with economic value, such as i) reuse of lime sludge from the IOLSM process as a coagulant (aid), and ii) capture of ammonia in atmospheric carbonation processes that can be used for the production of ammonium sulfate fertilizer.

The specific objectives of this thesis are:

1. Optimize the performance of the IOSLM process to treat industrial wastewater with variable characteristics, by studying the effect of the lime dose and precipitation pH;
2. Optimize the atmospheric carbonation process using:
    - Open systems, by evaluating the effect of carbonation time, reactor area/volume ratio, reaction pH, and the presence/absence of IOSLM precipitate on effluent neutralization;
    - Closed systems, through modeling and optimization of CO_2 and ammonia capture for a stirrer bubble column and a stepped continuous flow capillary column. For the bubbling process, the effects of aeration time, air flow rate, stirring speed, and effluent volume are evaluated. In the capillary process, the effects of effluent flow rate, air flow rate, and capillary area are evaluated;
3. Evaluate constructed wetlands as a refining process for low biodegradable and:
    - high nitrogen wastewater, through the study of the effect of flooding level, C/N ratio, and nitrogen load;
    - high organic wastewater, by evaluating the effect of organic matter load and bed depth;
4. Evaluate the adsorption process as a tuning process in the removal of organic matter, by studying the effect of the activated carbon dosage and contact time, and methods for activated carbon separation from water (magnetic separation filtration, and sedimentation);

5. Evaluate the reuse of lime sludge from the IOSLM process as a coagulant (aid) in the treatment of effluents with variable characteristics, through the effect of heat treatment and the successive reuse of sludge.

This thesis is divided into eight chapters. The chapters of this thesis are autonomous and are composed of sections: abstract, introduction, materials and methods, results and discussion, conclusion, and references. Chapter 1 is the introduction, and it describes the characteristics and strategies for treating industrial wastewater (including the main treatment processes studied here), as well as indicating the objectives of the thesis. Chapters 2 and 3 focus on the use of immediate one-step lime precipitation and atmospheric carbonation as pre-treatment for explosives industrial wastewater and slaughterhouse wastewater, respectively. In these chapters, the effect of the dose/pH of reaction applied in the removal of contaminants during the IOSLM process is analyzed, and then the effect of some operational variables (e.g., time) in the open system atmospheric carbonation process is studied. Chapter 4 seeks to model and optimize the capture of atmospheric CO_2 in a closed system with the simultaneous capture of ammonia, using response surface methodology. Chapters 5 and 6 focus on the application of refining processes (e.g., constructed wetland or adsorption) for explosives wastewater and slaughterhouse wastewater, respectively, both obtained by the IOSLM+AC pretreatment process. Chapter 7 is dedicated to the recovery of sludge obtained by the IOSLM as a coagulant (aid) process in the treatment of wastewater from the slaughterhouse. Finally, chapter 8 provides a conclusion and future outlook.

1.6. References

A. Ramos-Arcos, S., G. González-Mondragón, E., S. López-Hernández, E., R. Rodríguez-Luna, A., M. Morales-Bautista, C., Lagunas-Rivera, S., López-Martínez, S., 2022. Phytoremediation Potential of Chrysopogon zizanioides for Toxic Elements in Contaminated Matrices, in: Biodegradation Technology of Organic and Inorganic Pollutants. IntechOpen. https://doi.org/10.5772/intechopen.98235

Abdullah, N.H., Shameli, K., Abdullah, E.C., Abdullah, L.C., 2019. Solid matrices for fabrication of magnetic iron oxide nanocomposites: Synthesis, properties, and application for the adsorption of heavy metal ions and dyes. Compos. Part B Eng. 162, 538–568. https://doi.org/10.1016/J.COMPOSITESB.2018.12.075

Abira, M.A., van Bruggen, J.J.A., Denny, P., 2005. Potential of a tropical subsurface constructed wetland to remove phenol from pre-treated pulp and papermill wastewater. Water Sci. Technol. 51, 173–176. https://doi.org/10.2166/WST.2005.0312

Achak, M., Barka, N., Lamy, E., 2023. Constructed Wetlands Process for Treating Sewage to Improve the Quantitative and Qualitative Management of Groundwater Resources. IntechOpen. https://doi.org/10.5772/intechopen.110630

Agarry, S.E., Oghenejoboh, K.M., Latinwo, G.K., Owabor, C.N., 2020. Biotreatment of petroleum refinery wastewater in vertical surface-flow constructed wetland vegetated with *Eichhornia crassipes*: lab-scale experimental and kinetic modelling. Environ. Technol. 41, 1793–1813. https://doi.org/10.1080/09593330.2018.1549106

Agarry, S.E., Owabor, C.N., 2012. Evaluation of the Adsorption Potential of Rubber (*Hevea brasiliensis*) Seed Pericarp-Activated Carbon in Abattoir Wastewater Treatment and in the Removal of Iron (iii) Ions from Aqueous Solution. Niger. J. Technol. 31, 346–358. https://doi.org/10.4314/njt.v31i3.

Aguilar, M.I., Sáez, J., Lloréns, M., Soler, A., Ortuño, J.F., Meseguer, V., Fuentes, A., 2005. Improvement of coagulation-flocculation process using anionic polyacrylamide as coagulant aid. Chemosphere 58, 47–56. https://doi.org/10.1016/j.chemosphere.2004.09.008

Al-Abri, M., Al-Ghafri, B., Bora, T., Dobretsov, S., Dutta, J., Castelletto, S., Rosa, L., Boretti, A., 2019. Chlorination disadvantages and alternative routes for biofouling control in reverse osmosis desalination. npj Clean Water 2019 21 2, 1–16. https://doi.org/10.1038/s41545-018-0024-8

Alayu, E., Leta, S., 2021. Post treatment of anaerobically treated brewery effluent using pilot scale horizontal subsurface flow constructed wetland system. Bioresour. Bioprocess. 8, 1–19. https://doi.org/10.1186/S40643-020-00356-0/FIGURES/8

Alayu, E., Yirgu, Z., 2018. Advanced technologies for the treatment of wastewaters from agro-processing industries and cogeneration of by-products: a case of slaughterhouse, dairy and beverage industries. Int. J. Environ. Sci. Technol. 15, 1581–1596. https://doi.org/10.1007/S13762-017-1522-9/FIGURES/8

Ali, M.E., Hoque, M.E., Safdar Hossain, S.K., Biswas, M.C., 2020. Nanoadsorbents for wastewater treatment: next generation biotechnological solution. Int. J. Environ. Sci. Technol. 17, 4095–4132. https://doi.org/10.1007/S13762-020-02755-4/TABLES/5

Almanassra, I.W., Kochkodan, V., Mckay, G., Atieh, M.A., Al-Ansari, T., 2021. Review of phosphate removal from water by carbonaceous sorbents. J. Environ. Manage. 287, 112245. https://doi.org/10.1016/J.JENVMAN.2021.112245

Almandoz, M.C., Pagliero, C.L., Ochoa, N.A., Marchese, J., 2015. Composite ceramic membranes from natural aluminosilicates for microfiltration applications. Ceram. Int. 41, 5621–5633. https://doi.org/10.1016/J.CERAMINT.2014.12.144

Almazán-Sánchez, P.T., Linares-Hernández, I., Solache-Río, M.J., Martínez-Miranda, V., 2016. Textile wastewater treatment using iron-modified clay and copper-modified carbon in batch and column systems. Water. Air. Soil Pollut. 227. https://doi.org/10.1007/S11270-016-2801-7

Almeida, A., Jóźwiakowski, K., Kowalczyk-Juśko, A., Bugajski, P., Kurek, K., Carvalho, F., Durao, A., Ribeiro, C., Gajewska, M., 2020. Nitrogen removal in vertical flow constructed wetlands: influence of bed depth and high nitrogen loadings. Environ. Technol. 41, 2196–2209. https://doi.org/10.1080/09593330.2018.1557749

Almeida, A., Ribeiro, C., Carvalho, F., Durao, A., Bugajski, P., Kurek, K., Pochwatka, P., Jóźwiakowski, K., 2019. Phytoremediation potential of Vetiveria zizanioides and Oryza sativa to nitrate and organic substance removal in vertical flow constructed wetland systems. Ecol. Eng. 138, 19–27. https://doi.org/10.1016/J.ECOLENG.2019.06.020

Álvarez-Torrellas, S., Peres, J.A., Gil-Álvarez, V., Ovejero, G., García, J., 2017. Effective adsorption of non-biodegradable pharmaceuticals from hospital wastewater with different carbon materials. Chem. Eng. J. 320, 319–329. https://doi.org/10.1016/J.CEJ.2017.03.077

Amor, C., Marchão, L., Lucas, M.S., Peres, J.A., 2019. Application of advanced oxidation processes for the treatment of recalcitrant agro-industrial wastewater: A review. Water 11. https://doi.org/10.3390/W11020205

Amuda, O.S., Alade, A., 2006. Coagulation/flocculation process in the treatment of abattoir wastewater. Desalination 196, 22–31. https://doi.org/10.1016/j.desal.2005.10.039

An, B.H., Xu, D.M., Geng, R., Cheng, Y., Qian, R.B., Tang, X.C., Fan, Z.Q., Chen, H. Bin, 2023. The pretreatment effects of various target pollutant in real coal gasification gray water by coupling pulse electrocoagulation with chemical precipitation methods. Chemosphere 311, 136898. https://doi.org/10.1016/j.chemosphere.2022.136898

Anh, H.T.H., Shahsavari, E., J. Bott, N., Ball, A.S., 2021. Bioaugmentation of seafood processing wastewater enhances the removal of inorganic nitrogen and chemical oxygen demand. Aquaculture 542, 736818. https://doi.org/10.1016/J.AQUACULTURE.2021.736818

Ani, J.U., Okoro, U.C., Aneke, L.E., Onukwuli, O.D., Obi, I.O., Akpomie, K.G., Ofomatah, A.C., 2019. Application of response surface methodology for optimization of dissolved solids adsorption by activated coal. Appl. Water Sci. 9, 1–11. https://doi.org/10.1007/S13201-019-0943-7/TABLES/7

Aragaw, T.A., Bogale, F.M., Aragaw, B.A., 2021. Iron-based nanoparticles in wastewater treatment: A review on synthesis methods, applications, and removal mechanisms. J. Saudi Chem. Soc. 25, 101280. https://doi.org/10.1016/J.JSCS.2021.101280

Asaithambi, P., Yesuf, M.B., Govindarajan, R., Hariharan, N.M., Thangavelu, P., Alemayehu, E., 2022. A Review of Hybrid Process Development Based on Electrochemical and Advanced Oxidation Processes for the Treatment of Industrial Wastewater. Int. J. Chem. Eng. https://doi.org/10.1155/2022/1105376

Avellan, C.T., Ardakanian, R., Gremillion, P., 2017. The role of constructed wetlands for biomass production within the water-soil-waste nexus. Water Sci. Technol. 75, 2237–2245. https://doi.org/10.2166/WST.2017.106

Ayeche, R., 2012. Treatment by Coagulation-Flocculation of Dairy Wastewater with the Residual Lime of National Algerian Industrial Gases Company (NIGC-Annaba). Energy Procedia 18, 147–156. https://doi.org/10.1016/J.EGYPRO.2012.05.026

Ayoub, G.M., Hamzeh, A., Semerjian, L., 2011. Post treatment of tannery wastewater using lime/bittern coagulation and activated carbon adsorption. Desalination 273, 359–365. https://doi.org/10.1016/J.DESAL.2011.01.045

Ayoub, G.M., Merhebi, F., 2002. Characteristics and quantities of sludge produced by coagulating wastewater with seawater bittern, lime and caustic. Adv. Environ. Res. 6, 277–284. https://doi.org/10.1016/S1093-0191(01)00058-2

Badejo, A.A., Omole, D.O., Ndambuki, J.M., Kupolati, W.K., 2017. Municipal wastewater treatment using sequential activated sludge reactor and vegetated submerged bed constructed wetland planted with Vetiveria zizanioides. Ecol. Eng. 99, 525–529. https://doi.org/10.1016/J.ECOLENG.2016.11.012

Bahadur, N., Bhargava, N., 2022. TERI Advanced Oxidation Technology (TADOX®) to treat industrial wastewater with integration at pre- and post-biological stage: case studies from India. Water Pract. Technol. 17, 1692–1705. https://doi.org/10.2166/WPT.2022.065

Bal Krishna, K.C., Niaz, M.R., Sarker, D.C., Jansen, T., 2017. Phosphorous removal from aqueous solution can be enhanced through the calcination of lime sludge. J. Environ. Manage. 200, 359–365. https://doi.org/10.1016/j.jenvman.2017.06.003

Banerjee, R., Goswami, P., Lavania, S., Mukherjee, A., Lavania, U.C., 2019. Vetiver grass is a potential candidate for phytoremediation of iron ore mine spoil dumps. Ecol. Eng. 132, 120–136. https://doi.org/10.1016/j.ecoleng.2018.10.012

Barasarathi, J., Abdullah, P.S., Uche, E.C., 2022. Application of magnetic carbon nanocomposite from agro-waste for the removal of pollutants from water and wastewater. Chemosphere 305, 135384. https://doi.org/10.1016/J.CHEMOSPHERE.2022.135384

Bazrafshan, E., Zakeri, H.R., Vieira, M.G.A., Derakhshan, Z., Mohammadi, L., Mohammadpour, A., Mousavi Khaneghah, A., 2022. Slaughterhouse Wastewater Treatment by Integrated Chemical Coagulation and Electro-Fenton Processes. Sustain. 14, 11407. https://doi.org/10.3390/SU141811407

Besenhard, M.O., LaGrow, A.P., Hodzic, A., Kriechbaum, M., Panariello, L., Bais, G., Loizou, K., Damilos, S., Margarida Cruz, M., Thanh, N.T.K., Gavriilidis, A., 2020. Co-precipitation synthesis of stable iron oxide nanoparticles with NaOH: New insights and continuous production via flow chemistry. Chem. Eng. J. 399, 125740. https://doi.org/10.1016/J.CEJ.2020.125740

Bhanot, P., Celin, S.M., Sreekrishnan, T.R., Kalsi, A., Sahai, S.K., Sharma, P., 2020. Application of integrated treatment strategies for explosive industry wastewater—A critical review. J. Water Process Eng. 35, 101232. https://doi.org/10.1016/J.JWPE.2020.101232

Billore, S.K., Singh, N., Ram, H.K., Sharma, J.K., Singh, V.P., Nelson, R.M., Dass, P., 2001. Treatment of a molasses based distillery effluent in a constructed wetland in central India. Water Sci. Technol. 44, 441–448. https://doi.org/10.2166/WST.2001.0864

Biswal, B.K., Balasubramanian, R., 2022. Constructed Wetlands for Reclamation and Reuse of Wastewater and Urban Stormwater: A Review. Front. Environ. Sci. 10, 201. https://doi.org/10.3389/FENVS.2022.836289/BIBTEX

Bohdziewicz, J., Sroka, E., 2005. Integrated system of activated sludge-reverse osmosis in the treatment of the wastewater from the meat industry. Process Biochem. 40, 1517–1523. https://doi.org/10.1016/j.procbio.2003.11.047

Bojcevska, H., Tonderski, K., 2007. Impact of loads, season, and plant species on the performance of a tropical constructed wetland polishing effluent from sugar factory stabilization ponds. Ecol. Eng. 29, 66–76. https://doi.org/10.1016/J.ECOLENG.2006.07.015

Borghi, C.C., Fabbri, M., 2014. Magnetic recovery of modified activated carbon powder used for removal of endocrine disruptors present in water. Environ. Technol. 35, 1018–1026. https://doi.org/10.1080/09593330.2013.858776

Boukhoubza, F., Jail, A., Korchi, F., Idrissi, L.L., Hannache, H., Duarte, J.C., Hassani, L., Nejmeddine, A., 2009. Application of lime and calcium hypochlorite in the dephenolisation and discolouration of olive mill wastewater. J. Environ. Manage. 91, 124–132. https://doi.org/10.1016/J.JENVMAN.2009.07.004

Bulc, T.G., Ojstršek, A., 2008. The use of constructed wetland for dye-rich textile wastewater treatment. J. Hazard. Mater. 155, 76–82. https://doi.org/10.1016/J.JHAZMAT.2007.11.068

Burger, P., Landreau, A., Watson, M., Janci, L., Cassisa, V., Kempf, M., Azoulay, S., Fernandez, X., 2017. Vetiver Essential Oil in Cosmetics: What Is New? Medicines 4, 41. https://doi.org/10.3390/MEDICINES4020041

Bustillo-Lecompte, C., Mehrvar, M., 2017. Slaughterhouse Wastewater: Treatment, Management and Resource Recovery, in: Physico-Chemical Wastewater Treatment and Resource Recovery. InTech. https://doi.org/10.5772/65499

Bustillo-Lecompte, C., Mehrvar, M., Quiñones-Bolaños, E., 2016. Slaughterhouse wastewater characterization and treatment: An economic and public health necessity of the meat processing industry in Ontario, Canada, in: International Conference on Environmental Pollution and Public Health, EPPH 2016. Engineering Information Institute, 175–186. https://doi.org/10.4236/gep.2016.44021

Bustillo-Lecompte, C.F., Mehrvar, M., 2015. Slaughterhouse wastewater characteristics, treatment, and management in the meat processing industry: A review on trends and advances. J. Environ. Manage. 165, 287-302. https://doi.org/10.1016/j.jenvman.2015.07.008

Bustillo-Lecompte, C.F., Mehrvar, M., Quiñones-Bolaños, E., 2014. Cost-effectiveness analysis of TOC removal from slaughterhouse wastewater using combined anaerobic-aerobic and UV/H_2O_2 processes. J. Environ. Manage. 134, 145–152. https://doi.org/10.1016/j.jenvman.2013.12.035

Cao, W., Mehrvar, M., 2011. Slaughterhouse wastewater treatment by combined anaerobic baffled reactor and UV/H_2O_2 processes. Chem. Eng. Res. Des. 89, 1136–1143. https://doi.org/10.1016/j.cherd.2010.12.001

Carreau, R., VanAcker, S., VanderZaag, A.C., Madani, A., Drizo, A., Jamieson, R., Gordon, R.J., 2012. Evaluation of a Surface Flow Constructed Wetland Treating Abattoir Wastewater. Appl. Eng. Agric. 28, 757–766. https://doi.org/10.13031/2013.42416

Carrera, J., Vicent, T., Lafuente, J., 2004. Effect of influent COD/N ratio on biological nitrogen removal (BNR) from high-strength ammonium industrial wastewater. Process Biochem. 39, 2035–2041. https://doi.org/10.1016/J.PROCBIO.2003.10.005

Carvalho, P.N., Pirra, A., Basto, M.C.P., Almeida, C.M.R., 2013. Activated sludge systems removal efficiency of veterinary pharmaceuticals from slaughterhouse wastewater. Environ. Sci. Pollut. Res. Int. 20, 8790–8800. https://doi.org/10.1007/S11356-013-1867-7

Chauhan, R., Srivastava, V.C., 2020. Electrochemical denitrification of highly contaminated actual nitrate wastewater by Ti/RuO_2 anode and iron cathode. Chem. Eng. J. 386, 122065. https://doi.org/10.1016/J.CEJ.2019.122065

Chen, C.K., Lo, S.L., 2003. Treatment of slaughterhouse wastewater using an activated sludge/contact aeration process. Water Sci. Technol. 47, 285–292. https://doi.org/10.2166/WST.2003.0658

Chen, Q., Luo, Z., Hills, C., Xue, G., Tyrer, M., 2009. Precipitation of heavy metals from wastewater using simulated flue gas: Sequent additions of fly ash, lime and carbon dioxide. Water Res. 43, 2605–2614. https://doi.org/10.1016/J.WATRES.2009.03.007

Chen, Y., Hong, L., Han, W., Wang, L., Sun, X., Li, J., 2011. Treatment of high explosive production wastewater containing RDX by combined electrocatalytic reaction and anoxic–oxic biodegradation. Chem. Eng. J. 168, 1256–1262. https://doi.org/10.1016/J.CEJ.2011.02.032

Cheng, Q., Wu, Y., Huang, Y., Li, F., Liu, Z., Nengzi, L., Bao, L., 2021. An integrated process of calcium hydroxide precipitation and air stripping for pretreatment of flue gas desulfurization wastewater towards zero liquid discharge. J. Clean. Prod. 314, 128077. https://doi.org/10.1016/J.JCLEPRO.2021.128077

Cheng, S., Ran, X., Ren, G., Wei, Z., Wang, Z., Rao, T., Li, R., Ma, X., 2022. Comparison of Fenton and Ozone Oxidation for Pretreatment of Petrochemical Wastewater: COD Removal and Biodegradability Improvement Mechanism. Separations 9, 179. https://doi.org/10.3390/separations9070179

Chintani, Y.S., Butarbutar, E.S., Nugroho, A.P., Sembiring, T., 2021. Uptake and release of chromium and nickel by Vetiver grass (*Chrysopogon zizanioides* (L.) Roberty). SN Appl. Sci. 3, 1–13. https://doi.org/10.1007/S42452-021-04298-W/TABLES/5

Chitra, A. V., Lakshmanaperumalsamy, P., 2006. Biodegradation of nitrate in wastestreams from explosives manufacturing plants. Res. J. Microbiol. 1, 142–151. https://doi.org/10.3923/jm.2006.142.151

Comino, E., Riggio, V., Rosso, M., 2011. Mountain cheese factory wastewater treatment with the use of a hybrid constructed wetland. Ecol. Eng. 37, 1673–1680. https://doi.org/10.1016/J.ECOLENG.2011.06.048

Cooper, P., Job, G., Green, M., Shutes, R., 1996. Reed beds and constructed wetlands for wastewater treatment. Water Res. Cent. Publ. 154.

Correia, T., Regato, M., Almeida, A., Santos, T., Amaral, L., Carvalho, M. de F.N., 2020. Manual Treatment of Urban Wastewater by Chemical Precipitation for Production of Hydroponic Nutrient Solutions. J. Ecol. Eng. 21, 143–152. https://doi.org/10.12911/22998993/118286

Council of the European Communities, 1991. Urban Wastewater Treatment Directive 91/271/EEC, Official Journal of the European Communities.

Crini, G., 2006. Non-conventional low-cost adsorbents for dye removal: A review. Bioresour. Technol. 97, 1061–1085. https://doi.org/10.1016/J.BIORTECH.2005.05.001

Crini, G., 2005. Recent developments in polysaccharide-based materials used as adsorbents in wastewater treatment. Prog. Polym. Sci. 30, 38–70. https://doi.org/10.1016/J.PROGPOLYMSCI.2004.11.002

Crini, G., Lichtfouse, E., 2019. Advantages and disadvantages of techniques used for wastewater treatment. Environ. Chem. Lett. 17, 145–155. https://doi.org/10.1007/S10311-018-0785-9/TABLES/1

Crini, G., Lichtfouse, E., Wilson, L.D., Morin-Crini, N., 2019. Conventional and non-conventional adsorbents for wastewater treatment. Environ. Chem. Lett. 17, 195–213. https://doi.org/10.1007/S10311-018-0786-8

Cristóvão, R.O., Botelho, C.M., Martins, R.J.E., Loureiro, J.M., Boaventura, R.A.R., 2014. Primary treatment optimization of a fish canning wastewater from a Portuguese plant. Water Resour. Ind. 6, 51–63. https://doi.org/10.1016/J.WRI.2014.07.002

Cruz, K.D., Francisco, J.T.J., Mellendrez, K.J.M., Pineda, J.M.F., 2019. Electrocoagulation treatment of swine slaughterhouse wastewater: effect of electrode material. E3S Web Conf. 117, 00020. https://doi.org/10.1051/E3SCONF/201911700020

Cyplik, P., Marecik, R., Piotrowska-Cyplik, A., Olejnik, A., Drozdzyńska, A., Chrzanowski, Ł., 2012. Biological Denitrification of High Nitrate Processing Wastewaters from Explosives Production Plant. Water. Air. Soil Pollut. 223, 1791. https://doi.org/10.1007/S11270-011-0984-5

Danh, L.T., Truong, P., Mammucari, R., Tran, T., Foster, N., 2009. VETIVER GRASS, *VETIVERIA ZIZANIOIDES*: A CHOICE PLANT FOR PHYTOREMEDIATION OF HEAVY METALS AND ORGANIC WASTES. Int. J. Phytoremediation 11, 664–691. https://doi.org/10.1080/15226510902787302

Darajeh, N., Truong, P., Rezania, S., Alizadeh, H., Leung, D.W.M., 2019. Effectiveness of Vetiver grass versus other plants for phytoremediation of contaminated water. J. Environ. Treat. Tech. 7, 485–500.

Davamani, V., Indhu Parameshwari, C., Arulmani, S., Ezra John, J., Poornima, R., 2021. Hydroponic phytoremediation of paperboard mill wastewater by using vetiver (*Chrysopogon zizanioides*). J. Environ. Chem. Eng. 9, 105528. https://doi.org/10.1016/J.JECE.2021.105528

de Jesus, M.A.S., Aguiar Dutra, A.R. de, Cirani, C.B.S., Jesus, K.R.E., Neto, R.C.S., Guerra, J.B.A., 2022. Eco-innovation assessment of biodigesters technology: an application in cassava processing industries in the south of Brazil, Parana state. Clean Technol. Environ. Policy 24, 931–948. https://doi.org/10.1007/s10098-021-02232-7

de Nardi, I.R., Fuzi, T.P., Del Nery, V., 2008. Performance evaluation and operating strategies of dissolved-air flotation system treating poultry slaughterhouse wastewater. Resour. Conserv. Recycl. 52, 533–544. https://doi.org/10.1016/J.RESCONREC.2007.06.005

del Real-Olvera, J., Rustrian-Portilla, E., Houbron, E., Landa-Huerta, F.J., 2016. Adsorption of organic pollutants from slaughterhouse wastewater using powder of *Moringa oleifera* seeds as a natural coagulant. Desalin. Water Treat. 57, 9971–9981. https://doi.org/10.1080/19443994.2015.1033479

Derakhshan, M., Fazeli, M., 2018. Improved biodegradability of hardly-decomposable wastewaters from petrochemical industry through photo-Fenton method and determination of optimum operational conditions by response surface methodology. J. Biol. Eng. 12. https://doi.org/10.1186/S13036-018-0104-9

Deshannavar, U.B., K, B.R., N, Naik, ini M., 2012. High rate digestion of dairy industry effluent by upflow anaerobic fixed-bed reactor. J. Chem. Pharm. Res. 2012, 2895–2899.

Devda, V., Chaudhary, K., Varjani, S., Pathak, B., Patel, A.K., Singhania, R.R., Taherzadeh, M.J., Ngo, H.H., Wong, J.W.C., Guo, W., Chaturvedi, P., 2021. Recovery of resources from industrial wastewater employing electrochemical technologies: status, advancements and perspectives. Bioengineered 12, 4697–4718. https://doi.org/10.1080/21655979.2021.1946631

Dinesh Kumar, M., Gopikumar, S., Uan, D.K., Adishkumar, S., Rajesh Banu, J., 2020. Constructed Wetlands: An Emerging Green Technology for the Treatment of Industrial Wastewaters. pp. 21–44. https://doi.org/10.1007/978-981-15-1390-9_2

Dinesh Kumar, S., Mande, A.B., Premalatha, M., Sivasankar, T., 2022. Experimental studies on the impact of porous bed-induced solar evaporation (PBISE) and thermal degradation of the solid content of the distillery effluent using cocopeat- A sustainable approach. J. Clean. Prod. 377, 134250. https://doi.org/10.1016/J.JCLEPRO.2022.134250

Ding, R., Wang, Y., Chen, X., Gao, Y., Yang, M., 2019. Extended Fenton's process: toward improving biodegradability of drilling wastewater. Water Sci. Technol. 79, 1790–1797. https://doi.org/10.2166/WST.2019.179

Dlamini, D.S., Tesha, J.M., Vilakati, G.D., Mamba, B.B., Mishra, A.K., Thwala, J.M., Li, J., 2020. A critical review of selected membrane- and powder-based adsorbents for water treatment: Sustainability and effectiveness. J. Clean. Prod. 277, 123497. https://doi.org/10.1016/J.JCLEPRO.2020.123497

Do, M.H., Phan, N.H., Nguyen, T.D., Pham, T.T.S., Nguyen, V.K., Vu, T.T.T., Nguyen, T.K.P., 2011. Activated carbon/Fe_3O_4 nanoparticle composite: Fabrication, methyl orange removal and regeneration by hydrogen peroxide. Chemosphere 85, 1269–1276. https://doi.org/10.1016/J.CHEMOSPHERE.2011.07.023

Duong, H.C., Cao, H.T., Hoang, N.B., Nghiem, L.D., 2021. Reverse osmosis treatment of condensate from ammonium nitrate production: Insights into membrane performance. J. Environ. Chem. Eng. 9, 106457. https://doi.org/10.1016/J.JECE.2021.106457

Edokpayi, J.N., Odiyo, J.O., Durowoju, O.S., Edokpayi, J.N., Odiyo, J.O., Durowoju, O.S., 2017. Impact of Wastewater on Surface Water Quality in Developing Countries: A Case Study of South Africa. Water Qual. pp. 401-416. https://doi.org/10.5772/66561

Elkarrach, K., Atia, F., Omor, A., Laidi, O., Biyada, S., Benlmelih, M., Merzouki, M., 2022. Biological versus Physicochemical Technologies for Industrial Sewage Treatment: Which Is the Most Efficient and Inexpensive?, in: Sewage - Recent Advances, New Perspectives and Applications. IntechOpen. https://doi.org/10.5772/intechopen.100325

Engida, T., Alemu, T., Wu, J., Xu, D., Zhou, Q., Wu, Z., 2020. Analysis of constructed wetlands technology performance efficiency for the treatment of floriculture industry wastewater, in Ethiopia. J. Water Process Eng. 38. https://doi.org/10.1016/j.jwpe.2020.101586

European Commission, 2005. Reference Document on Best Available Techniques in the Slaughterhouses and Animal By-products Industries.

Fabricius, K., 2011. Nutrient pollution/eutrophication. Encycl. Earth Sci. Ser. Part 2, 722–731. https://doi.org/10.1007/978-90-481-2639-2_19/COVER

Fasani, E., DalCorso, G., Zerminiani, A., Ferrarese, A., Campostrini, P., Furini, A., 2019. Phytoremediatory efficiency of *Chrysopogon zizanioides* in the treatment of landfill leachate: a case study. Environ. Sci. Pollut. Res. Int. 26, 10057–10069. https://doi.org/10.1007/S11356-019-04505-7

Fawzy, M.E., Abdelfattah, I., Abuarab, M.E., Mostafa, E., Aboelghait, K.M., El-Awady, M.H., 2018. Sustainable approach for pharmaceutical wastewater treatment and reuse: Case study. J. Environ. Sci. Technol. 11, 209–219. https://doi.org/10.3923/JEST.2018.209.219

Fibbi, D., Doumett, S., Colzi, I., Coppini, E., Pucci, S., Gonnelli, C., Lepri, L., Del Bubba, M., 2011. Total and hexavalent chromium removal in a subsurface horizontal flow (h-SSF) constructed wetland operating as post-treatment of textile wastewater for water reuse. Water Sci. Technol. 64, 826–831. https://doi.org/10.2166/WST.2011.548

Fitch, M.W., 2013. 3.14 Constructed Wetlands, in: Comprehensive Water Quality and Purification. Elsevier, pp. 268–295. https://doi.org/10.1016/B978-0-12-382182-9.00053-0

Folino, A., Zema, D.A., Calabrò, P.S., 2020. Environmental and economic sustainability of swine wastewater treatments using ammonia stripping and anaerobic digestion: A short review. Sustainability. 12(12), 4971. https://doi.org/10.3390/su12124971

Folkman, Y., Wachs, A.M., 1973. Removal of algae from stabilization pond effluents by lime treatment. Water Res. 7, 419–435. https://doi.org/10.1016/0043-1354(73)90024-9

Forouzesh, M., Fatehifar, E., Khoshbouy, R., Daryani, M., 2023. Experimental investigation of iron removal from wet phosphoric acid through chemical precipitation process. Chem. Eng. Res. Des. 189, 308–318. https://doi.org/10.1016/J.CHERD.2022.11.041

García-Ávila, F., Avilés-Añazco, A., Cabello-Torres, R., Guanuchi-Quito, A., Cadme-Galabay, M., Gutiérrez-Ortega, H., Alvarez-Ochoa, R., Zhindón-Arévalo, C., 2023. Application of ornamental plants in constructed wetlands for wastewater treatment: A scientometric analysis. Case Stud. Chem. Environ. Eng. 7, 100307. https://doi.org/10.1016/J.CSCEE.2023.100307

Georgiou, D., Aivazidis, A., Hatiras, J., Gimouhopoulos, K., 2003. Treatment of cotton textile wastewater using lime and ferrous sulfate. Water Res. 37, 2248–2250. https://doi.org/10.1016/S0043-1354(02)00481-5

Gholipour, A., Zahabi, H., Stefanakis, A.I., 2020. A novel pilot and full-scale constructed wetland study for glass industry wastewater treatment. Chemosphere 247. https://doi.org/10.1016/J.CHEMOSPHERE.2020.125966

Ghorab, R.E.A., Pugazhendi, A., Jamal, M.T., Jeyakumar, R.B., Godon, J.J., Mathew, D.K., 2022. Tannery wastewater treatment coupled with bioenergy production in upflow microbial fuel cell under saline condition. Environ. Res. 212, 113304. https://doi.org/10.1016/J.ENVRES.2022.113304

Ghoreishi, S.M., Haghighi, R., 2003. Chemical catalytic reaction and biological oxidation for treatment of non-biodegradable textile effluent. Chem. Eng. J. 95, 163–169. https://doi.org/10.1016/S1385-8947(03)00100-1

Goli, A., Shamiri, A., Khosroyar, S., Talaiekhozani, A., Sanaye, R., Azizi, K., 2019. A review on different aerobic and anaerobic treatment methods in dairy industry wastewater. J. Environ. Treat. Tech.

Gomes, A.C., Silva, L., Albuquerque, A., Simões, R., Stefanakis, A.I., 2018. Investigation of lab-scale horizontal subsurface flow constructed wetlands treating industrial cork boiling wastewater. Chemosphere 207, 430–439. https://doi.org/10.1016/J.CHEMOSPHERE.2018.05.123

Goren, A.Y., Yucel, A., Sofuoglu, S.C., Sofuoglu, A., 2021. Phytoremediation of olive mill wastewater with *Vetiveria zizanioides* (L.) Nash and *Cyperus alternifolius* L. Environ. Technol. Innov. 24. https://doi.org/10.1016/j.eti.2021.102071

Gorgoglione, A., Torretta, V., 2018. Sustainable management and successful application of constructed wetlands: A critical review. Sustain. 10. https://doi.org/10.3390/SU10113910

Guo, Y., Qi, P.S., Liu, Y.Z., 2017. A Review on Advanced Treatment of Pharmaceutical Wastewater, in: IOP Conference Series: Earth and Environmental Science. IOP Publishing, p. 012025. https://doi.org/10.1088/1755-1315/63/1/012025

Gutiérrez-Sarabia, A., Fernández-Villagómez, G., Martínez-Pereda, P., Rinderknecht-Seijas, N., Poggi-Varaldo, H.M., 2004. Slaughterhouse wastewater treatment in a full-scale system with constructed wetlands. Water Environ. Res. 76, 334–343. https://doi.org/10.2175/106143004X141924

Habte, L., Shiferaw, N., Thriveni, T., Mulatu, D., Lee, M. hye, Jung, S. ho, Ahn, J.W., 2020. Removal of Cd(II) and Pb(II) from wastewater via carbonation of aqueous $Ca(OH)_2$ derived from eggshell. Process Saf. Environ. Prot. 141, 278–287. https://doi.org/10.1016/J.PSEP.2020.05.036

Hamza, R.A., Zaghloul, M.S., Iorhemen, O.T., Sheng, Z., Tay, J.H., 2019. Optimization of organics to nutrients (COD:N:P) ratio for aerobic granular sludge treating high-strength organic wastewater. Sci. Total Environ. 650, 3168–3179. https://doi.org/10.1016/J.SCITOTENV.2018.10.026

Han, B., Butterly, C., Zhang, W., He, J. zheng, Chen, D., 2021. Adsorbent materials for ammonium and ammonia removal: A review. J. Clean. Prod. 283, 124611. https://doi.org/10.1016/J.JCLEPRO.2020.124611

Hande Gursoy-Haksevenler, B., Arslan-Alaton, I., 2020. Effects of treatment on the characterization of organic matter in wastewater: A review on size distribution and structural fractionation. Water Sci. Technol. 82, 799–828. https://doi.org/10.2166/wst.2020.403

Haq, I., Raj, A., 2020. Pulp and Paper Mill Wastewater: Ecotoxicological Effects and Bioremediation Approaches for Environmental Safety, in: Bioremediation of Industrial Waste for Environmental Safety. Springer, Singapore, pp. 333–356. https://doi.org/10.1007/978-981-13-3426-9_14

Hassan, I., Chowdhury, S.R., Prihartato, P.K., Razzak, S.A., 2021. Wastewater treatment using constructed wetland: Current trends and future potential. Processes 9, 1917. https://doi.org/10.3390/pr9111917

Hatt, J.W., Germain, E., Judd, S.J., 2013. Granular activated carbon for removal of organic matter and turbidity from secondary wastewater. Water Sci. Technol. 67, 846–853. https://doi.org/10.2166/wst.2012.644

Hemalatha, G., Uma, S.G., Muthulakshmi, S., 2020. Sewage water treatment using vetiver grass. Mater. Today Proc. 46, 3795–3798. https://doi.org/10.1016/J.MATPR.2021.02.031

Heredia, C., Guédron, S., Point, D., Perrot, V., Campillo, S., Verin, C., Espinoza, M.E., Fernandez, P., Duwig, C., Achá, D., 2022. Anthropogenic eutrophication of Lake Titicaca (Bolivia) revealed by carbon and nitrogen stable isotopes fingerprinting. Sci. Total Environ. 845, 157286. https://doi.org/10.1016/J.SCITOTENV.2022.157286

Hota, A., Gopal Krishna Patro, S., Obaid, A.J., Khatak, S., Kumar, R., 2023. Constructed wetland challenges for the treatment of industrial wastewater in smart cities: A sensitive solution. Sustain. Energy Technol. Assessments 55, 102967. https://doi.org/10.1016/J.SETA.2022.102967

Hsieh, C.T., Teng, H., 2000. Influence of mesopore volume and adsorbate size on adsorption capacities of activated carbons in aqueous solutions. Carbon N. Y. 38, 863–869. https://doi.org/10.1016/S0008-6223(99)00180-3

Huang, X.F., Ling, J., Xu, J.C., Feng, Y., Li, G.M., 2011. Advanced treatment of wastewater from an iron and steel enterprise by a constructed wetland/ultrafiltration/reverse osmosis process. Desalination 269, 41–49. https://doi.org/10.1016/J.DESAL.2010.10.040

Hunt, P.G., Matheny, T.A., Vanotti, M.B., Stone, K.C., Szogi, A.A., 2012. Denitrification Enzyme Activity in Swine Wastewater Effluent of a Nitrification/Denitrification Treatment System. Trans. ASABE 55, 159–165. https://doi.org/10.13031/2013.41265

Hussain, Z., Arslan, M., Malik, M.H., Mohsin, M., Iqbal, S., Afzal, M., 2018. Integrated perspectives on the use of bacterial endophytes in horizontal flow constructed wetlands for the treatment of liquid textile effluent: Phytoremediation advances in the field. J. Environ. Manage. 224, 387–395. https://doi.org/10.1016/J.JENVMAN.2018.07.057

Hussein, A., Scholz, M., 2018. Treatment of artificial wastewater containing two azo textile dyes by vertical-flow constructed wetlands. Environ. Sci. Pollut. Res. 25, 6870–6889. https://doi.org/10.1007/S11356-017-0992-0/TABLES/7

Ioannou, L.A., Puma, G.L., Fatta-Kassinos, D., 2015. Treatment of winery wastewater by physicochemical, biological and advanced processes: A review. J. Hazard. Mater. 286, 343–368. https://doi.org/10.1016/J.JHAZMAT.2014.12.043

Ishak, S., Malakahmad, A., 2013. Optimization of Fenton process for refinery wastewater biodegradability augmentation. Korean J. Chem. Eng. 2013 305 30, 1083–1090. https://doi.org/10.1007/S11814-013-0002-2

Jain, M., Yadav, M., Kohout, T., Lahtinen, M., Garg, V.K., Sillanpää, M., 2018. Development of iron oxide/activated carbon nanoparticle composite for the removal of Cr(VI), Cu(II) and Cd(II) ions from aqueous solution. Water Resour. Ind. 20, 54–74. https://doi.org/10.1016/j.wri.2018.10.001

Ji, G.D., Sun, T.H., Ni, J.R., 2007. Surface flow constructed wetland for heavy oil-produced water treatment. Bioresour. Technol. 98, 436–441. https://doi.org/10.1016/j.biortech.2006.01.017

Jorgensen, T.C., Weatherley, L.R., 2003. Ammonia removal from wastewater by ion exchange in the presence of organic contaminants. Water Res. 37, 1723–1728. https://doi.org/10.1016/S0043-1354(02)00571-7

Justin, M.Z., Vrhovšek, D., Stuhlbacher, A., Bulc, T.G., 2009. Treatment of wastewater in hybrid constructed wetland from the production of vinegar and packaging of detergents. Desalination 246, 100–109. https://doi.org/10.1016/J.DESAL.2008.03.045

Kadlec, R.H., Wallace, S., 2008. Treatment Wetlands, Treatment Wetlands. CRC Press. https://doi.org/10.1201/9781420012514

Kafle, A., Timilsina, A., Gautam, A., Adhikari, K., Bhattarai, A., Aryal, N., 2022. Phytoremediation: Mechanisms, plant selection and enhancement by natural and synthetic agents. Environ. Adv. 8, 100203. https://doi.org/10.1016/J.ENVADV.2022.100203

Kajjumba, G.W., Emik, S., Öngen, A., Kurtulus Özcan, H., Aydın, S., 2019. Modelling of Adsorption Kinetic Processes—Errors, Theory and Application, in: Advanced Sorption Process Applications. IntechOpen. https://doi.org/10.5772/intechopen.80495

Kalam, S., Abu-Khamsin, S.A., Kamal, M.S., Patil, S., 2021. Surfactant Adsorption Isotherms: A Review. ACS Omega 6, 32342. https://doi.org/10.1021/ACSOMEGA.1C04661

Kapellakis, I.E., Paranychianakis, N. V., Tsagarakis, K.P., Angelakis, A.N., 2012. Treatment of olive mill wastewater with constructed wetlands. Water 4, 260–271. https://doi.org/10.3390/W4010260

Karungamye, P., 2021. Wastewater pretreatment methods for constructed wetland: Review. J. Mater. Environ. Sci. 12.

Keerthana, K., Thivyatharsan, R., 2018. Constructed wetland for slaughterhouse wastewater treatment. AGRIEAST J. Agric. Sci. 12, 7. https://doi.org/10.4038/agrieast.v12i1.47

Keerthana, K, Thivyatharsan, R., 2018. Evaluation of the efficiency of constructed wetland and activated charcoal for the treatment of slaughterhouse wastewater. Earth, Energy Environ. 6, 12.

Khajeh, M., Laurent, S., Dastafkan, K., 2013. Nanoadsorbents: Classification, preparation, and applications (with emphasis on aqueous media). Chem. Rev. 113, 7728–7768. https://doi.org/10.1021/CR400086V/ASSET/IMAGES/MEDIUM/CR-2013-00086V_0016.GIF

Khdair, A., Abu-Rumman, G., 2020. Sustainable environmental management and valorization options for olive mill byproducts in the Middle East and North Africa (MENA) region. Processes. https://doi.org/10.3390/PR8060671

Kinidi, L., Tan, I.A.W., Abdul Wahab, N.B., Tamrin, K.F. Bin, Hipolito, C.N., Salleh, S.F., 2018. Recent Development in Ammonia Stripping Process for Industrial Wastewater Treatment. Int. J. Chem. Eng. https://doi.org/10.1155/2018/3181087

Klomjek, P., 2016. Swine wastewater treatment using vertical subsurface flow constructed wetland planted with Napier grass. Sustain. Environ. Res. 26, 217–223. https://doi.org/10.1016/J.SERJ.2016.03.001

Kobya, M., Senturk, E., Bayramoglu, M., 2006. Treatment of poultry slaughterhouse wastewaters by electrocoagulation. J. Hazard. Mater. 133, 172–176. https://doi.org/10.1016/j.jhazmat.2005.10.007

Kokkinos, P., Venieri, D., Mantzavinos, D., 2021. Advanced Oxidation Processes for Water and Wastewater Viral Disinfection. A Systematic Review. Food Environ. Virol. 13, 283. https://doi.org/10.1007/S12560-021-09481-1

Kolev Slavov, A., 2017. Dairy Wastewaters – General Characteristics and Treatment Possibilities – A Review. Food Technol. Biotechnol. 55. https://doi.org/10.17113/FTB.55.01.17.4520

Krishna Mohan, T. V., Nancharaiah, Y. V., Venugopalan, V.P., Satya Sai, P.M., 2016. Effect of C/N ratio on denitrification of high-strength nitrate wastewater in anoxic granular sludge sequencing batch reactors. Ecol. Eng. 91, 441–448. https://doi.org/10.1016/J.ECOLENG.2016.02.033

Kriti, Basant, N., Singh, J., Kumari, B., Sinam, G., Gautam, A., Singh, G., Swapnil, Mishra, K., Mallick, S., 2021. Nickel and cadmium phytoextraction efficiencies of vetiver and lemongrass grown on Ni–Cd battery waste contaminated soil: A comparative study of linear and nonlinear models. J. Environ. Manage. 295, 113144. https://doi.org/10.1016/J.JENVMAN.2021.113144

Kumar, S., Choudhary, A.K., 2018. Constructed Wetland Technology for Pulp and Paper Mill Wastewater Treatment, in: Constructed Wetlands for Industrial Wastewater Treatment. John Wiley & Sons, Ltd, pp. 309–325. https://doi.org/10.1002/9781119268376.ch15

Kumari, P., Alam, M., Siddiqi, W.A., 2019. Usage of nanoparticles as adsorbents for waste water treatment: An emerging trend. Sustain. Mater. Technol. https://doi.org/10.1016/j.susmat.2019.e00128

Kuokkanen, V., Kuokkanen, M., Hynynen, I., Kuokkanen, T., 2021. Electrocoagulation treatment of metallurgical industry wastewater – A laboratory scale batch and pilot scale continuous study. Hydrometallurgy 202, 105596. https://doi.org/10.1016/J.HYDROMET.2021.105596

Kuptajit, P., Sano, N., Nakagawa, K., Suzuki, T., 2021. A study on pore formation of high surface area activated carbon prepared by microwave-induced plasma with KOH (MiWP-KOH) activation: Effect of temperature-elevation rate. Chem. Eng. Process. - Process Intensif. 167, 108511. https://doi.org/10.1016/j.cep.2021.108511

Kurama, H., Poetzschke, J., Haseneder, R., 2002. The application of membrane filtration for the removal of ammonium ions from potable water. Water Res. 36, 2905–2909. https://doi.org/10.1016/S0043-1354(01)00531-0

Ky, N.M., Hung, N.T.Q., Manh, N.C., Lap, B.Q., Dang, H.T.T., Ozaki, A., 2020. Assessment of nutrients removal by constructed wetlands using reed grass (*Phragmites australis* L.) and vetiver grass (*Vetiveria zizanioides* L.). J. Fac. Agric. Kyushu Univ. 65, 149–156. https://doi.org/10.5109/2558907

Laber, J., Perfler, R., Haberl, R., 1997. Two strategies for advanced nitrogen elimination in vertical flow constructed wetlands. Water Sci. Technol. 35, 71–77. https://doi.org/10.1016/S0273-1223(97)00054-1

Lajayer, B.A., Nobaharan, K., Moghiseh, E., Biglari Quchan Atigh, Z., Delangiz, N., Mosaferi, M., Aftab, T., Astatkie, T., 2022. Removal of pharmaceuticals and personal care products from water and wastewater through biological processes: an overview, in: Hazardous and Trace Materials in Soil and Plants: Sources, Effects, and Management. Academic Press, pp. 87–96. https://doi.org/10.1016/B978-0-323-91632-5.00005-7

Lakdawala MM, Lakdawala JM, 2013. Comparative Study of Effect of PAC and GAC on Removal of COD Contributing Component of Sugar Industry waste water. Res. J. Recent Sci. 2, 90–97.

Largitte, L., Pasquier, R., 2016. A review of the kinetics adsorption models and their application to the adsorption of lead by an activated carbon. Chem. Eng. Res. Des. 109, 495–504. https://doi.org/10.1016/J.CHERD.2016.02.006

Lee, S.H., Nishijima, W., Lee, C.H., Okada, M., 2003. Calcium accumulation on activated carbon deteriorates synthetic organic chemicals adsorption. Water Res. 37, 4631–4636. https://doi.org/10.1016/S0043-1354(03)00425-1

Li, Y., Nan, X., Li, D., Wang, L., Xu, R., Li, Q., 2021. Advances in the treatment of phosphorus-containing wastewater, in: IOP Conference Series: Earth and Environmental Science. IOP Publishing, p. 012163. https://doi.org/10.1088/1755-1315/647/1/012163

Li, Z., Ren, X., Zuo, J., Liu, Y., Duan, E., Yang, J., Chen, P., Wang, Y., 2012. Struvite precipitation for ammonia nitrogen removal in 7- aminocephalosporanic acid wastewater. Molecules 17, 2126–2139. https://doi.org/10.3390/molecules17022126

Liao, X., Luo, S., Wu, Y., Wang, Z., 2003. Studies on the abilities of *Vetiveria zizanioides* and *Cyperus alternifolius* for pig farm wastewater treatment. Int. Conf. Vetiver Exhib. 3, 174–181.

Lin, L., Yuan, S., Lin, L., Yuan, S., Chen, J., Xu, Z., Lu, X., 2009. Removal of ammonia nitrogen in wastewater by microwave radiation. J. Hazard. Mater. 161, 1063–1068. https://doi.org/10.1016/j.jhazmat.2008.04.053

Lippi, M., Gaudie Ley, M.B.R., Mendez, G.P., Felix Cardoso Junior, R.A., 2018. State of Art of Landfill Leachate Treatment: Literature Review and Critical Evaluation. Ciência e Nat. 40, 78. https://doi.org/10.5902/2179460X35239

Liu, D.H.F., Lipták, B.G., 2000. Wastewater treatment. Boca Raton, London.

Liu, F., Wang, S., Zhang, X., Qian, F., Wang, Y., Yin, Y., 2021. Nitrate Removal from Actual Wastewater by Coupling Sulfur-Based Autotrophic and Heterotrophic Denitrification under Different Influent Concentrations. Water 13, 2913. https://doi.org/10.3390/W13202913

Lompe, K.M., Menard, D., Barbeau, B., 2017. The influence of iron oxide nanoparticles upon the adsorption of organic matter on magnetic powdered activated carbon. Water Res. 123, 30–39. https://doi.org/10.1016/J.WATRES.2017.06.045

Luz, S., Rivas, J., Afonso, A., Carvalho, F., 2021. Immediate one-step lime precipitation process for the valorization of winery wastewater to agricultural purposes. Environ. Sci. Pollut. Res. 1–10. https://doi.org/10.1007/s11356-020-11933-3

Ma, C., Ran, Z., Yang, Z., Wang, L., Wen, C., Zhao, B., Zhang, H., 2019. Efficient pretreatment of industrial estate wastewater for biodegradability enhancement using a micro-electrolysis-circulatory system. J. Environ. Manage. 250, 109492. https://doi.org/10.1016/J.JENVMAN.2019.109492

Mahedi, M., Cetin, B., Dayioglu, A.Y., 2019. Leaching behavior of aluminum, copper, iron and zinc from cement activated fly ash and slag stabilized soils. Waste Manag. 95, 334–355. https://doi.org/10.1016/j.wasman.2019.06.018

Mahmood, T., Momin, S., Ali, R., Naeem, A., Khan, A., 2022. Technologies for Removal of Emerging Contaminants from Wastewater, in: Wastewater Treatment. IntechOpen. https://doi.org/10.5772/intechopen.104466

Mahtab, A., Tariq, M., Shafiq, T., Nasir, A., 2009. Coagulation/adsorption combined treatment of slaughterhouse wastewater. Desalin. Water Treat. 12, 270–275. https://doi.org/10.5004/dwt.2009.952

Makopondo, R.O.B., Rotich, L.K., Kamau, C.G., 2020. Potential Use and Challenges of Constructed Wetlands for Wastewater Treatment and Conservation in Game Lodges and Resorts in Kenya. Sci. World J. 2020. https://doi.org/10.1155/2020/9184192

Mangkoedihardjo, S., 2006. Biodegradability improvement of industrial wastewater using hyacinth. J. Appl. Sci. 6, 1409–1414. https://doi.org/10.3923/JAS.2006.1409.1414

Manh, L.H., Dung, N.N.X., Van Am, L., Le Minh, B.T., 2014. Treatment of wastewater from slaughterhouse by biodigester and *Vetiveria zizanioides* L. L. Livest. Res. Rural Dev. 26.

Marczewski, A.W., Seczkowska, M., Deryło-Marczewska, A., Blachnio, M., 2016. Adsorption equilibrium and kinetics of selected phenoxyacid pesticides on activated carbon: effect of temperature. Adsorption 22, 777–790. https://doi.org/10.1007/S10450-016-9774-0/FIGURES/11

Marecik, R., Biegańska-Marecik, R., Cyplik, P., Ławniczak, Ł., Chrzanowski, U., 2013. Phytoremediation of industrial wastewater containing nitrates, nitroglycerin, and nitroglycol. Polish J. Environ. Stud. 22, 773–780.

Mariliz, G., Benvenuti, J., Fontoura, J., Ortiz-Monsalve, S., 2015. Characterization of Raw Wastewater from Tanneries. Journal- Soc. Leather Technol. Chem. 99, 280–287.

Martínez-Cruz, A., Fernandes, A., Ciríaco, L., Pacheco, M.J., Carvalho, F., Afonso, A., Madeira, L., Luz, S., Lopes, A., 2020. Electrochemical Oxidation of Effluents from Food Processing Industries: A Short Review and a Case-Study. Water 12, 3546. https://doi.org/10.3390/w12123546

Martínez-Cruz, A., Fernandes, A., Ramos, F., Soares, S., Correia, P., Baía, A., Lopes, A., Carvalho, F., 2021. An Eco-Innovative Solution for Reuse of Leachate Chemical Precipitation Sludge: Application to Sanitary Landfill Coverage. Ecol. Eng. Environ. Technol. 22, 52–58. https://doi.org/10.12912/27197050/133329

Martinez, S.L., Torretta, V., Minguela, J.V., Siñeriz, F., Raboni, M., Copelli, S., Rada, E.C., Ragazzi, M., 2014. Treatment of slaughterhouse wastewaters using anaerobic filters. Environ. Technol. 35, 322–332. https://doi.org/10.1080/09593330.2013.827729

Masoud, A.M.N., Alfarra, A., Sorlini, S., 2022. Constructed Wetlands as a Solution for Sustainable Sanitation: A Comprehensive Review on Integrating Climate Change Resilience and Circular Economy. Water, 14(20), 3232. https://doi.org/10.3390/w14203232

Mechnou, I., Meskini, S., El Ayar, D., Lebrun, L., Hlaibi, M., 2022. Olive mill wastewater from a liquid biological waste to a carbon/oxocalcium composite for selective and efficient removal of methylene blue and paracetamol from aqueous solution. Bioresour. Technol. 365, 128162. https://doi.org/10.1016/J.BIORTECH.2022.128162

Melo, R., Cabo Verde, S., Branco, J., Botelho, M.L., 2008. Gamma radiation induced effects on slaughterhouse wastewater treatment. Radiat. Phys. Chem. 77, 98–100. https://doi.org/10.1016/j.radphyschem.2007.03.006

Metcalf, E., Eddy, H., 2003. Wastewater Engineering, Treatment, Disposal and Reuse. 4th edition, Mc Graw-Hill, New York.

Mihelcic, James R., Zimmerman, Julie Beth, Zhang, Q., 2002. Water Treatment and Design, in: Mihelcic, J.R., Zimmerman, J.B. (Eds.), Environmental Engineering : Fundamentals, Sustainability, Design. Wiley, pp. 397–455.

Milani, M., Marzo, A., Toscano, A., Consoli, S., Cirelli, G.L., Ventura, D., Barbagallo, S., 2019. Evapotranspiration from horizontal subsurface flow constructed wetlands planted with different perennial plant species. Water 11(10), 2159. https://doi.org/10.3390/W11102159

Millamena, O.M., 1992. Ozone treatment of slaughterhouse and laboratory wastewaters. Aquac. Eng. 11, 23–31. https://doi.org/10.1016/0144-8609(92)90018-S

Mirbagheri, S.A., Hosseini, S.N., 2005. Pilot plant investigation on petrochemical wastewater treatmentfor the removal of copper and chromium with the objective of reuse. Desalination 171, 85–93. https://doi.org/10.1016/J.DESAL.2004.03.022

Mlih, R., Bydalek, F., Klumpp, E., Yaghi, N., Bol, R., Wenk, J., 2020. Light-expanded clay aggregate (LECA) as a substrate in constructed wetlands – A review. Ecol. Eng. 148, 105783. https://doi.org/10.1016/j.ecoleng.2020.105783

Mohameda, A.M., Fouad, A.H., ElHefny, M.R., 2022. Reviewing Rotating Biological Contactor's Different Aspects for Wastewater Treatment with Experiment. Eng. Res. J. - Fac. Eng. 51, 180–187. https://doi.org/10.21608/erjsh.2022.239936

Mohammadi, M., Man, H.C., Hassan, M.A., Yee, P.L., 2010. Treatment of wastewater from rubber industry in Malaysia. African J. Biotechnol. 9(38), 6233-6243. https://doi.org/10.4314/AJB.V9I38

Mokhatab, S., Poe, W.A., Mak, J.Y., 2019. Natural Gas Dehydration and Mercaptans Removal, in: Handbook of Natural Gas Transmission and Processing. Elsevier, pp. 307–348. https://doi.org/10.1016/b978-0-12-815817-3.00009-5

Mollica, N.R., Guo, W., Cohen, A.L., Huang, K.F., Foster, G.L., Donald, H.K., Solow, A.R., 2018. Ocean acidification affects coral growth by reducing skeletal density. Proc. Natl. Acad. Sci. U. S. A. 115, 1754–1759. https://doi.org/10.1073/PNAS.1712806115/SUPPL_FILE/PNAS.201712806SI.PDF

Mosse, K.P.M., Patti, A.F., Christen, E.W., Cavagnaro, T.R., 2011. Review: Winery wastewater quality and treatment options in Australia. Aust. J. Grape Wine Res. 17, 111–122. https://doi.org/10.1111/J.1755-0238.2011.00132.X

Mudhiriza, T., Mapanda, F., Mvumi, B.M., Wuta, M., 2015. Removal of nutrient and heavy metal loads from sewage effluent using vetiver grass, *Chrysopogon zizanioides* (L.) Roberty. Water SA 41, 457–463. https://doi.org/10.4314/WSA.V41I4.04

Muñoz-Alegría, J.A., Muñoz-España, E., Flórez-Marulanda, J.F., 2021. Dissolved Air Flotation: A Review from the Perspective of System Parameters and Uses in Wastewater Treatment. TecnoLógicas 24 (52), e2111. https://doi.org/10.22430/22565337.2111

Mustapha, H.I., van Bruggen, J.J.A., Lens, P.N.L., 2018. Optimization of Petroleum Refinery Wastewater Treatment by Vertical Flow Constructed Wetlands Under Tropical Conditions: Plant Species Selection and Polishing by a Horizontal Flow Constructed Wetland. Water. Air. Soil Pollut. 229, 1–17. https://doi.org/10.1007/S11270-018-3776-3/TABLES/5

Nageeb, M., 2013. Adsorption Technique for the Removal of Organic Pollutants from Water and Wastewater, in: Organic Pollutants - Monitoring, Risk and Treatment. IntechOpen. https://doi.org/10.5772/54048

Navada, S., Knutsen, M.F., Bakke, I., Vadstein, O., 2020. Nitrifying biofilms deprived of organic carbon show higher functional resilience to increases in carbon supply. Sci. Reports 10, 1–11. https://doi.org/10.1038/s41598-020-64027-y

Newcombe, G., 2006. Chapter 8: Removal of natural organic material and algal metabolites using activated carbon. Interface Sci. Technol. 10, 133–153. https://doi.org/10.1016/S1573-4285(06)80077-3

Ng, M., Dalhatou, S., Wilson, J., Kamdem, B.P., Temitope, M.B., Paumo, H.K., Djelal, H., Assadi, A.A., Nguyen-tri, P., Kane, A., 2022. Characterization of Slaughterhouse Wastewater and Development of Treatment Techniques: A Review. Processes. https://doi.org/10.3390/pr10071300

Nguyen, M.K., Hung, N.T.Q., Nguyen, C.M., Lin, C., Nguyen, T.A., Nguyen, H.-L., 2023. Application of vetiver grass (*Vetiveria Zizanioides* L.) for organic matter removal from contaminated surface water. Bioresour. Technol. Reports 101431. https://doi.org/10.1016/J.BITEB.2023.101431

Niaounakis, M., Halvadakis, C.P., 2006. Olive Processing Waste Management: Literature Review and Patent Survey 2nd Edition. Elsevier.

Nizam, N.U.M., Hanafiah, M.M., Mahmoudi, E., Halim, A.A., Mohammad, A.W., 2021. The removal of anionic and cationic dyes from an aqueous solution using biomass-based activated carbon. Sci. Reports 11, 1–17. https://doi.org/10.1038/s41598-021-88084-z

Njau, K.N., Mlay, H., 2003. Wastewater Treatment and other Research Initiatives with Vetiver Grass, System.

Noworyta, A., Koziol, T., Trusek-Holownia, A., 2003. A system for cleaning condensates containing ammonium nitrate by the reverse osmosis method. Desalination 156, 397–402. https://doi.org/10.1016/S0011-9164(03)00373-4

Odong, R., Kansiime, F., Omara, J., Kyambadde, J., 2013. The potential of four tropical wetland plants for the treatment of abattoir effluent. Int. J. Environ. Technol. Manag. 16, 203–222. https://doi.org/10.1504/IJETM.2013.053640

Olguín, E.J., Sánchez-Galván, G., González-Portela, R.E., López-Vela, M., 2008. Constructed wetland mesocosms for the treatment of diluted sugarcane molasses stillage from ethanol production using *Pontederia sagittata*. Water Res. 42, 3659–3666. https://doi.org/10.1016/J.WATRES.2008.05.015

Omondi, O.D., Navalia, C.A., 2021. Constructed Wetlands in Wastewater Treatment and Challenges of Emerging Resistant Genes Filtration and Reloading, in: Inland Waters - Dynamics and Ecology. IntechOpen. https://doi.org/10.5772/intechopen.93293

Pandey, N., Keshavkant, S., 2021. Mechanisms of heavy metal removal using microorganisms as biosorbents, in: New Trends in Removal of Heavy Metals from Industrial Wastewater. Elsevier, pp. 1–21. https://doi.org/10.1016/B978-0-12-822965-1.00001-5

Panja, S., Sarkar, D., Datta, R., 2018. Vetiver grass (*Chrysopogon zizanioides*) is capable of removing insensitive high explosives from munition industry wastewater. Chemosphere 209, 920–927. https://doi.org/10.1016/J.CHEMOSPHERE.2018.06.155

Paramo-Vargas, J., Camargo, A.M.E., Gutierrez-Granados, S., Godinez, L.A., Peralta-Hernandez, J.M., 2015. Applying electro-Fenton process as an alternative to a slaughterhouse effluent treatment. J. Electroanal. Chem. 754, 80–86. https://doi.org/10.1016/j.jelechem.2015.07.002

Park, H.S., Koduru, J.R., Choo, K.H., Lee, B., 2015. Activated carbons impregnated with iron oxide nanoparticles for enhanced removal of bisphenol A and natural organic matter. J. Hazard. Mater. 286, 315–324. https://doi.org/10.1016/J.JHAZMAT.2014.11.012

Patel, H., 2018. Charcoal as an adsorbent for textile wastewater treatment. Sep. Sci. Technol. 53, 2797–2812. https://doi.org/10.1080/01496395.2018.1473880

Paulino, A.T., Santos, L.B., Nozaki, J., 2008. Removal of Pb^{2+}, Cu^{2+}, and Fe^{3+} from battery manufacture wastewater by chitosan produced from silkworm chrysalides as a low-cost adsorbent. React. Funct. Polym. 68, 634–642. https://doi.org/10.1016/J.REACTFUNCTPOLYM.2007.10.028

Phanwilai, S., Noophan, P., Li, C.W., Choo, K.H., 2020. Effect of COD:N ratio on biological nitrogen removal using full-scale step-feed in municipal wastewater treatment plants. Sustain. Environ. Res. 30, 1–9. https://doi.org/10.1186/s42834-020-00064-6

Philipp, M., Jabri, K.M., Wellmann, J., Akrout, H., Bousselmi, L., Geißen, S.U., 2021. Slaughterhouse wastewater treatment: A review on recycling and reuse possibilities. Water, 13(22), 3175. https://doi.org/10.3390/w13223175

Phothong, K., Tangsathitkulchai, C., Lawtae, P., 2021. The analysis of pore development and formation of surface functional groups in bamboo-based activated carbon during CO_2 activation. Molecules 26, 5641. https://doi.org/10.3390/molecules26185641

Pongthornpruek, S., 2017. Treatment of Piggery Wastewater by Three Grass Species Growing in a Constructed Wetland. Appl. Environ. Res. 39, 75–83. https://doi.org/10.35762/AER.2017.39.1.8

Portuguese Government, 2019. Decree-Law No. 119/2019 establishing the legal regime for producing water to be reused, obtained from wastewater treatment. Diário da República, I Série, No. 159, 21 August 2019.

Prasad, H., Lohchab, R.K., Singh, B., Nain, A., Kumari, M., 2019. Lime treatment of wastewater in a plywood industry to achieve the zero liquid discharge. J. Clean. Prod. 240, 118176. https://doi.org/10.1016/J.JCLEPRO.2019.118176

Prazeres, A.R., Afonso, A., Guerreiro, R., Jerónimo, E., 2021. Contamination reduction of real olive oil mill wastewater using innovative acid and basic chemical precipitation processes. Int. J. Environ. Sci. Technol. 18, 799–808. https://doi.org/10.1007/S13762-020-02924-5/FIGURES/5

Prazeres, A.R., Fernandes, F., Madeira, L., Luz, S., Albuquerque, A., Simões, R., Beltrán, F., Jerónimo, E., Rivas, J., 2019a. Treatment of slaughterhouse wastewater by acid precipitation (H_2SO_4, HCl and HNO_3) and oxidation ($Ca(ClO)_2$, H_2O_2 and CaO_2). J. Environ. Manage. 250, 109558. https://doi.org/10.1016/j.jenvman.2019.109558

Prazeres, A.R., Lelis, J., Alves-Ferreira, J., Carvalho, F., 2019b. Treatment of vinasse from sugarcane ethanol industry: H_2SO_4, NaOH and $Ca(OH)_2$ precipitations, $FeCl_3$ coagulation-flocculation and atmospheric CO_2 carbonation. J. Environ. Chem. Eng. 7, 103203. https://doi.org/10.1016/j.jece.2019.103203

Prazeres, A.R., Luz, S., Fernandes, F., Jerónimo, E., 2020. Cheese wastewater treatment by acid and basic precipitation: Application of H_2SO_4, HNO_3, HCl, $Ca(OH)_2$ and NaOH. J. Environ. Chem. Eng. 8, 103556. https://doi.org/10.1016/J.JECE.2019.103556

Prazeres, A.R., Rivas, J., Paulo, Ú., Ruas, F., Carvalho, F., 2016. Sustainable treatment of different high-strength cheese whey wastewaters: an innovative approach for atmospheric CO_2 mitigation and fertilizer production. Environ. Sci. Pollut. Res. 23, 13062–13075. https://doi.org/10.1007/s11356-016-6429-3

Pundlik, R.C., Dash, R.R., Bhunia, P., 2022. Constructed wetland system for the treatment of wastewater in a circular bioeconomy, in: Biomass, Biofuels, Biochemicals: Circular Bioeconomy: Technologies for Waste Remediation. Elsevier, pp. 365–386. https://doi.org/10.1016/B978-0-323-88511-9.00010-0

Qi, D., 2018. Treatment of Wastewater, Off-Gas, and Waste Solid, in: Hydrometallurgy of Rare Earths. Elsevier, pp. 743–777. https://doi.org/10.1016/b978-0-12-813920-2.00008-8

Radhi, A.A., 2020. Comparison of granulated and powdered activated carbon in the removal of organic matter from river water. Int. Res. J. Adv. Eng. Sci. 5, 191–197.

Raharjo, S., Fitriyah Irmawati, E.S., Manaf, M., 2018. Constructed Wetland with Flow Water Surface Type for Elimination of Aquaculture Wastewater from Catfish (*Clarias gariepinus*, Var). IOP Conf. Ser. Earth Environ. Sci. 187. https://doi.org/10.1088/1755-1315/187/1/012061

Rahman, M.A., Lee, S.H., Ji, H.C., Kabir, A.H., Jones, C.S., Lee, K.W., 2018. Importance of mineral nutrition for mitigating aluminum toxicity in plants on acidic soils: Current status and opportunities. Int. J. Mol. Sci. 19(10), 3073. https://doi.org/10.3390/ijms19103073

Rahman, M.E., Halmi, M.I.E. Bin, Samad, M.Y.B.A., Uddin, M.K., Mahmud, K., Shukor, M.Y.A., Abdullah, S.R.S., Shamsuzzaman, S.M., 2020. Design, Operation and Optimization of Constructed Wetland for Removal of Pollutant. Int. J. Environ. Res. Public Heal. 17, 8339. https://doi.org/10.3390/IJERPH17228339

Raj, S., Singh, H., Bhattacharya, J., 2023. Treatment of textile industry wastewater based on coagulation-flocculation aided sedimentation followed by adsorption: Process studies in an industrial ecology concept. Sci. Total Environ. 857, 159464. https://doi.org/10.1016/J.SCITOTENV.2022.159464

Ramalho, M., Jovanović, T., Afonso, A., Baía, A., Lopes, A., Fernandes, A., Almeida, A., Carvalho, F., 2022. Landfill leachate treatment by immediate one-step lime precipitation, carbonation, and phytoremediation fine-tuning. Environ. Sci. Pollut. Res. 1, 1–10. https://doi.org/10.1007/S11356-022-18729-7/TABLES/3

Rao, A.G., Reddy, T.S.K., Prakash, S.S., Vanajakshi, J., Joseph, J., Sarma, P.N., 2007. pH regulation of alkaline wastewater with carbon dioxide: A case study of treatment of brewery wastewater in UASB reactor coupled with absorber. Bioresour. Technol. 98, 2131–2136. https://doi.org/10.1016/J.BIORTECH.2006.08.011

Rashed, M.N., 2013. Adsorption Technique for the Removal of Organic Pollutants from Water and Wastewater, in: Organic Pollutants - Monitoring, Risk and Treatment. IntechOpen. https://doi.org/10.5772/54048

Renou, S., Poulain, S., Givaudan, J.G., Sahut, C., Moulin, P., 2009. Lime treatment of stabilized leachates. Water Sci. Technol. 59, 673–685. https://doi.org/10.2166/WST.2009.014

Renu, Agarwal, M., Singh, K., 2017. Heavy metal removal from wastewater using various adsorbents: a review. J. Water Reuse Desalin. 7, 387–419. https://doi.org/10.2166/WRD.2016.104

Reyes-Serrano, A., López-Alejo, J.E., Hernández-Cortázar, M.A., Elizalde, I., 2020. Removing contaminants from tannery wastewater by chemical precipitation using CaO and $Ca(OH)_2$. Chinese J. Chem. Eng. 28, 1107–1111. https://doi.org/10.1016/J.CJCHE.2019.12.023

Ribas, M.C., Adebayo, M.A., Prola, L.D.T., Lima, E.C., Cataluña, R., Feris, L.A., Puchana-Rosero, M.J., Machado, F.M., Pavan, F.A., Calvete, T., 2014. Comparison of a homemade cocoa shell activated carbon with commercial activated carbon for the removal of reactive violet 5 dye from aqueous solutions. Chem. Eng. J. 248, 315–326. https://doi.org/10.1016/J.CEJ.2014.03.054

Rodríguez, J., Castrillón, L., Marañón, E., Sastre, H., Fernández, E., 2004. Removal of non-biodegradable organic matter from landfill leachates by adsorption. Water Res. 38, 3297–3303. https://doi.org/10.1016/J.WATRES.2004.04.032

Roongtanakiat, N., Tangruangkiat, S., Meesat, R., 2007. Utilization of vetiver grass (*Vetiveria zizanioides*) for removal of heavy metals from industrial wastewaters. ScienceAsia 33, 397–403. https://doi.org/10.2306/SCIENCEASIA1513-1874.2007.33.397

Sabumon, P., 2016. Perspectives on Biological Treatment of Tannery Effluent. Adv. Recycl. Waste Manag. 01, 1. https://doi.org/10.4172/2475-7675.1000104

Sadegh, H., Ali, G.A.M., 2018. Potential Applications of Nanomaterials in Wastewater Treatment, in: Advanced Treatment Techniques for Industrial Wastewater. IGI Global, pp. 51–61. https://doi.org/10.4018/978-1-5225-5754-8.ch004

Saeed, T., Afrin, R., Muyeed, A. Al, Sun, G., 2012. Treatment of tannery wastewater in a pilot-scale hybrid constructed wetland system in Bangladesh. Chemosphere 88, 1065–1073. https://doi.org/10.1016/J.CHEMOSPHERE.2012.04.055

Saeed, T., Khan, T., 2019. Constructed wetlands for industrial wastewater treatment: Alternative media, input biodegradation ratio and unstable loading. J. Environ. Chem. Eng. 7, 103042. https://doi.org/10.1016/J.JECE.2019.103042

Saeed, T., Muntaha, S., Rashid, M., Sun, G., Hasnat, A., 2018. Industrial wastewater treatment in constructed wetlands packed with construction materials and agricultural by-products. J. Clean. Prod. 189, 442–453. https://doi.org/10.1016/J.JCLEPRO.2018.04.115

Saeed, T., Sun, G., 2012. A review on nitrogen and organics removal mechanisms in subsurface flow constructed wetlands: Dependency on environmental parameters, operating conditions and supporting media. J. Environ. Manage. 112, 429–448. https://doi.org/10.1016/J.JENVMAN.2012.08.011

Safarik, I., Horska, K., Pospiskova, K., Safarikova, M., 2012. Magnetically Responsive Activated Carbons for Bio - and Environmental Applications. Int. Rev. Chem. Eng. 4, 346–352.

Saha, N.K., Balakrishnan, M., Batra, V.S., 2005. Improving industrial water use: case study for an Indian distillery. Resour. Conserv. Recycl. 43, 163–174. https://doi.org/10.1016/J.RESCONREC.2004.04.016

Saha, S., Gupta, R., Sethi, S., Biswas, R., 2022. Enhancing the efficiency of nitrogen removing bacterial population to a wide range of C:N ratio (1.5:1 to 14:1) for simultaneous C & N removal. Front. Environ. Sci. Eng. 16, 1–15. https://doi.org/10.1007/S11783-022-1522-Y/METRICS

Sanmuga, Priya, E., Senthamil, Selvan, P., 2017. Water hyacinth (*Eichhornia crassipes*) – An efficient and economic adsorbent for textile effluent treatment – A review. Arab. J. Chem. 10, S3548–S3558. https://doi.org/10.1016/J.ARABJC.2014.03.002

Saravanathamizhan, R., Perarasu, V.T., 2021. Improvement of Biodegradability Index of Industrial Wastewater Using Different Pretreatment Techniques, in: Wastewater Treatment: Cutting-Edge Molecular Tools, Techniques and Applied Aspects. Elsevier, pp. 103–136. https://doi.org/10.1016/B978-0-12-821881-5.00006-4

Satyanarayan, S., Ramakant, Vanerkar, A.P., 2005. Conventional approach for abattoir wastewater treatment. Environ. Technol. 26, 441–448. https://doi.org/10.1080/09593332608618554

Schulz, C., Gelbrecht, J., Rennert, B., 2003. Treatment of rainbow trout farm effluents in constructed wetland with emergent plants and subsurface horizontal water flow. Aquaculture 217, 207–221. https://doi.org/10.1016/S0044-8486(02)00204-1

Semerjian, L., Ayoub, G.M., 2003. High-pH–magnesium coagulation–flocculation in wastewater treatment. Adv. Environ. Res. 7, 389–403. https://doi.org/10.1016/S1093-0191(02)00009-6

Seroja, R., Effendi, H., Hariyadi, S., 2018. Tofu wastewater treatment using vetiver grass (*Vetiveria zizanioides*) and zeliac. Appl. Water Sci. 8, 1–6. https://doi.org/10.1007/S13201-018-0640-Y/TABLES/3

Serra, A.P., Marchetti, M.E., Dupas, E., Carducci, C.E., Silva, E.F. da, Pinheiro, E.R., 2018. Phosphorus in Forage Production, in: New Perspectives in Forage Crops. InTech. https://doi.org/10.5772/intechopen.70202

Serrano, L., de la Varga, D., Ruiz, I., Soto, M., 2011. Winery wastewater treatment in a hybrid constructed wetland. Ecol. Eng. 37, 744–753. https://doi.org/10.1016/J.ECOLENG.2010.06.038

Shelly, Y., Kuk, M., Menashe, O., Zeira, G., Azerrad, S., Kurzbaum, E., 2021. Nitrate removal from a nitrate-rich reverse osmosis concentrate: Superior efficiency using the bioaugmentation of an Acinetobacter biofilm. J. Water Process Eng. 44, 102425. https://doi.org/10.1016/J.JWPE.2021.102425

Shen, J., He, R., Han, W., Sun, X., Li, J., Wang, L., 2009. Biological denitrification of high-nitrate wastewater in a modified anoxic/oxic-membrane bioreactor (A/O-MBR). J. Hazard. Mater. 172, 595–600. https://doi.org/10.1016/J.JHAZMAT.2009.07.045

Shen, Y.F., Tang, J., Nie, Z.H., Wang, Y.D., Ren, Y., Zuo, L., 2009. Preparation and application of magnetic Fe_3O_4 nanoparticles for wastewater purification. Sep. Purif. Technol. 68, 312–319. https://doi.org/10.1016/j.seppur.2009.05.020

Shende, A.D., Pophali, G.R., 2021. Anaerobic treatment of slaughterhouse wastewater: a review. Environ. Sci. Pollut. Res. 28, 35–55. https://doi.org/10.1007/S11356-020-10921-X

Sheth, N., Patel, M., Desai, M.D., 2017. A Study on Characterization & Treatment of Laundry Effluent. IJIRST-International J. Innov. Res. Sci. Technol. 4, 50–55.

Shi, Y., Zhang, G., Liu, J., Zhu, Y., Xu, J., 2011. Performance of a constructed wetland in treating brackish wastewater from commercial recirculating and super-intensive shrimp growout systems. Bioresour. Technol. 102, 9416–9424. https://doi.org/10.1016/J.BIORTECH.2011.07.058

Singh, A., Katoch, S.S., Bajpai, M., Rawat, A., 2022. Constructed Wetlands: A sustainable way of Treating Wastewater in Cold Climate - A review. Pollution 8, 373–396. https://doi.org/10.22059/POLL.2021.324626.1103

Singh, K., Lataye, D.H., Wasewar, K.L., Yoo, C.K., 2013. Removal of fluoride from aqueous solution: Status and techniques. Desalin. Water Treat. 51, 3233–3247. https://doi.org/10.1080/19443994.2012.749036

Singh, S., Sharma, A., Malviya, R., 2021. Industrial Wastewater: Health Concern and Treatment Strategies. Open Biol. J. 9, 1–10. https://doi.org/10.2174/1874196702109010001

Sivapragasam, C., Sharma, N.K., Vanitha, S., 2021. Modeling Wastewater Treatment Process: A Genetic Programming Approach, Soft Computing Techniques in Solid Waste and Wastewater Management. Elsevier. https://doi.org/10.1016/B978-0-12-824463-0.00026-4

Skrzypiec, K., Gajewska, M.H., 2017. The use of constructed wetlands for the treatment of industrial wastewater. J. Water L. Dev. 34, 233–240. https://doi.org/10.1515/jwld-2017-0058

Sohsalam, P., Englande, A.J., Sirianuntapiboon, S., 2008. Seafood wastewater treatment in constructed wetland: Tropical case. Bioresour. Technol. 99, 1218–1224. https://doi.org/10.1016/J.BIORTECH.2007.02.014

Soltani, R.D.C., Safari, M., Rezaee, A., Godini, H., 2015. Application of a compound containing silica for removing ammonium in aqueous media. Environ. Prog. Sustain. Energy 34, 105–111. https://doi.org/10.1002/EP.11969

Soni, R., Bhardwaj, S., Shukla, D.P., 2020. Various water-treatment technologies for inorganic contaminants: current status and future aspects, in: Inorganic Pollutants in Water. Elsevier, pp. 273–295. https://doi.org/10.1016/B978-0-12-818965-8.00014-7

Soroko, M., 2007. Treatment of wastewater from small slaughterhouse in hybrid constructed wetlands systems, in: Ecohydrology and Hydrobiology. Polish Academy of Sciences, pp. 339–343. https://doi.org/10.1016/S1642-3593(07)70117-9

Spellman, F.R., 2020. Handbook of Water and Wastewater Treatment Plant Operations, 4th ed. CRC Press. https://doi.org/10.1201/9781003038351

Stefanakis, A., Akratos, C.S., Tsihrintzis, V.A., 2014. Introduction, in: Vertical Flow Constructed Wetlands. Elsevier, pp. 1–16. https://doi.org/10.1016/b978-0-12-404612-2.00001-5

Stefanakis, A.I., 2020. Constructed wetlands for sustainable wastewater treatment in hot and arid climates: Opportunities, challenges and case studies in the Middle East. Water 12(6), 1665. https://doi.org/10.3390/W12061665

Subki, N.S., Akhir, N.M., Abdul Halim, N.S., Nik Yusoff, N.R., 2020. COD Reduction in Industrial Wastewater Using Activated Carbon Derived from Wodyetia Bifurcata Fruit. IOP Conf. Ser. Earth Environ. Sci. 549, 012066. https://doi.org/10.1088/1755-1315/549/1/012066

Sukmana, H., Bellahsen, N., Pantoja, F., Hodur, C., 2021. Adsorption and coagulation in wastewater treatment – Review. Prog. Agric. Eng. Sci. 17, 49–68. https://doi.org/10.1556/446.2021.00029

Tariq, M., Ahmad, M., Siddique, S., Waheed, A., Shafiq, T., Khan, M.H., 2012. Optimization of coagulation process for the treatment of the characterized slaughterhouse wastewater. Pak. J. Sci. Ind. Res. 55, 43–48.

Tee, H.C., Lim, P.E., Seng, C.E., Nawi, M.A.M., 2012. Newly developed baffled subsurface-flow constructed wetland for the enhancement of nitrogen removal. Bioresour. Technol. 104, 235–242. https://doi.org/10.1016/J.BIORTECH.2011.11.032

Tetteh, E.K., Rathilal, S., 2020. Application of Organic Coagulants in Water and Wastewater Treatment, in: Organic Polymers. IntechOpen. https://doi.org/10.5772/intechopen.84556

Thakur, I.S., Medhi, K., 2019. Nitrification and denitrification processes for mitigation of nitrous oxide from waste water treatment plants for biovalorization: Challenges and opportunities. Bioresour. Technol. 282, 502-513. https://doi.org/10.1016/j.biortech.2019.03.069

Ulu, F., Kobya, M., 2020. Ammonia removal from wastewater by air stripping and recovery struvite and calcium sulphate precipitations from anesthetic gases manufacturing wastewater. J. Water Process Eng. 38, 101641. https://doi.org/10.1016/J.JWPE.2020.101641

Upadhyayula, S., Chaudhary, A., 2021. Advanced Materials and Technologies for Wastewater Treatment. 1st Edition. CRC Press. Boca Raton. https://doi.org/10.1201/9781003138303

US Environmental Protection Agency, 2004. Effluent limitations guidelines and new source performance standards for the meat and poultry products point source category; Final Rule, Federal Register.

US Environmental Protection Agency, 1976. PART 457-EXPLOSIVES MANUFACTUR-ING POINT SOURCE CATEGORY.

Vargues, F., Brion, M.A., Rosa da Costa, A.M., Moreira, J.A., Ribau Teixeira, M., 2021. Development of a magnetic activated carbon adsorbent for the removal of common pharmaceuticals in wastewater treatment. Int. J. Environ. Sci. Technol. 18, 2805–2818. https://doi.org/10.1007/S13762-020-03029-9/FIGURES/9

Vasiraja, N., Saravana Sathiya Prabhahar, R., Joshua, A., 2023. Preparation and Physio–Chemical characterisation of activated carbon derived from prosopis juliflora stem for the removal of methylene blue dye and heavy metal containing textile industry effluent. J. Clean. Prod. 397, 136579. https://doi.org/10.1016/J.JCLEPRO.2023.136579

Venturini, M., Rossen, A., Paulo, P.S., 2021. Nitrification process in a nuclear wastewater with high load of nitrogen, uranium and organic matter under ORP controlled. Water 13(11), 1607. https://doi.org/10.3390/W13111607

Viktoryová, N., Szarka, A., Hrouzková, S., 2022. Recent Developments and Emerging Trends in Paint Industry Wastewater Treatment Methods. Appl. Sci. 12, 10678. https://doi.org/10.3390/APP122010678

Vinayagam, R., Pai, S., Murugesan, G., Varadavenkatesan, T., Narayanasamy, S., Selvaraj, R., 2022. Magnetic activated charcoal/Fe_2O_3 nanocomposite for the adsorptive removal of 2,4-Dichlorophenoxyacetic acid (2,4-D) from aqueous solutions: Synthesis, characterization, optimization, kinetic and isotherm studies. Chemosphere 286, 131938. https://doi.org/10.1016/j.chemosphere.2021.131938

Viswanaathan, S., Perumal, P.K., Sundaram, S., 2022. Integrated Approach for Carbon Sequestration and Wastewater Treatment Using Algal-Bacterial Consortia: Opportunities and Challenges. Sustain. 14, 1075. https://doi.org/10.3390/SU14031075

von Sperling, M., 2007. WASTEWATER CHARACTERISTICS, TREATMENT AND DISPOSAL, vol. 1. IWA Publishing, New York.

Vymazal, J., 2014. Constructed wetlands for treatment of industrial wastewaters: A review. Ecol. Eng. 73, 724–751. https://doi.org/10.1016/J.ECOLENG.2014.09.034

Vymazal, J., 2007. Removal of nutrients in various types of constructed wetlands. Sci. Total Environ. 380, 48–65. https://doi.org/10.1016/j.scitotenv.2006.09.014

Vymazal, J., Březinová, T., 2016. Accumulation of heavy metals in aboveground biomass of *Phragmites australis* in horizontal flow constructed wetlands for wastewater treatment: A review. Chem. Eng. J. 290, 232–242. https://doi.org/10.1016/J.CEJ.2015.12.108

Vymazal, J., Sochacki, A., Fučík, P., Šereš, M., Kaplická, M., Hnátková, T., Chen, Z., 2020. Constructed wetlands with subsurface flow for nitrogen removal from tile drainage. Ecol. Eng. 155. https://doi.org/10.1016/J.ECOLENG.2020.105943

Vymazal, J., Zhao, Y., Mander, Ü., 2021. Recent research challenges in constructed wetlands for wastewater treatment: A review. Ecol. Eng. 169, 106318. https://doi.org/10.1016/J.ECOLENG.2021.106318

Waly, M.M., Ahmed, T., Abunada, Z., Mickovski, S.B., Thomson, C., 2022. Constructed Wetland for Sustainable and Low-Cost Wastewater Treatment: Review Article. Land 11(9), 1388. https://doi.org/10.3390/land11091388

Wang, D., Li, T., Yan, C., Zhou, Y., Zhou, L., 2023. A novel bio-flocculation combined with electrodialysis process: Efficient removal of pollutants and sustainable resource recovery from swine wastewater. Sep. Purif. Technol. 304, 122330. https://doi.org/10.1016/J.SEPPUR.2022.122330

Wang, H., Sheng, L., Xu, J., 2021. Clogging mechanisms of constructed wetlands: A critical review. J. Clean. Prod. 295, 126455. https://doi.org/10.1016/j.jclepro.2021.126455

Wang, H., Song, Q., Wang, J., Zhang, H., He, Q., Zhang, W., Song, J., Zhou, J., Li, H., 2018. Simultaneous nitrification, denitrification and phosphorus removal in an aerobic granular sludge sequencing batch reactor with high dissolved oxygen: Effects of carbon to nitrogen ratios. Sci. Total Environ. 642, 1145–1152. https://doi.org/10.1016/J.SCITOTENV.2018.06.081

Wang, L., Hung, Y.T., Shammas, N.K., 2005. Physicochemical Treatment Processes. Humana Press, New Jersey. https://doi.org/10.5772/63666

Wang, L.K., Vaccari, D.A., Li, Y., Shammas, N.K., 2005. Chemical Precipitation. Physicochem. Treat. Process. 141–197. https://doi.org/10.1385/1-59259-820-X:141

Wang, W., Hua, Y., Li, S., Yan, W., Zhang, W. xian, 2016. Removal of Pb(II) and Zn(II) using lime and nanoscale zero-valent iron (nZVI): A comparative study. Chem. Eng. J. 304, 79–88. https://doi.org/10.1016/J.CEJ.2016.06.069

Wang, Y., 2016. Zero Discharge of wastewater Treatment Technology of Wet Desulfurization in Coal-fired Power Plants, in: 5th International Conference on Environment, Materials, Chemistry and Power Electronics. Atlantis Press. https://doi.org/10.2991/emcpe-16.2016.62

Wilcox, D.P., Chang, E., Dickson, K.L., Johansson, K.R., 1983. Microbial growth associated with granular activated carbon in a pilot water treatment facility. Appl. Environ. Microbiol. 46, 406. https://doi.org/10.1128/AEM.46.2.406-416.1983

World Bank Group, 2007. Environmental, Health and Safety (EHS) Guidelines for Meat Processing. General EHS Guidelines: Environmental Wastewater and Ambient Water Quality. URL http://www.ifc.org/ehsguidelines (accessed 4.18.23).

Wu, H., Zhang, J., Ngo, H.H., Guo, W., Hu, Z., Liang, S., Fan, J., Liu, H., 2015. A review on the sustainability of constructed wetlands for wastewater treatment: Design and operation. Bioresour. Technol. 175, 594–601. https://doi.org/10.1016/J.BIORTECH.2014.10.068

Wu, J., Doan, H., 2005. Disinfection of recycled red-meat-processing wastewater by ozone. J. Chem. Technol. Biotechnol. 80, 828–833. https://doi.org/10.1002/JCTB.1324

Wu, L., Peng, C., Peng, Y., Li, L., Wang, S., Ma, Y., 2012. Effect of wastewater COD/N ratio on aerobic nitrifying sludge granulation and microbial population shift. J. Environ. Sci. 24, 234–241. https://doi.org/10.1016/S1001-0742(11)60719-5

Wun Jern, N.G., 2006. Industrial wastewater treatment. Ind. Wastewater Treat. 1–153. https://doi.org/10.1142/P405/SUPPL_FILE/P405_CHAP01.PDF

Xu, X., Zhou, Q., Chen, X., Li, Y., Jiang, Y., 2022. The Efficiency of Green Technology Innovation and Its Influencing Factors in Wastewater Treatment Companies. Sep. 2022, Vol. 9, Page 263 9, 263. https://doi.org/10.3390/SEPARATIONS9100263

Yagub, M.T., Sen, T.K., Afroze, S., Ang, H.M., 2014. Dye and its removal from aqueous solution by adsorption: A review. Adv. Colloid Interface Sci. 209, 172–184. https://doi.org/10.1016/J.CIS.2014.04.002

Yaragal, R.R., Mutnuri, S., 2023. Nitrates removal using ion exchange resin: batch, continuous column and pilot-scale studies. Int. J. Environ. Sci. Technol. 20, 739–754. https://doi.org/10.1007/S13762-021-03836-8

Yeboah, S., Allotey, A., Biney, E., 2015. Purification of industrial wastewater with vetiver grasses (*Vetiveria zizanioides*): the case of food and beverages wastewater in Ghana. Asian J. Basic Appl. Sci. 2(2), 1-14.

Yegane Badi, M., Azari, A., Pasalari, H., Esrafili, A., Farzadkia, M., 2018. Modification of activated carbon with magnetic Fe_3O_4 nanoparticle composite for removal of ceftriaxone from aquatic solutions. J. Mol. Liq. 261, 146–154. https://doi.org/10.1016/J.MOLLIQ.2018.04.019

Ying, Z., Li, X., Zhang, L., Xi, B., Xia, X., Zhang, Z., Zhan, J., 2011. Coagulation pretreatment for constructed Wetlands. Fresenius Environ. Bull. 20, 2326–2334.

Yirong, C., Puetpaiboon, U., 2004. Performance of constructed wetland treating wastewater from seafood industry. Water Sci. Technol. 49, 289–294. https://doi.org/10.2166/WST.2004.0766

Zala, S.L., Ayyer, J., Desai, A.J., 2004. Nitrate removal from the effluent of a fertilizer industry using a bioreactor packed with immobilized cells of *Pseudomonas stutzeri* and *Comamonas testosteroni*. World J. Microbiol. Biotechnol. 20, 661–665. https://doi.org/10.1007/S11274-004-9982-8/METRICS

Zhang, J., Wang, M., Zhu, X., 2013. Treatment of HMX-Production Wastewater in an Aerobic Granular Reactor. Water Environ. Res. 85, 301–307. https://doi.org/10.2175/106143013X13596524516068

Zhang, X., Wang, T., Xu, Z., Zhang, L., Dai, Y., Tang, X., Tao, R., Li, R., Yang, Y., Tai, Y., 2020. Effect of heavy metals in mixed domestic-industrial wastewater on performance of recirculating standing hybrid constructed wetlands (RSHCWs) and their removal. Chem. Eng. J. 379, 122363. https://doi.org/10.1016/J.CEJ.2019.122363

Zhao, P., Ma, M., Hu, Y., Wu, W., Xiao, J., 2022. Comparison of international standards for irrigation with reclaimed water. Agric. Water Manag. 274, 107974. https://doi.org/10.1016/J.AGWAT.2022.107974

Zhao, Q., Han, H., Xu, C., Zhuang, H., Fang, F., Zhang, L., 2013. Effect of powdered activated carbon technology on short-cut nitrogen removal for coal gasification wastewater. Bioresour. Technol. 142, 179–185. https://doi.org/10.1016/J.BIORTECH.2013.04.051

Zhao, Z.L., Li, W.W., Wang, F., Zhang, Y.Q., 2018. Using of hydrated lime water as a novel degumming agent of silk and sericin recycling from wastewater. J. Clean. Prod. 172, 2090–2096. https://doi.org/10.1016/J.JCLEPRO.2017.11.213

Zhu, S., Qin, L., Feng, P., Shang, C., Wang, Z., Yuan, Z., 2019. Treatment of low C/N ratio wastewater and biomass production using co-culture of *Chlorella vulgaris* and activated sludge in a batch photobioreactor. Bioresour. Technol. 274, 313–320. https://doi.org/10.1016/J.BIORTECH.2018.10.034

Zodi, S., Louvet, J.-N., Michon, C., Potier, O., Pons, M.-N., Lapicque, F., Leclerc, J.-P., 2011. Electrocoagulation as a tertiary treatment for paper mill wastewater: Removal of non-biodegradable organic pollution and arsenic. Sep. Purif. Technol. 81, 62–68. https://doi.org/10.1016/j.seppur.2011.07.002

Chapter 2

Immediate one-step lime precipitation and atmospheric carbonation as pre-treatment for low biodegradable and high nitrogen wastewaters: A case study of explosives industry

This Chapter was published in:

Madeira, L., Almeida, A., Ribau Teixeira, M., Prazeres, A., Chaves, H., Carvalho, F. (2020). Immediate one-step lime precipitation and atmospheric carbonation as pre-treatment for low biodegradable and high nitrogen wastewaters: A case study of explosives industry. J. Environ. Chem. Eng. 8, 103808. https://doi.org/10.1016/j.jece.2020.103808

This Chapter resulted in a European Patent published as:

Carvalho, F.; Almeida, A., Ribau, M., Prazeres, A., Chaves, H.; Madeira, L. (2019). "Process for the Treatment and Recovery of Wastewater from the Explosives Industries". EP 3339251B1.

ABSTRACT

The treatment of some industrial wastewaters is complex since they usually contain complex non-biodegradable organic compounds or toxic compounds which are not easily treatable. These compounds are not removed by biological treatment in wastewater treatment plants and they may affect the removal of ammonium, nitrate, and organic nitrogen by these treatment systems. Therefore, this research proposes a new and innovative low-cost and easy-to-apply pre-treatment to treat low biodegradable and high nitrogen wastewaters, using explosive wastewaters as a case study. The pre-treatment is composed of immediate one-step lime precipitation (IOSLM) and atmospheric CO_2 carbonation (AC) processes. The novelty of the proposed pre-treatment is based firstly on the use of one reactant (hydrated lime) at high concentrations, added in one step, that produces immediately an abundant and insoluble precipitate able to sweep the organic matter and other contaminants from wastewater in a short time and ensure conditions (pH and Ca^{2+}) for the AC process. Secondly, the AC process uses the sludge produced in IOSLM to keep pH high for longer, allowing ammonia removal while simultaneously the pH is reduced by spontaneous reactions with atmospheric CO_2. IOSLM results showed 92.1%, 98.2%, and 100% of organic matter, oils and fats, and organic nitrogen removals, respectively, for the optimal hydrated lime dose (7.76 g L^{-1}). In the AC process, 61% of ammonium nitrogen was removed and the pH was reduced to 8.1 in 10 days.

2.1. Introduction

Industrial wastewaters usually contain complex non-biodegradable organic compounds or toxic compounds which are not easily treatable. Examples of these effluents can be found in the textile industry due to the dyes and organic sizing agents used in the manufacturing process (Ghoreishi and Haghighi, 2003), in the explosives industry as a result of the manufacture ammonium nitrate-fuel oil (ANFO), emulsion explosives, 2,4,6-trinitrotoluene (TNT), hexahydro-1,3,5-trinitro-1,3,5-triazine (RDX), and octahydro-1,3,5,7-tetranitro-1,3,5,7-tetrazocine (HMX) (Vijaya Chitra and Lakshmanaperumalsamy, 2006), in paper mills factories due to the amount of lignin, lignin derivatives, and arsenic (Zodi et al., 2011), and in tannery industry due to chemicals used in leather processing (Mariliz et al., 2015). Furthermore, some of these industries discharge high amounts of wastewaters, especially when coming from large-scale industrial parks, which may cause major environmental problems for the receiving water bodies. These compounds have a high potential impact on human health and environment (Chatterjee et al., 2017; Vijaya Chitra and Lakshmanaperumalsamy, 2006).

The treatment of these wastewaters is complex. Non-biodegradable compounds are not removed by the biological treatment of the wastewaters treatment plants (e.g., activated sludge) and they may affect the removal of ammonium, nitrate, organic nitrogen, and organic matter in these treatment systems (DeLaune and Reddy, 2005). Therefore, a pre-treatment is required for these industrial wastewaters since, if not applied, the effectiveness of the biological treatment will be compromised. The pre-treatment of low biodegradable effluents has been a real challenge, especially when the effluent has specific features (such as high concentrations of nitrogen) that could be removed biologically. In literature, some studies developed physical-chemical pre-treatment solutions to increase the biodegradability of the effluents, namely oxidation (Schröder, 1996; Van Leeuwen et al., 2009), electrochemical processes (Carboneras et al., 2018), and peroxi-coagulation (Ren et al., 2019), while other studies seek to remove non-biodegradable organic matter or toxic compounds of the effluents through membranes processes (Chan et al., 2007) or chemical precipitation and adsorption (Rodríguez et al., 2004). In chemical precipitation, the treatment of different industrial wastewaters with lime and hydrated lime has shown several benefits for the environment. Organic

compounds present as suspended particles can be substantially removed by sweep coagulation phenomena caused by the formation and simultaneous precipitation of calcium carbonate. Moreover, dissolved compounds can also be removed, leading to a significant reduction of several pollution parameters (Dowling et al., 2015; Georgiou et al., 2019). Georgiou et al. (2019) used hydrated lime as a pre-treatment step for pH-raising and reduction of residual particulates of an anaerobic digestate generated in the treatment of animal manure. Hydrated lime was preferred because of its fast reaction and low cost, with effective clarification of the anaerobic digestate at high pH (≥11.5) (Georgiou et al., 2019). These authors used air-stripping for ammonia removal, with removals ca. 100% at 50 °C and 90% at 30ºC (G/L= 2000) (Georgiou et al., 2019). In Chen et al. (2009) lime with fly ashes was preferred for the removal of heavy metals from industrial wastewater due to its relatively low cost. The application of carbonation improved the removal of heavy metals. Results showed that removals of Zn(II), Pb(II), Cu(II), and Cr(III) were enhanced between pH 7-11 and removals efficiencies as high as 99.37–99.69% obtained by the fly ash–lime-carbonation treatment (Chen et al., 2009). A high arsenic acidic wastewater from a sulfuric acid factory was effectively treated in a combined process of pre-oxidation, lime, and ferrous precipitation, ferric and manganese binary metal oxide (FMBO) adsorption, and polyaluminum chloride (PACl) coagulation (Wang et al., 2011). A lime pretreatment process, for efficient bioethanol production from rice straw was developed without a solid–liquid-separation (Park et al., 2010). Carbonation was made using CO_2 gas bubbled into the treated slurry. This pretreatment was very efficient (Park et al., 2010). These treatments were very efficient in removing the target compounds but some included several treatment processes and most were applied to remove heavy metals. In addition, some of these treatments have proven disadvantages, for example, air stripping presents high operating costs and often accumulates calcium carbonate on the walls of the stripping tower (Yuan et al., 2016), and activated sludge is poorly tolerant to load and flow variations, and to toxic compounds (Yuan et al., 2016). Moreover, some treatments are expensive or produce sub-products that can be more harmful to the environment than the initial ones (Gulyas, 1997). Therefore, it is necessary to find better alternatives for the treatment of these effluents. These alternatives should be technically feasible, low cost, have less environmental impacts, and consider future reuses.

Thus, this study proposes a novel low-cost and easy-to-apply pre-treatment, composed of immediate one-step lime precipitation (IOSLM) followed by atmospheric CO_2

carbonation (AC) process, for low biodegradable organic matter and ammonium removal, using ANFO and emulsion explosives wastewaters as a case study. This integrated pre-treatment is intended to improve the quality of this type of wastewaters to promote the viability of biological treatment or allow reuse within the factory processes. In addition, this environmental solution could mitigate greenhouse gas production, boost the capture of ammonia to be reused in industries, and recover the lime from the sludge produced through lime calcination processes. The research of the proposed integrated pre-treatment is based on the following assumption: (i) Hydrated lime is a low-cost reagent (Davis, 2010) that can be easily acquired, and has been used efficiently to adjust pH and to remove hardness and impurities from water and wastewater (Davis, 2010; Dowling et al., 2015; Renou et al., 2009; Zayen et al., 2016); (ii) Hydrated lime can be used as a soil amendment for in situ remediation of explosives (RDX) and metals stabilization, as demonstrated by Martin et al. (2012); (iii) The effect of hydrated lime on the effluent biodegradability and on the removal of non-biodegradable organic compounds from ANFO and emulsion effluents have not been studied yet as far as the authors' knowledge; (iv) Recent studies have shown that it is possible to reduce the pH by natural neutralization with atmospheric CO_2 (AC) at a low-cost process (Prazeres et al., 2019, 2016). However, no studies have referred to the AC's ability to remove ammonia or mentioned the effect of precipitated sludge (from chemical precipitation) in lowering the pH during the carbonation process.

2.2. Material and methods

2.2.1. Explosive wastewater (EW) characterization

EW was used as a case study. EW was collected from an international industry that manufactures ANFO and emulsion explosives in Portugal. ANFO and emulsion explosives are used in mining industry quarrying and construction activities, and their demand has been increasing relative to other types of explosives due to their low manufacturing cost and risk of accidental ignition, and ease of handling (Satsangi, 2016; Schoch et al., 2013). ANFO explosives are composed of a mixture of ammonium nitrate (AN) with diesel fuel in a ratio of about 94 to 6% (Hernandes et al., 2015). Emulsion explosives are composed of a dispersed phase (aqueous solution of inorganic oxidizing AN salt) surrounded by a continuous phase (emulsifying oil, Al-Sabagh et al., 2017). This

wastewater (EW) is a mixture of effluents from leaks and spills in process areas, equipment washing operations, floor and auto-tank washing, and on-site wastewater pre-treatment. The on-site wastewater pre-treatment consists in breaking down residual emulsion by adding a liquid detergent, which results in the oil separation from the liquid phase. Table 2.1 summarizes the characteristics of the EW.

Table 2.1 - Characteristics of the EW.

Parameters	Unit	Average ± standard deviation
COD	mg O_2 L^{-1}	5922 ± 1711
BOD_5	mg O_2 L^{-1}	50 ± 34
BOD_5 / COD	-	0.009 ± 0.006
TSS	mg L^{-1}	126 ± 3
Ammonium nitrogen	mg N-NH_4^+ L^{-1}	1553.9 ± 23.1
pH	Sorensen	7.63 ± 0.11
Redox Potential	mV	114.7 ± 74.3
Conductivity	mS cm^{-1}	12.21 ± 0.11
Nitrates	mg L^{-1}	7233 ± 47
Nitrites	mg N L^{-1}	10.96 ± 0.13
Chlorides	mg L^{-1}	290.0 ± 4.7
Dissolved oxygen	mg O_2 L^{-1}	6.505 ± 0.054
Calcium hardness	mg L^{-1} $CaCO_3$	203.4 ± 20.3
Calcium	mg L^{-1}	81.4 ± 8.1
Total hardness	mg L^{-1} $CaCO_3$	406.8 ± 20.3
Magnesium hardness	mg L^{-1} $CaCO_3$	203.4 ± 28.7
Magnesium	mg L^{-1}	49.4 ± 9.9
Phenolphthalein alkalinity	mg L^{-1} $CaCO_3$	47 ± 0.0
Total alkalinity	mg L^{-1} $CaCO_3$	560 ± 46.7
Bicarbonate	mg L^{-1} $CaCO_3$	558 ± 46.7
Carbonate	mg L^{-1} $CaCO_3$	2.2 ± 0.0
Kjeldahl-N	mg N-Kj. L^{-1}	1897.4 ± 0.0
Organic-N	mg N L^{-1}	343.5 ± 23.1
Oils and fats	mg L^{-1}	285.3
Total hydrocarbons	mg L^{-1}	46.0
Cadmium	mg Cd L^{-1}	< 0.025
Manganese	mg Mn L^{-1}	0.504 ± 2.51E-04

2.2.2. Experimental set-up

A scheme of the experimental unit used in this work is shown in Figure 2.1.

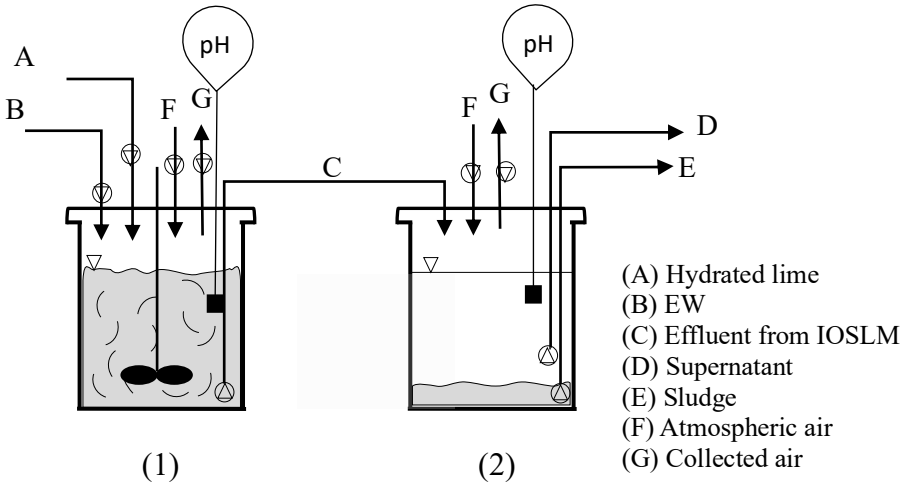

Figure 2.1 – Schematic diagram of the IOSLM (1) and AC (2) processes.

2.2.2.1. Immediate one-step lime precipitation (IOSLM) tests

IOSLM experiments were conducted using 1000 mL of explosive wastewater where different doses (from 2 to 19 g L^{-1}) of hydrated lime (≥95%, Spectrum® chemical) were added to raw water, under vigorous agitation (rotation speed of 3 Stirrer). Agitation was maintained until different precipitation pHs were reached, from 9 to 12.5. Once achieved, the agitation was kept for 1 minute and then stopped. After the stirring period, the effluent was immediately transferred to a normalized glass graduated cylinder (1 L, 37 cm height and 28 cm^2 of superficial area) and the sludge sedimentation operation started, so no agitation took place and the solution rested for 46 min. Then, the type of sedimentation, the sedimented sludge volume, and the physicochemical characteristics of the pre-treated water (supernatant) were analyzed.

2.2.2.2. Atmospheric CO_2 carbonation (AC) tests

The AC tests consisted in keeping 5 L of EW treated by IOSLM in a 189 cm^2 superficial area recipient at room temperature, without chemicals addition and agitation. Two sets of experiments were made.

Firstly, the AC process was tested for all the hydrated lime doses studied in ISOLM for sixteen days. In the first 14 days, the supernatant and the sludge were kept in the same recipient in contact with atmospheric air, at room temperature. After this time, the supernatant was separated from the sludge and it was exposed to air, for another two days. The influence of the sludge in the treated water characteristics was evaluated by pH and the Langelier Saturation Index.

In the second set of experiments, the AC process was made for the best hydrated lime dose found in the ISOLM process (section 2.2.2.1.) and the best condition found in the first AC set experiments. Process efficiency was monitored (section 2.2.3.) over time. These experiments were maintained until a maximum removal of ammonia was observed and when the supernatant pH was close to 8.

2.2.3. Analytical methods

pH and redox potential measurements were performed in a WTW InoLab apparatus, using the electrodes SenTix 41 and WTW SenTix ORP, respectively. Electrical conductivity was evaluated in a Jenway 4510 meter, using an electrode VWR CO 11. Chemical oxygen demand (COD) was determined by the standard dichromate closed reflux method (APHA et al., 2012), using a digester WPA HC 6016 and quantified by Pharmacia Biotech Ultrospec 2000 UV/Visible spectrophotometer model 80-2106-00. Total suspended solids (TSS) were quantified by the gravimetric method using filters Whatman^{TM} 1001-110 (APHA et al., 2012). Biological oxygen demand (BOD) was determined by the Mohr method using the system WTW's Oxitop® (APHA et al., 2012). Chlorides were determined by the Mohr method (APHA et al., 2012). Oil and fats were measured gravimetrically after Soxhlet extraction (Sawyer et al., 2003). Nitrate was determined by the sodium salicylate method (Monteiro et al., 2003). Ammonium nitrogen was measured by distillation method in BUCHI Distillation Unit B-316 and then by titration (APHA et al., 2012). Kjeldahl nitrogen was determined by the Kjeldahl method (APHA et al., 2012). Nitrites and dissolved oxygen were determined by colorimetric and modifications of the Winkler methods, respectively (APHA et al., 2012). Calcium and magnesium determinations were made by volumetric complexation with EDTA using eriochrome black T (calcium + magnesium) and calcon (calcium) indicators (APHA et al., 2012). Phenolphthalein and total alkalinity were measured by neutralization titration (APHA et

al., 2012). Heavy metals were determined by flame atomic absorption spectrometry using a Varian SpectraAA 220FS spectrometer (APHA et al., 2012). Total hydrocarbons were measured by the company "QUIMITESTE – Engenharia e Tecnologia, Lda", using infrared spectrophotometry. The carbonates and bicarbonates were determined by APHA et al. (APHA et al., 2012). Langelier Saturation Index was determined by the saturation index (APHA et al., 2012). Clarifying velocity was determined by Talmadge & Fitch method (Ramalho, 1996).

2.2.4. Statistical analysis

Experiments were made in triplicate for IOSLM and AC experiments as well as for parameter measurements, and their averages were calculated. The graphs were drawn by GraphPad Prism version 5.0 for Windows, GraphPad Software, La Jolla California USA. All data were submitted to one-way ANOVA using Tukey's test at a 95% confidence level for a distinction between averages, through the IBM SPSS Statistics for Windows, Version 20.0, Armonk, NY, IBM Corp. The correlation analysis was performed for IOSLM and AC experiments according to Pearson using RStudio^{TM} software, version 1.2.1335, Inc., Boston, MA. All correlations were considered statistically significant at P values < 0.05 or < 0.001.

2.3. Results and Discussion

2.3.1. EW characterization

Visually, EW is a homogeneous, turbid, and whitish mixture. EW smells fuel, due to one of the raw materials used in the formation of ANFO and emulsion explosives.

As shown in Table 2.1, the EW pH is neutral (7.63±0.11). The redox potential is positive (+114±74 mV), which indicates that the effluent presents an oxidative environment. The conductivity is 12.21±0.11 mS cm^{-1}, so the effluent has high mineralization. EW presents a high content of organic matter (5922±1711 mg COD L^{-1}), which may be due to the presence of residual detergent used in the wastewater pre-treatment and/or additives used

in the formation of explosives. The values of BOD_5 are low, about 50±34 mg L^{-1}. This effluent is difficult to biodegrade because it has a very low biodegradability index (BOD_5/COD ratio=0.009). The high concentrations of nitrate (7233±47 mg L^{-1}) and ammonium (1554±23 mg N-NH_4^+ L^{-1}) are characteristic of this type of effluent because they are part of the main raw materials used in the manufacture of explosives. Ghafari et al. (2008) reported effluents from the explosives industry, with nitrate concentration above 1000 mg L^{-1} N-NO_3^-. Nitrogenous organic matter is also high (344±23 mg N L^{-1}) but nitrites concentration is insignificant (11.0±0.1 mg N L^{-1}). The values of total suspended solids, oils and fats, and total hydrocarbons are 126±3, 285.3, and 46.0 mg L^{-1}, respectively. According to the hardness classification presented by Sawyer et al. (2003), EW is very hard with a total hardness of 406.8±20 mg L^{-1} $CaCO_3$.

2.3.2. Immediate one-step lime precipitation (IOSLM) process

The results of IOSLM bench tests are different from the typical lime precipitation (tested by Zayen et al. (2016) and Renou et al. (2009)) because a highly concentred lime solution is added in excess, at once, to the water under vigorous agitation (rotation speed of 3 Stirrer). This produces an instantaneous and intense precipitate followed by the "sweeping" phenomenon of particles, in a short time. In this process, the flocculation step did not take place because agitation would reduce the "sweeping" effect. In addition, hydrated lime is used in high concentrations because it is important for the next process (AC) since the presence of calcium ions in excess will promote reactions with atmospheric CO_2 and the pH decrease. This is a new technology that has been presented recently (Carvalho et al., 2019).

Figure 2.2A describes in detail the effect of hydrated lime dose on pH, phenolphthalein alkalinity, and total alkalinity of the EW. Results presented in Table 2.2 indicate that hydrated lime dose has a significant positive correlation with pH (r=0.88, P<0.001), phenolphthalein alkalinity (r=0.94, P<0.001), and total alkalinity (r=0.94, P<0.001). The hydrated lime dose added (2 to 18.98 g L^{-1}) increases the pH from 9 to 12.45 due to the addition of OH^- to the solution. Experimental tests have shown that it is not possible to increase the pH beyond 12.45 even if a higher dose of lime is added. Zayen et al. (2016) also observed this behavior in the neutralization of landfill leachate with lime. Between

2 and 10.5 g L^{-1} of hydrated lime added, the pH increase is proportional to the lime dose applied (Figure 2.2A). However, from 10.5 to 18.98 g L^{-1} of lime doses added, this behavior is not observed. Thus, a minimal dose of the hydrated lime applied may cause a significant increase in pH (P<0.05). Theoretically, at 10 g L^{-1} of hydrated lime (corresponding to a pH between 10.5 to 11) all the ammonium ions are converted to ammonia by consumption of OH^- ions (Lin et al., 2009; Wang et al., 2005) according to Eq. 1, which justifies the pH suddenly increase at this dose (Figure 2.2A).

$$NH_{3\,(g)} + H_2O_{\,(l)} \leftrightarrow NH_4^{+}{}_{(aq)} + OH^-_{(aq)} \qquad pK_a = 9.25 \quad (25^oC) \qquad (1)$$

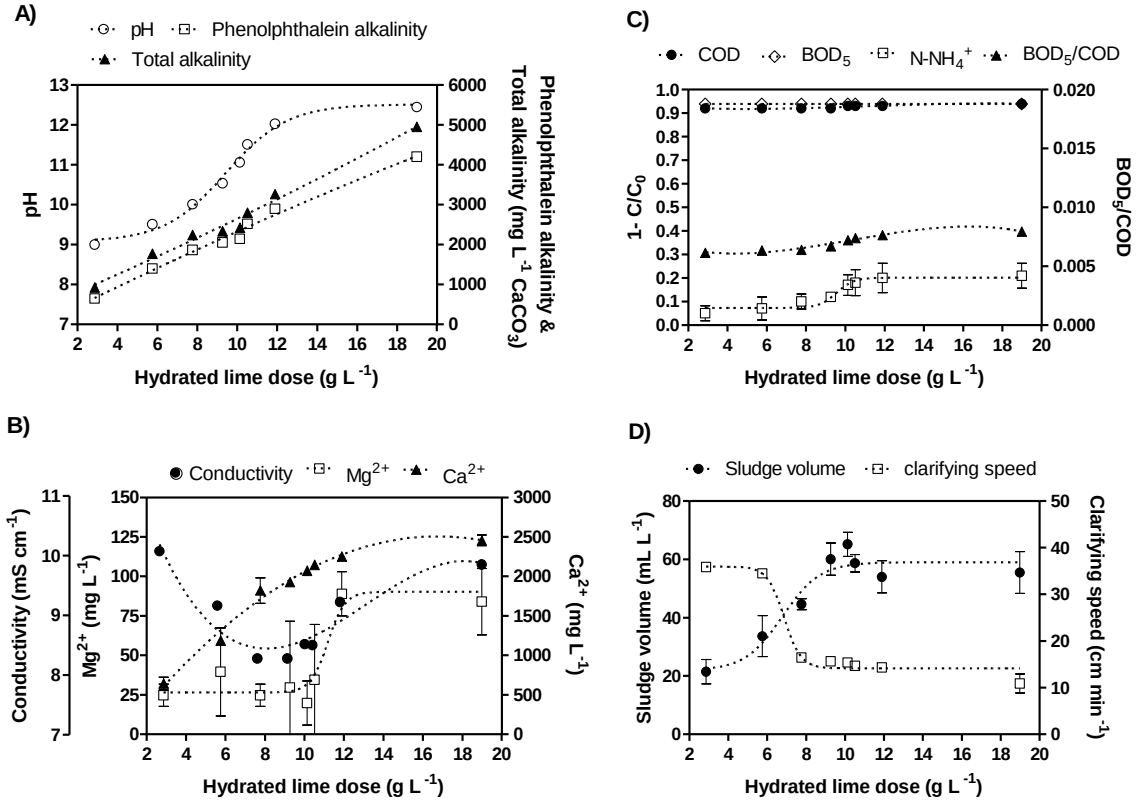

Figure 2.2 - Effect of the hydrated lime dose on the **A)** pH, phenolphthalein alkalinity, and total alkalinity; **B)** electrical conductivity, magnesium, and calcium concentration; **C)** COD, BOD_5 and ammonium removals and biodegradability index; and **D)** sludge volume produced and his clarifying speed.

Table 2.2 - Correlation matrix between parameters determined in immediate one-step lime precipitation tests.

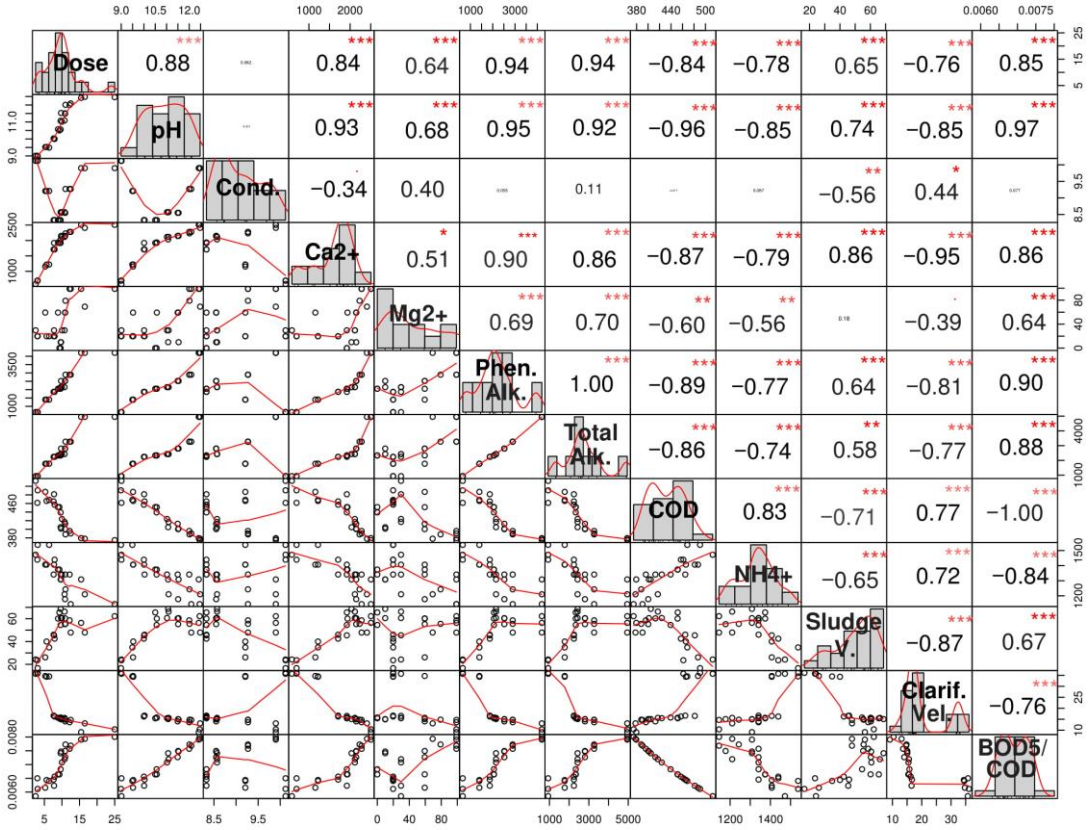

Notes: 1) Where it is written: "cond.", "Phen. Alk", "Total Alk", "Sludge V.", and "Clarif. Vel." mean conductivity, Phenolphthalein Alkalinity, Total Alkalinity, Sludge volume, and clarifying velocity, respectively; 2) The distribution of each variable is shown on the diagonal. On the bottom of the diagonal: the bivariate scatter plots with a fitted line are displayed. On the top of the diagonal: the value of the correlation plus the significance level as stars. Each significance level is associated to a symbol : p-values(0, 0.001, 0.01, 0.05, 0.1, 1) <=> symbols("***", "**", "*", ".", " ").

Renou et al. (2009) studied the pre-treatment of three different raw landfill leachates, using chemical precipitation with lime followed by flocculation. They dosed about 1.8, 3, and 4 g L^{-1} of $Ca(OH)_2$ to achieve a pH of 10, while in this work, about 8 g L^{-1} of hydrated lime was added to get the same pH. This difference in the lime dose consumed may be due to some differences in the physicochemical characteristics of the wastewater used, namely the initial pH (8.35, 8.55, and 8.60, respectively for the doses applied 1.8, 3, and 4 g L^{-1}), alkalinity (175, 285 and 495 mg L^{-1} $CaCO_3$) or the initial concentration of the ammonium ion (370, 468, and 730 mg L^{-1}) (Renou et al., 2009). The highest the ammonium ion concentration in the effluent, the highest hydrated lime will be needed. The phenolphthalein and total alkalinities mean values increase from 654 to 4203 mg L^{-1} $CaCO_3$ and from 934 to 4950 mg L^{-1} $CaCO_3$, respectively, for the hydrated lime doses tested (Figure 2.2A). This increase is related to the increase in hydroxide and carbonate content. Since the concentration of ammonium ion in EW is high, it may be possible that

the ammonia contributes to alkalinity (Sawyer et al., 2003) at all lime doses applied, but mainly for doses whose pH is greater than 9.25. Rounds (2012) mentioned that high quantities of titrant acid were needed to reach the first equivalence point (pH ≈ 8.3) which would otherwise be represented by carbonate and hydroxide since ammonia (NH_3) will react with hydrogen ions from the titrant to produce ammonium ion (NH_4^+).

Figure 2.2B presents the variation of conductivity, magnesium, and calcium concentrations with the hydrated lime dose added. According to Table 2.2, the hydrated lime dose shows significant positive correlations with magnesium (r=0.64, P<0.001) and calcium (r=0.84, P<0.001) concentrations, while no significant correlation is observed with conductivity. Conductivity concentration decreases and reaches the minimum of 8.3 mS cm^{-1} (corresponding to the maximum conductivity removal of 32%) between 7.76 and 9.26 g L^{-1} of hydrated lime (at pH 10 and 10.5, respectively). After the addition of 9.26 g L^{-1} of hydrated lime, conductivity starts to rise (Figure 2.2B). Usually, the conductivity reduction is due to the chemical precipitation of organic and inorganic (e.g. calcium and magnesium) salts in the form of hydroxides or carbonates, as explained below (Renou et al., 2009). Magnesium present in EW may precipitate as magnesium carbonates or magnesium hydroxide according to Eq. 2 and Eq. 3 (Prazeres et al., 2016; Renou et al., 2008b).

$$Ca(OH)_2 + Mg(HCO_3)_2 \leftrightarrow MgCO_3 + CaCO_3\,(s) + 2H_2O \quad (2)$$

$$Ca(OH)_2 + MgCO_3 \leftrightarrow Mg(OH)_2\,(s) + CaCO_3\,(s) \quad (3)$$

The conductivity demonstrates a weak and insignificant correlation with calcium (r=-0.34, P>0.05) and magnesium (r=0.40, P>0.05) for the range of hydrated lime dose studied; however, a significant positive correlation is observed between conductivity and calcium (r=0.95, P<0.001) or magnesium (r=0.78, P<0.001) from 9.26 g L^{-1} of hydrated lime added. Anyway, the conductivity never exceeds the initial value whatever the lime dose added. In addition, other metallic substances (such as zinc, nickel, or manganese) may be present in wastewater, since they are part of the raw fuel oil material and tend to precipitate in the form of hydroxides and/or carbonates contributing in this way to the conductivity variation. Furthermore, this wastewater has high concentrations of sodium, nitrates, and chlorides, which may be also responsible for the high conductivity. The magnesium concentration increases after 10.5 g L^{-1} of hydrated lime added (reaching ca.

80 g L^{-1}, Figure 2.2B). This increase may be due to the prevalence of other metals that precipitate first in relation to magnesium or magnesium contamination from the reagent.

For calcium, concentration increases from 642.8 to 2457.1 mg L^{-1} with hydrated lime doses (the initial calcium effluent concentration was 81.4 mg L^{-1}). This increase contrasts with conventional softening behavior because above pH 9.5 the calcium added and the existing in the solution (EW) should precipitate in the form of calcium carbonate, according to Eq. 4 and Eq. 5 (Prazeres et al., 2016; Renou et al., 2008b). The reason for the observed behavior is the fact that hydrated lime doses applied are, stoichiometric, too high for the bicarbonate in the solution, making bicarbonate a limiting reagent, even for the lowest lime dose applied. Thus, since the hydrated lime is poorly soluble, lime will contribute to sludge but also will be dissociated in calcium cations (Ca^{2+}) and hydroxide anions (OH^-) (Eq. 6), increasing the concentrations of these ions in solution at the studied doses. However, when the maximum solubility of $Ca(OH)_2$ is reached, at ca. pH 12 and 11.89 g L^{-1} of lime dose added (Figure 2.2B), calcium tends to remain constant even though more calcium hydroxide is added.

$$Ca(OH)_2 + H_2CO_3 \leftrightarrow CaCO_3\,(s) + 2H_2O \quad (4)$$

$$Ca(OH)_2 + Ca(HCO_3)_2 \leftrightarrow 2CaCO_3\,(s) + 2H_2O \quad (5)$$

$$Ca(OH)_{2(s)} \leftrightarrow Ca^{2+}{}_{(aq)} + 2\,OH^-{}_{(aq)} \quad (6)$$

Figure 2.2C shows the variation of COD, BOD_5, ammoniacal nitrogen, and biodegradability index as a function of the hydrated lime dose added. Hydrated lime dose shows significant negative correlations with COD (r=-0.84, P<0.001) and NH_4^+ (r=-0.78, P<0.001) concentrations, while a significant positive correlation with biodegradability index (r=0.85, P<0.001) is observed. No correlation between hydrated lime dose and BOD_5 is found because its removal was constant at 94%, independently of the dose applied. COD removals vary between 92 and 94%, for the lime doses applied. The biodegradability index is 0.0069±0.0007 for all the doses applied so no significant changes were observed from the initial effluent value (Table 2.1). The IOSLM process removed proportionally both biodegradable and non-biodegradable organic matter for all the lime doses tested. The removal of organic matter is related to the addition of calcium hydroxide in excess and its subsequent drag during sedimentation (Prazeres et al., 2016; Renou et al., 2008b). In fact, when an appreciable amount of hydrated lime is added, the

calcium carbonate and calcium hydroxide produced act as coagulating agents. Thus, they improve the drag of the organic matter, and the "sweeping effect" occurs (Renou et al., 2008a; U.S. EPA, 2000). Other contaminants like heavy metals, hydrocarbons, oils and fats, and other organic substances, at this pH, become prone to drag from the solution, helped by the produced precipitate. So, a sedimentation in mantle occurs and consequently, a liquid-solid interface is formed, which results in a clarified supernatant (without the flocculation step) and consolidated sludge. Martin et al. (2012) evaluated the potential of hydrated lime for metal immobilization and explosives transformation in soil. These authors concluded that hydrated lime reduced the RDX and zinc metal in leachates and runoff water by about 26-92% and 66-83%, respectively, and gave conditions for optimum explosives decomposition. In our study, hydrocarbons removals are ca. 96, 91, and 90% for the lime doses of 10.13, 11.89, and 18.98 g L^{-1}, respectively.

Ammoniacal nitrogen removals vary between 5 and 12% until 9 g L^{-1} of hydrated lime added and increase to 21% after the addition of 10.13 g L^{-1} of hydrated lime (Figure 2.2C). This increase in ammonia removal is related to the high availability of ammonia to be volatilized (Dowling et al., 2015) as a result of the displacement of the chemical equilibrium (Eq. 1) (conversion of ammonium ion to ammonia) due to increased pH (Lin et al., 2009). Thus, a significant negative correlation between NH_4^+ concentration and pH ($r=-0.85$, $P<0.001$) is observed in Table 2.2. Berge et al. (2005) and Wang et al. (2005) reported that pH is normally adjusted above 10.5-11.5 to convert all the ammoniacal nitrogen into ammonia. From the applied dose of 10.13 g L^{-1} (pH = 11.06), ammonia removal remained constant at around 21%. Renou et al. (2009, 2008a) obtained higher percentages of ammonia removals (25 to 56%) by applying lime precipitation to leachate. These higher removals are related to the operational conditions used in the processes. Renou et al. (2009, 2008a) applied rapid mixing at 300 rpm for 5 min followed by slow mixing at 30 rpm for 30 min and sedimentation for 30 min, while in this work a rapid mixing for 1 min and sedimentation for 46 min was applied. In fact, a higher time of operation contributes to higher ammonia removal. However, for the same time of operation, the agitation step promotes the release of ammonia into the atmosphere when compared to the sedimentation step. Water and ammonia are polar molecules, so the ammonia has some capacity to remain in solution unless there is turbulence (i.e., greater contact between water and air, as occurs in the agitation operation). Therefore, IOSLM should be coupled to an ammonia capture system, not only to recover and reuse ammonia

(e.g. in the explosives industry since ammonia is one of the ingredients used) but also to avoid air pollution. As expected, no removal of nitrates is observed in the tested conditions, because nitrates are soluble ionic compounds in water (Wang et al., 2018).

Figure 2.2D shows the variation of sludge volume produced and the clarifying velocity as a function of the hydrated lime dose. Sludge volume shows a significant positive correlation with hydrated lime dose (r=0.65, P<0,001), but the sludge volume only increases linearly (r=0.99) up to the dose of 9.26 g L^{-1} of hydrated lime, reaching a maximum value of ca. 60 mL L^{-1}. After 9.26 g L^{-1} of lime added, the sludge volume tends to remain constant even after doubling the lime dose added, because of the sludge compaction caused by its weight. Clarifying velocity shows a significant negative correlation with hydrated lime dose (r=-0.76, P<0.001) and sludge volume (r=-0.87, P<0.001). The latter high correlation was expected since the high quantities of sludge produced imply the increase of collisions between particles, causing retardation of sedimentation and, therefore, a slower clarifying velocity.

The optimal hydrated lime dose is 7.76 g L^{-1} for this EW and the tested conditions. This dose was selected based on the supernatant quality (COD and conductivity removals), the volume of the sludge produced associated with the needs of the hydrated lime, and the characteristics that may contribute to the success of the next treatment (ammonia removal), such as pH. This dose removes 98.2% of oils and fats, 100% of organic nitrogen, 92.1% of COD, and 10.2% of ammonium ions. Since hydrated lime can globally cost around US$110-125/ton, approximately US$0.97/$m^3$ will be spent with hydrated lime to treat this EW for the optimal dose in the IOSLM process (Lee et al., 2014; Wei et al., 2018). This cost can be reduced if the sludges are reused by the calcination process and if this effluent is properly treated and reused in industry processes operation. Some possibilities for lime sludge valorization are application in building construction materials (Vashistha et al., 2019), biofuel (Rughoonundun and Holtzapple, 2017), and bioethanol production (Mendes et al., 2014).

2.3.3. Atmospheric CO_2 carbonation (AC) process

2.3.3.1. Influence of sludge on the atmospheric CO_2 carbonation process

The influence of the IOSLM sludge on the AC supernatant was evaluated through pH (Figure 2.3A) and Langelier Saturation Index (Figure 2.3B) and for all the hydrated lime doses applied. Figure 2.3A demonstrates that pH decreases during the atmospheric CO_2 carbonation with IOSLM sludge (between 0 and 14th days) for all the hydrated lime doses applied. This decrease is less evident for the highest dose (18.96 g L^{-1}) because the supernatant was buffered in IOSLM. After the removal of the sludge from the AC process (between the 14th and 16th days), a higher decrease in the supernatant pH is observed, for all the lime doses applied, when compared with the previous situation. Thus, the contact between the sludge and the supernatant slows down the pH decrease of the supernatant.

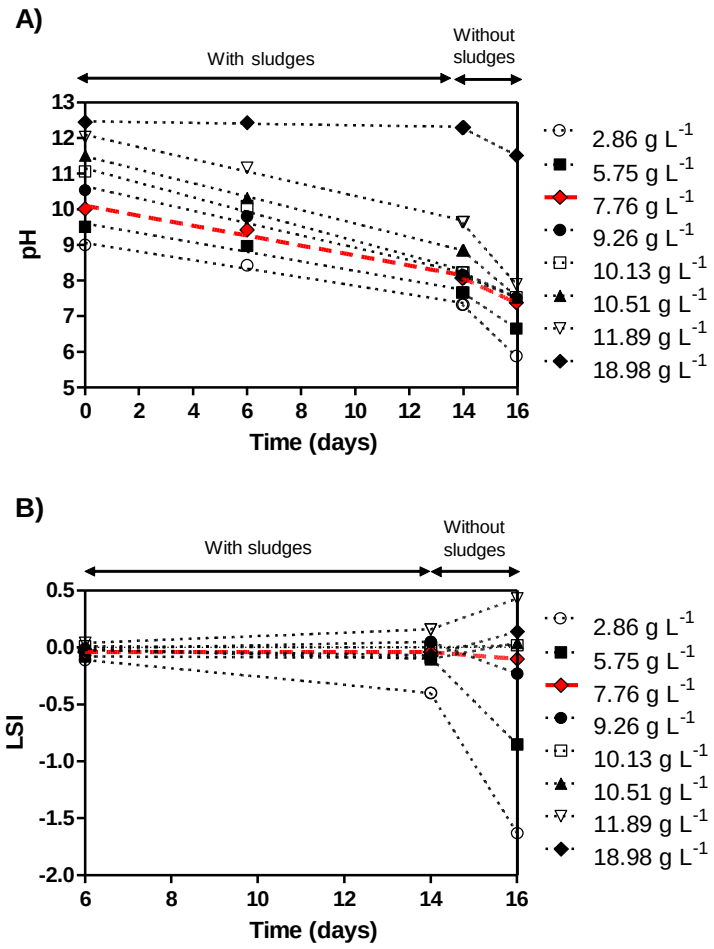

Figure 2.3 - Evolution of supernatant characteristics, in terms of **A**) pH and **B)** Langelier Saturation Index, for atmospheric CO_2 carbonation process, with and without sludges for different hydrated lime doses applied.

This observation can be an advantage for ammoniacal nitrogen removal since the sludge avoids a sudden drop in pH and, consequently, ammoniacal nitrogen will be in the form of ammonia for a longer time. As a result, ammonia can be captured in a separate process and reused in the explosives industry, for example. According to Eq. 1, the AC process must be applied for pH between 9.2 and 11, as proposed in ISOLM, where about 100% of the ammoniacal nitrogen is in the form of ammonia. However, after the removal of ammonia, sludge should be removed from the AC process because a rapid drop in pH is observed (Figure 2.3A). The pH range obtained ($6 < pH < 7.5$, Figure 2.3A) is considered optimal for some plants used in phytoremediation, as well as for soil microorganisms responsible for nitrification (pH 6.6 – 8.0) and denitrification (pH 6.0 – 8.0) processes (Vymazal, 2007). In the literature, no studies were found on the use of AC with sludge in wastewater treatment, so a new solution for ammonia recovery is presented. These results demonstrate that there are chemical equilibriums between sludge and supernatant, and between supernatant and atmospheric air during the AC process. However, even if a physical separation of these two phases (sludge and supernatant) is done and the supernatant is exposed again to the AC process, new residuals sludge could be formed or residual calcium carbonate in the supernatant could be dissolved, due to the chemical equilibrium with the atmosphere, and so a new chemical equilibrium between the supernatant and the new sludge will be restored, as can be seen in Figure 2.3B, particularly for lime doses of 2.86, 5.75, and 11.89 g L^{-1}, whose Langelier saturation index varied greatly on 16th day.

2.3.3.2. Optimised solution

The optimized integrated pre-treated solution was studied to guarantee the pH reduction and the removal of ammoniacal nitrogen and ammonia recovery of the low biodegradable wastewaters, which includes the best conditions obtained in ISOLM and AC processes. Thus, the optimal hydrated lime dose (7.76 g L^{-1}) from IOSLM and the 11 days of AC with the supernatant in contact with the sludge were tested.

According to Table 2.3, the AC time shows a significant negative correlation with pH ($r=-0.99$, $P<0.001$) and a significant positive correlation with redox potential ($r=0.97$, $P<0.001$). Figure 2.4A shows a pH decrease from 10 to 8.1, while the redox potential

increases from -14.8 to 118.5 mV, during experimental time. The observed decrease in pH over time is justified by the following reactions (Eqs. 7 to 10).

$$CO_2\ (g) \leftrightarrow CO_2\ (aq) \quad (7)$$

$$CO_2\ (aq) + H_2O\ (l) \leftrightarrow H_2CO_3\ (aq) \quad (8)$$

$$H_2CO_3 \leftrightarrow H^+ + HCO_3^- \quad (9)$$

$$HCO_3^- \leftrightarrow H^+ + CO_3^{2-} \quad (10)$$

Table 2.3 - Correlation matrix between parameters determined in atmospheric CO_2 carbonation process tests.

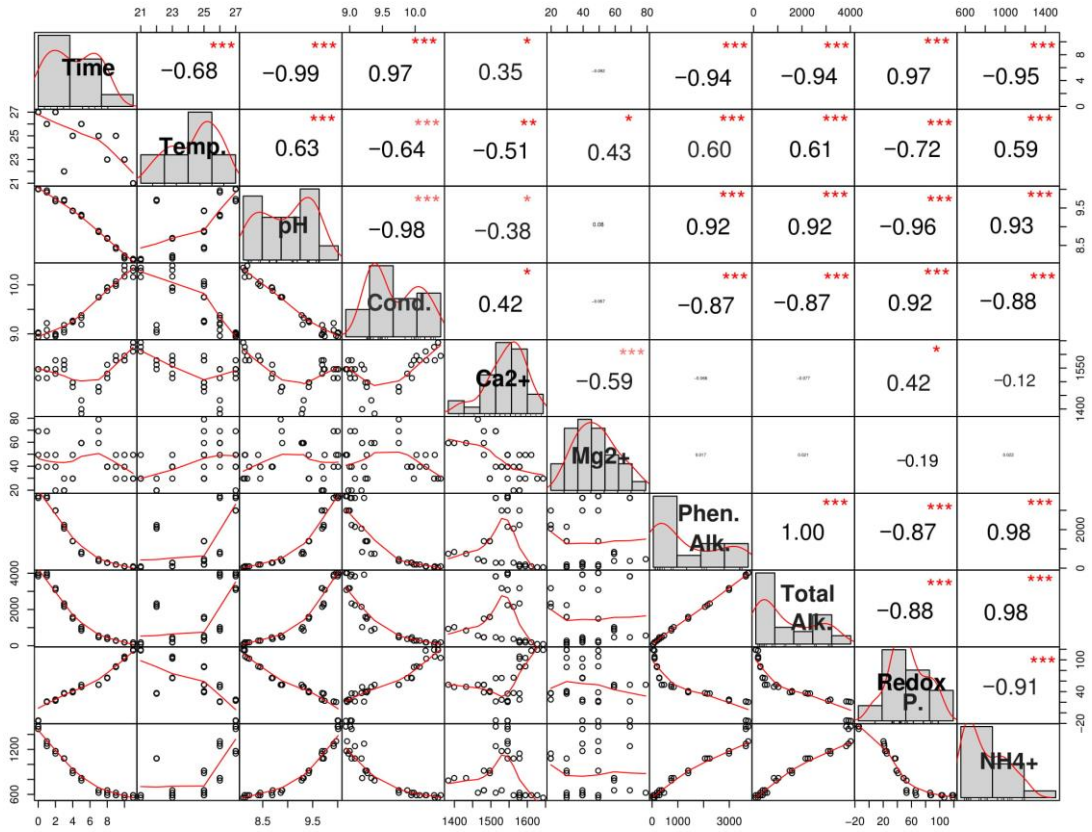

Notes: 1) Where it is written: "Temp", "cond.", "Phen. Alk", "Total Alk", and "Redox P." mean temperature, conductivity, Phenolphthalein Alkalinity, Total Alkalinity, and Redox Potential, respectively; 2) The distribution of each variable is shown on the diagonal. On the bottom of the diagonal: the bivariate scatter plots with a fitted line are displayed. On the top of the diagonal: the value of the correlation plus the significance level as stars. Each significance level is associated to a symbol : p-values(0, 0.001, 0.01, 0.05, 0.1, 1) <=> symbols("***", "**", "*", ".", " ").

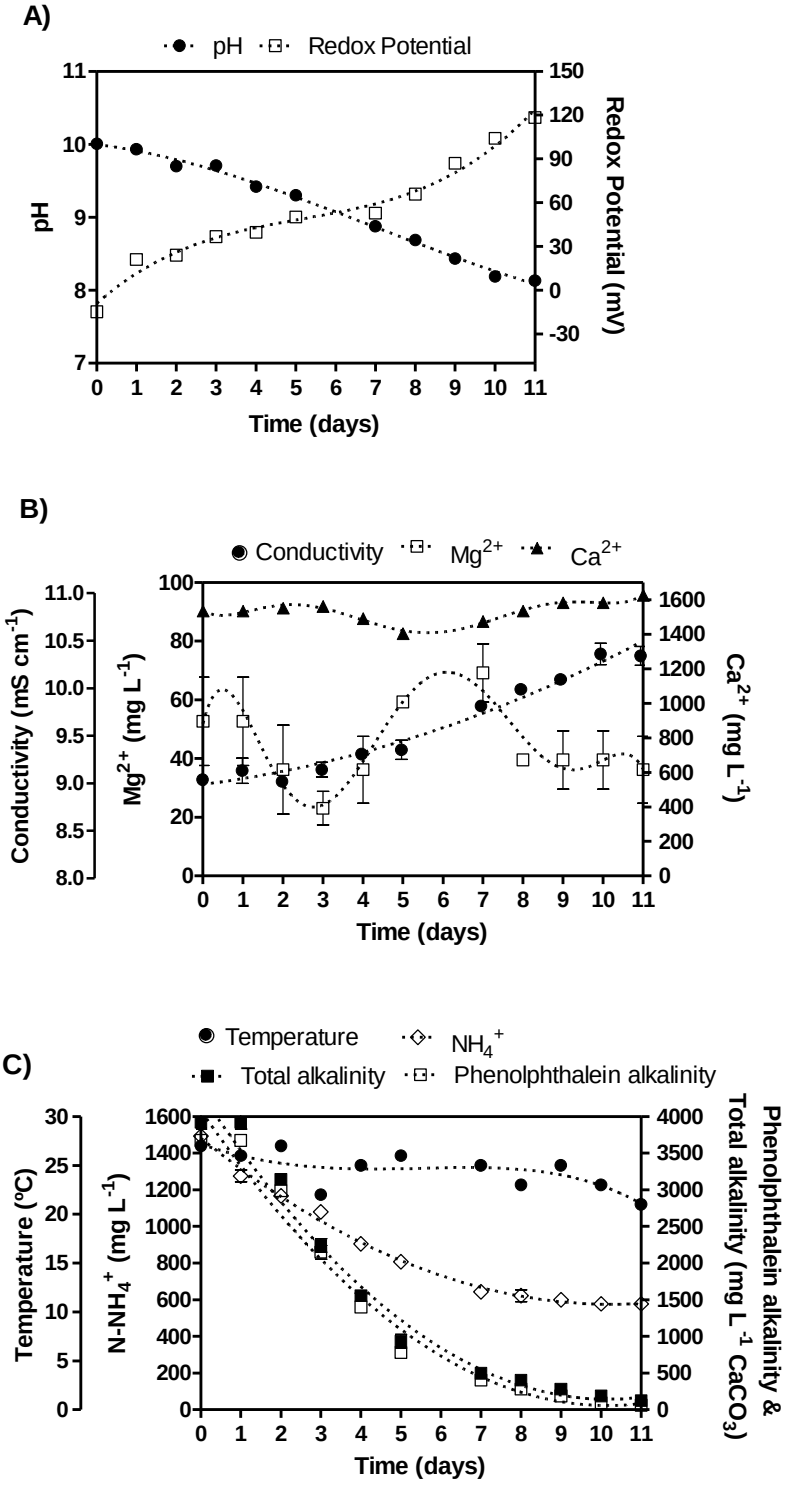

Figure 2.4 - Evolution of supernatant characteristics (EW treated with 7.76 g L^{-1} of hydrated lime) in terms of **A)** pH and redox potential; **B)** electrical conductivity, magnesium, and calcium concentration; and **C)** temperature, phenolphthalein alkalinity and total alkalinity and ammonium concentration, during 11 days of atmospheric CO_2 carbonation, in contact with the sludge.

The carbonic acid present in EW is totally consumed during the IOSLM to produce calcium carbonate (Eq. 4), causing a chemical disequilibrium of CO_2 between the supernatant and the atmosphere. As a way of counteracting this disequilibrium, the CO_2 present in the atmosphere tends to dissolve in the water through the water-air interface until reaching equilibrium (Eq. 7). During this phase, CO_2 dissolves in the effluent by combining with water molecules to form carbonic acid (Eq. 8) and then decomposes naturally into molecules of bicarbonate (Eq. 9) and carbonate (Eq. 10) producing hydrogen ions (H^+) and leading the pH decrease in the supernatant. When the equilibrium is reached, the pH will remain constant in the solution (Mihelcic et al., 2014). A decrease in pH during atmospheric CO_2 carbonation was also observed by Prazeres et al. (2016) using cheese whey wastewater but without sludge. The increase of redox potential is related to a pH decrease due to an increase in the concentration of hydrogen ions in solution (DeLaune and Reddy, 2005), which is confirmed by Table 2.3, whose correlation is negative and significant (r=-0.96, P<0.001). Redox potential influences the type of microbial metabolism developed and indicates the tendency of a given system to forward accepting electrons (if redox potential is positive) or donating electrons (if redox potential is negative), and predicting the stability of various compounds (Faulwetter et al., 2009; Reddy and DeLaune, 2008). Thus, at the end of 11 days, it is possible to obtain a supernatant with a pH very close to the ideal (pH = 8) and a redox potential within the appropriate range (i.e between 100 to 350 mV) for the occurrence of the denitrification process.

Conductivity and AC time are variables significantly and positively correlated (r=0.97, P<0.001), and conductivity increases from 9 to 10.3 mS cm^{-1} (Figure 2.4B), for 11 days. This increase may be related to evaporation phenomena and/or redissolution of ions (responsible for electrical conductivity) from sludge to the supernatant. According to Table 2.3, conductivity presents a weak correlation with calcium (r=0.42, P<0.05), and no correlation with magnesium is observed, as already obtained (section 2.3.2.). The calcium and magnesium concentrations vary between 1405 to 1627 mg L^{-1} and 23 to 69 mg L^{-1}, respectively, over time. The variation of calcium and magnesium in the supernatant is due to the complex interaction between sludge and supernatant, and between supernatant and atmosphere (explained in section 2.3.3.1.). Consequently, the dissolution rate (Eqs. 11 and 12) is higher or lower than the precipitation velocity (Eqs. 2 and 5) until an equilibrium is reached. It seems that this equilibrium is achieved from the

8th day since the concentration of calcium and magnesium tends to remain constant (Figure 2.4B). On the 11th day, the Langelier index value is -0.02±0.04, which means that the supernatant did not tend to precipitate, so it stabilized.

$$CaCO_3 + CO_2 + H_2O \rightarrow Ca^{2+} + 2HCO_3^- \quad (11)$$

$$MgCO_3 + CO_2 + H_2O \rightarrow Mg^{2+} + 2HCO_3^- \quad (12)$$

The influence of sludge on the supernatant during atmospheric carbonation has not been found in the literature for simultaneous pH and ammonia decreasing. Normally in water treatment systems that use softening, the addition of CO_2 to the water takes place soon, after the sludge is separated from the supernatant to convert the residual calcium carbonate into calcium bicarbonate (Davis, 2010).

Figure 2.4C shows that the total and phenolphthalein alkalinities decrease from 3923 to 125 mg $CaCO_3$ L^{-1} and 3674 to 62 mg $CaCO_3$ L^{-1}, respectively, for 11 days, with the same significant negative correlation (r=-0.94, P<0.001, Table 2.3). This decrease is mainly due to the hydroxides consumption during the reaction with atmospheric CO_2 and in the conversion of the ammonium ion to ammonia to maintain the chemical equilibrium NH_3/NH_4^+ (Eq. 1) which has been changing due to the loss of ammonia in the system (Lin et al., 2009). Ammonium concentration shows a significant negative correlation with AC time (r=-0.95, P<0.001, Table 2.3), and decreases from 1505 to 556 mg N-NH_4^+ L^{-1} over time, reaching a maximum removal of 61% and stabilizing at the 7th day of the experiment (Figure 2.4C). According to Berge et al. (2005), temperature and pH are two parameters that may influence the form of ammoniacal nitrogen (NH_3 or NH_4^+) in solution, and consequently its volatilization capacity. The temperature remained constant over time, around 24.5±2.0°C (Figure 2.4C), so the temperature has a weak and significant correlation with ammoniacal nitrogen (r=0.59, P<0.001, Table 2.3). Thus, pH is responsible for the observed decrease in the ammoniacal nitrogen concentration. In fact, when pH is above 9.25 the chemical balance (Eq. 1) is displaced in the direction of converting ammoniacal nitrogen into ammonia which favors the removal of ammoniacal nitrogen by volatilization of the ammonia. This equilibrium displacement decreases when the pH of the solution decreases to 9.25, reaching the same percentage of species NH_4^+ and NH_3 in the solution (Lin et al., 2009). Below pH 9.25, this equilibrium is displaced to the formation of ammonium ion, which is non-volatile so it remains in the solution (Lin

et al., 2009). On the 11th day, at pH=8.1 and 21°C, the percentage of ammonia is low (5.5%) compared with the ammonium ion (94.5%). So, the integrated treatment solution (IOSLM + AC) for the chosen hydrated lime dose can remove 62.8% of ammoniacal nitrogen. The collection and subsequent reuse of ammonia in the industry is an advantage since it will contribute to eliminate nitrification in biological treatment (i.e. to produce nitrate) and consequently in denitrification process organic matter may be added in fewer concentrations.

2.4. Conclusions

A novel integrated pre-treatment that combines immediate one-step lime precipitation (IOSLM) with atmospheric CO_2 carbonation (AC) in the presence of the sludge is proposed in this work. The integrated treatment, IOSLM and AC, was evaluated for low biodegradable organic matter and ammonia removal using ANFO and emulsion explosives wastewaters as a case study.

For the optimal hydrated lime dose (7.76 g L^{-1}), IOSLM removed 92.1% of organic matter, 98.2% of oils and fats, and 100 % of organic nitrogen, as well as reached the maximum conductivity reduction. However, as expected, it was not effective in ammonium nitrogen and nitrates removals, resulting in high concentrations of these compounds in the wastewater. These compounds are expected to be removed in the next sequence of treatment processes. AC process removed 61% of ammoniacal nitrogen in 7 days and pH decreased to approximately 8. Table 2.4 present the treated wastewater quality.

The proposed sequence is a low-cost and easy-to-apply wastewater treatment solution, since lime is a cheap product widely used in industry and wastewater treatment, and AC does not need chemicals or specialized maintenance and is a low energy consumption process. The idea of this integrated solution is to pre-treat wastewaters that can be used in subsequent conventional biological treatments, in green solutions like phytoremediation processes, or in the industry.

Table 2.4 - Characteristics of the treated effluent for the optimised conditions.

Parameters	Unit	
COD	mg O_2 L^{-1}	468±24
BOD_5	mg O_2 L^{-1}	3±1
BOD_5 / COD	-	0.006
Ammonium nitrogen	mg N-NH_4^+ L^{-1}	577.9±18.9
pH	Sorensen	8.13±0.02
Redox Potential	mV	118.5±0.78
Conductivity	mS cm^{-1}	10.3±0.1
Nitrates	mg L^{-1}	7230±50
Nitrites	mg N L^{-1}	11.0±0.1 3
Calcium hardness	mg L^{-1} $CaCO_3$	4068±40.7
Calcium	mg L^{-1}	1627
Total hardness	mg L^{-1} $CaCO_3$	4217±23.5
Magnesium hardness	mg L^{-1} $CaCO_3$	149.2
Magnesium	mg L^{-1}	36.2
Phenolphthalein alkalinity	mg L^{-1} $CaCO_3$	62.0±27.0
Total alkalinity	mg L^{-1} $CaCO_3$	125±53.9
Bicarbonate	mg L^{-1} $CaCO_3$	123.0±53.3
Carbonate	mg L^{-1} $CaCO_3$	1.40±0.66
Organic-N	mg N L^{-1}	Not detected
Oils and fats	mg L^{-1}	5.13
Total hydrocarbons	mg L^{-1}	5.34±0.12

2.5. References

Al-Sabagh, A.M., Hussien, M.A., Mishrif, M.R., El-Tabey, A.E., Elawady, A.A.A., 2017. Preparation and investigation of emulsion explosive matrix based on gas oil for mining process. J. Mol. Liq. 238, 198–207. https://doi.org/10.1016/j.molliq.2017.04.085

APHA, AWWA, WEF, 2012. Standard Methods for the Examination of Water and Wastewater, 22nd ed. American Public Health Association, Washington.

Berge, N.D., Reinhart, D.R., Townsend, T.G., 2005. The fate of nitrogen in bioreactor landfills. Crit. Rev. Environ. Sci. Technol. https://doi.org/10.1080/10643380590945003

Carboneras, M.B., Cañizares, P., Rodrigo, M.A., Villaseñor, J., Fernandez-Morales, F.J., 2018. Improving biodegradability of soil washing effluents using anodic oxidation. Bioresour. Technol. 252, 1–6. https://doi.org/10.1016/j.biortech.2017.12.060

Carvalho, M.F.N., Almeida, M.A.A., Teixeira, M.M.C.G.R., Prazeres, A.R., Chaves, H.M.I.T., Madeira, L.M.S., 2019. Process for treatment and recovery of waste water from explosive industries. EP 3339251B1.

Chan, G.Y.S., Chang, J., Kurniawan, T.A., Fu, C.X., Jiang, H., Je, Y., 2007. Removal of non-biodegradable compounds from stabilized leachate using VSEPRO membrane filtration. Desalination 202, 310–317. https://doi.org/10.1016/j.desal.2005.12.069

Chatterjee, S., Deb, U., Datta, S., Walther, C., Gupta, D.K., 2017. Common explosives (TNT, RDX, HMX) and their fate in the environment: Emphasizing bioremediation. Chemosphere 184, 438–451. https://doi.org/10.1016/J.CHEMOSPHERE.2017.06.008

Chen, Q., Luo, Z., Hills, C., Xue, G., Tyrer, M., 2009. Precipitation of heavy metals from wastewater using simulated flue gas: Sequent additions of fly ash, lime and carbon dioxide. Water Res. 43, 2605–2614. https://doi.org/10.1016/J.WATRES.2009.03.007

Davis, M.L., 2010. Water and wastewater engineering : design principles and practice, Profession. ed. McGraw-Hill, New York.

DeLaune, R.D., Reddy, K.R., 2005. Redox Potential. Encycl. Soils Environ. https://doi.org/10.1016/B0-12-348530-4/00212-5

Dowling, A., O'Dwyer, J., Adley, C.C., 2015. Lime in the limelight. J. Clean. Prod. https://doi.org/10.1016/j.jclepro.2014.12.047

Faulwetter, J.L., Gagnon, V., Sundberg, C., Chazarenc, F., Burr, M.D., Brisson, J., Camper, A.K., Stein, O.R., 2009. Microbial processes influencing performance of treatment wetlands: A review. Ecol. Eng. 35, 987–1004. https://doi.org/10.1016/j.ecoleng.2008.12.030

Georgiou, D., Liliopoulos, V., Aivasidis, A., 2019. Investigation of an integrated treatment technique for anaerobically digested animal manure: Lime reaction and settling, ammonia stripping and neutralization by biogas scrubbing. Bioresour. Technol. Reports 5, 127–133. https://doi.org/10.1016/J.BITEB.2019.01.001

Ghafari, S., Hasan, M., Aroua, M.K., 2008. Bio-electrochemical removal of nitrate from water and wastewater-A review. Bioresour. Technol. https://doi.org/10.1016/j.biortech.2007.05.026

Ghoreishi, S.M., Haghighi, R., 2003. Chemical catalytic reaction and biological oxidation for treatment of non-biodegradable textile effluent. Chem. Eng. J. 95, 163–169. https://doi.org/10.1016/S1385-8947(03)00100-1

Gulyas, H., 1997. Processes for the removal of recalcitrant organics from industrial wastewaters. Water Sci. Technol. 36, 9–16. https://doi.org/10.1016/S0273-1223(97)00364-8

Hernandes, V.V., Franco, M.F., Santos, J.M., Melendez-Perez, J.J., Morais, D.R. de, Rocha, W.F. de C., Borges, R., de Souza, W., Zacca, J.J., Lograd o, L.P.L., Eberlin, M.N., Correa, D.N., 2015. Characterization of ANFO explosive by high accuracy ESI(±)-FTMS with forensic identification on real samples by EASI(-)-MS. Forensic Sci. Int. 249, 156–164. https://doi.org/10.1016/j.forsciint.2015.01.006

Lee, C.S., Robinson, J., Chong, M.F., 2014. A review on application of flocculants in wastewater treatment. Process Saf. Environ. Prot. https://doi.org/10.1016/j.psep.2014.04.010

Lin, L., Yuan, S., Lin, L., Yuan, S., Chen, J., Xu, Z., Lu, X., 2009. Removal of ammonia nitrogen in wastewater by microwave radiation. J. Hazard. Mater. 161, 1063–1068. https://doi.org/10.1016/j.jhazmat.2008.04.053

Mariliz, G., Benventuri, J., Fontoura, S., Ortiz-Monsalve, S., 2015. Characterization of raw wastewater from tanneries. J. Soc. Leather Technol. Chem. 99, 280–287.

Martin, W.A., Larson, S.L., Nestler, C.C., Fabian, G., O'Connor, G., Felt, D.R., 2012. Hydrated lime for metals immobilization and explosives transformation: Treatability study. J. Hazard. Mater. 215–216, 280–286. https://doi.org/10.1016/j.jhazmat.2012.02.066

Mendes, C.V.T., Rocha, J.M.S., Carvalho, M.G.V.S., 2014. Valorization of residual streams from pulp and paper mills: Pretreatment and bioconversion of primary sludge to bioethanol. Ind. Eng. Chem. Res. 53, 19398–19404. https://doi.org/10.1021/IE503021Y/ASSET/IMAGES/LARGE/IE-2014-03021Y_0003.JPEG

Mihelcic, J.R., Zimmerman, J.B., Auer, M.T., 2014. Environmental engineering : fundamentals, sustainability, design, 2nd ed. Wiley Global Education.

Monteiro, M.I.C., Ferreira, F.N., De Oliveira, N.M.M., Ávila, A.K., 2003. Simplified version of the sodium salicylate method for analysis of nitrate in drinking waters. Anal. Chim. Acta 477, 125–129. https://doi.org/10.1016/S0003-2670(02)01395-8

Park, J. Y., Shiroma, R., Al-Haq, M. I., Zhang, Y., Ike, M., Arai-Sanoh, Y., Ida, A., Kondo, M., & Tokuyasu, K. (2010). A novel lime pretreatment for subsequent bioethanol production from rice straw - Calcium capturing by carbonation (CaCCO) process. Bioresource Technology, 101(17), 6805–6811. https://doi.org/10.1016/j.biortech.2010.03.098

Prazeres, A.R., Lelis, J., Alves-Ferreira, J., Carvalho, F., 2019. Treatment of vinasse from sugarcane ethanol industry: H_2SO_4, NaOH and $Ca(OH)_2$ precipitations, $FeCl_3$ coagulation-flocculation and atmospheric CO_2 carbonation. J. Environ. Chem. Eng. 7, 103203. https://doi.org/10.1016/j.jece.2019.103203

Prazeres, A.R., Rivas, J., Paulo, Ú., Ruas, F., Carvalho, F., 2016. Sustainable treatment of different high-strength cheese whey wastewaters: an innovative approach for atmospheric CO_2 mitigation and fertilizer production. Environ. Sci. Pollut. Res. Int. 23, 13062–75. https://doi.org/10.1007/s11356-016-6429-3

Ramalho, R.S., 1996. Tratamiento de aguas residuals, Revisada. ed. Editorial Reverté, S. A., Barcelona, España.

Reddy, K.R., DeLaune, R.D., 2008. Biogeochemistry of wetlands: science and applications, Biogeochemistry of Wetlands. CRC Press, Taylor & Francis Group, Boca Raton, New York. https://doi.org/10.1201/9780203491454

Ren, G., Zhou, M., Zhang, Q., Xu, X., Li, Y., Su, P., Paidar, M., Bouzek, K., 2019. Cost-efficient improvement of coking wastewater biodegradability by multi-stages flow through peroxi-coagulation under low current load. Water Res. 154, 336–348. https://doi.org/10.1016/j.watres.2019.02.013

Renou, S., Givaudan, J.G., Poulain, S., Dirassouyan, F., Moulin, P., 2008a. Landfill leachate treatment: Review and opportunity. J. Hazard. Mater. 150, 468–493. https://doi.org/10.1016/j.jhazmat.2007.09.077

Renou, S., Poulain, S., Givaudan, J.G., Moulin, P., 2009. Amelioration of ultrafiltration process by lime treatment: Case of landfill leachate. Desalination 249, 72–82. https://doi.org/10.1016/j.desal.2008.09.007

Renou, S., Poulain, S., Givaudan, J.G., Moulin, P., 2008b. Treatment process adapted to stabilized leachates: Lime precipitation-prefiltration-reverse osmosis. J. Memb. Sci. 313, 9–22. https://doi.org/10.1016/j.memsci.2007.11.023

Rodríguez, J., Castrillón, L., Marañón, E., Sastre, H., Fernández, E., 2004. Removal of non-biodegradable organic matter from landfill leachates by adsorption. Water Res. 38, 3297–3303. https://doi.org/10.1016/j.watres.2004.04.032

Rounds, S.A., 2012. Chapter A6. Section 6.6. Alkalinity and acid neutralizing capacity, U.S. Geological Survey Techniques of Water-Resources Investigations, Book 9. https://doi.org/10.3133/twri09A6.6

Rughoonundun, H., Holtzapple, M.T., 2017. Converting wastewater sludge and lime-treated sugarcane bagasse to mixed carboxylic acids – a potential pathway to ethanol biofuel production. Biomass and Bioenergy 105, 73–82. https://doi.org/10.1016/J.BIOMBIOE.2017.06.007

Satsangi, S., 2016. Industrial Explosives Market by Type, End-use Industry - Global Opportunity Analyses and Industry Forecast 2014-2022. Portland, United States.

Sawyer, C.N., McCarty, P.L., Parkin, G.F., 2003. Chemistry for Environmental Engineering, 5th ed. McGraw-Hill, Inc., New York, United States.

Schoch, S., Nikiforakis, N., Lee, B.J., Saurel, R., 2013. Multi-phase simulation of ammonium nitrate emulsion detonations. Combust. Flame 160, 1883–1899. https://doi.org/10.1016/j.combustflame.2013.03.033

Schröder, H.F., 1996. Non-biodegradable wastewater compounds treated by ozone or ozone/UV - Conversion monitoring by substance-specific analysis and biotoxicity testing. Water Sci. Technol. 33, 331–338. https://doi.org/10.1016/0273-1223(96)00283-1

U.S. EPA, 2000. Wastewater Technology Fact Sheet: Chemical Precipitation. Washington, D.C.

Van Leeuwen, J., Sridhar, A., Harrata, A.K., Esplugas, M., Onuki, S., Cai, L., Koziel, J.A., 2009. Improving the biodegradation of organic pollutants with ozonation during biological wastewater treatment. Ozone Sci. Eng. 31, 63–70. https://doi.org/10.1080/01919510802668380

Vashistha, P., Kumar, V., Singh, S.K., Dutt, D., Tomar, G., Yadav, P., 2019. Valorization of paper mill lime sludge via application in building construction materials: A review. Constr. Build. Mater. https://doi.org/10.1016/j.conbuildmat.2019.03.085

Vijaya Chitra, A., Lakshmanaperumalsamy, P., 2006. Biodegradation of nitrate in wastestreams from explosives manufacturing plants. Res. J. Microbiol. 1, 142–151. https://doi.org/10.3923/jm.2006.142.151

Vymazal, J., 2007. Removal of nutrients in various types of constructed wetlands. Sci. Total Environ. 380, 48–65. https://doi.org/10.1016/j.scitotenv.2006.09.014

Wang, H.J., Gong, W.X., Liu, R.P., Liu, H.J., Qu, J.H., 2011. Treatment of high arsenic content wastewater by a combined physical–chemical process. Colloids Surfaces A Physicochem. Eng. Asp. 379, 116–120. https://doi.org/10.1016/J.COLSURFA.2010.11.047

Wang, L., Hung, Y.T., Shammas, N.K., 2005. Physicochemical Treatment Processes, Physicochemical Treatment Processes. Humana Press, New Jersey. https://doi.org/10.5772/63666

Wang, Z., Jiang, Y., Awasthi, M.K., Wang, J., Yang, X., Amjad, A., Wang, Q., Lahori, A.H., Zhang, Z., 2018. Nitrate removal by combined heterotrophic and autotrophic denitrification processes: Impact of coexistent ions. Bioresour. Technol. 250, 838–845. https://doi.org/10.1016/j.biortech.2017.12.009

Wei, H., Gao, B., Ren, J., Li, A., Yang, H., 2018. Coagulation/flocculation in dewatering of sludge: A review. Water Res. 143, 608–631. https://doi.org/10.1016/J.WATRES.2018.07.029

Yuan, M.H., Chen, Y.H., Tsai, J.Y., Chang, C.Y., 2016. Ammonia removal from ammonia-rich wastewater by air stripping using a rotating packed bed. Process Saf. Environ. Prot. 102, 777–785. https://doi.org/10.1016/j.psep.2016.06.021

Zayen, A., Schories, G., Sayadi, S., 2016. Incorporation of an anaerobic digestion step in a multistage treatment system for sanitary landfill leachate. Waste Manag. 53, 32–39. https://doi.org/10.1016/j.wasman.2016.04.030

Zodi, S., Louvet, J.N., Michon, C., Potier, O., Pons, M.N., Lapicque, F., Leclerc, J.P., 2011. Electrocoagulation as a tertiary treatment for paper mill wastewater: Removal of non-biodegradable organic pollution and arsenic. Sep. Purif. Technol. 81, 62–68. https://doi.org/10.1016/J.SEPPUR.2011.07.002

Chapter 3

Optimization of atmospheric carbonation in the integrated treatment immediate one-step lime precipitation and atmospheric carbonation. The case study of slaughterhouse effluents

This Chapter was published in:

Madeira, L., Carvalho, F., Almeida, A., Ribau Teixeira, M. (2023). Optimization of atmospheric carbonation in the integrated treatment immediate one-step lime precipitation and atmospheric carbonation. The case study of slaughterhouse effluents. Results Eng. 17, 100807. https://doi.org/10.1016/j.rineng.2022.100807

ABSTRACT

Long carbonation time has been a common feature in the integrated process composed of immediate one-step lime precipitation and atmospheric carbonation. This work aims to understand how carbonation time can be influenced by reaction pH, as well as how reactor area/volume ratio affects carbonation time and ammonia removal, using slaughterhouse wastewater due to its variable characteristics. In the integrated immediate one-step lime precipitation and atmospheric carbonation process, the immediate one-step lime precipitation results showed that the reaction pH and the type of slaughterhouse wastewater influenced the removal, however, removals were the highest at reaction pH 12. In the atmospheric carbonation process, the carbonation time required to reach pH 8 was independent of the reaction pH used. Additionally, at reaction pH 12, the reactor area/volume ratios applied (from 0 to 155.4 m^2/m^3) showed that higher reactor area/volume ratios caused lower carbonation time, but ammonia removal was not affected. For reactor area/volume ratios of 5 and 155.4 m^2/m^3, 15 and 1 days were spent to reduce the pH from 11.9 to 8.2, with removals of 71 and 82.6% for NH_4^+ and 10 and 79.1% for calcium, respectively. High removals of total Kjeldahl nitrogen (≥71%), biological oxygen demand (≥80%), ammonium nitrogen (≥52%), total phosphorus (98%), total suspended solids (≥52%), turbidity (≥62%), absorbance at 254 nm (≥87%), absorbance at 410 nm (≥83%) and oils & fats (≥47%) were obtained using immediate one-step lime precipitation and atmospheric carbonation integrated process to treatment slaughterhouse wastewater, indicating that this process is an efficient pretreatment for slaughterhouse wastewaters.

3.1. Introduction

Although most municipal wastewater treatment plants are capable of removing biodegradable compounds (e.g. organic matter, phosphorus, and nitrogen), they are not designed to remove high concentrations of these compounds, so on-site pre-treatment is required (Ajala et al., 2022; Iloms et al., 2020). The integrated process, immediate one-step lime precipitation (IOSLM) followed by atmospheric carbonation (AC), has been used as a pretreatment for industrial wastewaters, such as explosives (Madeira et al. (2020), chapter 2), vinasse from sugarcane ethanol industry (Prazeres et al., 2019b), winery (Luz et al., 2021), cheese whey (Prazeres et al., 2016), urban wastewaters (Correia et al., 2020), and landfill leachate (Ramalho et al., 2022). This integrated solution is recognized for its low cost, simplicity, eco-friendly technology, and high efficiency in removing contaminants, like organic matter and nitrogen (Madeira et al. (2020), chapter 2). However, this treatment process needs to be studied in detail, since the ability of the atmospheric CO_2 to be transferred to the aqueous phase depends on factors, such as concentration of CO_2 in the atmosphere, area at gas-liquid interface, contact time, and solution properties (including pH, temperature, concentration of dissolved salts, and others) (Viswanaathan et al. (2022)). Lately, the capture of atmospheric CO_2 has deserved the attention of several researchers (Odunlami et al., 2022). In the AC process, the atmospheric CO_2 is transferred to the aqueous phase reducing the pH, but long retention times are needed to reduce the pH of the effluent (Ramalho et al., 2022). Madeira et al. (2020) (chapter 2) and Prazeres et al. (2019b) observed that the AC process in the presence of sludge precipitate (resulting from the IOSLM process) needs a long time to reduce the pH from 12 to 8, but significant advantages in the removal of ammoniacal nitrogen were observed (Madeira et al. (2020), chapter 2). On the other hand, Correia et al. (2020) observed that the injection of air (at 85 L h^{-1}) to urban effluent treated by IOSLM, in the presence of the sludge IOSLM precipitate, reduced the carbonatation time from 220 to 100 hours to reduce the pH from 11.5 to 8, but its effect on ammonia removal was not analyzed. Even so, aeration systems have been recognized as a significant energy cost in wastewater treatment plants (Aziz et al., 2019; Chen et al., 2022). In addition, since the transfer of CO_2 to water must be maximized, the reactor area/volume (A/V) ratio in the AC process is very important. According to the literature, low reactor A/V ratios such as 3.78 m^2/m^3 (Madeira et al. (2020), chapter 2), 6.23 m^2/m^3 (Prazeres et al., 2019b),

4.63 m^2/m^3 (Prazeres et al., 2016), 5.00 m^2/m^3 (Correia et al., 2020), and 5.00 to 6.67 m^2/m^3 (Ramalho et al., 2022) have been used in the AC process. However, it is not possible to establish any relationship between these reactors' A/V ratios and the carbonation time, as the characteristics of effluent (e.g. pH, temperature, nitrogen, and organic contents) and experimental conditions were different among the various authors. Therefore, the effect of high reactor A/V ratios on the carbonation time of the AC process and hence its effect on ammonia removal is unknown.

This work aims to fill these gaps in the integrated IOSLM and AC process, namely evaluate the effect of the reaction pH and reactor A/V ratio on the carbonation time and ammonium nitrogen removal. Slaughterhouse wastewater was used as a case study, given that current slaughterhouse coagulation pre-treatment systems use coagulants (such as ferric chloride or ferric sulfate) (Bustillo-Lecompte and Mehrvar, 2017) that do not remove ammonium nitrogen (Aguilar et al., 2002). Thus, the subsequent treatment processes, such as biological treatments (e.g. activated sludge) or constructed wetlands, need alternating aerobic and anoxic phases and consequently, a longer hydraulic retention time, to effectively remove ammonium nitrogen and organic matter, as heterotrophic and nitrifying bacteria compete for available oxygen (Madeira et al. (2021), chapter 5). This effluent is recognized for the great variability in its composition (for organic matter, nitrogen and total phosphorus (TP), and total suspended solids (TSS)) due to the number and type of animals slaughtered, and water consumption (Al Smadi et al., 2019; Bustillo-Lecompte and Mehrvar, 2017; Njoya et al., 2019). Lime precipitation has been applied by several authors in slaughterhouse wastewater treatment (Hossaini et al., 2013; Mahtab et al., 2009; Satyanarayan et al., 2005; Tariq et al., 2012), but this treatment has never been integrated with the AC process, neither the impact of different slaughterhouse wastewater characteristics. In this way, this work also intends to know if the reaction pH can be a determining factor in the treatment of slaughterhouse wastewater with variable characteristics.

3.2. Materials and Methods

3.2.1. Slaughterhouse wastewater sampling

Slaughterhouse wastewater (SWW) used in this study is Portuguese on-site wastewater that resulted from the slaughtering process (cattle, pigs, goats, sheep, and ratite) and the cleaning facilities. The slaughterhouse wastewater is pretreated in an on-site pretreatment plant (SWPP), after which is discharged to the municipal sewage treatment plant (MSTP). Three slaughterhouse wastewaters coming from different SWPP stages were studied: SWW1 was collected in the aeration and homogenization tank, SWW2 was collected at the output of the rotary drum screen filter, and SWW3 was collected at the output of the flocculation/dissolved air flotation (DAF) system. All samples were collected during working hours and only once. If not immediately analyzed, the collected samples were stored at 4 ºC until use. Table 3.1 shows the SWW1, SWW2, and SWW3 physicochemical characterization.

Table 3.1 – Physicochemical characterization of SWW1, SWW2, and SWW3 effluents.

Parameters	Unit	SWW1	SWW2	SWW3
pH	Sorensen	7.2±0.1	7.2±0.2	7.5±0.1
Conductivity	mS cm^{-1}	3.1±0.3	3.0±0.1	3.0±0.1
COD	mg O_2 L^{-1}	5430±1646	1810±274	226±41
SCOD	mg O_2 L^{-1}	172±38	450±47	183±2
BOD_5	mg O_2 L^{-1}	2813±208	1013±29	40±0
BOD_5/COD	-	0.52±0.16	0.56±0.09	0.18±0.03
TKN	mg N-Kj. L^{-1}	212±2	97±2	58±0
COD/TKN	-	25.6	18.7	3.9
NH_4^+	mg N L^{-1}	88±1	69±0	52±0
Organic-N	mg N L^{-1}	124±2	28±2	6±0
TP	mg L^{-1}	491.6±89.6	255.6±90.1	147.6±12.0
TSS	mg L^{-1}	3703±10	848±17	61±7
Turbidity	NTU	1193±84	469±42	17±6
STurbidity	NTU	24±1	38±1	11±1
Abs. at 254 nm	cm^{-1}	1.659±0.298	0.884±0.150	0.198±0.040
Abs. at 410 nm	cm^{-1}	2.072±0.295	1.471±0.296	0.314±0.099
Oils & Fats	mg L^{-1}	1736±170	376±96	86±8
P. Alkalinity	mg $CaCO_3$ L^{-1}	0±0	0±0	0±0
T. Alkalinity	mg $CaCO_3$ L^{-1}	560±16	675±16	583±16
Calcium	mg L^{-1}	101.2±6.0	158.7±6.9	190.5±0.0
Magnesium	mg L^{-1}	54.1±3.6	74.6±4.2	60.2±4.2
Color	-	dark brown	dark brown	yellowish
Odor	-	unpleasant	unpleasant	slight smell

Note: COD - chemical oxygen demand; SCOD - soluble chemical oxygen demand total; BOD - biological oxygen demand; TKN – total Kjeldahl nitrogen; TP - total phosphorus; TSS - total suspended solids; STurbidity – soluble turbidity; P. Alkalinity - phenolphthalein alkalinity; T. Alkalinity - total alkalinity.

3.2.2. Experimental set-up

The experimental set-up used in this work is presented in Figure 3.1, which includes the IOSLM followed by the AC process.

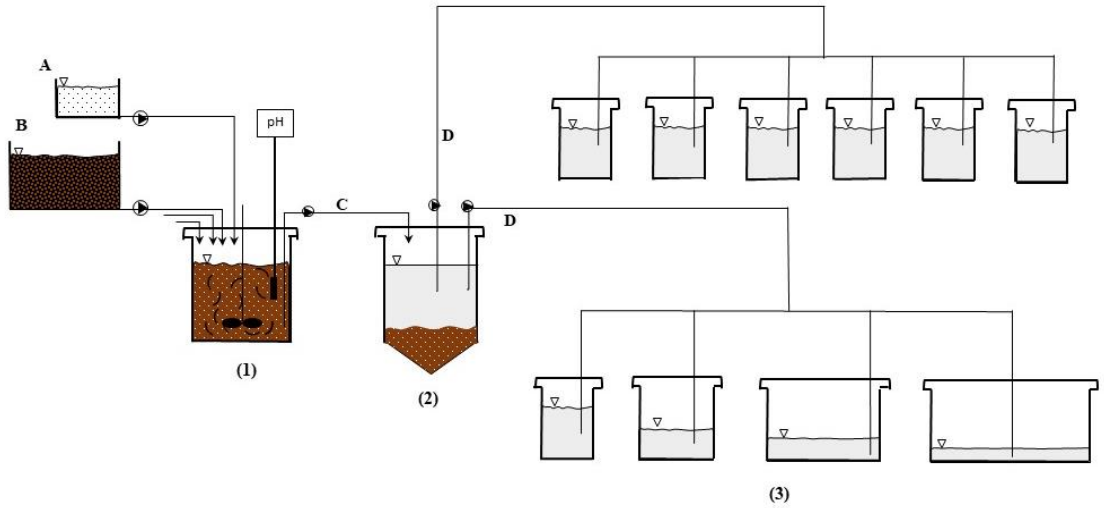

Figure 3.1 – Schematic diagram of the treatment processes used in this work, namely, (1) IOSLM process, (2) sedimentation process, and (3) AC process. A – hydrated lime tank, B – SWW tank, C – IOSLM effluent, D – supernatant.

3.2.2.1. Immediate one-step lime precipitation (IOSLM)

The IOSLM process is already described in Madeira et al. (2020) (chapter 2). Various hydrated lime concentrations were added to pretreated wastewaters SWW1, SWW2, and SWW3, drop by drop, under vigorous agitation (magnetic stirrer at speed of 3 s^{-1}) and agitation was maintained until precipitation pH reached, from 9.5 to 12 (called in this work reaction pH). The agitation was kept for 1 min and then stopped, and the effluent was transferred to the sedimentation tank (without agitation) for 1 hour. After that, the physicochemical characteristics of the supernatant were analyzed (section 3.2.3.) and the effluent passed to the AC process. Calcium hydroxide (≥95%, PanReac S.A) was used to prepare the hydrated lime solution at a concentration of 200 g L^{-1}.

3.2.2.2. Atmospheric CO_2 carbonation (AC) tests

In all these experiments, 1 to 2 L of IOSLM supernatants from SWW1, SWW2, and SWW3 were tested and applied to AC reactors. Three AC tests were made. In the first set of experiments, the carbonation time was studied for the different IOSLM supernatants and pH (from 9.5 to 12) and was tested in AC reactors with 9.5 m^2/m^3 of A/V ratio for SWW1 supernatant, and 5 m^2/m^3 for SWW2 and SWW3 supernatants. In the second set, the supernatant pHs were maintained at 12 and the carbonation time was studied for different reactors' area/volume (A/V) ratios, from 0 to 155.4 m^2/m^3. Finally, in the third experimental set, the best conditions were studied to maximize ammonium removal. In all experiments, the IOSLM supernatants were kept in contact with atmospheric air without any chemical and agitation. Process efficiency was monitored (section 3.2.3.) over time, once a day, until the supernatant pH was close to 8 or kept constant over time. All AC tests were at room temperature 23 ± 2ºC.

Subsequently, to estimate the amount of atmospheric CO_2 captured during the carbonation process, the IOSLM supernatant at pH 12 was neutralized with different volumes of pure CO_2 from a CO_2 cylinder (CEVIK brand), and the pH obtained was recorded. CO_2 was quantified by Stevin's law and the ideal gas law, applying the sample in a U-Tube attached to a CO_2 bottle and subsequent vigorous mixing between the added CO_2 gas and the sample.

3.2.3. Analytical methods

The parameters and methods used are shown in Table 3.2. Chemical oxygen demand (COD), total Kjeldahl nitrogen (TKN), ammonium nitrogen (NH_4^+), total phosphorus (TP), total suspended solids (TSS), oils and fats, biological oxygen demand (BOD), calcium, magnesium, phenolphthalein alkalinity, total alkalinity, and turbidity were determined according to Standard Methods (Baird et al., 2017). Absorbance at 410 nm indicates the presence of compounds responsible for color, while absorbance at 254 nm indicates the presence of high molecular weight organic compounds with a high degree of aromaticity, high number of double and triple bonds, and phenolic groups (Rivas et al., 2010).

Table 3.2 – The parameters analyzed and analytical methods used.

Parameters	Method	Equipment
pH	Potentiometric method	WTW InoLab pH Level 1 apparatus and a pH electrode SenTix® 41
Conductivity	Electrometric method	Jenway 4510 conductivity meter and a conductivity sensor VWR phenomenal CO 11
COD and SCOD	Closed reflux colorimetric method	COD digester WPA Hydrocheck HC 6016, UV/Vis spectrophotometer Pharmacia Biotech Ultrospec 2000; 0.45-µm pore-size filter for soluble COD.
BOD_5	Respirometric method	WTW OxiTop® IS 12 system
TKN	Kjeldahl method	Digester Bloc Digest 6 P-Selecta; distillation unit BUCHI B-316
NH_4^+	Distillation method	Distillation unit BUCHI B-316
TP	Vanadomolybdophosphoric acid colorimetric method	Muffle P SELECTA-HORN 186331, UV/Vis spectrophotometer Pharmacia Biotech Ultrospec 2000
TSS	Gravimetric method	Whatman® glass microfiber filters (Grade 934-AH®)
Turbidity and STurbidity	Nephelometric method	HACH 2100N turbidimeter; 0.45-µm pore-size filter for soluble turbidity.
Abs. at 254 nm	Spectroscopic method	UV/Vis spectrophotometer Pharmacia Biotech Ultrospec 2000
Abs. at 410 nm	Spectroscopic method	UV/Vis spectrophotometer Pharmacia Biotech Ultrospec 2000
Oils and Fats	Gravimetric method	Soxhlet extractor with petroleum ether and Soxhlet heating mantles electrothermal EM O250/CE
P. Alkalinity	Neutralization titration	
T. Alkalinity	Neutralization titration	
Calcium	Volumetric complexation with EDTA	
Magnesium	Difference between total hardness and calcium hardness. Total hardness determined by Volumetric complexation with EDTA.	

Note: P. Alkalinity - phenolphthalein alkalinity; T. Alkalinity - total alkalinity; SCOD – soluble COD; STurbidity – soluble turbidity.

3.2.4. Statistical analysis

All samples and experimental treatments were analyzed in triplicate, and the results were presented as means ± standard deviation. For comparison between averages, the data were submitted to One-way ANOVA with Tukey's test at a 95% confidence level, using IBM SPSS Statistics for Windows. Principal component analysis (PCA) and correlation analysis were performed using the XLSTAT 2021 statistical software. GraphPad Prism for Windows (version 5.0, GraphPad Software, La Jolla California USA) was used to draw the graphs.

3.3. Results and discussion

3.3.1. Physicochemical characterization of SWW

SWW physicochemical characteristics are shown in Table 3.1. Briefly, the COD concentrations vary according to the collected place at SWPP, being the highest COD concentrations for SWW1 (5430 ± 1646 mg O_2 L^{-1}) and the lowest for SWW3 (226 ± 41 mg O_2 L^{-1}). SWW1 and SWW2 organic matter are in an insoluble form, while SWW3 organic matter is practically soluble. The biodegradability index (BOD_5/COD ratio) of SWW1 and SWW2 is around 0.5, similar to Al Smadi et al. (2019), which means that these effluents have moderate biodegradability. SWW3 has a low BOD_5/COD ratio (around 0.18), which according to Dinçer (2020) it is not possible to treat using conventional biological treatments. For nitrogen, all SWW present considerable values of TKN (58 to 212 mg TKN L^{-1}), either in the form of ammonia (52 to 88 mg N-NH_4^+ L^{-1}) or organic nitrogen (6 to 124 mg N L^{-1}), as well as rich in phosphorus (148 to 492 mg L^{-1}). Turbidity values are high in SWW1 (1193 ± 84 NTU) and SWW2 (469 ± 42 NTU), and much lower in SWW3 (17 ± 6 NTU), which is excepted since this wastewater was collected after flocculation/DAF processes. The presence of aromatic and unsaturated compounds given by absorbance at 254 nm (Table 3.1) is common in SWW due to the use of pharmaceutical drugs (Aguilar et al., 2006; Shao et al., 2009). Other SWW characteristics can be seen in Table 3.1.

3.3.2. Immediate one-step lime precipitation (IOSLM)

The supernatant quality and removals after IOSLM are presented in Figures 3.2 and 3.3. For TKN, NH_4^+, organic-N, and COD removals practically did not vary with reaction pH for all the studied waters. After the IOSLM, the supernatants' quality was very similar between reaction pHs in each SWW but different between SWW, because the initial concentrations of these parameters were different between SWW (Figure 3.2). Thus, for these parameters, the final supernatant quality is not dependent on reaction pH, and it seems that lower pH may be used in the IOSLM process (pH of 9.5). This is very important in sludge production and consumption (Figure 3.4).

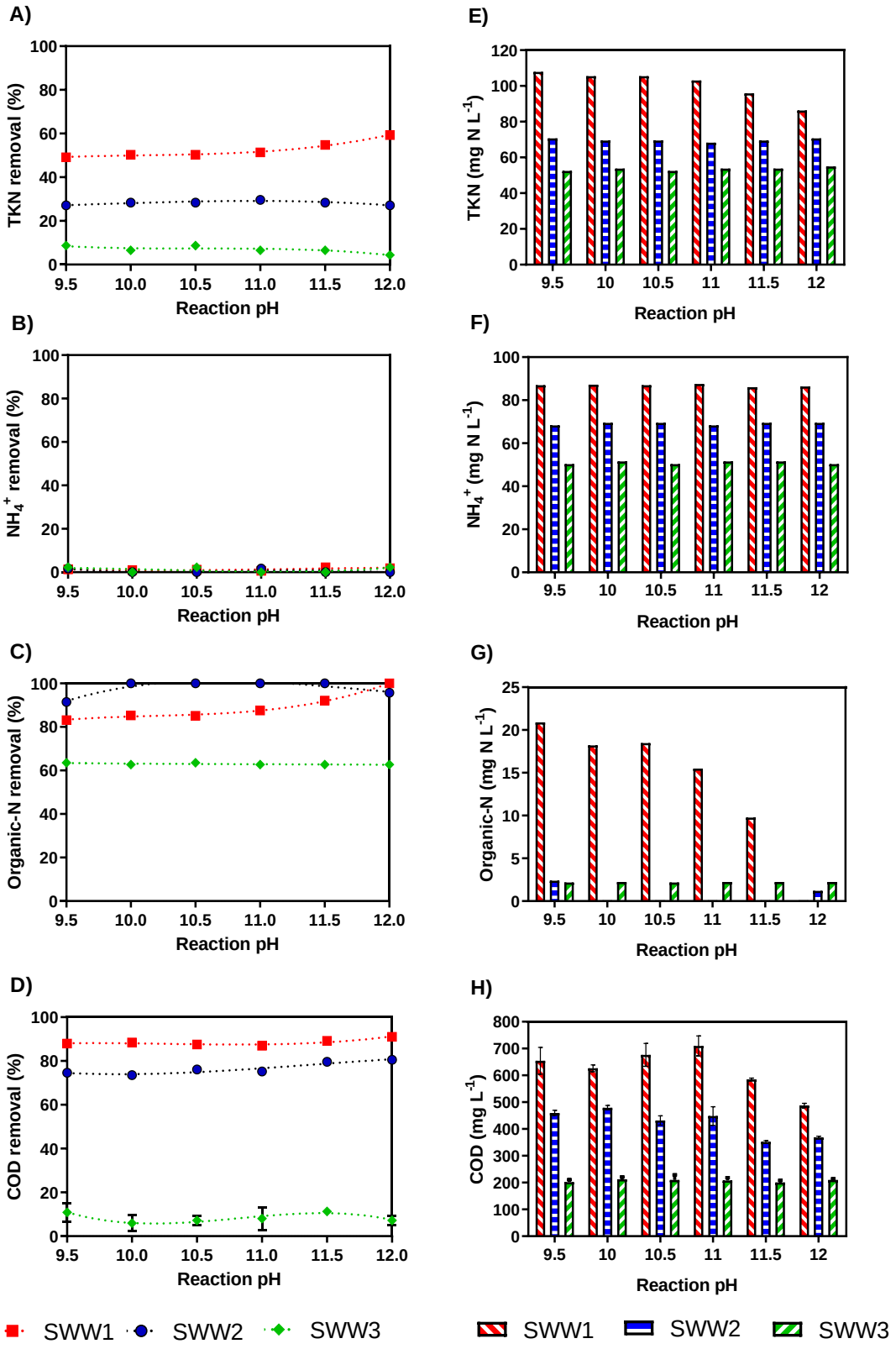

Figure 3.2 - Effect of the reaction pH in IOSLM tests on some parameters removal efficiency: a) TKN, b) ammonium nitrogen, c) organic N and d) COD, and on the effluent quality: e) TKN concentration, f) ammonium nitrogen concentration, g) organic-N concentration and h) COD concentration, for SWW1, SWW2, and SWW3. Bars represent the standard deviation of the mean.

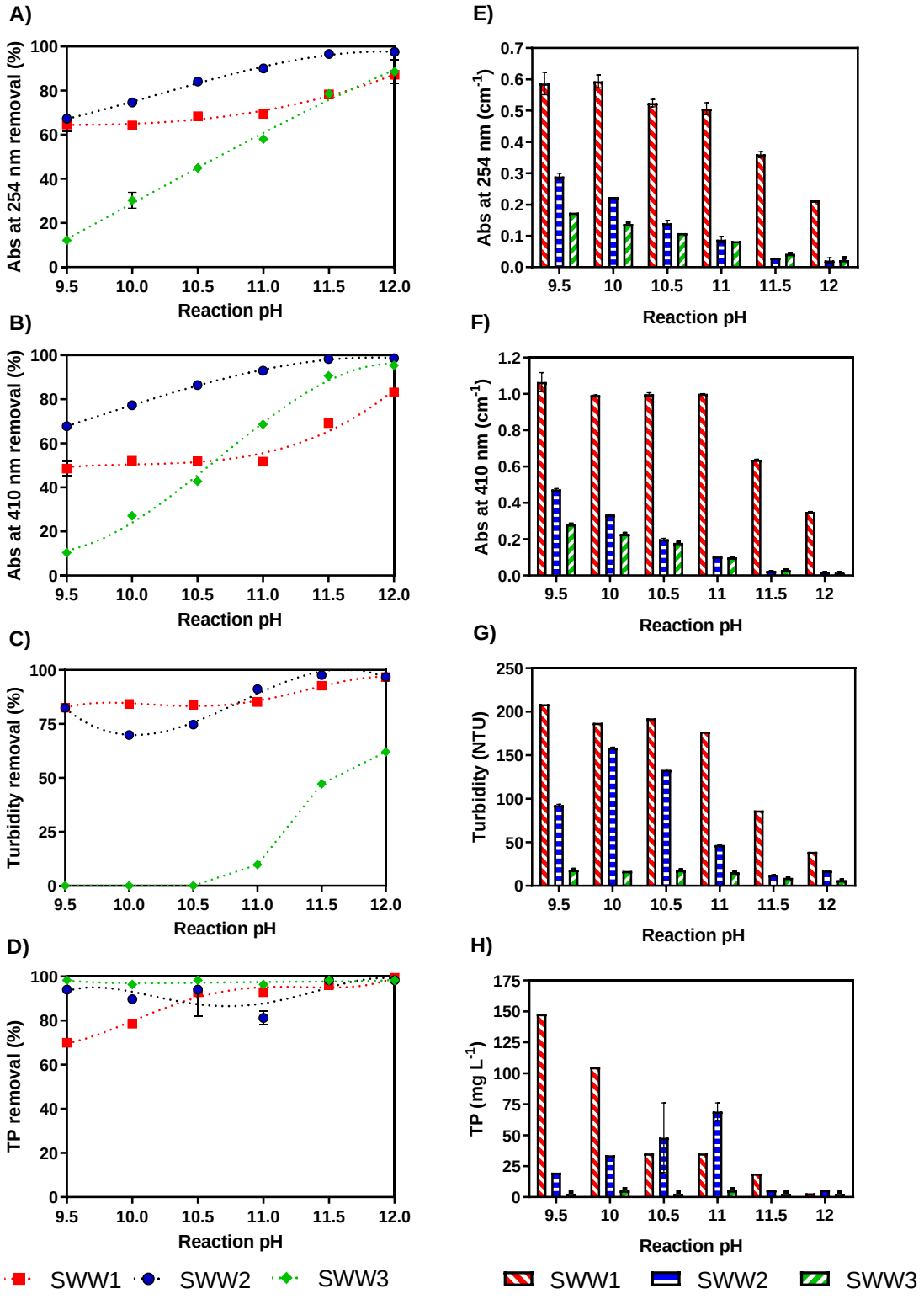

Figure 3.3 - Effect of the reaction pH in IOSLM tests on some parameters removal efficiency: a) absorbance at 254 nm, b) absorbance at 410 nm, c) turbidity, and d) TP), and on the effluent quality: e) absorbance at 254 nm, f) absorbance at 410 nm, g) turbidity, and h) TP concentration, for SWW1, SWW2, and SWW3. Bars represent the standard deviation of the mean.

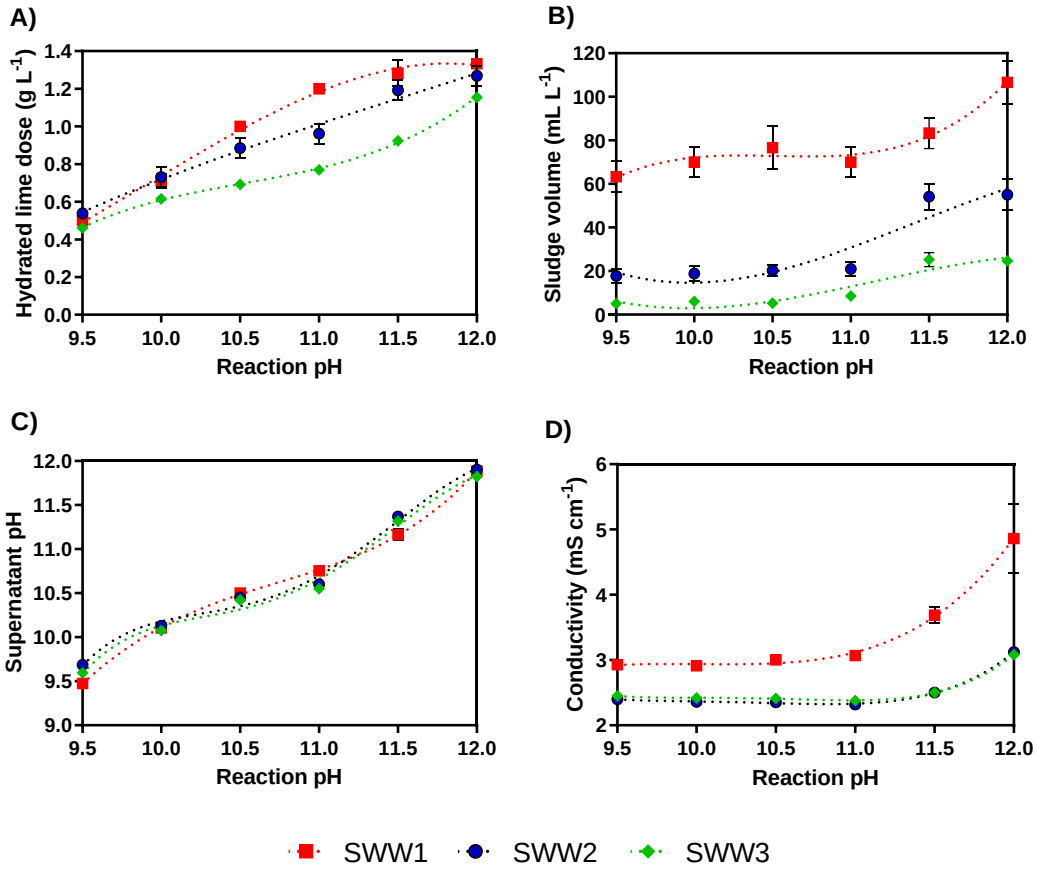

Figure 3.4 - Effect of the reaction pH in IOSLM tests on the: a) hydrated lime dose and b) sludge volume (after 1 hour of sedimentation), c) supernatant pH, and d) conductivity, for SWW1, SWW2, and SWW3. Bars represent the standard deviation of the mean.

The TKN removals were essentially due to the removal of organic nitrogen since the ammonium nitrogen removals were insignificant (P<0.05). Although the studied pH range is greater than 9.3 (pKa of the reaction between NH_3 and NH_4^+ is 9.26, so at higher pH than 9.26 the ammoniacal nitrogen is in the non-ionized form (NH_3) and susceptible to being volatilized (Gupta et al., 2015)), the removal of ammonia was negligible since the IOSLM process was quick. The IOSLM process was not very effective in removing COD for SWW3 (6.0 to 11.3%, Figure 3.2d), which indicates that this effluent presents non-precipitable organic matter (in addition to being non-biodegradable). In this way, this effluent can only be treated by unconventional treatment processes (e.g., advanced oxidation processes or adsorption processes). Low COD removals in the lime precipitation process have also been found in the treatment of winery wastewater (Luz et al., 2021) and landfill leachate (Ramalho et al., 2022). On the other hand, high COD removals were obtained for SWW1 (86.9 to 91.0%) and SWW2 (73.5 to 80.6%), similar

to those obtained by Tariq et al. (2012). These removals are justified by the addition of lime in excess to wastewater which results in the destabilization and aggregation of charged particles, as well as the formation of an intense and spontaneous precipitate (Madeira et al. (2020), chapter 2). This in addition to precipitate adsorptive capacity, contributes to a vigorous "sweeping" of suspended impurities and organic matter (Madeira et al., 2020; Prasad et al., 2019). Moreover, the removal of some organic matter is also due to the sedimentation operation since these effluents present easily sedimentable organic matter, as observed by Satyanarayan et al. (2005).

For absorbances at 254 and 410 nm, turbidity, and TP, the removals increased with reaction pH and the supernatant quality was much better for pH 12 (Figure 3.3) for all the studied waters. In fact, it is at high pH that larger precipitates of $CaCO_3$, $MgCO_3$, and $Mg(OH)_2$ are formed, as a result of the reaction between lime and different chemical species (such as carbonic acid, calcium bicarbonate, magnesium bicarbonate, magnesium carbonate) present in SWW (Madeira et al. (2020), chapter 2). These precipitates have a high adsorption capacity for some organic compounds (Hakim et al., 2017; Lawler, 2004; Zeng et al., 2012) and phosphorus (Yagi and Fukushi, 2012). According to Zhao et al. (2015), the $Mg(OH)_2$ precipitate can neutralize the charge and cause enmeshment of colloidal particles, beyond its adsorptive capacity. The magnesium concentration was reduced in the entire reaction pH range and for all effluents (Figure 3.5B).

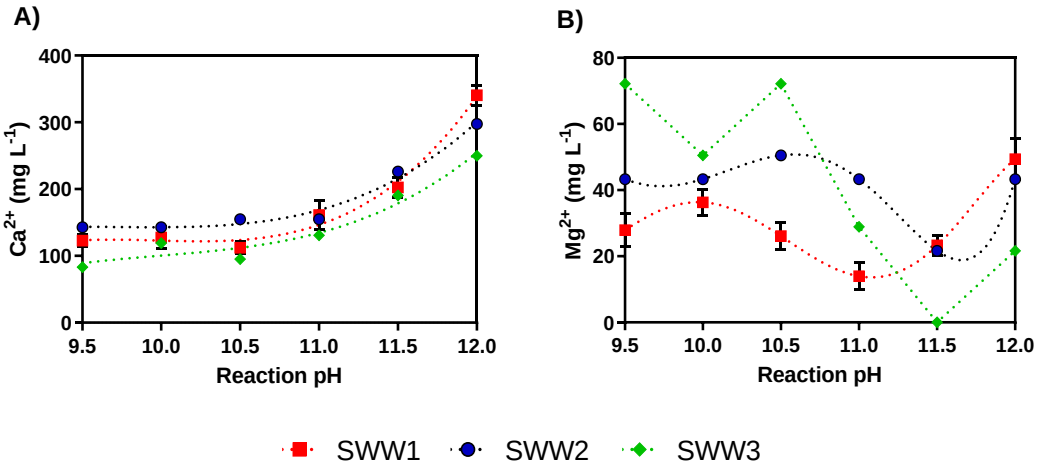

Figure 3.5 - Effect of the reaction pH in IOSLM tests on the: a) calcium concentration and b) magnesium concentration, for SWW1, SWW2, and SWW3. Bars represent the standard deviation of the mean.

The observed decrease in turbidity appears to be related to the removal of absorbances at 254 nm and 410 nm, and COD since strong and positive correlations were found between these parameters and turbidity, for all SWW types (Table 3.3). On the other hand, TP had a negative correlation with calcium, which varies between strong (r=-0.63, for SWW1 and r=-0.66 for SWW2) and weak (r=-0.24 for SWW3) correlation (Table 3.3). In fact, phosphorus removals involve also large amounts of soluble calcium and alkaline conditions (pH>9) (Anawar et al., 2019), being associated with the formation of hydroxyapatite precipitate (Eq. 1), calcium phosphate (Eq. 2) and octacalcium phosphate (Eq. 3) (Dai et al., 2018).

$$5Ca^{2+} + 3PO_4^{3-} + OH^- \rightarrow Ca_5H(PO_4)_3OH \downarrow \quad (1)$$

$$3Ca(OH)_2 + 2PO_4^{3-} \rightarrow Ca_3(PO_4)_2 \downarrow + 6\ OH^- \quad (2)$$

$$4Ca(OH)_2 + 3PO_4^{3-} + H_2O \rightarrow Ca_4H(PO_4)_3 \downarrow + 9\ OH^- \quad (3)$$

Despite the reduction in contamination observed for the pH range studied, the calcium was not completely consumed in the IOSLM process, for all SWW (Figure 3.5a), which may be important in the following AC process. On the contrary, the calcium that is present seems to be responsible for the conductivity since high and positive correlations were found, for all SWW (Table 3.3). As a result of the IOSLM process, only SWW1 (pH≥11.5) showed a higher conductivity than it had initially (Figure 3.4).

Table 3.3 – Correlation matrix between all parameters analyzed in IOSLM process, for treated SWW1 (represented by letter A and beige color), treated SWW2 (represented by letter B and blue color), and treated SWW3 (represented by letter C and green color). Values in bold are different from 0 with a significance level alpha=0.05.

Parameters	Reaction pH	Supernatant pH	Dose	Cond.	Turb.	Ca	Mg	Abs 254	Abs 410	COD	TP	NH_4^+	TKN	Sludge V.
Reaction pH														
Supernatant pH	**0.99** A **0.98** B **0.98** C													
Dose	**0.98** A **0.99** B **0.98** C	**0.96** A **0.98** B **0.99** C												
Cond.	0.30 A 0.70 B 0.67 C	0.38 A 0.79 B 0.75 C	0.16 A 0.66 B 0.79 C											
Turb.	**-0.90** A -0.79 B -0.75 C	**-0.91** A -0.76 B -0.72 C	**-0.84** A -0.75 B -0.70 C	-0.54 A -0.57 B -0.56 C										
Ca	**0.84** A **0.87** B **0.91** C	**0.87** A **0.94** B **0.95** C	0.73 A **0.86** B **0.96** C	0.73 A **0.93** B **0.85** C	**-0.94** A -0.74 B -0.64 C									
Mg	0.25 A -0.39 B **-0.82** C	0.36 A -0.41 B -0.80 C	0.13 A -0.44 B -0.77 C	**0.88** A -0.06 B -0.38 C	-0.53 A 0.60 B 0.55 C	0.63 A -0.35 B -0.80 C								
Abs 254	**-0.93** A **-0.98** B **-1.00** C	**-0.94** A **-0.94** B **-0.98** C	**-0.86** A **-0.99** B **-0.97** C	-0.58 A -0.55 B -0.64 C	**0.98** A 0.76 B 0.73 C	**-0.95** A -0.77 B **-0.91** C	-0.50 A 0.43 B **0.84** C							
Abs 410	**-0.87** A **-0.97** B **-0.99** C	**-0.89** A **-0.92** B **-0.96** C	-0.79 A **-0.97** B **-0.95** C	-0.64 A -0.50 B -0.59 C	**0.99** A 0.72 B 0.75 C	**-0.96** A -0.73 B **-0.89** C	-0.63 A 0.41 B **0.88** C	**0.98** A **1.00** B **0.99** C						
COD	-0.63 A **-0.85** B 0.04 C	-0.68 A **-0.89** B 0.04 C	-0.52 A **-0.88** B 0.12 C	-0.77 A -0.65 B 0.17 C	**0.89** A 0.81 B 0.47 C	**-0.88** A **-0.87** B 0.03 C	**-0.84** A 0.63 B 0.23 C	**0.84** A **0.84** B -0.02 C	**0.93** A 0.80 B 0.06 C					
TP	**-0.93** A -0.28 B -0.21 C	**-0.93** A -0.45 B -0.30 C	**-0.98** A -0.32 B -0.25 C	-0.10 A -0.63 B -0.41 C	0.72 A 0.39 B 0.63 C	-0.63 A -0.66 B -0.24 C	-0.07 A 0.53 B -0.03 C	0.78 A 0.17 B 0.21 C	0.69 A 0.11 B 0.18 C	0.39 A 0.63 B 0.51 C				
NH_4^+	-0.56 A 0.41 B 0.10 C	-0.55 A 0.52 B 0.02 C	-0.55 A 0.50 B 0.00 C	-0.36 A 0.38 B -0.44 C	0.78 A 0.09 B 0.30 C	-0.60 A 0.47 B 0.03 C	-0.40 A -0.19 B -0.54 C	0.73 A -0.41 B -0.13 C	0.77 A -0.41 B -0.20 C	0.77 A -0.46 B 0.00 C	0.42 A -0.44 B 0.71 C			
TKN	**-0.91** A -0.07 B 0.78 C	**-0.93** A 0.10 B 0.79 C	**-0.83** A -0.08 B **0.84** C	-0.63 A 0.60 B 0.75 C	**0.99** A -0.06 B -0.34 C	**-0.98** A 0.42 B **0.90** C	-0.58 A 0.07 B -0.75 C	**0.99** A 0.22 B -0.77 C	**0.99** A 0.29 B -0.75 C	**0.88** A -0.23 B 0.30 C	0.73 A -0.78 B 0.17 C	0.69 A 0.17 B 0.24 C		
Sludge v.	**0.87** A **0.86** B **0.87** C	**0.91** A **0.92** B **0.92** C	0.81 A **0.88** B **0.88** C	0.69 A 0.77 B 0.70 C	**-0.93** A -0.80 B -0.73 C	**0.93** A **0.94** B **0.94** C	0.68 A -0.64 B **-0.87** C	**-0.96** A -0.80 B **-0.89** C	**-0.96** A -0.77 B **-0.89** C	**-0.88** A **-0.96** B -0.28 C	-0.75 A -0.72 B -0.41 C	-0.66 A 0.50 B 0.09 C	**-0.96** A 0.30 B 0.73 C	

Finally, a PCA was applied for the IOSLM results (Figure 3.6). The first principal component separates the three SWWs treated at different reaction pH, showing greater contamination of SWW1, followed by SWW2 and then SWW3. For the three treated SWW, the increase in reaction pH decreases the concentration of several pollutants, although this decrease was more noticeable for treated SWW1, followed by SWW2, and finally SWW3. This means that the application of the same reaction pH did not guarantee the same effluent quality for the three SWWs. Thus, the reaction pH is not a key parameter for slaughterhouse water treatment, which will depend on the characteristics of the SWW to be treated. However, at the reaction pH 12 the quality of the three treated SWWs is better for the studied parameters than raw SWWs. SWW1 had higher lime consumption and sludge production than SWW2 or SWW3, and SWW2 higher than SWW3, justified by the different initial contaminations (Figure 3.4). This lime consumption (which ranged from 0.46 to 1.33 g L^{-1}) was lower than that found in the treatment of explosive effluents (about 6 to 12 g L^{-1}) (Madeira et al. (2020), chapter 2), for the same range of reaction pH (9.5 to 12), and can be justified by the differences in ammonium nitrogen concentrations existing in these effluents (about 52 to 88 mg N L^{-1} for SWW and 1554 mg N L^{-1} for explosive wastewater). In general, the supernatant pH values were close to the reaction pH values, for the three SWW types (Figure 3.4).

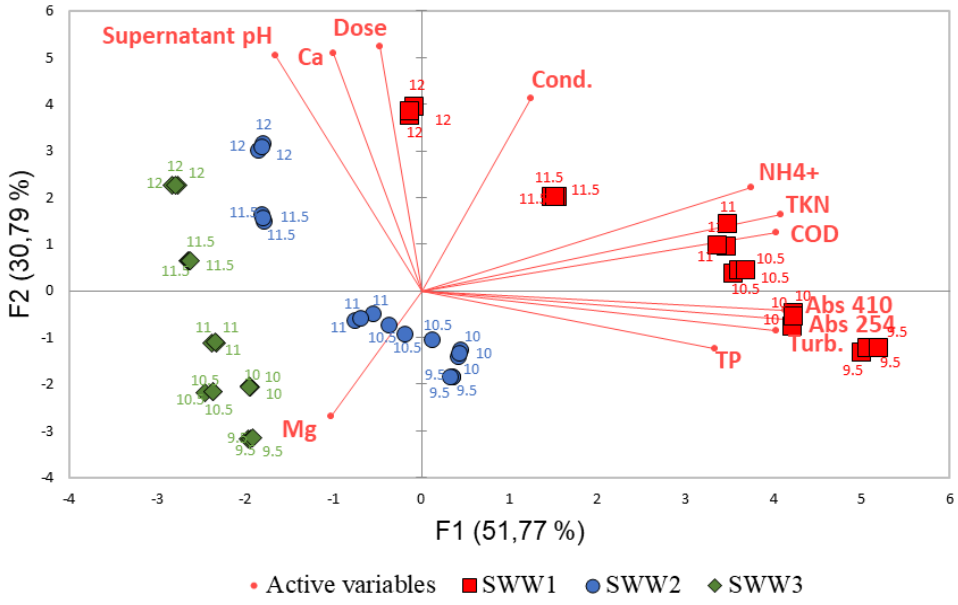

Figure 3.6 – Principal Component Analysis (PCA) biplot (axes F1 and F2: 82.56 %) based on results obtained by the IOSLM process, for the SWW1, SWW2, and SWW3. Score plots colored by type of SWW sample applied (SWW1 samples in red square, SWW2 samples in blue circles, and SWW3 samples in green rhombus). Score names are designated by reaction pH applied (9.5 to 12).

3.3.3. Atmospheric CO_2 carbonation (AC)

3.3.3.1. Effect of the reaction pH

Figure 3.7 shows the variation of the supernatant quality with carbonatation time and reaction pH in the AC process, for the SWW1, SWW2, and SWW3. According to Figure 3.7A, the supernatant pH decreased linearly with time for all reaction pH studied, except for pH 12. At this pH, the supernatant pH slightly decreased in the first seven days for all SWW, after which a sudden drop in supernatant pH was observed. This behavior could be related to the buffer capacity of the supernatant, that is, the ability of the supernatant to neutralize (through its alkalinity) the protons that were meanwhile released (Middelburg et al., 2020). Similar behavior was observed by Luz et al. (2021) when the authors applied the AC process to pretreated winery wastewater at the reaction pH 12. On the 9^{th} day (for SWW1), the 10^{th} day (for SWW2), and the 12^{th} day (for SWW3) all the reaction pH had reached the same supernatant pH.

The decrease in supernatant pH over time was due to the reaction of the supernatant with atmospheric CO_2 (Madeira et al. (2020), chapter 2). Very strong and significant (P<0.05) negative correlations were observed between supernatant pH and time, SWW1 ($r \geq -0.95$, Table 3.4), SWW2 ($r \geq -0.92$, Table 3.5) and SWW3 ($r \geq -0.90$, Table 3.6), at different reaction pH (9.5 to 12).

No significant variation in conductivity with time was observed for the studied reaction pH, being very close the final values of the conductivity to the initial ones before the integrated treatment processes by IOSLM +AC (Figures 3.7B).

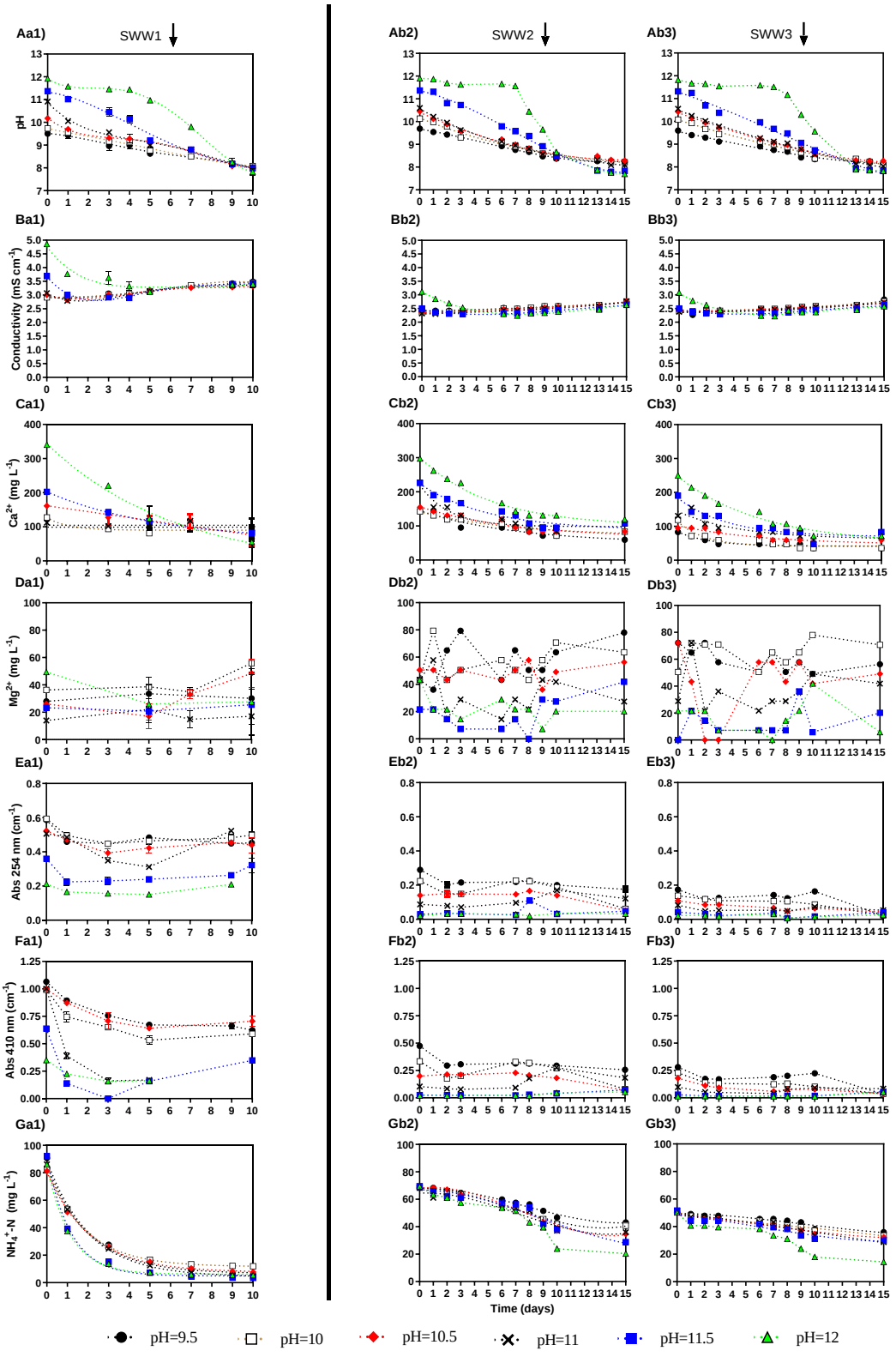

Figure 3.7 – Variation of **A)** supernatant pH; **B)** electrical conductivity; **C)** calcium concentration; **D)** magnesium concentration; **E)** absorbance at 254 nm; **F)** absorbance at 410 nm, and **G)** ammonium nitrogen concentration, over experimental time at different reaction pH (9.5 and 12), in AC process. Numbers **1**, **2,** and **3** mean SWW1, SWW2, and SWW3, respectively. Lowercase letters **a** and **b** mean the A/V ratio, a for 9.5 m^2 m^{-3} was used for SWW1, and b for 5 m^2 m^{-3} was used for SWW2 and SWW3 pretreated by IOSLM. Bars represent the standard deviation of the mean.

Table 3.4 – Correlation matrix between all parameters analyzed in AC process, for SWW1 pretreated at different reaction pH (such as 9.5, 10, 10.5, 11, 11.5, and 12, represented by letters A, B, C, D, E, and F, respectively). Values in bold are different from 0 with a significance level alpha=0.05.

Parameters	Time		Supernatant pH		Cond.		NH_4^+		Ca		Mg		Abs 254		Abs 410	
Time																
Supernatant pH	**-0.99** A	**-0.98** D														
	-1.00 B	**-0.99** E														
	-0.99 C	**-0.95** F														
Cond.	**0.97** A	0.82 D	**-0.93** A	-0.69 D												
	0.98 B	-0.07 E	**-0.97** B	0.13 E												
	0.95 C	-0.75 F	**-0.89** C	0.52 F												
NH_4^+	-0.86 A	-0.86 D	**0.90** A	**0.94** D	-0.80 A	-0.49 D										
	-0.83 B	-0.80 E	0.88 B	0.82 E	-0.77 B	0.62 E										
	-0.86 C	-0.79 F	**0.89** C	0.58 F	-0.73 C	**0.98** F										
Ca	-0.67 A	-0.40 D	0.74 A	0.46 D	-0.58 A	0.04 D	**0.95** A	0.35 D								
	-0.69 B	**-0.95** E	0.74 B	**0.96** E	-0.54 B	0.25 E	0.88 B	**0.91** E								
	-0.95 C	**-0.95** F	**0.98** C	0.82 F	-0.84 C	0.87 F	0.79 C	**0.88** F								
Mg	0.28 A	0.02 D	-0.34 A	-0.24 D	0.25 A	-0.51 D	-0.71 A	-0.43 D	-0.85 A	-0.55 D						
	0.70 B	0.34 E	-0.65 B	-0.25 E	0.61 B	0.62 E	-0.37 B	0.22 E	-0.51 B	-0.02 E						
	0.72 C	-0.70 F	-0.67 C	0.47 F	0.80 C	**0.96** F	-0.28 C	**0.99** F	-0.73 C	0.81 F						
Abs 254	-0.74 A	0.53 D	0.77 A	-0.33 D	-0.69 A	0.75 D	**0.94** A	-0.04 D	**0.95** A	-0.11 D	-0.76 A	-0.73 D				
	-0.47 B	-0.14 E	0.53 B	0.20 E	-0.36 B	**0.91** E	0.87 B	0.71 E	0.83 B	0.41 E	-0.07 B	0.79 E				
	-0.40 C	0.56 F	0.51 C	-0.78 F	-0.13 C	0.13 F	0.76 C	0.05 F	0.46 C	-0.32 F	0.23 C	0.17 F				
Abs 410	-0.88 A	0.25 D	**0.91** A	-0.03 D	-0.81 A	0.69 D	**1.00** A	0.22 D	**0.94** A	0.28 D	-0.69 A	**-0.95** D	**0.92** A	**0.91** D		
	-0.77 B	-0.30 E	0.82 B	0.32 E	-0.71 B	0.85 E	**0.99** B	0.80 E	0.85 B	0.53 E	-0.23 B	0.66 E	**0.88** B	**0.97** E		
	-0.71 C	0.12 F	0.73 C	-0.40 F	-0.57 C	0.50 F	**0.97** C	0.47 F	0.60 C	0.18 F	-0.04 C	0.57 F	0.81 C	0.83 F		

Table 3.5 – Correlation matrix between all parameters analyzed in AC process, for SWW2 pretreated at different reaction pH (such as 9.5, 10, 10.5, 11, 11.5, and 12, represented by letters A, B, C, D, E, and F, respectively). Values in bold are different from 0 with a significance level alpha=0.05.

Parameters	Time	Supernatant pH	Cond.	NH_4^+	Ca	Mg	Abs 254	Abs 410
Time								
Supernatant pH	**-0.97** A **-0.96** B **-0.96** C	**-0.97** D **-0.99** E **-0.92** F						
Cond.	**0.98** A **0.99** B **0.97** C	**0.95** D 0.56 E -0.51 F	**-0.92** A **-0.92** B **-0.87** C	**-0.85** D -0.53 E 0.24 F				
NH_4^+	**-0.98** A **-0.97** B **-0.96** C	**-0.96** D **-0.97** E **-0.96** F	**0.97** A **0.97** B **0.94** C	**0.95** D **0.97** E **0.97** F	**-0.97** A **-0.94** B **-0.94** C	**-0.89** D -0.62 E 0.48 F		
Ca	**-0.89** A **-0.89** B **-0.87** C	**-0.80** D **-0.86** E **-0.87** F	**0.91** A **0.94** B **0.95** C	**0.89** D **0.90** E 0.70 F	**-0.80** A **-0.83** B -0.75 C	-0.61 D -0.14 E **0.80** F	**0.87** A **0.96** B **0.82** C	**0.78** D **0.81** E **0.85** F
Mg	0.42 A 0.74 B 0.59 C	-0.02 D 0.55 E -0.46 F	-0.35 A -0.75 B -0.51 C	0.06 D -0.55 E 0.31 F	0.38 A 0.73 B 0.58 C	0.05 D **0.86** E **0.76** F	-0.37 A **-0.81** B -0.46 C	-0.09 D -0.68 E 0.47 F	-0.63 A **-0.87** B -0.58 C	-0.13 D -0.29 E 0.59 F
Abs 254	-0.72 A -0.49 B -0.67 C	0.69 D 0.27 E 0.30 F	0.70 A 0.38 B 0.45 C	-0.71 D -0.25 E -0.34 F	-0.67 A -0.55 B **-0.81** C	0.61 D -0.01 E -0.25 F	0.69 A 0.34 B 0.62 C	**-0.84** D -0.12 E -0.39 F	**0.79** A 0.26 B 0.27 C	-0.68 D -0.17 E -0.38 F	**-0.79** A -0.43 B -0.35 C	0.45 D -0.43 E -0.62 F
Abs 410	-0.68 A -0.43 B -0.75 C	0.69 D **0.85** E **0.83** F	0.69 A 0.33 B 0.54 C	-0.71 D **-0.81** E **-0.94** F	-0.60 A -0.48 B **-0.87** C	0.62 D **0.86** E -0.11 F	0.63 A 0.28 B 0.71 C	**-0.83** D **-0.89** E **-0.89** F	**0.79** A 0.21 B 0.34 C	-0.62 D -0.50 E -0.63 F	**-0.76** A -0.37 B -0.47 C	0.38 D **0.81** E -0.25 F	**0.98** A **0.99** B **0.96** C	**0.97** D 0.10 E 0.54 F

Calcium concentrations decreased in the first 10 days, after which remain practically unchanged, despite the concentration of the wastewaters after the IOSLM process (Figures 3.7C). Thus, the AC process is efficient in removing calcium added to the IOSLM process. On the 10th day for SWW1 and 15th day for SWW2 and SWW3, the calcium concentrations were below the initial values (ca. 101 mg L^{-1} for SWW1, 159 mg L^{-1} for SWW2 and ca. 191 mg L^{-1} for SWW3, Table 3.1) before applying the IOSLM process. Despite the high calcium removal, the calcium was not a limiting factor in the AC process to drop pH to neutral values, as was observed by Ramalho et al. (2022). Ramalho et al. (2022) observed that the calcium concentration was totally consumed during the AC process, leading to a decrease in pH from only 12.5 to 10.1, after 32 days of AC. The calcium removal is justified by the formation of calcium carbonate (Eq. 4) since the carbonate ions are formed by dissolving atmospheric CO_2 in water and reducing pH (Prazeres et al., 2016) (a strong positive correlation between calcium and supernatant pH, r≥0.46, P<0.05, for SWW1 (Table 3.4), r≥0.70, P<0.05, for SWW2 (Table 3.5), and r≥0.53, P<0.05, for SWW3 (Table 3.6)).

$$CO_3^{2-} + Ca^{2+} \rightarrow CaCO_3 \downarrow \quad (4)$$

Regarding the magnesium (Figures 3.7D), its concentration varied considerably over time for all SWW, regardless of the reaction pH. In this way, there is no significant correlation (P<0.05) between magnesium and time, for reaction pHs and waters (Tables 3.4, 3.5, and 3.6). This variation may be due to the simultaneous occurrence of a set of reactions, namely the formation of magnesium carbonate (Eq. 5), dissolution reactions of magnesium precipitates (Eq. 6), and evaporation phenomena.

$$CO_3^{2-} + Mg^{2+} \rightarrow MgCO_3 \downarrow \quad (5)$$

$$MgCO_3 + CO_2 + H_2O \rightarrow Mg^{2+} + 2HCO_3^- \quad (6)$$

Table 3.6 – Correlation matrix between all parameters analyzed in AC process, for SWW3 pretreated at different reaction pH (such as 9.5, 10, 10.5, 11, 11.5, and 12, represented by letters A, B, C, D, E, and F, respectively). Values in bold are different from 0 with a significance level alpha=0.05.

Parameters	Time	Supernatant pH	Cond.	NH_4^+	Ca	Mg	Abs 254	Abs 410
Time								
Supernatant pH	**-0.98** A **-0.98** B **-0.98** C	**-0.99** D **-1.00** E **-0.90** F						
Cond.	**0.84** A **0.96** B **0.97** C	**0.96** D 0.54 E -0.49 F	-0.74 A **-0.91** B **-0.90** C	**-0.91** D -0.50 E 0.16 F				
NH_4^+	**-0.96** A **-0.97** B **-0.98** C	**-0.97** D **-0.96** E **-0.97** F	**0.96** A **0.99** B **0.98** C	**0.97** D **0.98** E **0.90** F	**-0.85** A **-0.91** B **-0.92** C	**-0.93** D -0.39 E 0.54 F		
Ca	-0.75 A **-0.86** B **-0.84** C	**-0.79** D **-0.85** E **-0.76** F	**0.76** A **0.92** B **0.89** C	**0.86** D **0.86** E 0.53 F	-0.48 A -0.69 B -0.73 C	-0.64 D -0.07 E **0.77** F	0.67 A **0.92** B **0.84** C	**0.82** D **0.90** E **0.80** F
Mg	-0.70 A -0.32 B 0.24 C	0.66 D 0.59 E -0.09 F	**0.78** A 0.25 B -0.18 C	-0.68 D -0.59 E -0.08 F	-0.34 A -0.37 B 0.36 C	0.66 D 0.32 E 0.21 F	0.69 A 0.14 B -0.13 C	-0.72 D -0.56 E -0.11 F
Abs 254	-0.66 A **-0.93** B **-0.91** C	-0.25 D -0.11 E -0.05 F	0.56 A **0.88** B **0.93** C	0.28 D 0.14 E -0.04 F	**-0.76** A **-0.96** B **-0.79** C	-0.06 D 0.48 E 0.05 F	0.58 A **0.91** B **0.89** C	0.23 D 0.26 E 0.10 F
Abs 410	-0.70 A **-0.90** B **-0.85** C	0.21 D 0.58 E 0.70 F	0.63 A **0.90** B **0.89** C	-0.13 D -0.54 E **-0.84** F	-0.72 A **-0.82** B -0.71 C	0.40 D **0.92** E 0.08 F	0.63 A **0.94** B **0.84** C	-0.25 D -0.39 E -0.60 F

Parameters	Ca	Mg	Abs 254	Abs 410
Ca	0.34 A 0.02 B -0.35 C	**-0.78** D -0.50 E -0.04 F		
Mg	0.52 A 0.72 B **0.89** C	0.26 D 0.33 E -0.13 F	0.20 A 0.12 B -0.08 C	0.32 D 0.18 E -0.42 F
Abs 254	0.61 A **0.89** B **0.78** C	0.11 D -0.11 E -0.21 F	0.25 A -0.12 B 0.12 C	0.44 D 0.57 E -0.35 F
Abs 410			**0.97** A **0.92** B **0.90** C	0.70 D 0.52 E 0.26 F

Overall, the AC process proved to be effective in removing aromatic and unsaturated compounds (Figures 3.7E) and compounds responsible for color (Figures 3.7F). It is expected that the sedimentability of small particles will still occur during the first days of the carbonation process. The decrease in absorbances (at 254 and 410 nm) may also be associated with the interaction of organic compounds with the precipitates formed during the AC process, through adsorption processes since some positive correlations were found between absorbances and calcium or magnesium (Tables 3.4, 3.5, and 3.6).

A decrease in the concentration of nitrogen ammonium over time was observed, for all reaction pH and waters (Figures 3.7G). Very strong negative correlations were observed for SWW1 ($-0.79 \leq r \leq -0.86$, Table 3.4), SWW2 ($-0.96 \leq r \leq -0.98$, Table 3.5), and SWW3 ($-0.96 \leq r \leq -0.98$, Table 3.6). At the end of the AC process, about 93 to 96% of ammonium nitrogen was removed in SWW1 at reaction pH 11.5 and 12, while 70.7 and 71.4%, respectively, in SWW2 and SWW3 at the reaction pH 12. It is observed that, over time, the decrease of ammonium nitrogen concentration is hampered due to the decrease in pH (Figures 3.7A). In fact, since the supernatant pH decreases over time, ammonia tends to be converted to ammonium nitrogen, while the other part of the ammonia is available to be removed (Berge et al. 2005). Ammonium nitrogen is not removed from the supernatant by volatilization (Chen et al., 2016). In this way, higher reaction pHs provide greater removal of ammonia during the carbonation process, as can be seen in Figures 3.7G. Ramalho et al. (2022) obtained 100% ammonia removal during the carbonation process of a leachate effluent, as the pH decrease was slower over time due to calcium limitation, using an A/V ratio of 5 to 6.7 m^2/m^3. These authors also observed the presence of nitrogen in the sludge resulting from the carbonation process, thus indicating that in addition to volatilization, it is also possible to have some adsorption of ammonia nitrogen during this process.

Finally, after 15 days, the best quality for the tested parameters was observed at the reaction pH of 12 for all the studied supernatants and the final supernatant pH was 8 (Figure 3.7). Therefore, independently of the water characteristics, it is possible to use the AC process after the IOSLM to decrease IOSLM supernatants' pH and remove ammonia.

3.3.3.2. Effect of the reactor A/V ratio

Figure 3.8 shows the variation of supernatant pH with experimental time in the AC process, for different reactor A/V ratios (0 to 155.4 m^2/m^3), for SWW1 (Figure 3.8a), SWW2 (Figure 3.8b), and SWW3 supernatants (Figure 3.8c), at reaction pH 12. These results show that below an A/V ratio (A/V ratio of 9.5 m^2/m^3 for SWW1, and A/V ratio of 3 m^2/m^3 for SWW2 and SWW3, Figure 3.8), the AC process was not efficient to decrease the supernatant pH to values that allow its discharge or reuse, requiring more time (>7 days). However, for SWW2 and SWW3 at A/V ratio of 19 m^2/m^3, 7 days were enough to put the supernatant pH at 8, and using a high A/V ratio (≥ 52.4 m^2/m^3) 2 days were enough. For the highest A/V ratio, 155.4 m^2/m^3 a more detailed analysis was made (Figure 3.8B) showing that the supernatant pH was 9.5 after 8 h and 8 after 24 h.

A decrease in the supernatant pH from 12 to 8 during the AC process was obtained by Prazeres et al. (2019b) and Prazeres et al. (2016), using a reactor A/V ratio of 6.23 m^2/m^3 (for 10 days with vinasse effluent) and 4.63 m^2/m^3 (for 8 days with cheese whey wastewaters). However, longer carbonation times (about 13 days) were achieved in this work using similar A/V ratios (5 m^2/m^3). This means that the A/V ratio is not the only factor determining the pH drop. In fact, other factors (e.g., the concentration of CO_2 in the atmosphere during the experiments, as discussed below) can change the ability of the atmospheric CO_2 to be transferred to the aqueous phase (Viswanaathan et al. 2022), and justify these differences in carbonation times. Results of SWW2 supernatant using A/V ratios of 5 and 155.4 m^2/m^3 to reach the pH 8 (13 days and 1 day for 5 and 155.4 m^2/m^3, respectively) showed higher NH_4^+ removals for the highest A/V ratio (82% for 155.4 m^2/m^3 compared 68% for 5 m^2/m^3) (Table 3.7). This means that despite the rapid decrease in pH, NH_4^+ removal is not hampered, on the contrary, it allows greater volatilization due to its larger area of exposure. Thus, a higher reactor A/V ratio did not decrease the NH_4^+ removal of the system.

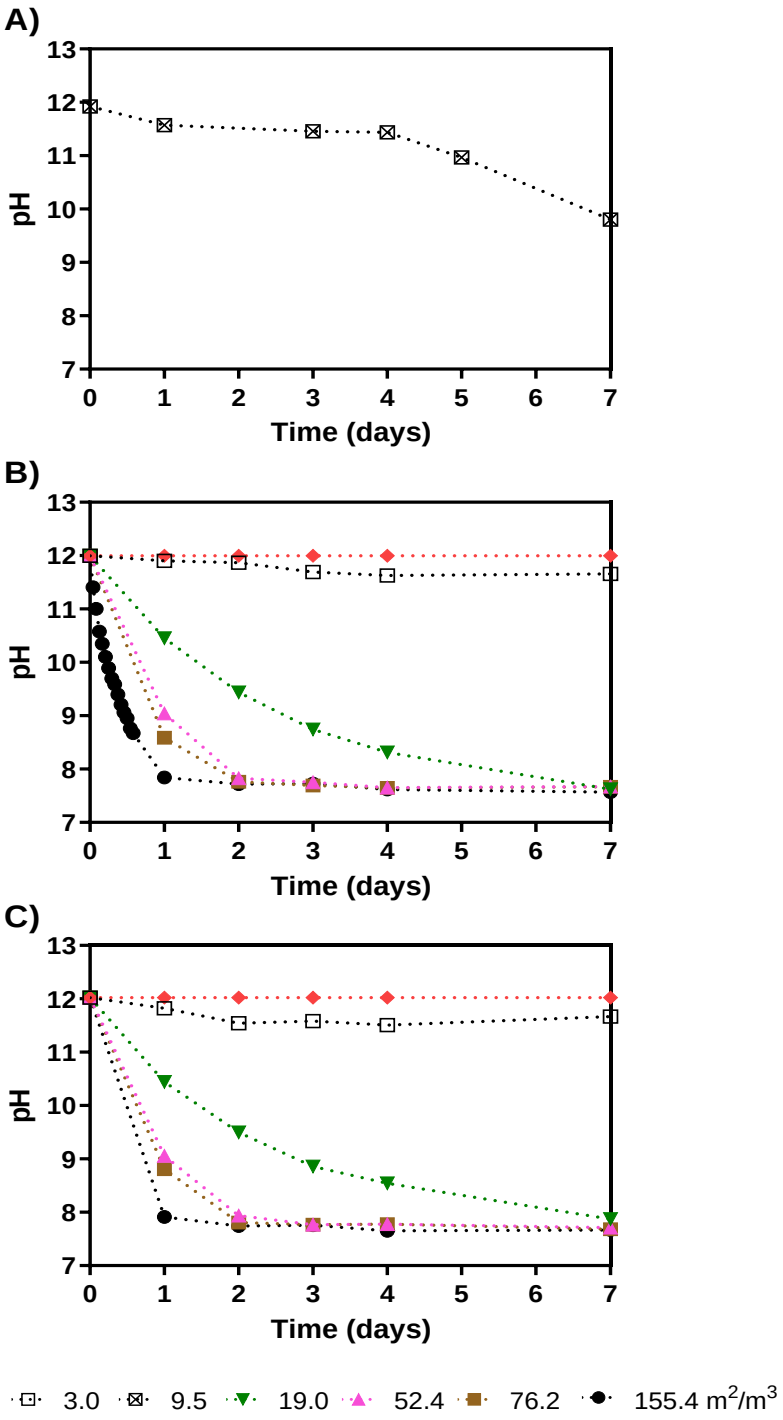

Figure 3.8 – Variation of the supernatant pH over time in the AC process, using a) SWW 1, b) SWW 2, and c) SWW 3 supernatants, all pretreated by IOSLM process (at pH 12), for different reactor A/V ratios (0 to 155.4 m^2/m^3). Bars represent the standard deviation of the mean.

Table 3.7 - Results of the SWW2 supernatant in the AC process, using A/V ratios of 5 m^2/m^3 (after 1 day) and 155.4 m^2/m^3 (after 13 days) to reach a pH of about 8.

Parameters	Unit	Initial	Final	
			A/V = 5 m^2/m^3	A/V = 155.4 m^2/m^3
pH	Sorensen	11.9±0.2	7.9±0.2	8.2±0.1
Conductivity	mS cm^{-1}	3.12±0.02	2.46±0.01	2.40±0.01
NH_4^+	mg N L^{-1}	69±0	22±1	12±1
Abs. 254 nm	cm^{-1}	0.022±0.012	0.035±0.006	0.025±0.002
Abs. 410 nm	cm^{-1}	0.020±0.001	0.047±0.001	0.012±0.000
P. Alkalinity	mg $CaCO_3$ L^{-1}	549±40	-	0±0
T. Alkalinity	mg $CaCO_3$ L^{-1}	694±87	-	234±40
Calcium	mg L^{-1}	297.6±3.4	130.9±8.4	62.2±6.9
Magnesium	mg L^{-1}	43.3±2.1	20.2±1.1	31.4±7.2
Evaporation rate	%	-	6.0±0.4	4.0±0.6

Note: P. Alkalinity - phenolphthalein alkalinity; T. Alkalinity - total alkalinity.

The impact of CO_2 concentration was analyzed. The amount of CO_2 that would be necessary to reduce the pH of 12 to 8 during the AC process was estimated by adding CO_2 and by reaction stoichiometry, for all waters studied. About 0.48 g of CO_2 L^{-1} was necessary to reduce the pH from 12 to 8, for the three SWWs (Figure 3.9), while lower quantities of about 0.35, 0.24, and 0.22 g CO_2 L^{-1} were estimated by reaction stoichiometry, for SWW1, SWW2, and SWW3, respectively. This same amount of CO_2 injected for all SWW is justified by the similarity of the initial values of phenolphthalein alkalinity (about 480±40, 549±40 and 556±35 mg L^{-1} $CaCO_3$, for SWW1, SWW2, and SWW3, respectively), total alkalinity (about 709±79, 694±87, and 610±13 mg L^{-1} $CaCO_3$, for SWW1, SWW2, and SWW3, respectively), and pH. However, these CO_2 quantities are overestimated for the addition of injected CO_2 and underestimated for the reaction stoichiometry. According to Eq. 7, part of the injected CO_2 was consumed by the reaction with the ammonia present in the SWWs forming ammonium bicarbonate, since the immediate injection of CO_2 prevents the volatilization of ammonia.

$$NH_3 + CO_2 + H_2O \rightarrow NH_4HCO_3 \quad (7)$$

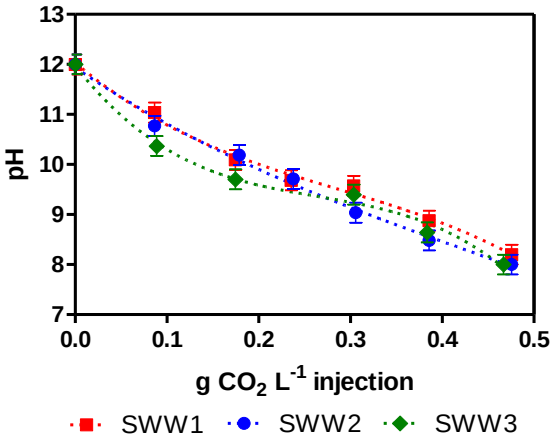

Figure 3.9 – Supernatant pH reached as a function of added CO_2, for SWW1, SWW2, and SWW3 supernatants treated by the IOSLM process at reaction pH 12. Bars represent the standard deviation of the mean.

On the other hand, for stoichiometric calculation the occurrence of evaporation during the AC process leads to higher concentrations of calcium or magnesium in the SWWs and the differences obtained in CO_2 calculated for SWW1, SWW2, and SWW3 reflect this. Calcium was the ion that most contributed (in about 81 to 89%) to CO_2 sequestration in this work compared to the magnesium ion. Thus, the estimate of the value of CO_2 captured during the AC process must be considered by CO_2 injection. Quantifying the air-water flux of carbon dioxide is still a challenge (Herrmann et al., 2020).

3.3.4. IOSLM + AC integrated process

Table 3.8 shows the characteristics and removals obtained by the IOSLM + AC integrated process, using the optimized conditions (IOSLM process at pH 12 and AC process at A/V ratios of 9.5 m^2/m^3 for SWW1 during 10 days and 5 m^2/m^3 for SWW2 and SWW3 during 15 days). According to Table 3.8, the effluents treated by the IOSLM + AC integrated process had a pH of around 7.8 and conductivity values close to the initial values. High TKN (97, 78, and 71%), BOD_5 (86, 82, and 80%), NH_4^+ (88, 69, and 52%), TP (99, 98, and 98%), TSS (99, 98, and 52%), turbidity (97, 96, and 62%), absorbance at 254 nm (87, 96, and 87%), absorbance at 410 nm (92, 96, and 83%) and oils & fats (92, 71, and 47%) removals were obtained for SWW1, SWW2, and SWW3, respectively. COD removals were 91 and 80% for SWW1 and SWW2, respectively, and 7% for SWW3 due to their previous treatment on-site pretreatment plant. The quality of the treated effluents showed

concentrations of COD (for all SWWs), BOD (for SWW1 and SWW2), TSS (for SWW1), TN (SWW2 and SWW3), and TP (for all SWWs) still above EU standards for discharge (COD = 125 mg L^{-1}; BOD = 25 mg L^{-1}; TSS = 35 mg L^{-1}; TN = 10 mg L^{-1}; TP = 1 mg L^{-1}). Therefore, additional treatments will be necessary for all SWWs. Biological treatments could be a solution for SWW1 and SWW2 since both presented high biodegradability index values after IOSLM + AC integrated process. On the other hand, constructed wetlands could be a solution to treat low biodegradable effluents such as SWW3 after IOSLM + AC integrated process (Madeira et al. (2021), chapter 5).

Table 3.8 – Characteristics and removals of three SWWs after the IOSLM + AC integrated process. Removals are shown in parentheses (at IOSLM reaction pH = 12, and A/V ratios of 9.5 m^2/m^3 for SWW1 during 10 days and 5 m^2/m^3 for SWW2 and SWW3 during 15 days).

Parameters	Unit	SWW1	SWW2	SWW3
pH	Sorensen	7.8±0.2	7.7±0.1	7.8±0.1
Conductivity	mS cm^{-1}	3.4±0.1	2.6±0.1	2.6±0.1
COD	mg O_2 L^{-1}	488±8 (91%)	368±5 (80%)	210±5 (7%)
TKN	mg N-Kj. L^{-1}	6±1 (97%)	22±1 (78%)	17±1 (71%)
BOD_5	mg O_2 L^{-1}	390±14 (86%)	180±0 (82%)	8±4 (80%)
NH_4^+	mg N L^{-1}	5±1 (88%)	20±1 (69%)	14±1 (52%)
TP	mg L^{-1}	3.0±1.6 (99%)	5.6±0.5 (98%)	2.5±2.0 (98%)
TSS	mg L^{-1}	47±10 (99%)	21±1 (98%)	29±4 (52%)
Turbidity	NTU	39±0 (97%)	17±0 (96%)	6±0 (62%)
Abs. at 254 nm	cm^{-1}	0.210±0.015 (87%)	0.033±0.005 (96%)	0.026±0.001 (87%)
Abs. at 410 nm	cm^{-1}	0.164±0.001 (92%)	0.054±0.005 (96%)	0.053±0.000 (83%)
Oils & Fats	mg L^{-1}	131±17 (92%)	110±15 (71%)	46±3 (47%)
Calcium	mg L^{-1}	55.7±15.7 (45%)	119.0±7.5 (25%)	71.4±3.7 (63%)
Magnesium	mg L^{-1}	27.6±24.3 (49%)	20.2±1.1 (73%)	5.8±1.8 (90%)

3.4. Conclusion

This work investigated the AC process in immediate one-step lime precipitation and atmospheric carbonation integrated processes for slaughterhouse wastewaters treatment. Slaughterhouse wastewaters with different characteristics were evaluated.

IOSLM results showed that the reaction pH was not a key parameter for slaughterhouse wastewaters treatment, which will depend on the characteristics of the SWW to be treated. However, at reaction pH 12 the SWW characteristics were better for the studied parameters where higher removals were obtained.

The AC process, as a solution for atmospheric mitigation of CO_2 emissions, proved to be efficient in reducing supernatant pH, conductivity, ammonium nitrogen, and calcium concentrations over time. Longer carbonation times are required using higher reaction pHs to achieve a supernatant pH of 9.5, however, if the objective is to achieve a supernatant pH of 8, the carbonation time may be the same regardless of the reaction pH applied. The reactor A/V ratio can be a significant factor in reducing supernatant pH, where high reactor A/V ratios mean less carbonation time. Ammonia removal was not affected by the reduction in carbonation time caused by the increase in the A/V ratio.

IOSLM + AC integrated process proved to be an efficient pre-treatment in the removal of contamination from the slaughterhouse wastewater for discharge into the municipal sewage treatment plant, however, an effluent tuning is still necessary if it is to be discharged into the water environment or to be reused in agriculture.

3.5. References

Aguilar, C.P., Peruzzolo, M., Luccio, M. Di, Dallago, R.M., Filho, I.D.N., 2006. Qualitative Study of Organic Compounds in Wastewaters of a Swine Slaughterhouse. Environ. Monit. Assess. 116, 103–110. https://doi.org/10.1007/s10661-006-7230-4

Aguilar, M.I., Sáez, J., Lloréns, M., Soler, A., Ortuño, J.F., 2002. Nutrient removal and sludge production in the coagulation-flocculation process. Water Res. 36, 2910–2919. https://doi.org/10.1016/S0043-1354(01)00508-5

Ajala, O.J., Tijani, J.O., Salau, R.B., Abdulkareem, A.S., Aremu, O.S., 2022. A review of emerging micro-pollutants in hospital wastewater: Environmental fate and remediation options. Results Eng. 16, 100671 https://doi.org/10.1016/j.rineng.2022.100671

Al Smadi, B.M., Al-Hayek, W., Abu Hajar, H.A., 2019. Treatment of Amman Slaughterhouse Wastewater by Anaerobic Baffled Reactor. Int. J. Civ. Eng. 17, 1445–1454. https://doi.org/10.1007/s40999-019-00406-5

Anawar, M.H., Strezov, V., Abhilash, A., 2019. Sustainable and economic waste management : resource recovery techniques. CRC Press.

Aziz, N.F.A., Ramli, N.A., Hamid, M.F.A., 2019. Energy efficiency of wastewater treatment plant through aeration system. Desalin. Water Treat. 156, 38–45. https://doi.org/10.5004/dwt.2019.24134

Baird, R., Eaton, A.D., Rice, E.W., Bridgewater, L., American Public Health Association, American Water Works Association, Water Environment Federation, 2017. Standard Methods for the Examination of Water and Wastewater, 23rd ed. ed. American Public Health Association, American Water Works Association, Water Environment Federation.

Berge, N.D., Reinhart, D.R., Townsend, T.G., 2005. The fate of nitrogen in bioreactor landfills. Crit. Rev. Environ. Sci. Technol. https://doi.org/10.1080/10643380590945003

Bustillo-Lecompte, C., Mehrvar, M., 2017. Slaughterhouse Wastewater: Treatment, Management and Resource Recovery, in: Physico-Chemical Wastewater Treatment and Resource Recovery. InTech. https://doi.org/10.5772/65499

Chen, Y., Xiong, C., Nie, J., 2016. Removal of Ammonia Nitrogen from Wastewater Using Modified Activated Sludge. Polish J. Environ. Stud. 25, 419–425. https://doi.org/10.15244/PJOES/60859

Chen, Y., Zhang, H., Yin, Y., Zeng, F., Cui, Z., 2022. Smart energy savings for aeration control in wastewater treatment. Energy Reports 8, 1711–1721. https://doi.org/10.1016/j.egyr.2022.02.038

Correia, T., Regato, M., Almeida, A., Santos, T., Amaral, L., Carvalho, M. de F.N., 2020. Manual Treatment of Urban Wastewater by Chemical Precipitation for Production of Hydroponic Nutrient Solutions. J. Ecol. Eng. 21, 143–152. https://doi.org/10.12911/22998993/118286

Dai, H., Tan, X., Zhu, H., Sun, T., Wang, X., 2018. Effects of Commonly Occurring Metal Ions on Hydroxyapatite Crystallization for Phosphorus Recovery from Wastewater. Water 10, 1619. https://doi.org/10.3390/w10111619

Dinçer, A.R., 2020. Increasing BOD_5/COD ratio of non-biodegradable compound (reactive black 5) with ozone and catalase enzyme combination. SN Appl. Sci. 2, 1–10. https://doi.org/10.1007/s42452-020-2557-y

Gupta, V.K., Sadegh, H., Yari, M., Shahryari Ghoshekandi, R., Maazinejad, B., Chahardori, M., 2015. Removal of ammonium ions from wastewater A short review in development of efficient methods. Glob. J. Environ. Sci. Manag. 1, 149–158. https://doi.org/10.7508/gjesm.2015.02.007

Hakim, S.S., Olsson, M.H.M., Sørensen, H.O., Bovet, N., Bohr, J., Feidenhans'l, R., Stipp, S.L.S., 2017. Interactions of the calcite {10.4} surface with organic compounds: Structure and behaviour at mineral-organic interfaces. Sci. Rep. 7, 1–11. https://doi.org/10.1038/s41598-017-06977-4

Herrmann, M., Najjar, R.G., Da, F., Friedman, J.R., Friedrichs, M.A.M., Goldberger, S., Menendez, A., Shadwick, E.H., Stets, E.G., St-Laurent, P., 2020. Challenges in Quantifying Air-Water Carbon Dioxide Flux Using Estuarine Water Quality Data: Case Study for Chesapeake Bay. J. Geophys. Res. Ocean. 125. https://doi.org/10.1029/2019JC015610

Hossaini, H., Fatehizadeh, A., Yousefi, N., Reshadat, S., Gilan, N.R., Ghasemi, S.R., Ahmadian, & M., 2013. Application of enhanced softening process in slaughterhouse wastewater treatment. Indian J. Chem. Technol. 20 (3):217-221.

Iloms, E., Ololade, O.O., Ogola, H.J.O., Selvarajan, R., 2020. Investigating industrial effluent impact on municipal wastewater treatment plant in Vaal, South Africa. Int. J. Environ. Res. Public Health. 17 (3): 1096. https://doi.org/10.3390/ijerph17031096

Lawler, D., 2004. Integrated Water Treatment Softening And Ultrafiltration. Intl Water Assn.

Luz, S., Rivas, J., Afonso, A., Carvalho, F., 2021. Immediate one-step lime precipitation process for the valorization of winery wastewater to agricultural purposes. Environ. Sci. Pollut. Res. 1–10. https://doi.org/10.1007/s11356-020-11933-3

Madeira, L., Almeida, A., Ribau Teixeira, M., Prazeres, A., Chaves, H., Carvalho, F., 2020. Immediate one-step lime precipitation and atmospheric carbonation as pre-treatment for low biodegradable and high nitrogen wastewaters: A case study of explosives industry. J. Environ. Chem. Eng. 8, 103808. https://doi.org/10.1016/j.jece.2020.103808

Madeira, L., Carvalho, F., Teixeira, M.R., Ribeiro, C., Almeida, A., 2021. Vertical flow constructed wetland as a green solution for low biodegradable and high nitrogen wastewater: A case study of explosives industry. Chemosphere 272, 129871. https://doi.org/10.1016/j.chemosphere.2021.129871

Mahtab, A., Tariq, M., Shafiq, T., Nasir, A., 2009. Coagulation/adsorption combined treatment of slaughterhouse wastewater. Desalin. Water Treat. 12, 270–275. https://doi.org/10.5004/dwt.2009.952

Middelburg, J.J., Soetaert, K., Hagens, M., 2020. Ocean Alkalinity, Buffering and Biogeochemical Processes. Rev Geophys. 58. https://doi.org/10.1029/2019RG000681

Njoya, M., Basitere, M., Ntwampe, S.K.O., 2019. Analysis of the characteristics of poultry slaughterhouse wastewater (PSW) and its treatability. Water Pract. Technol. 14, 959–970. https://doi.org/10.2166/wpt.2019.077

Odunlami, O.A., Vershima, D.A., Oladimeji, T.E., Nkongho, S., Ogunlade, S.K., Fakinle, B.S., 2022. Advanced techniques for the capturing and separation of CO_2 – A review. Results Eng. 15, 100512. https://doi.org/10.1016/j.rineng.2022.100512

Prasad, H., Lohchab, R.K., Singh, B., Nain, A., Kumari, M., 2019. Lime treatment of wastewater in a plywood industry to achieve the zero liquid discharge. J. Clean. Prod. 240, 118176. https://doi.org/10.1016/j.jclepro.2019.118176

Prazeres, A.R., Fernandes, F., Madeira, L., Luz, S., Albuquerque, A., Simões, R., Beltrán, F., Jerónimo, E., Rivas, J., 2019a. Treatment of slaughterhouse wastewater by acid precipitation (H_2SO_4, HCl and HNO_3) and oxidation ($Ca(ClO)_2$, H_2O_2 and CaO_2). J. Environ. Manage. 250, 109558. https://doi.org/10.1016/j.jenvman.2019.109558

Prazeres, A.R., Lelis, J., Alves-Ferreira, J., Carvalho, F., 2019b. Treatment of vinasse from sugarcane ethanol industry: H_2SO_4, NaOH and $Ca(OH)_2$ precipitations, $FeCl_3$ coagulation-flocculation and atmospheric CO_2 carbonation. J. Environ. Chem. Eng. 7, 103203. https://doi.org/10.1016/j.jece.2019.103203

Prazeres, A.R., Rivas, J., Paulo, Ú., Ruas, F., Carvalho, F., 2016. Sustainable treatment of different high-strength cheese whey wastewaters: an innovative approach for atmospheric CO_2 mitigation and fertilizer production. Environ. Sci. Pollut. Res. 23, 13062–13075. https://doi.org/10.1007/s11356-016-6429-3

Ramalho, M., Jovanović, T., Afonso, A., Baía, A., Lopes, A., Fernandes, A., Almeida, A., Carvalho, F., 2022. Landfill leachate treatment by immediate one-step lime precipitation, carbonation, and phytoremediation fine-tuning. Environ. Sci. Pollut. Res. 1, 1–10. https://doi.org/10.1007/S11356-022-18729-7/TABLES/3

Rivas, J., Prazeres, A.R., Carvalho, F., Beltrán, F., 2010. Treatment of cheese whey wastewater: Combined Coagulation - Flocculation and aerobic biodegradation. J. Agric. Food Chem. 58, 7871–7877. https://doi.org/10.1021/jf100602j

Satyanarayan, S., Ramakant, Vanerkar, A.P., 2005. Conventional approach for abattoir wastewater treatment. Environ. Technol. 26, 441–448. https://doi.org/10.1080/09593332608618554

Shao, B., Chen, D., Zhang, J., Wu, Y., Sun, C., 2009. Determination of 76 pharmaceutical drugs by liquid chromatography-tandem mass spectrometry in slaughterhouse wastewater. J. Chromatogr. A 1216, 8312–8318. https://doi.org/10.1016/j.chroma.2009.08.038

Tariq, M., Ahmad, M., Siddique, S., Waheed, A., Shafiq, T., Khan, M.H., 2012. Optimization of coagulation process for the treatment of the characterized slaughterhouse wastewater. Pak. J. Sci. Ind. Res. 55, 43–48.

Viswanaathan, S., Perumal, P.K., Sundaram, S., 2022. Integrated Approach for Carbon Sequestration and Wastewater Treatment Using Algal-Bacterial Consortia: Opportunities and Challenges. Sustain. 14, 1075. https://doi.org/10.3390/SU14031075

Yagi, S., Fukushi, K., 2012. Removal of phosphate from solution by adsorption and precipitation of calcium phosphate onto monohydrocalcite. J. Colloid Interface Sci. 384, 128–136. https://doi.org/10.1016/j.jcis.2012.06.063

Zeng, H., Zou, F., Horvath-Szabo, G., Andersen, S., 2012. Effects of brine composition on the adsorption of benzoic acid on calcium carbonate, in: Energy and Fuels. American Chemical Society, pp. 4321–4327. https://doi.org/10.1021/ef300165m

Zhao, J., Liu, S., Chi, Y., Feng, N., 2015. Magnesium hydroxide coagulation performance and floc properties in treating kaolin suspension under high pH. Desalin. Water Treat. 53, 579–585. https://doi.org/10.1080/19443994.2013.842502

Chapter 4

Modeling and optimization of atmospheric CO_2 capture for neutralization of high alkaline wastewaters using response surface methodology

This chapter is in preparation to submit a patent.

ABSTRACT

In this work, a lab-scale stirrer bubble column (SBC) and a lab-scale stepped continuous flow capillary column (SCFCR) were developed to neutralize lime precipitation treated slaughterhouse wastewater (SWW), using atmospheric CO_2. These experiments were carried out based on the response surface methodology using central composite design. Aeration time (2, 11.5, and 21 h), air flow rate (60, 90, and 120 L h^{-1}), stirring speed (0, 100, and 200 rpm), and SWW volume (178, 328, and 478 mL) were the independent variables studied for the bubbling process, while SWW flow rate (1.2, 1.6, and 2.0 mL min^{-1}), air flow rate (90, 180, and 270 L h^{-1}) and capillary area (150, 425, and 700 cm^2) in case of capillary process. The results showed that all the independent variables studied had a significant effect on the response variables studied (pH, conductivity, calcium, total alkalinity, and ammonium nitrogen), except the air flow rate variable on pH, conductivity, and calcium in the bubbling process, and the airflow rate variable in relation to all parameters studied in the capillary process. The carbonation process occurred in both processes. For the bubbling process, numerical optimization indicated a final pH 8 with calcium and ammonium nitrogen removals of 76.0 and 66.2%, respectively, applying 21 h, air flow rate at 65 L h^{-1}, the stirring speed at 52 rpm, and SWW volume at 178 mL. On the other hand, for the capillary process, pH 8.2 and calcium and ammonium nitrogen removals of 81.0 and 57.5% were achieved, applying SWW flow rate at 1.2 mL min^{-1}, air flow rate at 90 L h^{-1} and capillary area at 700 cm^2. Under optimal conditions, the SCFCR was able to neutralize different SWW volumes, 178 to 478 mL, without significant differences in the collected samples, with the operation time varying between 4.48 and 10.20 h, respectively.

4.1. Introduction

High alkaline wastewaters are usually generated from some industrial processes (Filimonova et al., 2019; Qi, 2018; Velts et al., 2013) and lime precipitation-based wastewater treatment systems (Martínez-Cruz et al., 2021; Mortula et al., 2020; Prasad et al., 2019; Prazeres et al., 2020). In the case of discharge or additional biological treatment, this type of effluent requires neutralization at adequate pH values (Madeira et al., 2020). Strong acids (e.g. sulfuric acid, hydrochloric acid, and nitric acid) have traditionally been used for neutralizing alkaline wastewater (Goel et al., 2005). However, its use has some disadvantages such as high economic cost, handling/storage concern of strong acids, corrosion of equipment and distribution networks, and significant discharge of strong acid salts (sulfates, chlorides, etc.) downstream of the treatment (Park and Lee, 2020). The neutralization of industrial alkaline wastewaters by biological means using alkalophilic bacteria has been reported as a possibility, but this process requires a source of carbon for acid production (Kumar et al., 2011). The use of CO_2 from simulated or real flue gas as a neutralizing agent for alkaline wastewater has been also considered given its advantages: CO_2 is not corrosive, its solubility in water is very high and allows greater control in the pH drop as CO_2 forms a weak acid in aqueous solution (Kang et al., 2016). Several strategies have been investigated to promote the absorption of gaseous CO_2 in alkaline aqueous solutions for carbonate production (Cruz-Navarro et al., 2020; Salmón et al., 2018). Different types of gas−liquid contactors have been used: rotating packed bed (Sun et al., 2011), tube-in-tube microreactor (Liang et al., 2014), microstructure mini reactor (Henthorn and Peppas, 2007), gas-liquid membrane contactor (Jia et al., 2013), surface-aerated stirred tank (Ding et al., 2018), gas sparged stirred tank (García Carmona et al., 2003), continuously stirred bubbling reactor (Liendo et al., 2021), packed bed reactor (Liendo et al., 2021), spray column (Wang et al., 2022) and tubular reactor (Azizi et al., 2022), among others. A rapid decrease in pH around neutrality and substantial reductions in conductivity and calcium concentration has been observed when the Ca-rich alkaline wastewater is neutralized with CO_2-containing flue gases, allowing to reduce the CO_2 emissions (Uibu et al., 2008). Although high CO_2 gas flow rates can significantly reduce the neutralization time to reach pH values below 8.5, there is some percentage of the CO_2 gas injected into the solution that is not consumed, which is released into the atmosphere and increases soluble calcium (Yoo et al., 2017). Recently, atmospheric CO_2 capture has

deserved attention in wastewater treatment systems (e.g., by microbial electrolytic carbon capture, microbial electrosynthesis, microalgae cultivation, constructed wetlands, and biochar production), since it contributes to negative carbon emissions (Lu et al., 2018). However, the atmospheric CO_2 capture for the neutralization of alkaline wastewaters resulting from the lime precipitation is not yet fully developed. Long carbonation time (≥ 7 days) to reduce the effluent pH from 12 to 8 has been observed in static and open systems using atmospheric CO_2 capture (Luz et al., 2021; Madeira et al., 2020 (chapter 2); Prazeres et al., 2019; Ramalho et al., 2022). The low concentration of CO_2 in the atmosphere (when compared to CO_2-containing flue gases) (Viswanaathan et al., 2022), the low reactor area/volume ratio used (≤ 7 m^2/m^3), and the presence of the lime precipitation process precipitate during carbonation process (Madeira et al., 2020) (chapter 2) may justify the high carbonation time. A high reactor area/volume ratio could decrease the pH (Madeira et al., 2023) (chapter 3), but this would require a large amount of available land. On the other hand, the aeration tank has contributed to better mixing of atmospheric air and liquid (Shibata et al., 2016). Correia et al. (2020) observed that the carbonation time of urban effluent treated by lime precipitation process (at pH 11.5) could be reduced from 220 to 100 hours to reach pH 8, using an aeration tank (A/V ratio of 5 m^2/m^3) with atmospheric air injection at 85 L h^{-1} during carbonation. However, as this carbonation process is performed in an open system, the ammonia if present in the effluent may be released into the atmosphere during CO_2 capture (Madeira et al., 2020 (chapter 2); Ramalho et al., 2022). Thus, there is a necessity to develop new cost-effective ways to promote a greater liquid-air interface to capture atmospheric CO_2 and the ammonia released in the meantime. Stirred bubble column (SBC) is a technology that has been applied in different industries due to its low cost, simple design, and high CO_2 absorption capacity derived from the large gas-liquid contact area caused by the stirring speed (Pashaei et al., 2018). Different aqueous solutions namely: slurry CaO (Liendo et al., 2021), diethanolamine solutions (Pashaei et al., 2017), and piperazine solutions (Pashaei et al., 2018), among others, have been successfully tested to capture CO_2. To the best of our knowledge, no investigations were reported on the neutralization of alkaline wastewater in stirred bubble columns using atmospheric CO_2, as well as their behavior in removing ammonia. On the other hand, recently the use of materials (e.g. cotton, polyester, among others) with capillary action has drawn the attention of several researchers in the treatment of supply waters (e.g., for iron (Radovenchyk et al., 2021; Trus et al., 2022) and manganese removal (Ayoub, 2018), and for water desalination

(Ahmadvand et al., 2019)) and wastewater treatment (e.g., for organic contaminants removal (Deng et al., 2022)). Such attention is because, without energy, the movement of water within the spaces of a porous material occurs due to the forces of adhesion, cohesion, and surface tension. The effect of capillary action on the neutralization of alkaline wastewater and on the volatilization of ammonia is not reported in the literature.

This work aims to evaluate the effectiveness of the stirrer bubble column (SBC) and stepped continuous flow capillary column (SCFCR) in neutralizing slaughterhouse wastewater (SWW) treated by lime precipitation using atmospheric CO_2. The effect of the operational variables of each of the two reactors, as well as the capture of ammonia in an acidic medium, will be studied. For both technologies proposed, mathematical models for the neutralization of alkaline effluents using atmospheric CO_2 have never been developed. Herein, these two technologies were designed to model and optimize through the response surface methodology.

4.2. Materials and methods

4.2.1. Raw and pretreated slaughterhouse wastewater (SWW)

Raw slaughterhouse wastewater (SWW) was collected from the output of the rotary drum screen filter in a slaughterhouse located in Portugal. Then, raw SWW was treated by IOSLM at pH 12, according to Madeira et al. (2023) (chapter 3). The pretreated SWW samples were characterized in terms of pH, conductivity, calcium, total alkalinity, and ammonium nitrogen. If not immediately analyzed, the collected samples were stored at 4 ºC until use. The SWW characteristics are provided in Table 4.1. According to Table 4.1, the effluents used are characterized by high pH (around 12), conductivity (around 5 mS cm^{-1}), and calcium (between 500 and 600 mg L^{-1}), which are characteristics of the effluents after the IOSLM process, and contains substantial amounts of ammonium nitrogen (between 60 and 80 mg $N\text{-}NH_4^+$ L^{-1}).

Table 4.1 - Physicochemical characterization of pretreated SWW resulting by IOSLM at pH 12.

Parameter	Unit	Used in experiments of:	
		Bubbling process	Capillary process
pH	Sorensen scale	11.88±0.05	12.13±0.02
Conductivity	mS cm^{-1}	5.23±0.15	5.03±0.34
Calcium	mg L^{-1}	633.1±18.6	509.7±7.6
Total alkalinity	mg $CaCO_3$ L^{-1}	1614±0	1296±0
Ammonium nitrogen	mg N-NH_4^+ L^{-1}	84.5±0.9	61.7±1.4

4.2.2. Experimental setup and procedure

The experimental tests of atmospheric CO_2 carbonation were conducted in three experiments.

In the first experiment, the bubbling process took place (Figure 4.1a). Between 178 to 478 mL of pretreated SWW was added to a lab-scale stirrer bubble column (SBC) (bottle column volume 750 mL and diameter 6.8 cm), under variable magnetic stirring (0 to 200 rpm) and atmospheric air injection (60 to 120 L h^{-1}) by an air pump. The reactor was hermetically sealed. The injected air was dispersed continuously (during 2 to 21 h) in the effluent by a bubble air diffuser (length 2.7 cm and diameter 1.3 cm) which was immersed in the bottle column. Then, the air was collected at the bottom of a beaker (height 35.3 cm and diameter 6 cm) containing 1 L of a sulfuric acid solution at pH 5, under dispersion by a bubble air diffuser (length 2.7 cm and diameter 1.3 cm). After the established time, the effluent was sedimented for 30 minutes and then analyzed according to section 4.2.4.

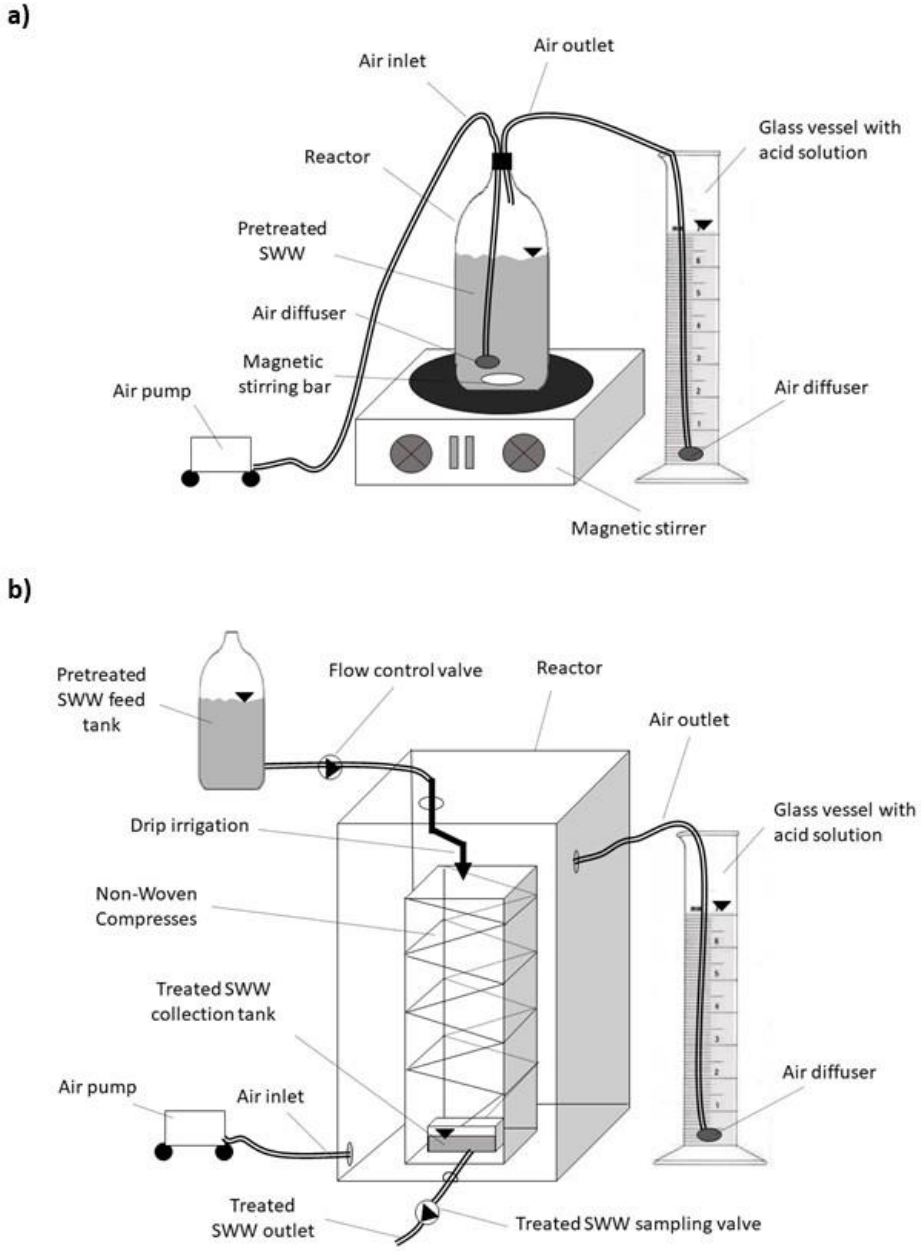

Figure 4.1 – Schematic diagrams of experimental systems relating to the atmospheric CO_2 carbonation process: a) stirrer bubble column and b) stepped continuous flow capillary column.

In the second experiment, the capillary process was used (Figure 4.1b). The pretreated SWW was gravitationally displaced, through a capillary located inside the lab-scale stepped continuous flow capillary column (SCFCR) (length, width, and height of 18.5, 14.5, and 35 cm, respectively), Figure 4.1b, while atmospheric air was continuously injected using an air pump at 90 to 270 L h^{-1}. The pretreated SWW flow rate used varied between 1.2 to 2.0 mL min^{-1} and was controlled by a flow regulation valve and by the height of the water level in the pretreated SWW feed tank. The SCFCR was hermetically

sealed. The capillary material used was a non-woven compress (width 5 cm, area 150 to 700 cm^2, and thickness 1 mm), made of 70% viscose and 30% polyester, which was arranged in a zigzag pattern with a slope of 17.7% in the SCFCR. The SCFCR injected air was collected in a beaker (height 35.3 cm and diameter 6 cm) filled with 1 L of sulfuric acid solution (at pH 5) and with a bubble air diffuser (length 2.7 cm and diameter 1.3 cm). After collecting 50 mL of effluent from the SCFCR, the experiment was terminated and the sample was analyzed according to section 4.2.4.

Finally, in the third experiment, the capillary process was performed again to evaluate the efficiency of the process in obtaining different volumes collected. Thus, 178, 328, and 478 mL of pretreated SWW were collected, using the best conditions found in the previous tests.

For both processes, the ammonia capture capacity was analyzed using the optimized conditions defined according to the selected criteria for independent variables and response variables (see section 4.2.3). The samples were analyzed according to section 4.2.4.

Throughout these experimental tests, the indoor air quality status (Table 4.2) was monitored (see section 4.2.4).

Table 4.2 – Indoor air quality states during the experiments.

Parameter		Experiments	
		Bubbling process	Capillary process
Temperature (ºC)	Min.	14.3	19.6
	Mean	15.9	19.8
	Max.	16.5	20.3
CO_2 (mg L^{-1})	Min.	222	206
	Mean	288	271
	Max.	389	420

4.2.3. Experimental design, optimization, and statistical analysis

In this work, the bubbling and the capillary experiments were carried out based on the Response Surface Methodology (RSM) using the full face central composite design (CCD). RSM was used to analyze the effect of independent variables and their

interactions on response variables, design experiments, build models, and find optimal operating conditions, through Design Expert 11 software (version 11.1.2.0).

A set of independent variables with a possible potential effect on the transfer of atmospheric CO_2 to the aqueous phase was evaluated for both processes. Four independent variables, aeration time, air flow rate, stirring speed, and SWW volume were performed for the bubbling process, while three variables, SWW flow rate, capillary area, and air flow rate, were for the capillary process. This set of variables was chosen for the following reasons. Aeration time has been the main variable studied in atmospheric carbonation processes. Shorter times may be associated with lower CO_2 capture and energy costs (e.g. running an air pump), and vice versa. Agitation may be a variable that promotes a greater area of gas-liquid contact since standing liquids result in less gas exchange with water. The air flow can be an important variable in the renewal of the air in closed systems, in addition to allowing a greater area of contact between the gas and the liquid as has been observed in the aeration tanks. On the other hand, larger volumes of effluent to be treated may be associated with a smaller space of contact between the air and the liquid inside the closed system, as well as greater needs for the capture of atmospheric CO_2. The capillary area is the contact medium between the gas and the liquid. Finally, the pretreated SWW flow rate is a variable that is related to the aeration time and the volume to be treated, as already mentioned before. Each of these variables was coded at three levels (-1, 0, +1), whose studied range is shown in Table 4.3. pH, conductivity, calcium, total alkalinity, and ammonium nitrogen were the response variables.

Table 4.3 – Experimental range and levels of the independent variables in the bubbling and capillary processes.

Process	Independent variable	Symbol	Coded levels		
			-1	0	1
Bubbling	Time (h)	A	2	11.5	21
	Air flow rate (L h^{-1})	B	60	90	120
	Stirring speed (rpm)	C	0	100	200
	SWW volume (mL)	D	178	328	478
Capillary	SWW flow rate (mL min^{-1})	A	1.2	1.6	2.0
	Air flow rate (L h^{-1})	B	90	180	270
	Capillary area (cm^2)	C	150	425	700

The experimental conditions are shown in Tables 4.4 and 4.5 for the bubbling and the capillary processes, respectively. These experimental matrices of capillary and bubbling processes are composed of 19 (with 5 central points and 14 non-central points) and 30 experiments (with 6 central points and 24 non-central points), respectively. The central point was repeated 5 (for the capillary process) and 6 times (for the bubbling process) to determine the experimental deviation between them, providing more robust statistical support to the results.

A quadratic model was applied for both processes to model the relationship between response variables and the independent variables, using the following second-order polynomial equation (1):

$$Y = \beta_0 + \sum_{i=1}^{n} \beta_i x_i + \sum_{i=1}^{n} \beta_{ii} x_i^2 + \sum_{i=1}^{n-1} \sum_{j=i+1}^{n} \beta_{ij} x_i x_j \quad (1)$$

where Y is the response variable, x_i and x_j are coded independent variables, and β_0, β_i, β_{ii}, and β_{ij} are coefficients of intercept, linear, quadratic, and interaction terms, respectively. The model was evaluated by R^2 and F values. Subsequently, the model was validated as to its reproducibility of results by repeating (in triplicate) an experiment carried out under optimal conditions. Once the model was validated, three-dimensional response surface graphs and contour plots were obtained.

The optimization was performed according to the constraint conditions defined for the response variables and independent variables, for both processes. These constraint conditions were mainly related to energy consumption and pH limit.

To confirm the statistical significance of the model, the effects of the input variables, and the interactions between the variables in the response, an analysis of variance (ANOVA) was performed with a *P*-value at the confidence level of 95 %, using the Design Expert software. GraphPad Prism for Windows (version 8.0.1) was used to draw the graphs. XLSTAT 2022 statistical software (version 2022.2.1) was used to correlate the response variables.

Table 4.4 – Experimental conditions (at four-factor and three-level) and results actual and predicted for pH, conductivity, calcium, total alkalinity, and ammonium by the bubbling process.

Run	Independent coded variables				pH		Conductivity (mS cm^{-1})		Calcium (mg L^{-1})		Total alkalinity (mg $CaCO_3$ L^{-1})		Ammonium (mg N L^{-1})	
	A	B	C	D	Actual	Predicted	Actual	Predicted	Actual	Predicted	Actual	Predicted	Actual	Predicted
1	1	0	0	0	9.60	9.56	1.57	1.72	158.14	177.28	50.08	41.40	31.68	37.65
2	0	0	0	0	11.42	11.14	2.64	2.49	253.02	275.93	230.69	339.59	58.09	51.07
3	0	0	0	0	11.06	11.14	2.79	2.49	284.64	275.93	230.69	339.59	51.49	51.07
4	-1	-1	-1	1	11.95	12.05	5.30	5.49	634.07	652.93	1401.04	1418.05	86.49	90.07
5	0	0	0	0	10.82	11.14	2.60	2.49	257.53	275.93	230.69	239.59	44.89	51.07
6	1	-1	1	1	10.66	10.69	1.71	1.81	178.41	186.17	184.55	208.16	47.53	48.43
7	1	1	1	-1	7.90	7.82	1.58	1.49	147.59	135.93	22.80	16.26	24.04	20.02
8	0	0	0	1	11.46	11.37	2.64	2.58	290.00	265.53	392.17	307.10	54.13	52.40
9	0	-1	0	0	11.04	11.30	2.17	2.50	292.34	311.62	401.20	377.97	45.64	50.97
10	0	0	1	0	11.29	11.34	2.39	2.72	263.56	292.98	346.03	317.59	56.85	61.90
11	-1	1	1	1	11.90	11.83	4.54	4.56	527.12	522.43	1038.09	1005.03	81.85	81.30
12	0	0	0	0	10.94	11.14	2.78	2.49	257.53	275.93	115.34	239.59	55.45	51.07
13	1	1	1	1	10.29	10.43	1.57	1.55	168.68	170.77	70.67	85.02	40.93	41.10
14	-1	-1	-1	-1	11.82	11.67	4.26	4.14	527.12	520.62	900.52	899.38	76.57	75.86
15	-1	-1	1	-1	11.68	11.66	3.63	3.59	432.24	433.04	784.34	771.23	72.61	70.30
16	0	0	-1	0	11.80	11.74	3.55	3.43	432.24	391.63	590.21	523.95	72.61	71.47
17	1	1	-1	1	11.19	11.23	2.29	2.43	274.10	280.49	346.03	369.60	52.81	54.67
18	1	1	-1	-1	8.23	8.29	1.54	1.56	169.84	175.88	23.01	8.02	27.72	28.41
19	1	-1	-1	-1	8.50	8.59	2.15	2.23	242.47	254.36	230.69	274.22	44.89	44.99
20	0	1	0	0	11.49	11.22	2.50	2.37	316.27	285.80	320.30	248.84	45.09	43.68
21	-1	-1	1	1	11.78	11.71	4.32	4.15	506.03	495.59	968.89	997.08	80.53	79.31
22	-1	0	0	0	11.77	11.80	4.12	4.17	516.58	486.24	900.00	813.98	75.25	73.19
23	1	-1	1	-1	8.04	7.95	1.53	1.35	129.00	103.72	50.04	13.51	30.36	28.77
24	0	0	0	0	11.14	11.14	2.04	2.49	316.27	275.93	138.41	239.59	56.77	51.07
25	-1	1	-1	-1	11.76	11.75	4.14	4.14	484.95	484.38	777.40	764.26	69.97	68.62
26	0	0	0	-1	9.80	9.88	1.60	1.87	168.68	181.95	23.01	13.39	29.12	34.76
27	0	0	0	0	11.41	11.14	2.67	2.49	253.02	275.93	207.62	239.59	51.49	51.07
28	-1	1	1	-1	11.78	11.91	4.35	4.40	495.49	507.48	853.54	905.07	67.33	70.88
29	1	-1	-1	1	11.79	11.65	3.70	3.50	422.96	406.57	800.02	761.69	73.93	69.84
30	-1	1	-1	1	11.93	12.00	5.08	5.10	548.20	569.08	1107.30	1157.04	83.17	84.23

Note: A: Time; B: Air flow rate; C: Stirring speed; D: SWW volume.

Table 4.5 – Experimental conditions (at three-factor and three-level) and results actual and predicted for pH, conductivity, calcium, total alkalinity, and ammonium by the capillary process.

Run	Independent coded variables			pH		Conductivity (mS cm^{-1})		Calcium (mg L^{-1})		Total alkalinity (mg $CaCO_3$ L^{-1})		Ammonium (mg N L^{-1})	
	A	B	C	Actual	Predicted	Actual	Predicted	Actual	Predicted	Actual	Predicted	Actual	Predicted
1	0	0	0	9.98	9.70	1.63	1.43	128.77	110.29	235.57	221.49	24.17	25.21
2	-1	-1	-1	11.81	11.73	2.99	2.97	268.26	269.46	471.15	458.50	29.70	29.73
3	-1	1	1	8.16	8.13	1.73	1.78	101.94	106.90	235.57	244.13	29.34	29.61
4	0	0	0	9.89	9.70	1.52	1.43	107.30	110.29	235.57	221.49	26.40	25.21
5	0	-1	0	9.12	9.27	1.53	1.60	96.57	105.18	176.68	203.71	22.00	22.56
6	0	0	0	9.67	9.70	1.49	1.43	123.40	110.29	176.68	221.49	26.40	25.21
7	0	0	1	8.87	8.93	1.67	1.60	107.30	108.40	235.57	220.20	23.73	23.79
8	1	-1	1	9.17	9.16	1.64	1.60	85.84	81.68	176.68	169.92	22.47	22.46
9	1	-1	-1	12.03	11.99	3.78	3.73	311.18	305.41	742.06	724.70	45.21	44.84
10	0	0	-1	11.93	12.15	3.08	3.16	278.99	281.16	530.04	580.63	33.00	33.34
11	1	1	-1	12.04	12.00	3.31	3.27	289.72	288.78	647.83	629.29	39.91	40.00
12	-1	0	0	9.38	9.57	1.34	1.24	107.30	97.67	176.68	173.09	27.63	27.62
13	1	0	0	10.07	10.15	1.40	1.50	107.30	120.20	235.57	274.38	32.18	32.58
14	-1	1	-1	11.82	11.75	2.74	2.77	225.34	228.69	412.26	410.21	26.40	26.32
15	0	0	0	9.77	9.70	1.28	1.43	96.57	110.29	294.47	221.49	25.67	25.21
16	1	1	1	9.04	9.04	1.51	1.53	118.03	116.02	176.68	180.52	24.56	24.44
17	-1	-1	1	8.28	8.25	1.56	1.60	96.57	96.70	176.68	186.41	26.40	26.21
18	0	1	0	9.10	9.22	1.53	1.46	107.30	101.96	176.68	184.87	22.00	21.84
19	0	0	0	9.72	9.70	1.26	1.43	101.94	110.29	235.57	221.49	24.17	25.21

Note: A: SWW flow rate; B: Air flow rate; C: Capillary area.

4.2.4. Analytical methods

All chemical analyses were performed following the Standard Methods (Baird et al., 2017). pH was measured by the potentiometric method, using WTW InoLab pH Level 1 apparatus and a pH electrode SenTix® 41. Electrical conductivity was determined by the electrometric method, using Jenway 4510 conductivity meter and a conductivity sensor VWR phenomenal CO 11. Ammonium nitrogen was measured by distillation method using a nitrogen distillation unit BUCHI B-316, followed by titration with hydrochloric acid. Calcium was measured by volumetric complexation with EDTA, using a calcon indicator. Total alkalinity was determined by neutralization titration.

Indoor air quality was assessed by a 3M™ EVM 7 Environmental Monitor Kit, which is a portable device whose measurement is continuous and in real-time. This equipment is equipped with a junction diode sensor and a non-dispersive infrared sensor for measuring temperature and carbon dioxide concentration levels, respectively, over a defined time interval.

4.3. Results and discussion

4.3.1. Experimental design and statistical analysis

The actual and predicted values of the different response variables referring to the experimental conditions applied to the bubbling process and the capillary process are shown in Tables 4.4 and 4.5, respectively. It can be seen from Table 4.4, that the pH, conductivity, calcium concentration, total alkalinity, and ammonium nitrogen concentration ranged from 7.90 to 11.95, 1.5 to 5.3 mS cm^{-1}, 129 to 634 mg L^{-1}, 23 to 1401 mg $CaCO_3$ L^{-1}, and 24 to 86 mg N L^{-1}, respectively, in the bubbling process. Regarding the capillary process (Table 4.5), the values varied between 8.16 and 12.04 for pH, 1.26 and 3.78 mS cm^{-1} for conductivity, 86 and 311 mg L^{-1} for calcium, 177 and 742 mg $CaCO_3$ L^{-1} for total alkalinity, and 22 and 45 mg N L^{-1} for ammonium nitrogen concentration. Minimum pH values observed around neutrality (of 7.90 and 8.16 for the bubbling process and the capillary process, respectively) indicated that there were experimental conditions that lead to the occurrence of the carbonation process. Overall, the actual and predicted values were quite close. These similarities are confirmed by the

proximity of most of the points to the diagonal axis (Figures 4.2 and 4.3), indicating that the quadratic polynomial models chosen seem suitable to predict the response variables of both processes.

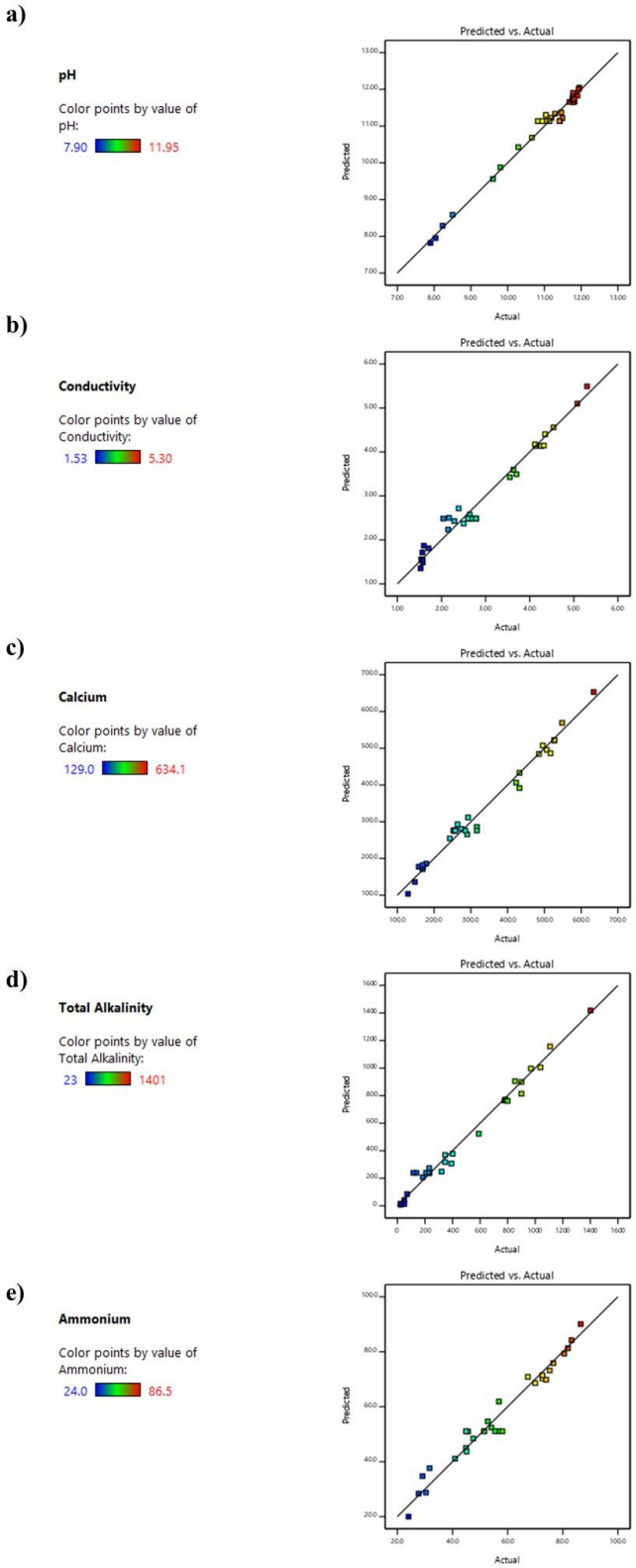

Figure 4.2 – Correlation between the actual value and the predicted values for a) pH, b) conductivity, c) calcium concentration, d) total alkalinity, and e) ammonium nitrogen concentration, using the bubbling process.

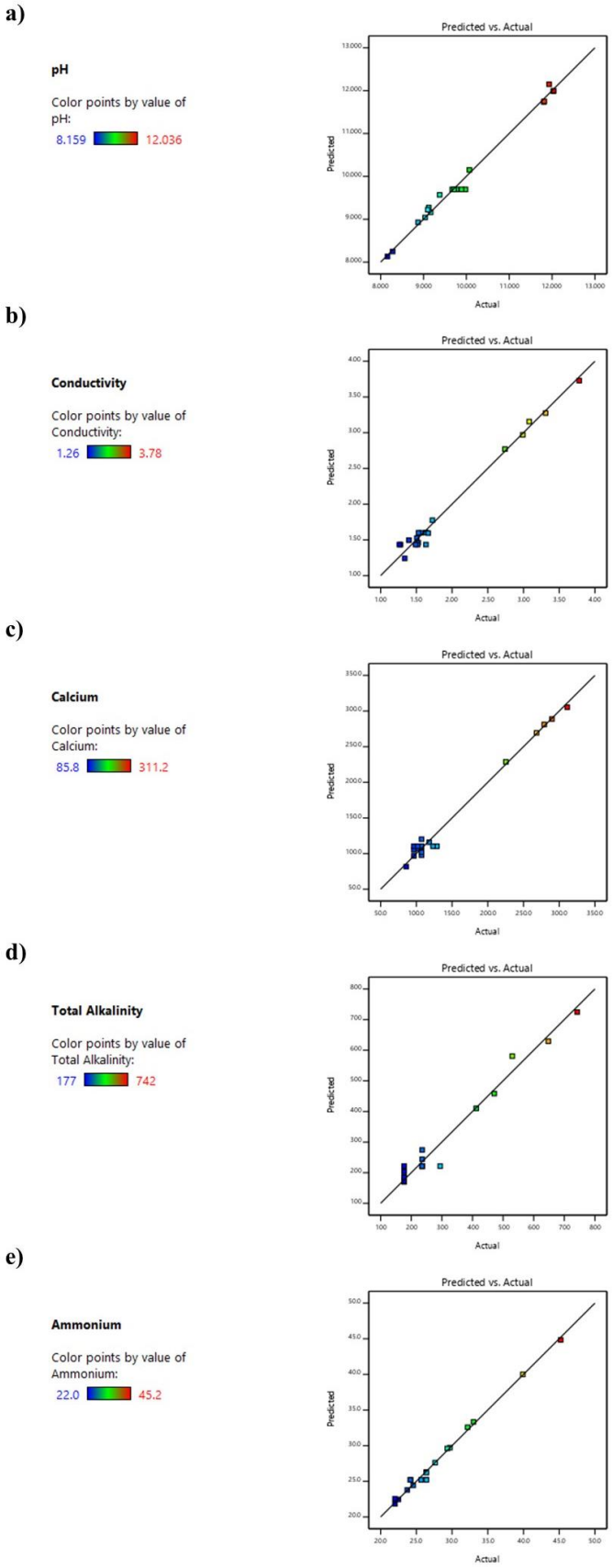

Figure 4.3 - Correlation between the actual value and the predicted values for a) pH, b) conductivity, c) calcium concentration, d) total alkalinity, and e) ammonium nitrogen concentration, using the capillary process.

Thus, the regression models to predict the response variables were described by the second-order polynomial equations given in Table 4.6 (Y_1 to Y_5 for the bubbling process and Y_6 to Y_{10} for the capillary process), which relates the response variable with the independent variables. Through the regression equations, it is possible to identify the effects of the independent variables on the response variables. Model components such as *A* (i.e., time), *B* (i.e., air flow rate) *C* (i.e., stirring speed), and *D* (i.e., SWW volume) for the bubbling process, and *A* (i.e., SWW flow rate), *B* (i.e., air flow rate), and *C* (i.e., capillary area) for the capillary process, represent the linear effects of the main independent variables. On the other hand, the model components *AB*, *AC*, *AD*, *BC*, *BD,* and *CD* for the bubbling process and *AB*, *AC*, and *BC* for the capillary process represent the interaction between two independent variables, while A^2, B^2, C^2, and D^2 for bubbling process, and A^2, B^2, C^2 for capillary process represent their quadratic effects. The positive coefficients of the equation indicate the synergistic effect of the independent variables on the response variables, while negative coefficients indicate antagonistic effects.

Table 4.6 – Regression equations for different parameters in the bubbling and capillary processes.

Parameters	Equations	
	Bubbling process	**Capillary process**
pH	$Y_1 = 11.14 - 1.12A - 0.0439B - 0.2028C + 0.7467D - 0.0950AB - 0.1562AC + 0.6713AD + 0.0413BC - 0.0312BD - 0.0825CD - 0.4551A^2 + 0.1249B^2 + 0.4049C^2 - 0.5101D^2$	$Y_6 = 9.70 + 0.2903A - 0.0259B - 1.61C - 0.0016AB + 0.1651AC - 0.0334BC + 0.1657A^2 - 0.4473B^2 + 0.8432C^2$
Conductivity (mS cm^{-1})	$Y_2 = 2.49 - 1.23A - 0.0652B - 0.3554C + 0.3542D - 0.1690AB - 0.0849AC - 0.0240AD + 0.2010BC - 0.0989BD - 0.2015CD + 0.4590A^2 - 0.0490B^2 + 0.5860C^2 - 0.2640D^2$	$Y_7 = 1.43 + 0.1271A - 0.0692B - 0.7802C - 0.0635AB - 0.1885AC + 0.0940BC - 0.0656A^2 + 0.0959B^2 + 0.9409C^2$
Calcium (mg L^{-1})	$Y_3 = 275.93 - 154.48A - 12.91B - 49.32C + 41.79D - 10.56AB - 15.77AC + 4.98AD + 27.67BC - 11.90BD - 17.44CD + 55.83A^2 + 22.78B^2 + 66.37C^2 - 52.19D^2$	$Y_8 = 110.29 + 11.27A - 1.61B - 86.38C + 6.04AB - 12.74AC + 12.74BC - 1.36A^2 - 6.72B^2 + 84.49C^2$
Total alkalinity (mg $CaCO_3$ L^{-1})	$Y_4 = 239.59 - 386.29A - 64.56B - 103.18C + 146.86D - 32.77AB - 33.14AC - 7.80AD + 67.24BC - 31.47BD - 73.21CD + 188.11A^2 + 73.82B^2 + 181.19C^2 - 79.34D^2$	$Y_9 = 221.49 + 50.65A - 9.42B - 180.21C - 11.78AB - 70.67AC + 26.50BC + 2.25A^2 - 27.20B^2 + 178.93C^2$
Ammonium (mg N L^{-1})	$Y_5 = 51.07 - 17.77A - 3.65B - 4.79C + 8.82D - 2.33AB - 2.66AC + 2.66AD + 1.96BC + 0.3525BD - 1.30CD + 4.35A^2 - 3.75B^2 + 15.61C^2 - 7.49D^2$	$Y_{10} = 25.21 + 2.48A - 0.3577B - 4.77C - 0.3554AB - 4.71AC + 1.70BC + 4.89A^2 - 3.01B^2 + 3.36C^2$

Note: A: Time; B: Air flow rate; C: Stirring speed; D: SWW volume, for the bubbling process. A: SWW flow rate; B: Air flow rate; C: Capillary area for the capillary process.

Tables 4.7 and 4.8 present the values of these coefficients of the regression equations, for the bubbling and capillary processes, respectively. From Table 4.7, the model components

such as *A*, *B,* and *C* in the bubbling process appear to contribute to the reduction of pH, conductivity, calcium, total alkalinity, and ammonia. On the other hand, model component *A* seems to contribute to the increase of all response variables (Table 4.7). Regarding the capillary process (Table 4.8), model component *A* seems to contribute to the increase in the response variables studied, unlike model components *B* and *C*, which seem to be responsible for its decrease. As with individual effects, the interactive effect between independent variables on response variables must also be considered. For example, for the pH, the model components such as *D*, *AD*, *BC*, B^2, and C^2 of the bubbling process (Table 4.7), and *A*, *AC*, A^2, and C^2 of the capillary process (Table 4.8) indicate favorable effects for pH increase, while other model components such as *A*, *B*, *C*, *AB*, *AC*, *BD*, *CD*, A^2, and D^2 for the bubbling process (Table 4.7), and *B*, *C*, *AB*, *BC,* and B^2 for the capillary process (Table 4.8) are responsible for the pH decrease. Although the coefficients of the terms *B* and *BD* (for the bubbling process) and, *B* and *AB* (for the capillary process) were negative, it can be said that their influence on pH was practically null since the values of the coefficients were close to zero. Therefore, it seems that air flow rate had not any influence on pH in both processes studied. Other favorable or unfavorable effects of the model components on the other response variables can be observed in Tables 4.7 and 4.8 for the bubbling process and capillary process, respectively. However, it will still be necessary to see the level of significance of these model components on the response variables, using ANOVA analysis.

Table 4.7 – Estimated coefficient from regression equations for predicting the response variables in the bubbling process.

	pH	Conductivity (mS cm^{-1})	Calcium (mg L^{-1})	Total alkalinity (mg $CaCO_3$ L^{-1})	Ammonium (mg N L^{-1})
Constant	+ 11.14	+ 2.49	+ 275.93	+ 239.59	+ 51.07
A	- 1.12	- 1.23	- 154.48	- 386.29	- 17.77
B	- 0.0439	- 0.0652	- 12.91	- 64.56	- 3.65
C	- 0.2028	- 0.3554	- 49.32	- 103.18	- 4.79
D	+ 0.7467	+ 0.3542	+ 41.79	+ 146.86	+ 8.82
AB	- 0.0950	- 0.1690	- 10.56	- 32.77	- 2.33
AC	- 0.1562	- 0.0849	- 15.77	- 33.14	- 2.66
AD	+ 0.6713	-0.0240	+ 4.98	- 7.80	+ 2.66
BC	+ 0.0413	+ 0.2010	+ 27.67	+ 67.24	+ 1.96
BD	- 0.0312	- 0.0989	- 11.90	- 31.47	+ 0.3525
CD	- 0.0825	- 0.2015	- 17.44	- 73.21	- 1.30
A^2	- 0.4551	+ 0.4590	+ 55.83	+ 188.11	+ 4.35
B^2	+ 0.1249	- 0.0490	+ 22.78	+ 73.82	- 3.75
C^2	+ 0.4049	+ 0.5860	+ 66.37	+ 181.19	+ 15.61
D^2	- 0.5101	- 0.2640	- 52.19	- 79.34	- 7.49

Note: A: Time; B: Air flow rate; C: Stirring speed; D: SWW volume.

Table 4.8 - Estimated coefficient from regression equations for predicting the response variables in the capillary process.

	pH	Conductivity ($mS\ cm^{-1}$)	Calcium ($mg\ L^{-1}$)	Total alkalinity ($mg\ CaCO_3\ L^{-1}$)	Ammonium ($mg\ N\ L^{-1}$)
Constant	+ 9.70	+ 1.43	+ 110.29	+ 221.49	+ 25.21
A	+ 0.2903	+ 0.1271	+ 11.27	+ 50.65	+ 2.48
B	- 0.0259	- 0.0692	- 1.61	- 9.42	- 0.3577
C	- 1.61	- 0.7802	- 86.38	- 180.21	- 4.77
AB	- 0.0016	- 0.0635	+ 6.04	- 11.78	- 0.3554
AC	+ 0.1651	- 0.1885	- 12.74	- 70.67	- 4.71
BC	- 0.0334	+ 0.0940	+ 12.74	+ 26.50	+ 1.70
A^2	+ 0.1657	- 0.0656	- 1.36	+ 2.25	+ 4.89
B^2	- 0.4473	+ 0.0959	- 6.72	- 27.20	- 3.01
C^2	+ 0.8432	+ 0.9409	+ 84.49	+ 178.93	+ 3.36

Note: A: SWW flow rate; B: Air flow rate; C: Capillary area.

The model adequacy was evaluated for different response variables using ANOVA (Table 4.9), both for the bubbling process and for the capillary process. According to Table 4.9, the models defined for pH, conductivity, calcium, and ammonia have excellent reproducibility (CV ≤ 10%), while the model defined for total alkalinity has good reproducibility (CV between 10 and 20%), for both processes. High determination coefficient (R^2) values were obtained (≥ 0.96 for the bubbling process and ≥ 0.97 for the capillary process), indicating a high correlation between the predicted and actual values, for all response variables. Furthermore, high predicted R^2 values (≥ 0.86 for the bubbling process and ≥ 0.89 for the capillary process) were obtained, indicating that the regression model can make predictions.

For all response variables and both processes, the predicted coefficient of determination is in reasonable agreement with the adjusted coefficient of determination since its difference is less than 0.2. All response variables had an adequate precision > 4, which indicates an adequate signal, and the model can be used to navigate the design space and for optimization. *F*-values of 78.24, 40.43, 54.70, 70.85, and 28.38 for the bubbling process, and *F*-values of 109.43, 72.57, 87.98, 37.53, and 107.34 for the capillary process, were obtained for pH, conductivity, calcium, total alkalinity, and ammonium nitrogen, respectively, which the *P*-value was less than 0.05 ($P < 0.0001$). These results suggest that the quadratic model was significant for all response variables. The *P*-value of lack of fit greater than 0.05 was observed for all response variables, either for the bubbling process (Table 4.10) or the capillary process (Table 4.11), which means that the regression models are not poor models of the data.

Table 4.9 – ANOVA results of the response surface quadratic model, for the bubbling process and the capillary process.

Process	Model	SD	Mean	CV (%)	R^2	Adjusted R^2	Predicted R^2	Adeq. Precision	Sum of Squares	*df*	Mean Square	*F*-value	*P*-value	Remark
Bubbling	pH	0.1995	10.87	1.83	0.9865	0.9739	0.9521	29.9732	43.59	14	3.11	78.24	< 0.0001	Significant
	Conductivity	0.2586	2.92	8.84	0.9742	0.9501	0.9066	22.6301	37.85	14	2.70	40.43	< 0.0001	Significant
	Calcium	27.98	331.60	8.44	0.9808	0.9629	0.9226	27.7572	6.00E+05	14	42828.71	54.70	< 0.0001	Significant
	Total alkalinity	66.59	457.85	14.54	0.9851	0.9712	0.9441	29.9446	4.40E+06	14	3.14E+05	70.85	< 0.0001	Significant
	Ammonium	4.81	56.31	8.55	0.9636	0.9297	0.8615	20.5816	9202.32	14	657.31	28.38	< 0.0001	Significant
Capillary	pH	0.1738	9.99	1.74	0.9909	0.9819	0.9656	31.8473	29.74	9	3.30	109.43	< 0.0001	Significant
	Conductivity	0.1302	1.95	6.69	0.9864	0.9728	0.9525	26.3337	11.06	9	1.23	72.57	< 0.0001	Significant
	Calcium	11.74	150.51	7.8	0.9888	0.9775	0.9577	26.2670	1.09E+05	9	12127.80	87.98	< 0.0001	Significant
	Total alkalinity	39.55	302.53	13.07	0.9740	0.9481	0.8984	19.3348	5.28E+05	9	58711.70	37.53	< 0.0001	Significant
	Ammonium	0.8243	27.97	2.95	0.9908	0.9815	0.9758	38.4510	656.41	9	72.93	107.34	< 0.0001	Significant

Note: SD – standard deviation; CV – coefficient of variation; R^2 - determination coefficient; Adeq. Precision – Adequate Precision; *df* – degrees of freedom; *F*-value – Fisher´s exact test value. A $P>0.10$ is considered not significant, while a $P<0.05$ is significant.

Table 4.10 – ANOVA of the prediction results for different parameters by quadratic modeling, in the bubbling process.

Source	Sum of Squares	*df*	Mean Square	*F*-value	*P*-value	Remark
pH model	43.59	14	3.11	78.24	< 0.0001	Significant
A	22.60	1	22.60	568.00	< 0.0001	Significant
B	0.0347	1	0.0347	0.8714	0.3654	Not significant
C	0.7401	1	0.7401	18.60	0.0006	Significant
D	10.04	1	10.04	252.20	< 0.0001	Significant
AB	0.1444	1	0.1444	3.63	0.0761	Not significant
AC	0.3906	1	0.3906	9.82	0.0068	Significant
AD	7.21	1	7.21	181.18	< 0.0001	Significant
BC	0.0272	1	0.0272	0.6842	0.4211	Not significant
BD	0.0156	1	0.0156	0.3927	0.5403	Not significant
CD	0.1089	1	0.1089	2.74	0.1188	Not significant
A^2	0.5366	1	0.5366	13.49	0.0023	Significant
B^2	0.0404	1	0.0404	1.02	0.3295	Not significant
C^2	0.4248	1	0.4248	10.68	0.0052	Significant
D^2	0.6741	1	0.6741	16.94	0.0009	Significant
Residual	0.5969	15	0.0398			
Lack of Fit	0.2972	10	0.0297	0.4958	0.8385	Not significant
Pure Error	0.2997	5	0.0599			
Cor Total	44.18	29				
Conductivity model	37.85	14	2.70	40.43	< 0.0001	Significant
A	27.16	1	27.16	406.21	< 0.0001	Significant
B	0.0766	1	0.0766	1.15	0.3015	Not significant
C	2.27	1	2.27	34.01	< 0.0001	Significant
D	2.26	1	2.26	33.77	< 0.0001	Significant
AB	0.4570	1	0.4570	6.83	0.0195	Significant
AC	0.1153	1	0.1153	1.72	0.2090	Not significant
AD	0.0092	1	0.0092	0.1378	0.7156	Not significant
BC	0.6464	1	0.6464	9.67	0.0072	Significant
BD	0.1564	1	0.1564	2.34	0.1470	Not significant
CD	0.6496	1	0.6496	9.71	0.0071	Significant
A^2	0.5459	1	0.5459	8.16	0.0120	Significant
B^2	0.0062	1	0.0062	0.0929	0.7647	Not significant
C^2	0.8898	1	0.8898	13.31	0.0024	Significant
D^2	0.1805	1	0.1805	2.70	0.1212	Not significant
Residual	1.00	15	0.0669			
Lack of Fit	0.6155	10	0.0616	0.7942	0.6474	Not significant
Pure Error	0.3875	5	0.0775			
Cor Total	38.85	29				
Calcium model	5.996E+05	14	42828.71	54.70	< 0.0001	Significant
A	4.295E+05	1	4.295E+05	548.60	< 0.0001	Significant
B	3000.29	1	3000.29	3.83	0.0692	Not significant
C	43791.40	1	43791.40	55.93	< 0.0001	Significant
D	31432.43	1	31432.43	40.14	< 0.0001	Significant
AB	1783.71	1	1783.71	2.28	0.1520	Not significant
AC	3976.64	1	3976.64	5.08	0.0396	Significant
AD	396.15	1	396.15	0.5060	0.4878	Not significant
BC	12250.60	1	12250.60	15.65	0.0013	Significant
BD	2265.91	1	2265.91	2.89	0.1095	Not significant
CD	4866.27	1	4866.27	6.22	0.0248	Significant
A^2	8075.14	1	8075.14	10.31	0.0058	Significant
B^2	1344.17	1	1344.17	1.72	0.2098	Not significant
C^2	11412.82	1	11412.82	14.58	0.0017	Significant
D^2	7056.94	1	7056.94	9.01	0.0089	Significant
Residual	11744.62	15	782.97			
Lack of Fit	8501.88	10	850.19	1.31	0.4034	Not significant
Pure Error	3242.74	5	648.55			
Cor Total	6.113E+05	29				

Note: *df* – degrees of freedom; *F*-value – Fisher´s exact test value; A $P > 0.10$ is considered not significant, while a $P < 0.05$ is significant.

Table 4.10 - (continued). ANOVA of the prediction results for different parameters by quadratic modeling, in the bubbling process.

Source	Sum of Squares	*df*	Mean Square	*F*-value	*P*-value	Remark
Total alkalinity model	3.919E+06	14	2.799E+05	36.93	< 0.0001	Significant
A	2.673E+06	1	2.673E+06	352.66	< 0.0001	Significant
B	44985.25	1	44985.25	5.93	0.0278	Significant
C	2.089E+05	1	2.089E+05	27.56	< 0.0001	Significant
D	4.305E+05	1	4.305E+05	56.79	< 0.0001	Significant
AB	10408.34	1	10408.34	1.37	0.2596	Not significant
AC	15078.07	1	15078.07	1.99	0.1788	Not significant
AD	15.83	1	15.83	0.0021	0.9642	Not significant
BC	88791.34	1	88791.34	11.71	0.0038	Significant
BD	12090.93	1	12090.93	1.59	0.2259	Not significant
CD	66362.11	1	66362.11	8.75	0.0098	Significant
A^2	39194.94	1	39194.94	5.17	0.0381	Significant
B^2	12420.98	1	12420.98	1.64	0.2200	Not significant
C^2	74115.39	1	74115.39	9.78	0.0069	Significant
D^2	61310.09	1	61310.09	8.09	0.0123	Significant
Residual	1.137E+05	15	7580.64			
Lack of Fit	58640.55	10	5864.05	0.5324	0.8147	Not significant
Pure Error	55069.10	5	11013.82			
Cor Total	4.033E+06	29				
Ammonium model	9202.32	14	657.31	28.38	< 0.0001	Significant
A	5684.57	1	5684.57	245.41	< 0.0001	Significant
B	239.40	1	239.40	10.34	0.0058	Significant
C	412.14	1	412.14	17.79	0.0007	Significant
D	1399.90	1	1399.90	60.44	< 0.0001	Significant
AB	87.07	1	87.07	3.76	0.0716	Not significant
AC	113.45	1	113.45	4.90	0.0428	Significant
AD	113.45	1	113.45	4.90	0.0428	Significant
BC	61.33	1	61.33	2.65	0.1245	Not significant
BD	1.99	1	1.99	0.0858	0.7736	Not significant
CD	26.94	1	26.94	1.16	0.2978	Not significant
A^2	49.10	1	49.10	2.12	0.1660	Not significant
B^2	36.39	1	36.39	1.57	0.2292	Not significant
C^2	631.65	1	631.65	27.27	0.0001	Significant
D^2	145.31	1	145.31	6.27	0.0243	Significant
Residual	347.46	15	23.16			
Lack of Fit	230.98	10	23.10	0.9915	0.5391	Not significant
Pure Error	116.48	5	23.30			
Cor Total	9549.77	29				

Note: *df* – degrees of freedom; *F*-value – Fisher´s exact test value; A $P>0.10$ is considered not significant, while a $P<0.05$ is significant.

Table 4.11 – ANOVA of the prediction results for different parameters by quadratic modeling, in the capillary process.

Source	Sum of Squares	*df*	Mean Square	*F*-value	*P*-value	Remark
pH model	29.74	9	3.30	109.43	< 0.0001	Significant
A	0.8427	1	0.8427	27.90	0.0005	Significant
B	0.0067	1	0.0067	0.2221	0.6486	Not significant
C	25.93	1	25.93	858.51	< 0.0001	Significant
AB	0.0000	1	0.0000	0.0007	0.9795	Not significant
AC	0.2181	1	0.2181	7.22	0.0249	Significant
BC	0.0089	1	0.0089	0.2951	0.6002	Not significant
A^2	0.0750	1	0.0750	2.48	0.1496	Not significant
B^2	0.5468	1	0.5468	18.11	0.0021	Significant
C^2	1.94	1	1.94	64.32	< 0.0001	Significant
Residual	0.2718	9	0.0302			
Lack of Fit	0.2079	5	0.0416	2.60	0.1874	Not significant
Pure Error	0.0639	4	0.0160			
Cor Total	30.02	18				
Conductivity model	11.06	9	1.23	72.57	< 0.0001	Significant
A	0.1615	1	0.1615	9.54	0.0130	Significant
B	0.0479	1	0.0479	2.83	0.1270	Not significant
C	6.09	1	6.09	359.35	< 0.0001	Significant
AB	0.0323	1	0.0323	1.90	0.2009	Not significant
AC	0.2843	1	0.2843	16.78	0.0027	Significant
BC	0.0707	1	0.0707	4.17	0.0714	Not significant
A^2	0.0117	1	0.0117	0.6936	0.4265	Not significant
B^2	0.0251	1	0.0251	1.48	0.2541	Not significant
C^2	2.42	1	2.42	142.81	< 0.0001	Significant
Residual	0.1525	9	0.0169			
Lack of Fit	0.0491	5	0.0098	0.3805	0.8411	Not significant
Pure Error	0.1033	4	0.0258			
Cor Total	11.22	18				
Calcium model	1.092E+05	9	12127.80	87.98	< 0.0001	Significant
A	1269.44	1	1269.44	9.21	0.0141	Significant
B	25.91	1	25.91	0.1879	0.6748	Not significant
C	74614.81	1	74614.81	541.31	< 0.0001	Significant
AB	291.45	1	291.45	2.11	0.1799	Not significant
AC	1298.94	1	1298.94	9.42	0.0134	Significant
BC	1298.94	1	1298.94	9.42	0.0134	Significant
A^2	5.02	1	5.02	0.0364	0.8529	Not significant
B^2	123.40	1	123.40	0.8953	0.3688	Not significant
C^2	19504.54	1	19504.54	141.50	< 0.0001	Significant
Residual	1240.57	9	137.84			
Lack of Fit	469.12	5	93.82	0.4865	0.7754	Not significant
Pure Error	771.45	4	192.86			
Cor Total	1.104E+05	18				
Total alkalinity model	5.284E+05	9	58711.70	37.53	< 0.0001	Significant
A	25652.83	1	25652.83	16.40	0.0029	Significant
B	887.93	1	887.93	0.5676	0.4705	Not significant
C	3.248E+05	1	3.248E+05	207.62	< 0.0001	Significant
AB	1109.91	1	1109.91	0.7095	0.4214	Not significant
AC	39956.82	1	39956.82	25.54	0.0007	Significant
BC	5618.93	1	5618.93	3.59	0.0906	Not significant
A^2	13.79	1	13.79	0.0088	0.9273	Not significant
B^2	2021.60	1	2021.60	1.29	0.2850	Not significant
C^2	87477.95	1	87477.95	55.92	< 0.0001	Significant
Residual	14078.57	9	1564.29			
Lack of Fit	7141.62	5	1428.32	0.8236	0.5910	Not significant
Pure Error	6936.95	4	1734.24			
Cor Total	5.425E+05	18				

Note: *df* – degrees of freedom; *F*-value – Fisher´s exact test value; A $P>0.10$ is considered not significant, while a $P<0.05$ is significant.

Table 4.11 - (continued). ANOVA of the prediction results for different parameters by quadratic modeling, in the capillary process.

Source	Sum of Squares	*df*	Mean Square	*F*-value	*P*-value	Remark
Ammonium model	656.41	9	72.93	107.34	< 0.0001	Significant
A	61.70	1	61.70	90.81	< 0.0001	Significant
B	1.28	1	1.28	1.88	0.2032	Not significant
C	227.69	1	227.69	335.09	< 0.0001	Significant
AB	1.01	1	1.01	1.49	0.2536	Not significant
AC	177.78	1	177.78	261.64	< 0.0001	Significant
BC	23.20	1	23.20	34.15	0.0002	Significant
A^2	65.41	1	65.41	96.26	< 0.0001	Significant
B^2	24.72	1	24.72	36.38	0.0002	Significant
C^2	30.81	1	30.81	45.35	< 0.0001	Significant
Residual	6.12	9	0.6795			
Lack of Fit	1.02	5	0.2040	0.1601	0.9650	Not significant
Pure Error	5.10	4	1.27			
Cor Total	662.52	18				

Note: *df* – degrees of freedom; *F*-value – Fisher´s exact test value; A $P>0.10$ is considered not significant, while a $P<0.05$ is significant.

4.3.2. Individual and interactive effects of model parameters on response variables

For the bubbling and capillary processes, the individual and interactive effects of independent variables on pH, conductivity, calcium, total alkalinity, and ammonium nitrogen were evaluated.

Tables 4.10 and 4.11 show the ANOVA results for the bubbling process and capillary process, respectively. As seen from Table 4.10, all independent variables of the bubbling process, such as time (*A*), air flow rate (*B*) stirring speed (*C*), and SWW volume (*D*), had significant effects ($P<0.05$) on the tested parameters models, except air flow rate which had no significant effect on pH, conductivity, and calcium. For the capillary process (Table 4.11), unlike air flow rate (*B*), the variables SWW flow rate (*A*), and capillary area (*C*) had significant effects ($P<0.05$) on pH, conductivity, calcium, total alkalinity, and ammonium nitrogen. Significant effects ($P<0.05$) of squared terms were observed for pH (e.g., A^2, C^2, and D^2), conductivity (e.g., A^2, and C^2), calcium (e.g., A^2, C^2, and D^2), total alkalinity (e.g., A^2, C^2, and D^2), and ammonium nitrogen (e.g., C^2 and D^2), in the bubbling process (Table 4.10). In the capillary process (Table 4.11), there was also significance ($P<0.05$) in terms A^2 (only for ammonium nitrogen), B^2 (only for pH and ammonium nitrogen), and C^2 (for all response variables).

The comparative effects of independent variables on the response variables in the bubbling and the capillary processes, through the perturbation plot, are shown in Figures

4.4a1 to 4.4e1 and Figures 4.4a2 to 4.4e2, respectively. From Figures 4.4a1 to 4.4e1 (for the bubbling process), it is possible to observe that the time variable (curve *A*) was the independent variable that had the greatest influence on response variables, given its more accentuated curvature. Time has been a determining factor in the carbonation process (Correia et al., 2020; Luz et al., 2021; Madeira et al., 2020 (chapter 2); Prazeres et al., 2019, 2016; Ramalho et al., 2022). The increase in time (curve A, from 2 to 21 h) and in stirring speed (curve *C*, from 0 to 200 rpm) contributed to the decrease in pH (Figure 4.4a1), conductivity (Figure 4.4b1), calcium (Figure 4.4c1), total alkalinity (Figure 4.4d1), and ammonium nitrogen (Figure 4.4e1). However, the increase in SWW volume (curve D, from 178 to 478 mL) increased for all the response variables (Figures 4.4a1 to 4.4e1), indicating that higher volumes of SWW impact the carbonation process. As can be seen in Figure 4.4c1, the calcium concentration never reached zero, which indicates that the carbonation process was not inhibited. On the other hand, the air flow rate applied (curve *B*, from 60 to 120 L h^{-1}) did not affect the response variables change, except for total alkalinity and ammonium nitrogen which decreased slightly at 60 to 90 L h^{-1} (Figure 4.4d1) and at 90 to 120 L h^{-1} (Figure 4.4e1), respectively. Even so, the use of air injection has deserved importance in the carbonation process as it contributes to a significant reduction in the carbonatation time of effluent treated by IOSLM (Correia et al., 2020). In fact, the injection of air (Legendre and Zevenhoven, 2017) or the turbulence of the water surface (Yang et al., 2021) can increase the gas-liquid interface and promote carbonation reactions. In this work, the turbulence at the water surface observed in the bubbling process was created by the air flow rate and the stirring speed variables, contributing to the increase of the gas-liquid interface area, even though the physical dimensions of the reactor are unchanged. From Figures 4.4a1 to 4.4e1, stirring speed had a greater effect on the response variables than the air flow rate. For the capillary process (Figures 4.4a2 to 4.4e2), the capillary area was the independent variable that had the greatest influence on response variables, given its clear sharp curve. The increase in air flow rate (curve *B*, from 90 to 270 L h^{-1}) did not influence the response variables. All response variables increased with an increase in the SWW flow rate (curve *A*, from 1.2 to 2.0 mL min^{-1}). On the other hand, in the opposite direction, an increase in the capillary area (curve *C*, from 150 to 700 cm^2) contributed to the decrease in pH, conductivity, calcium, total alkalinity, and ammonium nitrogen. This means that the carbonation process can be compromised if there is not enough contact time between air and SWW, either by controlling the SWW flow rate and/or by the capillary area.

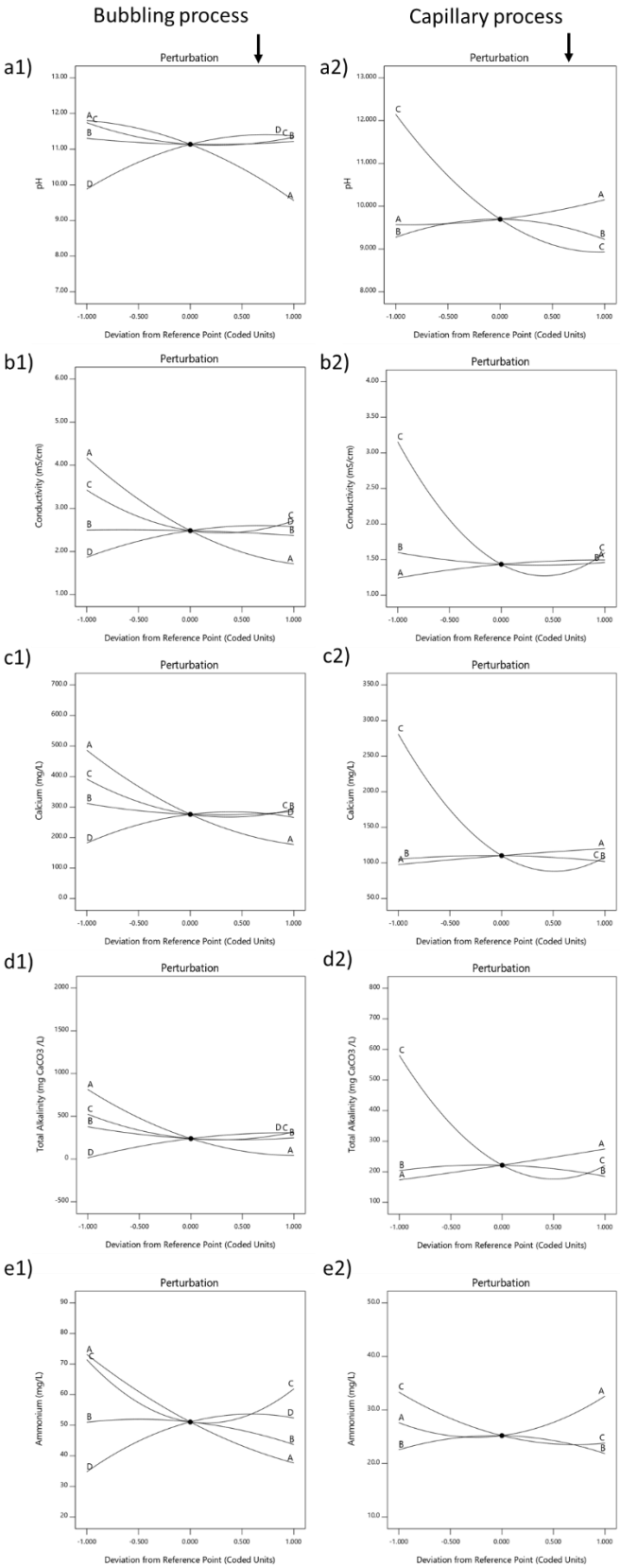

Figure 4.4 - Perturbation plot showing the effect of all independent variables on the a) pH, b) conductivity, c) calcium, d) total alkalinity, and e) ammonium nitrogen. Numbers **1** and **2** refer to the bubbling process and the capillary process, respectively. Capital letters inside the figures represent the following independent variables: A - Time, B - Air flow rate, C - Stirring speed, and D - SWW volume, for the bubbling process, and A - SWW flow rate, B - Air flow rate, and C - Capillary area, for the capillary process.

The decrease in pH, calcium, conductivity, and total alkalinity that was observed in both processes is related to carbonation reactions with atmospheric CO_2 (Eqs.2 to 5).

$$CO_2\ (g) \rightleftarrows CO_2\ (aq) \quad (2)$$

$$CO_2\ (aq) + H_2O\ (l) \rightleftarrows H_2CO_3\ (aq) \quad (3)$$

$$H_2CO_3 \rightleftarrows H^+ + HCO_3^- \quad (4)$$

$$HCO_3^- \rightleftarrows H^+ + CO_3^{2-} \quad (5)$$

$$CO_3^{2-} + Ca^{2+} \rightleftarrows CaCO_3 \quad (6)$$

In fact, free CO_2 is not available in the pretreated SWW by IOSLM at pH 12, which causes a chemical imbalance of CO_2 between the water and the air inside the reactor of both processes. As a way of counteracting this imbalance, the CO_2 present inside the reactor tends to dissolve in water through the water-air interface until reaching equilibrium (Eq. 2). After dissolution in water, the dissolved CO_2 is subjected to a hydration reaction by reacting with water to form H_2CO_3 (Eq. 3). As H_2CO_3 is a weak acid, it dissociates in two steps, the first step (Eq. 4) being the formation of HCO_3^- and H^+ ions, and the second step (Eq. 5) the formation of CO_3^{2-} and ions H^+, from HCO_3^-. The production of H^+ ions leads to a decrease in the pH of the effluent. In turn, the carbonate ions react with the calcium ions present in the water, forming the precipitated calcium carbonate (Eq. 6) (Mitchell et al., 2010). Consequently, the conductivity may decrease with the removal of calcium. In fact, in this work, high correlations ($r = 0.98$, $P<0.05$, Tables 4.12 and 4.13) were found between calcium and conductivity, in both processes. During the carbonation process, alkalinity is consumed due to the reaction with hydroxide ions and ammonium nitrogen removal (Madeira et al., 2020 (chapter 2); Ramalho et al., 2022). The decrease in ammonium nitrogen in the water is due to the volatilization of ammonia at pH > 9.2, since at high pH most of the ammoniacal nitrogen is in the form of ammonia which can be volatilized. As the pH decreases, ammonia will tend to be in equilibrium with the ammonium ion (Eq. 7), and its removal will be more difficult (Mohammed-Nour et al., 2019).

$$NH_4^+ + OH^- \rightarrow H_2O + NH_3 \quad (7)$$

Table 4.12 – Correlation matrix between response variables, using actual values from the bubbling process. Values in bold are different from 0 with a significance level alpha=0.05.

Variables	pH	Conductivity	Calcium	Total alkalinity	Ammonium
pH					
Conductivity	**0.735**				
Calcium	**0.751**	**0.975**			
Total alkalinity	**0.692**	**0.963**	**0.971**		
Ammonium	**0.835**	**0.938**	**0.943**	**0.919**	

Table 4.13 – Correlation matrix between response variables, using actual values from the capillary process. Values in bold are different from 0 with a significance level alpha=0.05.

Variables	pH	Conductivity	Calcium	Total alkalinity	Ammonium
pH					
Conductivity	**0.856**				
Calcium	**0.919**	**0.977**			
Total alkalinity	**0.879**	**0.953**	**0.953**		
Ammonium	**0.678**	**0.794**	**0.789**	**0.874**	

According to Viswanaathan et al. (2022), the rate of dissolution of atmospheric CO_2 in water depends on factors, such as contact time, area at the gas-liquid interface, concentration of CO_2 in the atmosphere, and solution properties (including pH, temperature, concentration of dissolved salts, and others). This dissolution can be enhanced if all these factors are considered. In this way, significant combined effects (P<0.05) on the bubbling process (Table 4.10) were observed between time and air flow rate (*AB*) for conductivity; time and stirring speed (*AC*) for pH, calcium, and ammonium nitrogen; time and SWW volume (*AD*) for pH and ammonium nitrogen; air flow rate and stirring speed (*BC*) for conductivity, calcium, and total alkalinity; and stirring speed and SWW volume (*CD*) for conductivity, calcium, and total alkalinity.

Response surface graphs show the combined effects of the independent variables (which the other variables were held at center level) on the response variables, for both processes studied (Figures 4.5 to 4.9). Concerning the bubbling process and the combined effect time and stirring speed (*AC*) (at 90 L h^{-1} of air flow rate and 328 mL of SWW volume) on pH, calcium, and ammonium nitrogen (Figures 4.5b, 4.7b, and 4.9b, respectively), it was possible to observe a greater decrease in pH, calcium, and ammonium nitrogen when the time was increased from 2 to 21 h, and the stirring speed was increased from 0 to 100-200 rpm. According to the combined effect of time and air flow rate (*AB*) (at 100 rpm of

stirring speed and 328 mL of SWW volume) shown in Figure 4.6a, lower conductivity values were achieved with increasing time from 0 to 21 h and increasing air flow rate from 60 to 120 L h^{-1}. On the other hand, the minimum pH and ammonium nitrogen values were reached when the combined effect of time and SWW volume (*AD*) (at 90 L h^{-1} of air flow rate and 100 rpm of stirring speed) occurred (Figures 4.5c and 4.9c, respectively), that is, when the time was increased from 0 to 21 h and the SWW volume was reduced from 478 to 178 mL. Low values of conductivity, calcium, and total alkalinity were also observed for the combined effects of air flow rate and stirring speed (*BC*) (at 11.5 h of time and 328 mL of SWW volume) in the range of 60 to 120 L h^{-1} and 75 to 175 rpm (Figures 4.6d, 4.7d, and 4.8d, respectively), as well as for stirring speed and SWW volume (*CD*) (at 11.5 h of time and 90 L h^{-1} of air flow rate) in the range 50 to 150 rpm and 178 to 238 mL (Figures 4.6f, 4.7f and 4.8f, respectively).

For the capillary process (Table 4.11), significant (P<0.05) combined effects were also found, namely between SWW flow rate and capillary area (*AC*) for all response variables, and between air flow rate and capillary area (*BC*) for calcium and ammonium nitrogen. In the case of the combined effect of SWW flow rate and capillary area (*AC*) (at 180 L h^{-1} of air flow rate) (Figures 4.5h, 4.6h, 4.7h, 4.8h, and 4.9h), all response variables had their minimum values when the capillary area increased from 150 to 700 cm^2, and the SWW flow rate was between 1.2 and 2.0 mL min^{-1} (although for pH (Figure 4.5h) and ammonium nitrogen (Figure 4.9h) it was preferable to reach low and high values of this range, respectively). For the combined effect of air flow rate and capillary area (*BC*) (at 1.6 mL min^{-1} of SWW flow rate) on calcium (Figure 4.7i) and ammonium (Figure 4.9i), the values of these parameters were minimal when the capillary area increased from 150 to 700 cm^2, regardless of air flow.

Bubbling process

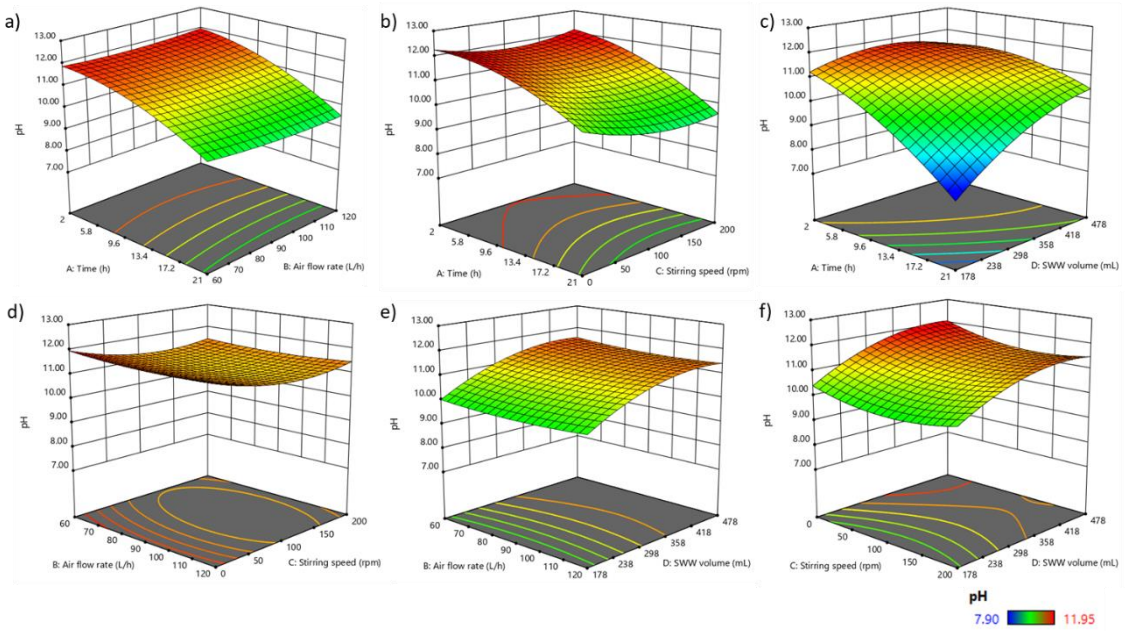

Capillary process

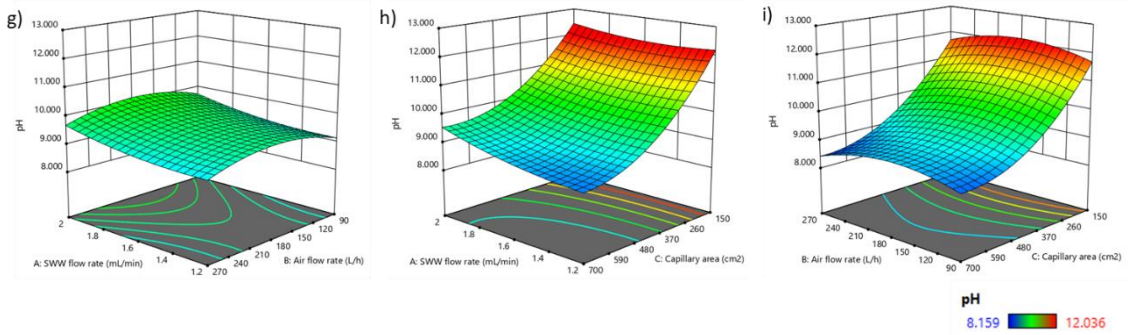

Figure 4.5 – Three-dimensional response surface graphs and contour plots of the pH, showing the effect of two variables (while the other two variables are held at center level), for the bubbling process: a) time and air flow rate; b) time and stirring speed; c) time and SWW volume; d) air flow rate and stirring speed; e) air flow rate and SWW volume; and f) stirring speed and SWW volume, for the bubbling process, as well as g) SWW flow rate and air flow rate; h) SWW flow rate and capillary area; and i) air flow rate and capillary area, for the capillary process.

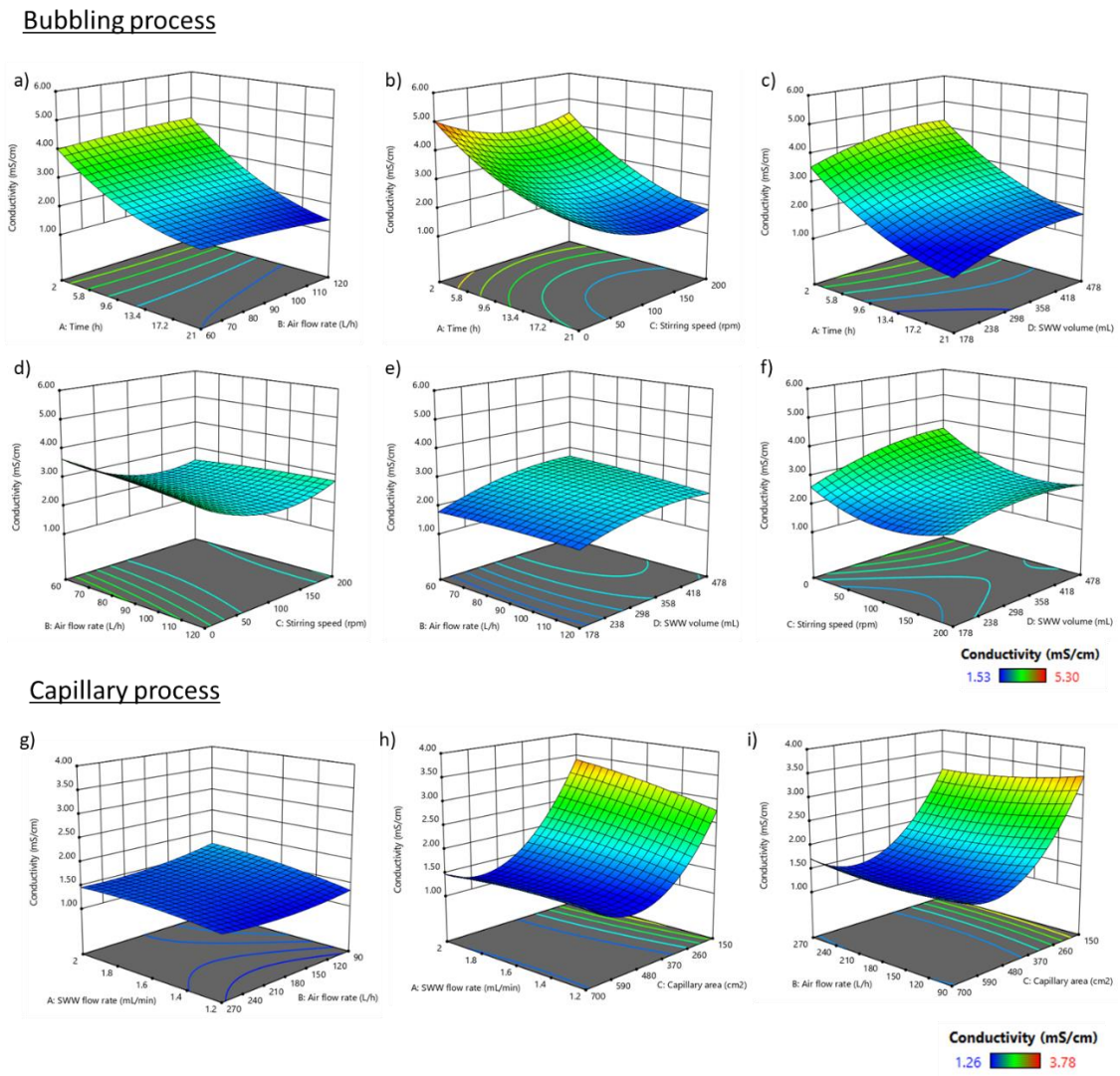

Figure 4.6 – Three-dimensional response surface graphs and contour plots of the conductivity, showing the effect of two variables (while the other two variables are held at center level), for the bubbling process: a) time and air flow rate; b) time and stirring speed; c) time and SWW volume; d) air flow rate and stirring speed; e) air flow rate and SWW volume; and f) stirring speed and SWW volume, for the bubbling process, as well as g) SWW flow rate and air flow rate; h) SWW flow rate and capillary area; and i) air flow rate and capillary area, for the capillary process.

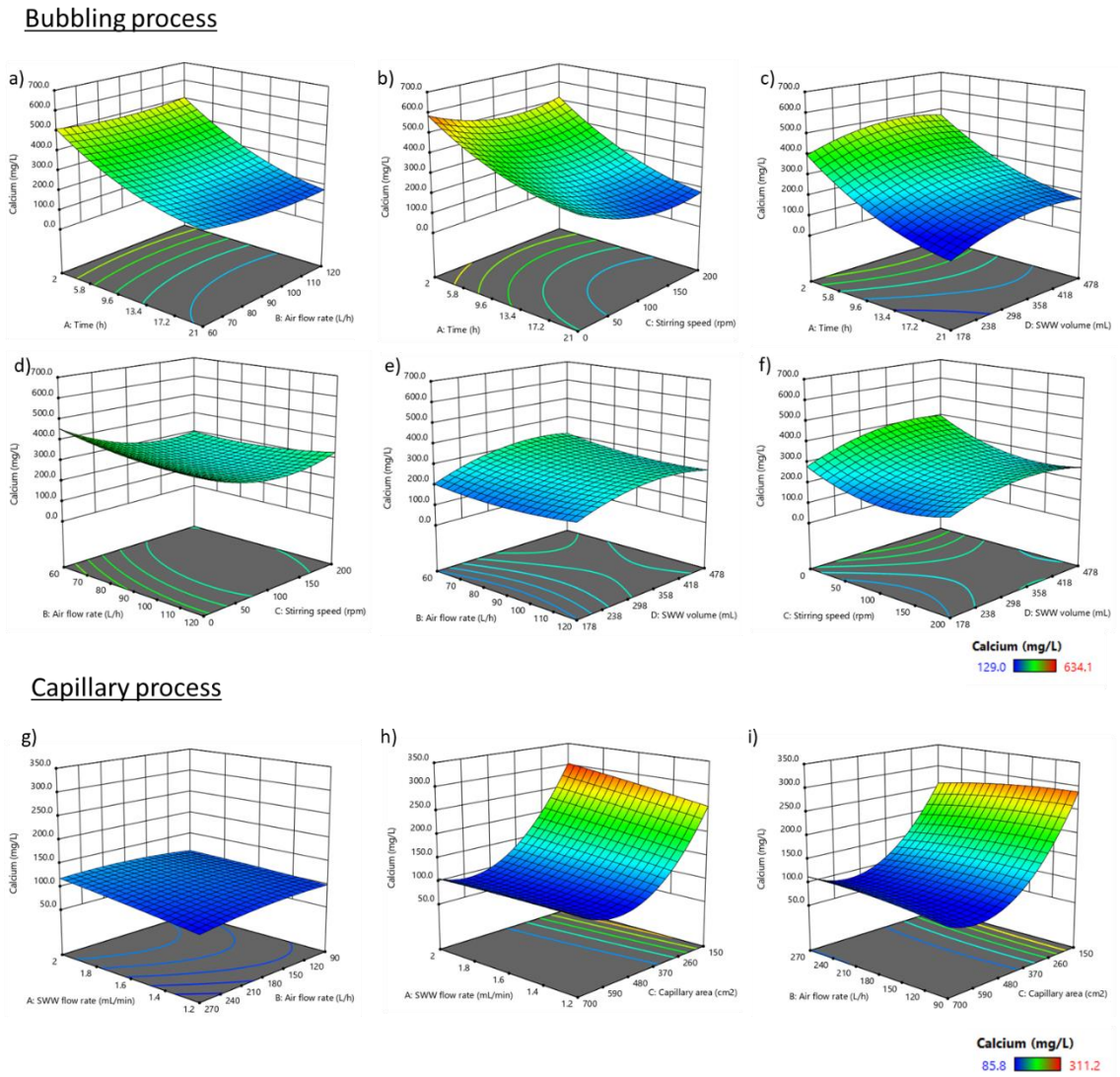

Figure 4.7 – Three-dimensional response surface graphs and contour plots of the calcium, showing the effect of two variables (while the other two variables are held at center level), for the bubbling process: a) time and air flow rate; b) time and stirring speed; c) time and SWW volume; d) air flow rate and stirring speed; e) air flow rate and SWW volume; and f) stirring speed and SWW volume, for the bubbling process, as well as g) SWW flow rate and air flow rate; h) SWW flow rate and capillary area; and i) air flow rate and capillary area, for the capillary process.

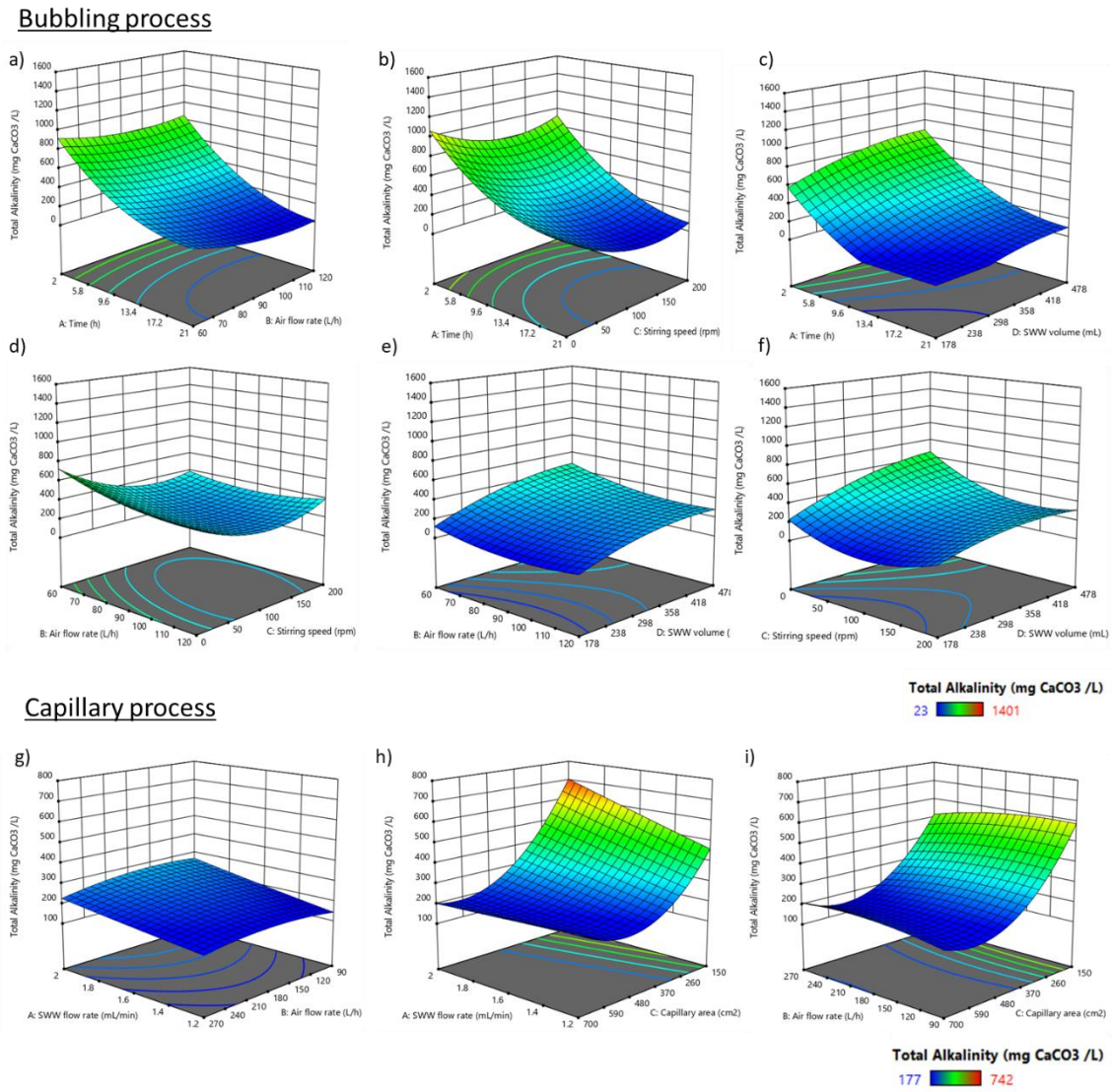

Figure 4.8 – Three-dimensional response surface graphs and contour plots of the total alkalinity, showing the effect of two variables (while the other two variables are held at center level), for the bubbling process: a) time and air flow rate; b) time and stirring speed; c) time and SWW volume; d) air flow rate and stirring speed; e) air flow rate and SWW volume; and f) stirring speed and SWW volume, for the bubbling process, as well as g) SWW flow rate and air flow rate; h) SWW flow rate and capillary area; and i) air flow rate and capillary area, for the capillary process.

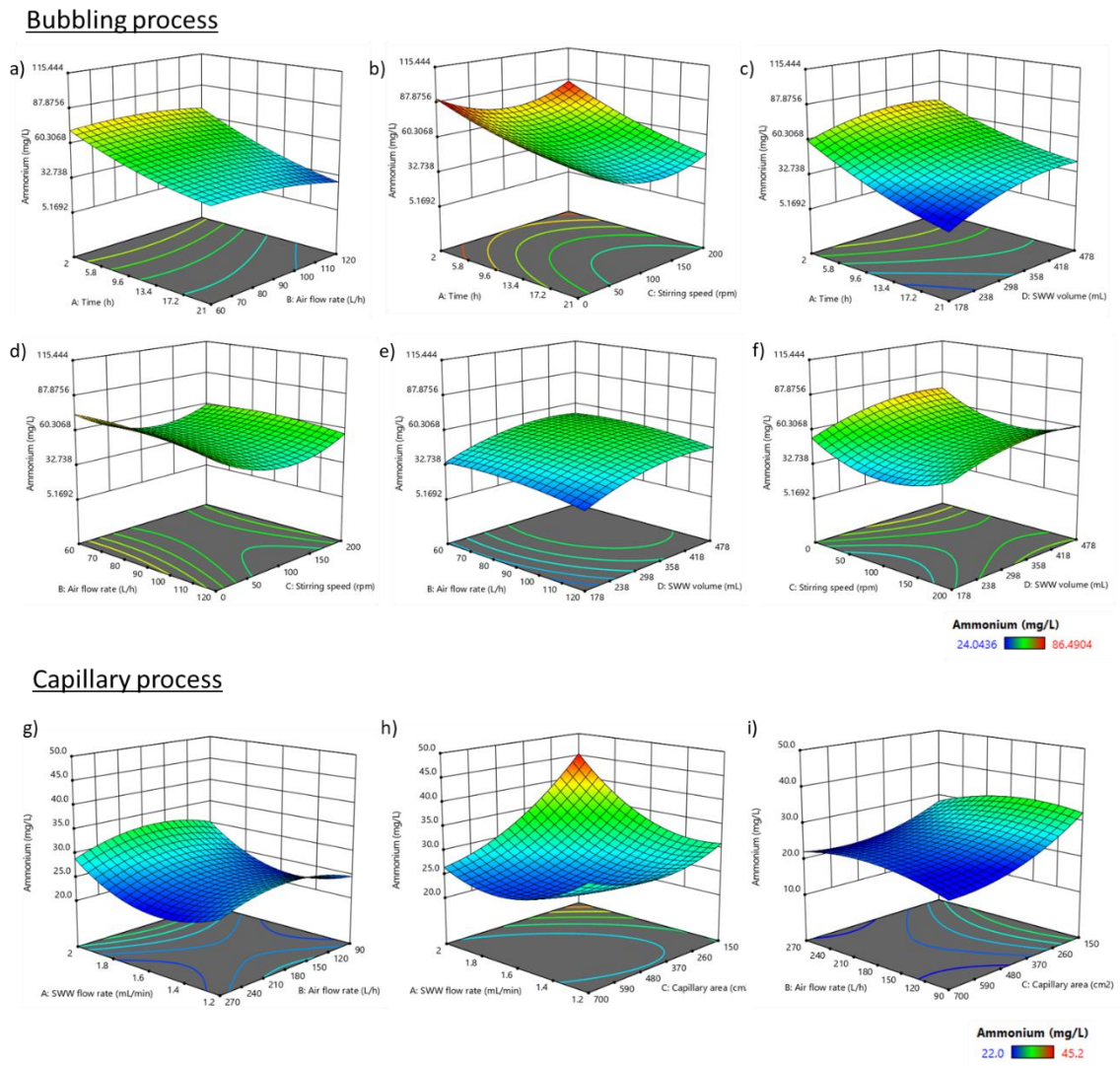

Figure 4.9 – Three-dimensional response surface graphs and contour plots of the ammonium nitrogen, showing the effect of two variables (while the other two variables are held at center level), for the bubbling process: a) time and air flow rate; b) time and stirring speed; c) time and SWW volume; d) air flow rate and stirring speed; e) air flow rate and SWW volume; and f) stirring speed and SWW volume, for the bubbling process, as well as g) SWW flow rate and air flow rate; h) SWW flow rate and capillary area; and i) air flow rate and capillary area, for the capillary process.

4.3.3. Optimization of operating conditions

The values of independent and response variables that simultaneously satisfy the intended objectives for the atmospheric carbonation process were found through numerical optimization. Tables 4.14 and 4.15 show the goals, the upper and lower limits, and the importance intended for each of the independent and response variables in the numerical optimization, for the bubbling and the capillary processes, respectively. According to Tables 4.14 and 4.15, all response variables were limited by the range of current values defined by Tables 4.4 and 4.5, respectively, except for pH. For pH, the target pH value

was set to 7.9 for the bubbling process and 8.2 for the capillary process (based on the minimum pH value that was found), and the upper limit of the range was restricted to 8.5 since it is the maximum pH value usually used in biological treatment (Englande et al., 2015). On the other hand, the defined pH ranges reduce the experimental conditions in which atmospheric carbonation did not occur efficiently. Regarding the independent variables, all of these were limited by their levels (established in Table 4.3), although the air flow rate variable was designated to minimize energy costs since it was a variable that did not have a significant effect on most parameters responses analyzed in both processes.

Table 4.14 – The selected criteria for numerical optimization, in the bubbling process.

	Variable types	Limits		Goals	Importance
		Lower	Upper		
Independent variables	A: Time (h)	2	21	is in range	3
	B: Air flow rate (L h^{-1})	60	120	minimize	3
	C: Stirring speed (rpm)	0	200	is in range	3
	D: SWW volume (mL)	178	478	is in range	3
Response variables	pH	7.9	8.5	is target = 7.9	3
	Conductivity (mS cm^{-1})	1.5	5.3	is in range	3
	Calcium (mg L^{-1})	129.0	634.1	is in range	3
	Total Alkalinity (mg $CaCO_3$ L^{-1})	22.8	1401.0	is in range	3
	Ammonium (mg N-NH_4^+ L^{-1})	24.0	86.5	is in range	3

Table 4.15 - The selected criteria for numerical optimization, in the capillary process.

	Variable types	Limits		Goals	Importance
		Lower	Upper		
Independent variables	A: SWW flow rate (mL min^{-1})	1.2	2	is in range	3
	B: Air flow rate (L h^{-1})	90	270	minimize	3
	C: Capillary area (cm^2)	150	700	is in range	3
Response variables	pH	8.2	8.5	is target = 8.2	3
	Conductivity (mS cm^{-1})	1.3	3.8	is in range	3
	Calcium (mg L^{-1})	85.8	311.1	is in range	3
	Total Alkalinity (mg $CaCO_3$ L^{-1})	176.7	742.1	is in range	3
	Ammonium (mg N-NH_4^+ L^{-1})	22.0	45.2	is in range	3

Thus, considering the restrictions presented in Tables 4.14 and 4.15, about 56 optimal solutions (Table 4.16) for the bubbling process and 22 optimal solutions (Table 4.17) for the capillary process were found, respectively.

Table 4.16 – Possible optimal solutions based on the selected criteria, for the bubbling process.

Number	Time	Air flow rate	Stirring speed	SWW volume	pH	Conductivity	Calcium	Total Alkalinity	Ammonium	Desirability	
1	**21.000**	**65.277**	**52.224**	**178.000**	**8.047**	**1.527**	**152.138**	**25.390**	**28.628**	**0.830**	**Selected**
2	21.000	61.803	53.942	178.000	8.075	1.527	157.327	46.727	28.315	0.829	
3	21.000	63.771	53.345	178.493	8.064	1.527	154.373	34.500	28.507	0.825	
4	21.000	63.998	53.564	178.955	8.068	1.527	154.117	33.261	28.535	0.820	
5	21.000	66.464	50.145	178.000	8.048	1.541	152.498	22.908	29.055	0.820	
6	21.000	64.856	53.874	180.176	8.076	1.528	153.263	28.886	28.658	0.806	
7	21.000	60.000	50.740	178.002	8.120	1.567	165.883	70.862	29.049	0.796	
8	20.903	60.000	57.029	181.006	8.152	1.527	161.007	58.913	28.249	0.762	
9	21.000	72.192	37.641	178.000	8.085	1.636	158.987	22.817	31.751	0.742	
10	20.612	60.001	55.175	178.000	8.192	1.527	161.096	55.968	28.380	0.717	
11	21.000	60.464	40.308	178.000	8.193	1.677	180.149	101.145	31.668	0.713	
12	20.999	75.384	31.645	178.001	8.107	1.680	162.172	22.801	33.030	0.698	
13	21.000	60.166	38.121	178.000	8.214	1.704	184.284	111.310	32.261	0.689	
14	21.000	75.964	32.101	180.111	8.133	1.685	162.830	22.800	33.201	0.670	
15	21.000	78.143	26.942	178.000	8.124	1.713	164.685	22.800	33.991	0.661	
16	21.000	79.309	24.760	178.000	8.135	1.729	166.187	23.938	34.454	0.642	
17	20.275	64.837	53.543	178.000	8.234	1.527	154.035	22.802	29.022	0.638	
18	21.000	60.822	65.253	192.769	8.255	1.527	161.159	57.481	28.522	0.635	
19	21.000	63.941	36.189	181.506	8.243	1.730	182.336	95.875	33.348	0.633	
20	20.730	75.407	31.349	178.000	8.181	1.688	163.527	22.800	33.362	0.629	
21	21.000	80.628	23.049	178.000	8.141	1.738	166.783	22.800	34.743	0.627	
22	21.000	82.114	20.841	178.000	8.150	1.752	168.008	22.906	35.147	0.607	
23	20.699	60.000	40.878	179.346	8.296	1.685	182.892	105.019	32.009	0.584	
24	20.978	83.905	18.075	178.000	8.170	1.770	169.881	23.866	35.678	0.575	
25	20.938	85.925	15.697	178.001	8.191	1.781	171.045	22.800	36.038	0.540	
26	21.000	87.873	13.032	178.000	8.190	1.794	172.607	24.121	36.391	0.526	
27	21.000	73.885	12.223	178.000	8.300	1.936	197.122	106.385	39.353	0.506	
28	20.999	88.902	9.911	178.000	8.216	1.824	176.489	31.642	37.186	0.496	
29	20.953	93.744	7.158	178.000	8.235	1.809	175.653	22.800	36.822	0.440	
30	20.989	95.152	5.902	178.000	8.232	1.808	176.186	22.800	36.791	0.430	
31	20.995	88.023	0.070	178.000	8.325	1.968	194.922	76.081	40.954	0.395	
32	20.819	96.477	4.685	178.000	8.287	1.814	177.601	22.800	36.971	0.373	
33	21.000	61.660	76.775	208.140	8.420	1.527	161.634	56.288	29.027	0.361	
34	21.000	101.220	1.247	178.000	8.262	1.797	178.747	22.886	36.366	0.352	
35	21.000	66.842	199.960	213.423	8.420	1.547	129.000	38.237	34.740	0.344	
36	21.000	102.723	0.243	178.000	8.270	1.792	179.393	23.173	36.167	0.332	
37	20.991	67.318	199.465	214.170	8.426	1.549	129.000	36.275	34.765	0.329	
38	21.000	92.030	0.002	183.355	8.393	1.961	195.715	71.695	40.849	0.288	
39	20.763	64.471	199.990	209.366	8.449	1.527	129.000	42.756	34.322	0.281	
40	20.791	64.986	198.906	210.870	8.453	1.527	129.000	40.218	34.288	0.269	
41	21.000	113.591	199.955	206.551	8.211	1.590	145.525	22.800	26.947	0.227	
42	20.494	102.338	0.470	178.000	8.405	1.809	181.366	22.800	36.777	0.216	
43	21.000	108.614	1.359	184.416	8.361	1.744	181.352	22.800	34.553	0.210	
44	21.000	112.183	199.400	213.889	8.305	1.609	147.698	24.077	28.359	0.206	
45	21.000	113.149	198.471	212.430	8.284	1.594	147.316	22.800	27.583	0.203	

Table 4.16 - (continued). Possible optimal solutions based on the selected criteria, for the bubbling process.

Number	Time	Air flow rate	Stirring speed	SWW volume	pH	Conductivity	Calcium	Total Alkalinity	Ammonium	Desirability
46	20.641	115.980	200.000	195.941	8.176	1.574	144.894	22.800	25.100	0.190
47	21.000	115.672	197.786	205.897	8.199	1.563	146.369	22.800	25.555	0.190
48	20.998	61.533	200.000	213.881	8.478	1.527	133.984	62.543	34.434	0.189
49	20.650	116.376	199.714	195.434	8.166	1.568	144.859	22.800	24.786	0.183
50	20.667	117.093	200.000	192.114	8.117	1.558	143.885	22.800	24.044	0.176
51	20.394	116.751	200.000	191.366	8.186	1.572	144.924	22.800	24.529	0.168
52	21.000	114.767	200.000	213.350	8.312	1.611	152.160	34.902	27.562	0.165
53	20.999	113.119	0.004	184.222	8.376	1.699	182.154	22.800	32.981	0.154
54	19.590	116.826	200.000	183.958	8.316	1.598	146.503	22.800	24.763	0.127
55	20.468	107.856	0.000	181.684	8.474	1.772	183.308	22.801	35.461	0.094
56	20.998	60.689	200.000	214.801	8.500	1.527	135.582	68.046	34.481	0.015

Table 4.17 – Possible optimal solutions based on the selected criteria, for the capillary process.

Number	SWW flow rate	Air flow rate	Capillary area	pH	Conductivity	Calcium	Total Alkalinity	Ammonium	Desirability	
1	**1.200**	**90.000**	**700.000**	**8.249**	**1.599**	**96.702**	**186.414**	**26.207**	**0.858**	**Selected**
2	1.200	90.001	697.662	8.250	1.589	96.006	184.541	26.165	0.857	
3	1.205	90.000	699.998	8.251	1.600	96.639	186.247	26.056	0.855	
4	1.200	90.000	692.737	8.251	1.568	94.580	180.681	26.079	0.854	
5	1.200	90.030	689.341	8.253	1.554	93.634	178.113	26.023	0.851	
6	1.214	90.000	699.997	8.254	1.603	96.537	185.981	25.816	0.850	
7	1.200	90.355	695.606	8.253	1.579	95.476	183.242	26.159	0.849	
8	1.224	90.000	699.998	8.257	1.606	96.415	185.672	25.539	0.844	
9	1.216	90.000	687.978	8.258	1.554	93.083	176.682	25.552	0.842	
10	1.258	90.000	700.000	8.271	1.617	95.975	184.608	24.614	0.820	
11	1.324	90.000	691.500	8.305	1.599	92.738	176.681	22.965	0.757	
12	1.371	90.000	693.086	8.333	1.616	92.520	176.681	22.050	0.700	
13	1.200	107.094	700.000	8.392	1.583	99.981	201.246	27.564	0.536	
14	1.200	110.030	700.000	8.413	1.580	100.495	203.596	27.776	0.476	
15	1.200	118.672	699.999	8.470	1.576	101.926	210.177	28.360	0.270	
16	1.200	249.381	700.000	8.328	1.716	108.455	248.554	30.440	0.240	
17	1.200	248.547	699.999	8.335	1.714	108.503	248.672	30.467	0.240	
18	1.200	250.416	699.999	8.320	1.719	108.393	248.399	30.405	0.240	
19	1.200	249.386	697.292	8.330	1.703	107.427	245.924	30.361	0.239	
20	1.220	249.493	699.999	8.334	1.717	108.741	246.855	29.831	0.235	
21	1.407	255.824	700.000	8.380	1.724	110.950	230.269	25.154	0.166	
22	1.200	123.275	700.000	8.497	1.574	102.637	213.478	28.649	0.079	

According to Table 4.16, pH, conductivity, calcium, total alkalinity, and ammonium nitrogen ranged from 8.0 to 8.5, 1.527 to 1.968 mS cm^{-1}, 129.0 to 197.1 mg L^{-1}, 22.8 to 111.3 mg $CaCO_3$ L^{-1}, and 24.0 to 41.0 mg $N\text{-}NH_4^+$ L^{-1}, respectively, when 19.6 to 21.0 h

for time, 60 to 117 L h^{-1} for air flow rate, 0 to 200 rpm for stirring speed, and 178 to 215 mL for SWW volume were applied in the bubbling process, reaching desirability values between 0.015 and 0.830. For the capillary process (Table 4.17), pH values from 8.2 to 8.5, conductivity from 1.554 to 1.724 mS cm^{-1}, calcium from 92.5 to 111.0 mg L^{-1}, total alkalinity from 177 to 249 mg $CaCO_3$ L^{-1}, and ammonium of 22.1 to 30.5 mg N-NH_4^+ L^{-1} were obtained using SWW flow rate from 1.2 to 1.4 mL min^{-1}, air flow rate from 90 to 256 L h^{-1}, and capillary area from 688 to 700 cm^2, reaching desirability values of 0.079 and 0.858. In fact, the values of the response variables were substantially lower than the initial values before treatment (Table 4.1), clearly indicating the occurrence of the carbonation process in both processes. For the bubbling process and capillary process, the optimal solution selected was the one that had the greatest desirability. Desirability values close to 1 mean that all variables meet the objective, while values close to 0 mean that there is at least 1 variable that does not meet the objective. According to Table 4.16 (for the bubbling process), this happens with a desirability of 0.830 with the following characteristics of the response variables (pH (8.0), conductivity (1.527 mS cm^{-1}), calcium (152.1 mg L^{-1}, corresponding a 76% of removal), total alkalinity (25.4 mg $CaCO_3$ L^{-1}) and ammonium (28.6 mg N-NH_4^+ L^{-1}, corresponding a 66.2% of removal)) and independent variables (time (21 h), air flow rate (65 L h^{-1}), stirring speed (52 rpm) and SWW volume (178 mL)). For the capillary process, with a desirability of 0.858 (Table 4.17), the selected optimal solution found the following values of pH (8.2), conductivity (1.599 mS cm^{-1}), calcium (96.7 mg L^{-1}, corresponding a 81.0% of removal), total alkalinity (186 mg $CaCO_3$ L^{-1}), and ammonium (26.2 mg N-NH_4^+ L^{-1}, corresponding a 57.5% of removal), associated with the values of the independent variables: SWW flow rate (1.2 mL min^{-1}), air flow rate (90 L h^{-1}) and capillary area (700 cm^2).

On the other hand, the optimization process was also complemented with graphic optimization, as can be seen in Figures 4.10 (for the bubbling process) and 4.11 (for the capillary process). The graphical optimization process produces an overlay plot for the optimal region based on the constraints of the previously defined response variables (Tables 4.14 and 4.15) as well as the values of the independent variables of the previously selected optimal solutions (Tables 4.16 and 4.17). In fact, the graphical optimization results allow a faster search for the ideal settings for the occurrence of atmospheric carbonation, where the colored areas on the graphical optimization plot indicate the region of interest (that is, the fulfillment of the objectives selected for each of the response

variables and for the selected factor pair), while the regions do not meet the proposed criteria are shaded out.

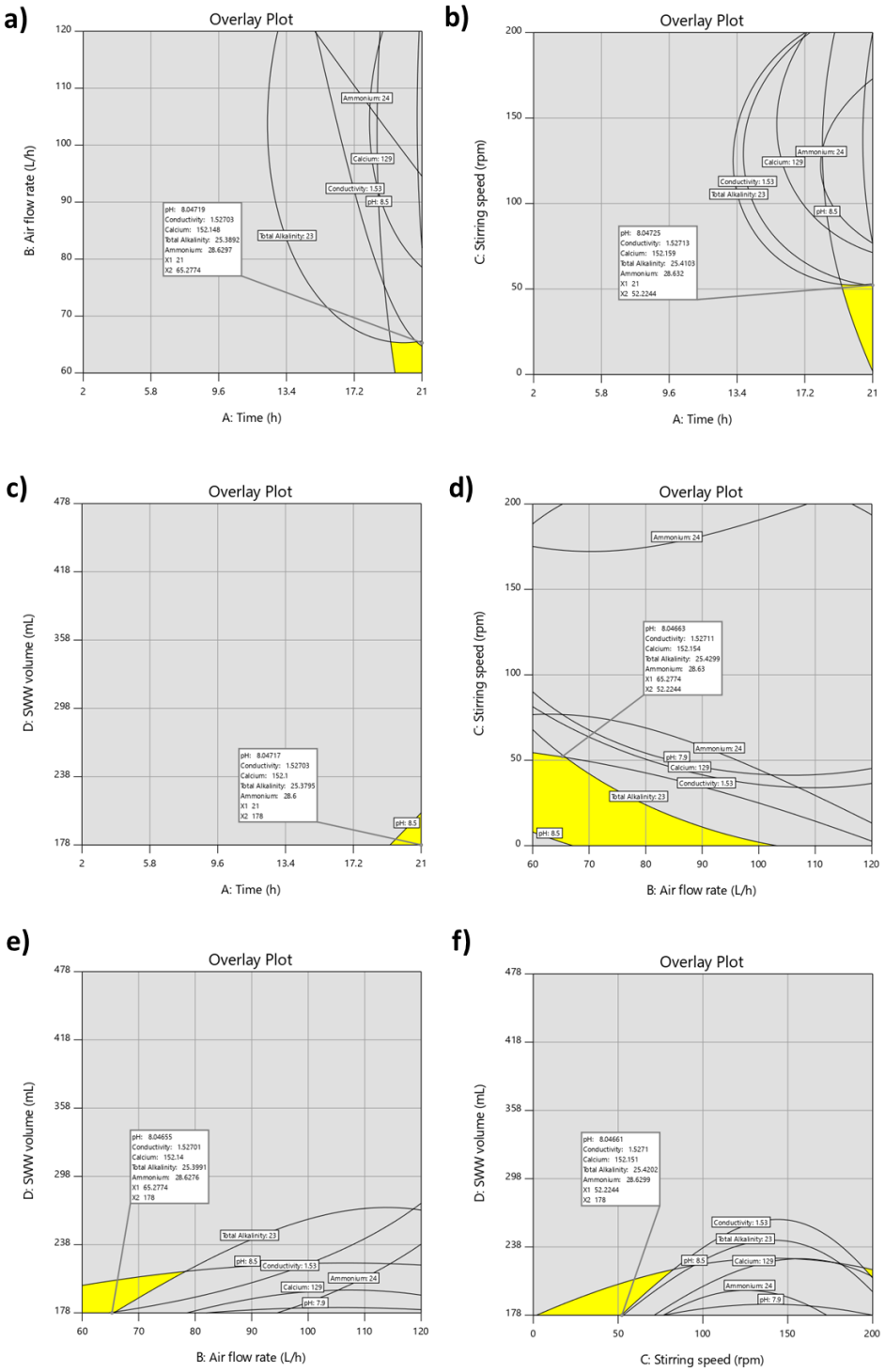

Figure 4.10 – Overlay plot for optimal region based on the criterion defined for the bubbling process, namely: a) time versus air flow rate at stirring speed of 52 rpm and SWW volume of 178 mL; b) time versus stirring speed at an air flow rate of 65 L h^{-1} and SWW volume of 178 mL; c) time versus SWW volume at an air flow rate of 65 L h^{-1} and stirring speed of 52 rpm; d) air flow rate versus stirring speed at the time of 21 h and SWW volume of 178 mL; e) air flow rate versus SWW volume at the time of 21 h and stirring speed of 52 rpm; and f) stirring speed versus SWW volume at the time of 21 h and air flow rate of 65 L h^{-1}.

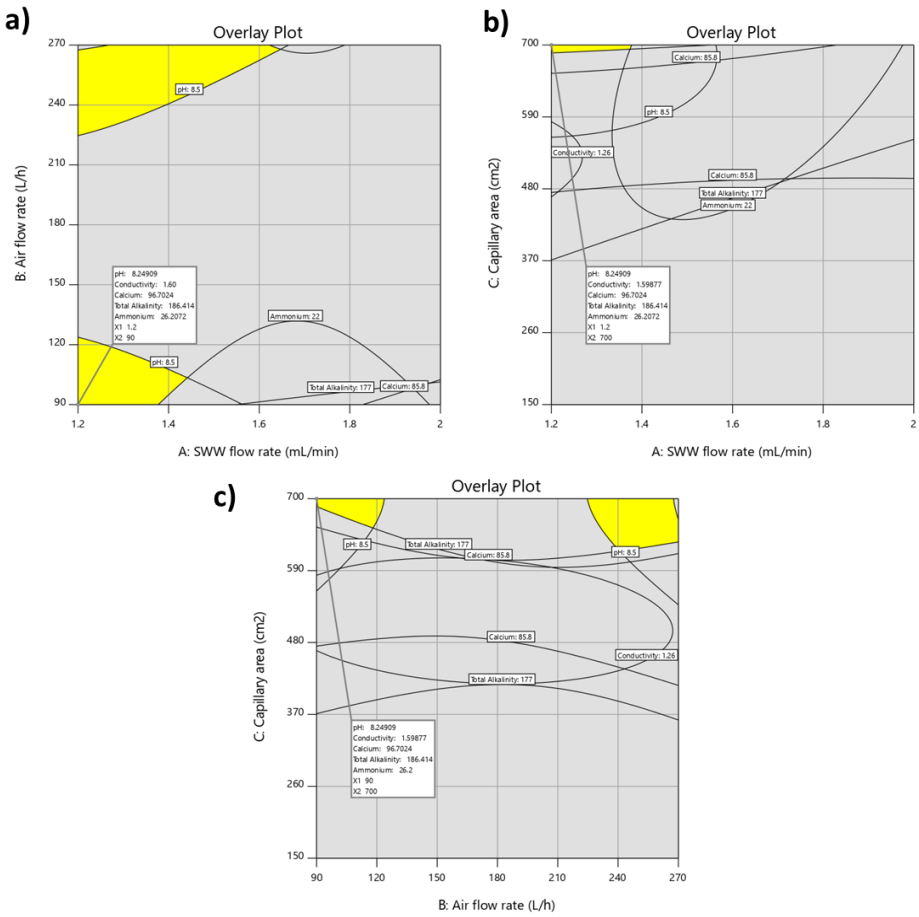

Figure 4.11 – Overlay plot for optimal region based on the criterion defined for capillary process, namely: a) SWW flow rate versus air flow rate at the capillary area of 700 cm^2; b) SWW flow rate versus capillary area at an air flow rate of 90 L h^{-1}; and c) air flow rate versus capillary area at SWW flow rate of 1.2 mL min^{-1}.

According to the graphic optimization shown in Figure 4.10 (for the bubbling process), all the colored regions were limited by the time from 19.5 to 21 h, simultaneously with the following independent variables: air flow rate between 60 and 65 L h^{-1} (under stirring speed at 52 rpm and SWW volume of 178 mL) (Figure 4.10a), stirring speed between 0 and 55 rpm (under an air flow rate of 65 L h^{-1} and SWW volume of 178 mL) (Figure 4.10b) and SWW volume between 178 and 215 mL (under air flow rate at 65 L h^{-1} and stirring speed at 52 rpm) (Figure 4.10c). In fact, time seems to be the determining factor in the bubbling process, requiring about 19 to 21 hours for atmospheric carbonation to be achieved. As can be seen in Figure 4.10d, the colored region can be reached with an air flow rate of around 67 to 103 L h^{-1} and stirring speed of around 8 to 54 rpm, if the time of 21 h and SWW volume of 178 mL were considered. However, in terms of energy costs, it may be preferable to apply only an air flow rate of 67 L h^{-1} without agitation. On the other hand, according to Figures 4.10e and 4.10f, the SWW volume can be increased from

178 mL to 214 and 216 mL, respectively, if, in the first case, the air flow rate is increased to 77 L h^{-1} (keeping constant time to 21 h and stirring speed to 52 rpm) or in the second case, stirring speed is increased to 82 rpm (keeping constant time to 21 h and air flow rate to 65 L h^{-1}).

For the capillary process, Figures 4.11a and 4.11c showed two distinct colored regions. One of the regions is limited by the low values of air flow rate (about 90 to 123 L h^{-1}) when they are applied simultaneously with low values of SWW flow rate (about 1.20 to 1.41) under capillary area at 700 cm^2 (Figure 4.11a), or high capillary area values (657 to 700 cm^2) under constant SWW flow rate at 1.2 mL min^{-1} (Figure 4.11c). The other region is limited by the high values of air flow rate (224 to 270 L h^{-1}) when they are applied together with low values of SWW flow rate (1.2 to 1.64 mL min^{-1}) under capillary constant area at 700 cm^2 (Figure 4.11a), or high capillary area values (619 to 700 cm^2) under constant SWW flow rate at 1.2 mL min^{-1} (Figure 4.11c). Although the SWW flow rate range of 1.2 to 1.64 mL min^{-1} can be achieved in the colored region (Figure 4.11a), the results indicated that 1.2 and 1.6 mL min^{-1} corresponded to the minimum and maximum of the defined pH range 8.2 to 8.5, respectively. In fact, as noted above, the increase in the SWW flow rate contributed to the increase in the effluent pH. In terms of energy costs, it is preferable to choose the region with low air flow rate values. Moreover, for both processes studied, the identification of optimal regions at low air flow rates, indicates that the air flows used were not too low to prevent a restoration of atmospheric CO_2 in the system and consequently limit the atmospheric carbonation process. Concerning Figure 4.11b, the colored region is limited by high capillary area values (687 to 700 cm^2) and low SWW flow rates (1.2 to 1.38 mL min^{-1}), when an air flow rate of 90 L h^{-1} is applied.

Table 4.18 shows the validation of the optimal conditions for the bubbling process (using time of 21 h, air flow rate of 90 L h^{-1}, no stirring speed, and SWW volume of 178 mL, as can be seen in Figure 4.10) and capillary process (using SWW flow rate of 1.2 mL min^{-1}, air flow rate of 90 L h^{-1} and capillary area of 700 cm^2, in Figure 4.11). According to Table 4.18, the differences between the actual values and the predicted values were small, in all the response variables, for both processes, which means that the developed models can predict the response variables with significant accuracy. For the bubbling process and the capillary process, the ammonium nitrogen capture under these operating conditions was

about 99±2%. Thus, it can be said that these processes, compared to atmospheric carbonation processes in open systems, can contribute to the capture and recovery of ammonium nitrogen.

Table 4.18 – Results of the model validation for the bubbling and the capillary processes, using optimal conditions.

Variables	Bubbling process[a)]			Capillary process[b)]		
	Predicted value	Actual value [c)]	Error (%)	Predicted value	Actual value [c)]	Error (%)
pH	8.31	8.26	0.61	8.25	8.30	0.60
Conductivity (mS cm^{-1})	1.95	1.91	2.09	1.60	1.57	1.91
Calcium (mg L^{-1})	192.3	187	2.83	96.7	91.2	6.03
Total alkalinity (mg $CaCO_3$ L^{-1})	67	74	9.46	186	206	9.71
Ammonium (mg N-NH_4^+ L^{-1})	40.4	38.5	4.94	26.2	27.0	2.96

Note: a) Optimal conditions: A = 21 h, B = 90 L/h, C = 0 rpm, and D = 178 mL; b) Optimal conditions: A = 1.2 mL min^{-1}, B = 90 L/h, and C = 700 cm^2; c) N = 3. The experimental values obtained are part of the 95% confidence interval.

The effectiveness of the capillary process to treat different SWW volumes (178 to 478 mL) under the previously found optimal condition was investigated (Figure 4.12). The time required to collect the pretreated SWW volumes of 178, 328, and 478 mL was 4.48, 7.38, and 10.20 hours, respectively. According to Figure 4.12, there were no significant (P<0.05) differences in the values of pH (Figure 4.12a), conductivity (Figure 4.12b), calcium (Figure 4.12c), total alkalinity (Figure 4.12d), and ammonium nitrogen (Figure 4.12e), for the different volumes collected (i.e., 178, 328, and 478 mL). Therefore, regardless of the volume collected, calcium, and ammonium removals were around 82.6 and 57.2%, respectively, with a substantial reduction in pH to 8.2 and conductivity to 1.5 mS cm^{-1}.

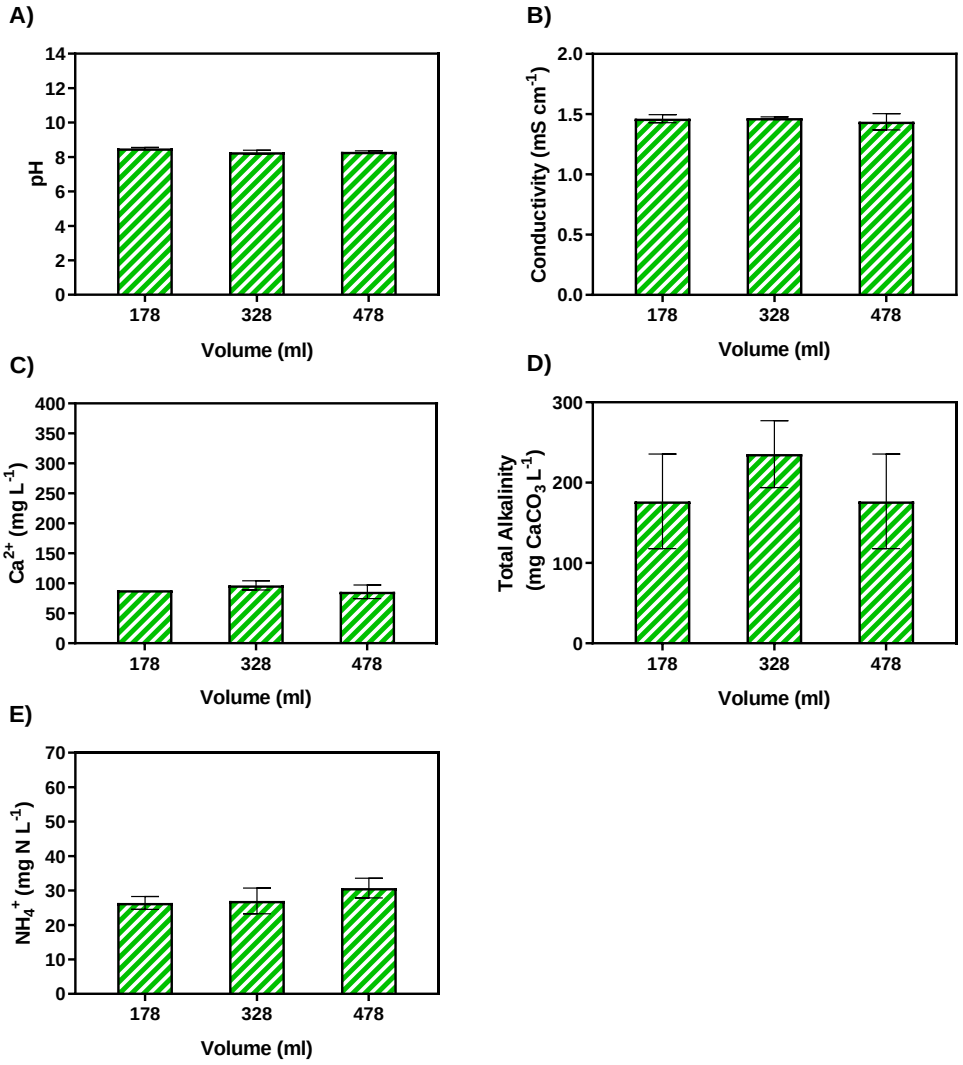

Figure 4.12 – Water quality analyzed in terms of a) pH; b) conductivity; c) calcium; d) total alkalinity; and e) ammonium nitrogen, at different SWW volumes collected (178 to 478 mL), applying the optimal conditions of the capillary process (SWW flow rate at 1.2 mL min^{-1}, air flow rate at 90 L/h, and capillary area at 700 cm^2). Bars represent the standard deviation of the mean.

These results indicate that, unlike the batch bubbling process which was only effective for SWW volumes around 178 mL (Figures 4.10c, 4.10e, and 4.10f), the capillary process can treat the effluent continuously and dispose of the effluent immediately for the following treatment processes. Furthermore, the capillary process proved to be more efficient than the bubbling process, requiring about 4.48 h to reduce the pH to around 8 for 178 mL of SWW, while the bubbling process would take 19-21 h and result in greater energy expenditure by the air pump. Moreover, the bubbling process still requires a settling time to remove the calcium carbonate precipitate from the solution, which does

not happen in the capillary process whose collected effluent was clean. Anyway, the static atmospheric carbonation processes found in the literature (Luz et al., 2021; Madeira et al., 2020 (chapter 2); Prazeres et al., 2019, 2016; Ramalho et al., 2022) seem to be less efficient than both processes studied, in which the former have long carbonation times (≥ 7 days) to reach pH 8. In fact, the contact areas between air and water are greater in processes studied than in static atmospheric carbonation processes. In the bubbling process occurs the creation of water splashing in the air. On the other hand, in the capillary process happens the distribution of water along the entire length of the capillary, whose area of contact between the air and water is twice the capillary area since the capillary can be wet either at the top or at the bottom. In static atmospheric carbonation processes, the water is at rest and the area of contact between the air and the water is just the surface area of the reactor. However, when the neutralization of effluent is reached, it is observed that the ammonium nitrogen removal in the bubbling process (about 54.4% according to results from Tables 4.1 and 4.18) or in the capillary process (about 56.2% according to results from Tables 4.1 and 4.18) seems to be less efficient than the static atmospheric carbonation processes found in the literature (e.g. by the authors Madeira et al. (2023) (chapter 3) who obtained 68.1-82.6% ammonium removal). In fact, in the former, there is a possibility of the volatilized ammonia being mixed again with water, given the turbulence of the water or air in the reactors. Reducing the pH to around neutrality with simultaneous low nitrogen removal in the processes studied favors the production of nitrogen-rich effluents that could be used by plants.

4.4. Conclusion

The purpose of this study was to evaluate the neutralization of slaughterhouse wastewaters treated by lime precipitation, by capturing atmospheric CO_2 in the lab-scale stirrer bubble column and lab-scale stepped continuous flow capillary column. Response surface methodology was used to model and optimize the lab-scale stirrer bubble column (studying the effect of the variables: aeration time, air flow rate, stirring speed, and SWW volume) and lab-scale stepped continuous flow capillary column (studying the effect of the variables SWW flow rate, air flow rate, and capillary area), through the analysis of the response parameters (pH, conductivity, calcium, total alkalinity, and ammonium nitrogen). Both processes were able to neutralize the lime precipitation treated slaughterhouse effluent. Time at 21 h, air flow rate at 65 L h^{-1}, stirring speed at 52 rpm,

and SWW volume at 178 mL was the optimal condition to reach pH 8, and removals of 76.0% of calcium and 66.2% of ammonium nitrogen were obtained in the bubbling process. On the other hand, SWW flow rate at 1.2 mL min^{-1}, air flow rate at 90 L h^{-1}, and capillary area at 700 cm^2 was the optimal condition observed by the capillary process optimization, reaching pH 8.2 and removals of 81.0 % calcium and 57.5% ammonium nitrogen. Both processes proved to be more efficient compared to carbonation processes carried out in static reactors since significantly shorter carbonation times were obtained. Compared to the bubbling process, the capillary process was more efficient in neutralizing the effluent, contributing to a faster drop in pH, without the need for prior sedimentation to remove the precipitated $CaCO_3$ and greater energy consumption. Both processes provide a low-cost and eco-friendly alternative neutralization of alkaline wastewaters, with the recovery of volatilized ammonia during the carbonation process, and without loss of ammonia to the atmosphere.

4.5. References

Ahmadvand, S., Abbasi, Behrooz, Azarfar, B., Elhashimi, M., Zhang, X., Abbasi, Bahman, 2019. Looking Beyond Energy Efficiency: An Applied Review of Water Desalination Technologies and an Introduction to Capillary-Driven Desalination. Water. 11 (4), 696. https://doi.org/10.3390/W11040696

Ayoub, M., 2018. Removal of Iron and Manganese by the Fabric Capillary Action Mohamed Ayoub. Int. J. Eng. Sci. 7, 28–31.

Azizi, F., Kaady, L., Al-Hindi, M., 2022. Chemical absorption of CO_2 in alkaline solutions using an intensified reactor. Can. J. Chem. Eng. 100, 2172–2190. https://doi.org/10.1002/CJCE.24420

Baird, R., Eaton, A.D., Rice, E.W., Bridgewater, L., American Public Health Association, American Water Works Association, Water Environment Federation, 2017. Standard Methods for the Examination of Water and Wastewater, 23rd ed. American Public Health Association, American Water Works Association, Water Environment Federation.

Correia, T., Regato, M., Almeida, A., Santos, T., Amaral, L., Carvalho, M. de F.N., 2020. Manual Treatment of Urban Wastewater by Chemical Precipitation for Production of Hydroponic Nutrient Solutions. J. Ecol. Eng. 21, 143–152. https://doi.org/10.12911/22998993/118286

Cruz-Navarro, D.S., Mugica-Álvarez, V., Gutiérrez-Arzaluz, M., Torres-Rodríguez, M., 2020. CO_2 Capture by Alkaline Carbonation as an Alternative to a Circular Economy. Appl. Sci. 10, 863. https://doi.org/10.3390/APP10030863

Deng, R., Xia, X.Z., Han, J.C., Wu, Q.Y., Yang, H.C., 2022. Siphon-driven interfacial photocatalytic reactors enhanced by capillary flow for continuous wastewater treatment. Sep. Purif. Technol. 300, 121835. https://doi.org/10.1016/J.SEPPUR.2022.121835

Ding, L., Wu, B., Luo, P., 2018. Preparation of $CaCO_3$ nanoparticles in a surface-aerated tank stirred by a long-short blades agitator. Powder Technol. 333, 339–346. https://doi.org/10.1016/J.POWTEC.2018.04.057

Englande, A.J., Krenkel, P., Shamas, J., 2015. Wastewater Treatment & Water Reclamation, in: Reference Module in Earth Systems and Environmental Sciences. Elsevier. https://doi.org/10.1016/b978-0-12-409548-9.09508-7

Filimonova, A.A., Chichirova, N.D., Chichirov, A.A., Minibaev, A.I., Buskin, R. V., 2019. Processing of Alkaline Wastewater of TPP Evaporative Water Treatment Plant With Electromembrane Methods. IOP Conf. Ser. Earth Environ. Sci. 288, 012009. https://doi.org/10.1088/1755-1315/288/1/012009

García Carmona, J., Gómez Morales, J., Rodríguez Clemente, R., 2003. Rhombohedral–scalenohedral calcite transition produced by adjusting the solution electrical conductivity in the system $Ca(OH)_2$–CO_2–H_2O. J. Colloid Interface Sci. 261, 434–440. https://doi.org/10.1016/S0021-9797(03)00149-8

Goel, R.K., Flora, J.R. V., Chen, J.P., 2005. Flow Equalization and Neutralization, in: Physicochemical Treatment Processes. Humana Press, pp. 21–45. https://doi.org/10.1385/1-59259-820-x:021

Henthorn, D.B., Peppas, N.A., 2007. Molecular simulations of recognitive behavior of molecularly imprinted intelligent polymeric networks. Ind. Eng. Chem. Res. 46, 6084–6091. https://doi.org/10.1021/IE061369L

Jia, Z., Chang, Q., Qin, J., Mamat, A., 2013. Preparation of Calcium Carbonate Nanoparticles with a Continuous Gas-liquid Membrane Contactor: Particles Morphology and Membrane Fouling. Chinese J. Chem. Eng. 21, 121–126. https://doi.org/10.1016/S1004-9541(13)60449-8

Kang, D.Y., Kim, M.R., Lim, J.H., Lee, T.Y., Lee, J.K., 2016. Neutralization of Alkaline Wastewater with CO_2 in a Continuous Flow Jet Loop Reactor. Korean J. Chem. Eng. 54, 101–107. https://doi.org/10.9713/KCER.2016.54.1.101

Kumar, R., Sharma, A., Dhall, P., Kulshreshtha, N.M., Kumar, A., 2011. Neutralization of Alkaline Waste-Waters using a Blend of Microorganisms. Int. J. Biotechnol. Bioeng. 5, 224–227. https://doi.org/10.5281/ZENODO.1058705

Legendre, D., Zevenhoven, R., 2017. Detailed experimental study on the dissolution of CO_2 and air bubbles rising in water. Chem. Eng. Sci. 158, 552–560. https://doi.org/10.1016/J.CES.2016.11.004

Liang, Y., Chu, G., Wang, J., Huang, Y., Chen, J., Sun, B., Shao, L., 2014. Controllable preparation of nano-$CaCO_3$ in a microporous tube-in-tube microchannel reactor. Chem. Eng. Process. Process Intensif. 79, 34–39. https://doi.org/10.1016/J.CEP.2014.03.006

Liendo, F., Arduino, M., Deorsola, F.A., Bensaid, S., 2021. Optimization of $CaCO_3$ synthesis through the carbonation route in a packed bed reactor. Powder Technol. 377, 868–881. https://doi.org/10.1016/j.powtec.2020.09.036

Lu, L., Guest, J.S., Peters, C.A., Zhu, X., Rau, G.H., Ren, Z.J., 2018. Wastewater treatment for carbon capture and utilization. Nat. Sustain. 1, 750–758. https://doi.org/10.1038/S41893-018-0187-9

Luz, S., Rivas, J., Afonso, A., Carvalho, F., 2021. Immediate one-step lime precipitation process for the valorization of winery wastewater to agricultural purposes. Environ. Sci. Pollut. Res. 1–10. https://doi.org/10.1007/s11356-020-11933-3

Madeira, L., Almeida, A., Ribau Teixeira, M., Prazeres, A., Chaves, H., Carvalho, F., 2020. Immediate one-step lime precipitation and atmospheric carbonation as pre-treatment for low biodegradable and high nitrogen wastewaters: A case study of explosives industry. J. Environ. Chem. Eng. 8, 103808. https://doi.org/10.1016/j.jece.2020.103808

Madeira, L., Carvalho, F., Almeida, A., Ribau Teixeira, M., 2023. Optimization of atmospheric carbonation in the integrated treatment immediate one-step lime precipitation and atmospheric carbonation. The case study of slaughterhouse effluents. Results Eng. 17, 100807. https://doi.org/10.1016/J.RINENG.2022.100807

Martínez-Cruz, A., Fernandes, A., Ramos, F., Soares, S., Correia, P., Baía, A., Lopes, A., Carvalho, F., 2021. An Eco-Innovative Solution for Reuse of Leachate Chemical Precipitation Sludge: Application to Sanitary Landfill Coverage. Ecol. Eng. Environ. Technol. 22, 52–58. https://doi.org/10.12912/27197050/133329

Mitchell, M.J., Jensen, O.E., Cliffe, K.A., Maroto-Valer, M.M., 2010. A model of carbon dioxide dissolution and mineral carbonation kinetics. Proc. R. Soc. A Math. Phys. Eng. Sci. 466, 1265–1290. https://doi.org/10.1098/RSPA.2009.0349

Mohammed-Nour, A., Al-Sewailem, M., El-Naggar, A.H., 2019. The Influence of Alkalization and Temperature on Ammonia Recovery from Cow Manure and the Chemical Properties of the Effluents. Sustain. 11, 2441. https://doi.org/10.3390/SU11082441

Mortula, M., Ali, T., Elaksher, A., 2020. Municipal wastewater treatment using different coagulants. Desalin. Water Treat. 179, 1–7. https://doi.org/10.5004/DWT.2020.24989

Park, Y.-J., Lee, H.-C., 2020. A Study on the Field Application of Alkaline Tunnel Wastewater to Neutralization Using CO_2. J. Korean Geotech. Soc. 36, 27–34. https://doi.org/10.7843/KGS.2020.36.8.27

Pashaei, H., Ghaemi, A., Nasiri, M., Heydarifard, M., 2018. Experimental Investigation of the Effect of Nano Heavy Metal Oxide Particles in Piperazine Solution on CO_2 Absorption Using a Stirrer Bubble Column. Energy and Fuels 32, 2037–2052. https://doi.org/10.1021/ACS.ENERGYFUELS.7B03481

Pashaei, H., Zarandi, M.N., Ghaemi, A., 2017. Experimental study and modeling of CO_2 absorption into diethanolamine solutions using stirrer bubble column. Chem. Eng. Res. Des. 121, 32–43. https://doi.org/10.1016/J.CHERD.2017.03.001

Prasad, H., Lohchab, R.K., Singh, B., Nain, A., Kumari, M., 2019. Lime treatment of wastewater in a plywood industry to achieve the zero liquid discharge. J. Clean. Prod. 240, 118176. https://doi.org/10.1016/J.JCLEPRO.2019.118176

Prazeres, A.R., Lelis, J., Alves-Ferreira, J., Carvalho, F., 2019. Treatment of vinasse from sugarcane ethanol industry: H_2SO_4, NaOH and $Ca(OH)_2$ precipitations, $FeCl_3$ coagulation-flocculation and atmospheric CO_2 carbonation. J. Environ. Chem. Eng. 7, 103203. https://doi.org/10.1016/j.jece.2019.103203

Prazeres, A.R., Luz, S., Fernandes, F., Jerónimo, E., 2020. Cheese wastewater treatment by acid and basic precipitation: Application of H_2SO_4, HNO_3, HCl, $Ca(OH)_2$ and NaOH. J. Environ. Chem. Eng. 8, 103556. https://doi.org/10.1016/J.JECE.2019.103556

Prazeres, A.R., Rivas, J., Paulo, Ú., Ruas, F., Carvalho, F., 2016. Sustainable treatment of different high-strength cheese whey wastewaters: an innovative approach for atmospheric CO_2 mitigation and fertilizer production. Environ. Sci. Pollut. Res. 23, 13062–13075. https://doi.org/10.1007/s11356-016-6429-3

Qi, D., 2018. Treatment of Wastewater, Off-Gas, and Waste Solid, in: Hydrometallurgy of Rare Earths. Elsevier, pp. 743–777. https://doi.org/10.1016/b978-0-12-813920-2.00008-8

Radovenchyk, I., Trus, I., Halysh, V., Krysenko, T., Chuprinov, E., Ivanchenko, A., 2021. Evaluation of Optimal Conditions for the Application of Capillary Materials for the Purpose of Water Deironing. Ecol. Eng. Environ. Technol. 22, 1–7. https://doi.org/10.12912/27197050/133256

Ramalho, M., Jovanović, T., Afonso, A., Baía, A., Lopes, A., Fernandes, A., Almeida, A., Carvalho, F., 2022. Landfill leachate treatment by immediate one-step lime precipitation, carbonation, and phytoremediation fine-tuning. Environ. Sci. Pollut. Res. 1, 1–10. https://doi.org/10.1007/S11356-022-18729-7/TABLES/3

Salmón, I.R., Cambier, N., Luis, P., 2018. CO_2 Capture by Alkaline Solution for Carbonate Production: A Comparison between a Packed Column and a Membrane Contactor. Appl. Sci. 8, 996. https://doi.org/10.3390/APP8060996

Shibata, K., Terasaka, K., Fujioka, S., Kato, K., 2016. Oxygen Transfer from a Free Surface and Dispersed Bubbles in an Aeration Tank. J. Chem. Eng. JAPAN 49, 391–398. https://doi.org/10.1252/JCEJ.15WE180

Sun, B.C., Wang, X.M., Chen, J.M., Chu, G.W., Chen, J.F., Shao, L., 2011. Synthesis of nano-$CaCO_3$ by simultaneous absorption of CO_2 and NH_3 into $CaCl_2$ solution in a rotating packed bed. Chem. Eng. J. 168, 731–736. https://doi.org/10.1016/J.CEJ.2011.01.068

Trus, I., Radovenchyk, I., Halysh, V., Chuprinov, E., Benatov, D., Olena, H., Sirenko, L., 2022. Innovative Method for Water Deiron Ions Using Capillary Material. J. Ecol. Eng. 23, 174–182. https://doi.org/10.12911/22998993/145467

Uibu, M., Velts, O., Trikkel, A., Kuusik, R., 2008. Reduction of CO_2 emissions by carbonation of alkaline wastewater. WIT Trans. Ecol. Environ. 116, 311–320. https://doi.org/10.2495/AIR080321

Velts, O., Uibu, M., Kallas, J., Kuusik, R., 2013. CO_2 Mineralisation: Concept for Co-utilization of Oil Shale Energetics Waste Streams in $CaCO_3$ Production. Energy Procedia 37, 5921–5928. https://doi.org/10.1016/J.EGYPRO.2013.06.518

Viswanaathan, S., Perumal, P.K., Sundaram, S., 2022. Integrated Approach for Carbon Sequestration and Wastewater Treatment Using Algal-Bacterial Consortia: Opportunities and Challenges. Sustain. 14, 1075. https://doi.org/10.3390/SU14031075

Wang, Z ;, Liu, X ;, Li, K, Wang, Zhongcheng, Liu, Xiaoyu, Li, Ke, 2022. Study of Absorbing CO_2 from Emissions Using a Spray Tower. Atmos. 13, 1315. https://doi.org/10.3390/ATMOS13081315

Yang, M., Smyth, T.J., Kitidis, V., Brown, I.J., Wohl, C., Yelland, M.J., Bell, T.G., 2021. Natural variability in air-sea gas transfer efficiency of CO_2. Sci. Rep. 11, 13584. https://doi.org/10.1038/s41598-021-92947-w

Yoo, J., Shin, H., Ji, S., 2017. An Eco-Friendly Neutralization Process by Carbon Mineralization for Ca-Rich Alkaline Wastewater Generated from Concrete Sludge. Met. 7, 371. https://doi.org/10.3390/MET7090371

Chapter 5

Vertical flow constructed wetland as a green solution for low biodegradable and high nitrogen wastewater: A case study of the explosives industry

This Chapter was published in:

Madeira, L., Carvalho, F., Teixeira, M.R., Ribeiro, C., Almeida, A. (2021). Vertical flow constructed wetland as a green solution for low biodegradable and high nitrogen wastewater: A case study of explosives industry. Chemosphere 272, 129871. https://doi.org/10.1016/j.chemosphere.2021.129871

ABSTRACT

The removal of nitrogen compounds from a pretreated explosives wastewater in a vertical flow constructed wetland planted with *Vetiveria zizanioides* (0.24 m^2× 0.70 m), filled with light expanded clay aggregates (Leca®NR 10/20), was studied. Experiments under constant hydraulic load, 50±4 L m^{-2} d^{-1} and 83±5 L m^{-2} d^{-1} without and with flooding level (25%), respectively, were made at different ammonium (3 to 48 mg NH_4^+-N L^{-1}), nitrate (56 to 160 mg NO_3^--N L^{-1}) and nitrite (0.3 to 1.1 mg NO_2^--N L^{-1}) concentrations. Results indicate that without flooding level (unsaturated) the removal efficiencies obtained were 30±9, 7±1, and 96±2%, respectively to NH_4^+-N, NO_3^--N, and NO_2^--N. When using flooding level and an external carbon source (C/N ratio from 1.3±0.19 to 2.5±0.20), the organic matter (COD) removal efficiencies were above 90%, 75% for NH_4^+-N, and 55% for NO_3^--N. Increasing the C/N ratio from 2.9±0.21 to 4±0.22 did not contribute to upgrading the efficiencies of COD, NH_4^+-N, and NO_3^--N removal. The denitrification process occurred in aerobic conditions and nitrite has been produced, probably due to the presence of aerobic conditions that inhibited partially the denitrification.

5.1. Introduction

Nitrogen compounds release from human activities (domestic, industrial, and agriculture) have a high impact on environmental nitrogen pollution and degrade water resources (OECD, 2017). Reactive nitrogen compounds in the form of nitrites (NO_2^-), nitrates (NO_3^-) and ammonium (NH_4^+), and dissolved organic nitrogen affect soil pH and water quality through surface run-off and leaching into surface and groundwaters leading to water pollution (EU, 2013; Zhou et al., 2017; Holmes et al., 2019). Most of the nitrogen leaching from agricultural soils is in the form of nitrate and comes from synthetic fertilizers, as well as from livestock manure (Hussain et al., 2020; De Boer, 2017). In addition, localized peaks in pollution may be associated with run-off from urban spaces, poorly treated sewage, and industrial sources (Sutton and Billen, 2010; WRI, 2013). Recent estimative revealed an increase in nitrogen discharges of 35 to 46% in water resources between 2000 and 2050 (IFPRI and Veolia, 2015). According to EU (2013), in the absence of human influence, around 0.5 kg $ha^{-1}year^{-1}$ of nitrogen is generally deposited in ecosystems, but in many areas of the world, the average nitrogen deposition rates exceed 10 kg nitrogen $ha^{-1}year^{-1}$.

Tertiary wastewater treatment practices have been developed to avoid the deleterious effects of excess reactive nitrogen in the environment, ensuring the removal of reactive nitrogen species (Holmes et al., 2019). Many efficient technologies rely on physicochemical treatments (e.g., reverse osmosis membranes, ion exchange, air stripping, electrodialysis) to remove nitrogen compounds (Ahn, 2006; Metcalf & Eddy, 2014). However, biological nitrogen removal practices (e.g., modified activated sludge) are much more environmentally friendly and cost-effective (Holmes et al., 2019). In this line, constructed wetlands (CWs) are an alternative to conventional treatments to remove nitrogen and organic matter. In CWs, removal and transformation mechanisms can occur such as filtration, sedimentation, adsorption, chemical precipitation, volatilization, bacterial metabolism (e.g., nitrification, anammox, denitrification), and phytoremediation (phytoextraction, phytodegradation, phytostabilization, phytovolatilization, rhizodegradation, and rhizofiltration) (Rajan et al., 2019).

Nitrogen (ammonium or nitrate) removals in CWs are dependent on the water flow regime, substrate matrix, plant, bed depth, applied operational parameters (such as hydraulic load (H_L), organic and nitrogen loads, C/N ratio, feeding regime, flooding level), and climatic conditions (e.g., temperature) (Almeida et al., 2018; Liu et al., 2018; Saeed and Sun, 2012; Wang et al., 2019). If effluents have low biodegradable organic matter, the nitrate reduction to molecular nitrogen can be compromised since the denitrification process involves the donation of electrons from biodegradable organic matter (Tjelldén et al., 2015). However, this may not be detrimental to certain plants since some plants may contribute to the denitrification process by releasing weak organic acid exudates through their root system and by producing enzymes that can transform complex organic matter into the simplest forms (Tjelldén et al., 2015). Some plants, such as *Phragmites australis, Typha latifolia, Cyperus papyrus, Typha domingensis*, are recognized for their great potential for wastewaters phytoremediation, but recently the interest in *Vetiveria zizanioides* plant has increased (Badejo et al., 2018; Almeida et al., 2019). This plant has wide tolerance to adverse conditions such as weather, soil, pH (between 3 to 10.5), and salinity (until 47.5 dS m^{-1} although its productivity decreases from 8 dS m^{-1}) (Danh et al., 2009), and has high potential for the removal of total nitrogen, ammonia, total suspended solids (TSS), and chemical oxygen demand (COD) from wastewaters (Badejo et al., 2018). Wang et al. (2009) used *Vetiveria zizanioides* in subsurface vertical flow constructed wetland (VFCW) with gravel and coal slag as a substrate to treat domestic wastewater. These authors obtained high COD (71%), ammonium nitrogen (67%), and total nitrogen (80%) removals using 5 days of hydraulic retention time and H_L of 600 to 800 L m^{-2} d^{-1}. The use of subsurface VFCW has some advantages compared with other water flow regimes since it requires less space and provides higher levels of oxygen transfer for the occurrence of the nitrification process and degradation of organic matter (Stefanakis, 2019). However, it does not provide good conditions for the denitrification process since this process occurs in low oxygen conditions (Stefanakis, 2019). In turn, subsurface horizontal flow constructed wetland (HFCW) is usually used for the denitrification process because of the low oxygen content provided in the system (Kadlec and Wallace, 2009). Xinshan et al. (2010) tested the combined systems VFCW-HFCW to treat sequentially an effluent containing ammonium and nitrate and low organic matter. VFCW allowed the conversion of ammonium to nitrate and then HFCW converted to nitrate (the formed and the present in the effluent) to molecular nitrogen using additional organic matter sources (Xinshan et al., 2010).

However, if wastewater has initially high amounts of organic matter nitrification can be inhibited, so a combined system of HFCW-VFCW with recirculation can be a good option (Cooper, 2005; Vymazal, 2013, 2005). Moreover, according to Kadlec (2010), nitrification and denitrification processes can occur simultaneously in the CWs bed. CWs have alternated zones with different oxygenation states in the proximities of the plant roots, where nitrification occurs and the produced nitrate is diffused to the soil anaerobic microzones to be denitrified (Kadlec, 2010). VFCW with flooding level (using *Vetiveria zizanioides*) also demonstrated good results in simultaneous nitrification and denitrification of wastewaters (Almeida et al., 2017; Almeida, 2012). In the flooding level, the dissolved oxygen (DO) content in the bed decreases when the bed flooding level increases, providing anoxic conditions for the occurrence of denitrification.

Explosives wastewaters (EW), from the ammonium nitrate-fuel oil (ANFO) and emulsion industries, are industrial wastewaters with high amounts of nitrogen (in the form of nitrates and/or ammonium nitrogen) and high non-biodegradable organic matter. Due to these characteristics, these wastewaters are very difficult to treat (Madeira et al. (2020), chapter 2). The present work aims to: (i) evaluate the use of VFCW planted with *Vetiveria zizanioides* to remove ammonium and nitrate from a pretreated explosives wastewaters (PEW), using two different flooding conditions; (ii) analyze the increase of organic mass load in the nitrogen forms removal; and (iii) study the impact of the different C/N ratios on the removal of nitrogen compounds.

5.2. Material and methods

5.2.1. Experimental setup characteristics

Experiments were carried out in a pilot-scale VFCW (0.4 m × 0.6 m × 0.70 m), planted with *Vetiveria zizanioides* (plant density higher than 120 plants per m^2) (Figure 5.1), filled with light-expanded clay aggregates (Leca® NR 10/20). A bottom slope of 2% was applied in the bed to enable the hydraulic collection of the effluent. A layer of gravel (diameter 10–50 mm) was placed around the outlet valve to prevent clogging by fine particles. The flooding levels were modified through a flexible siphon in the outlet. This VFCW was fed in continuous mode, through network sprinklers, equidistantly located

over the whole VFCW using a submersible pump (Eheim1250, Deizisan, Germany) in the feeding tank. The VFCW was acclimatized using PEW at the same concentration that trials were done until the system was pseudo-stationary.

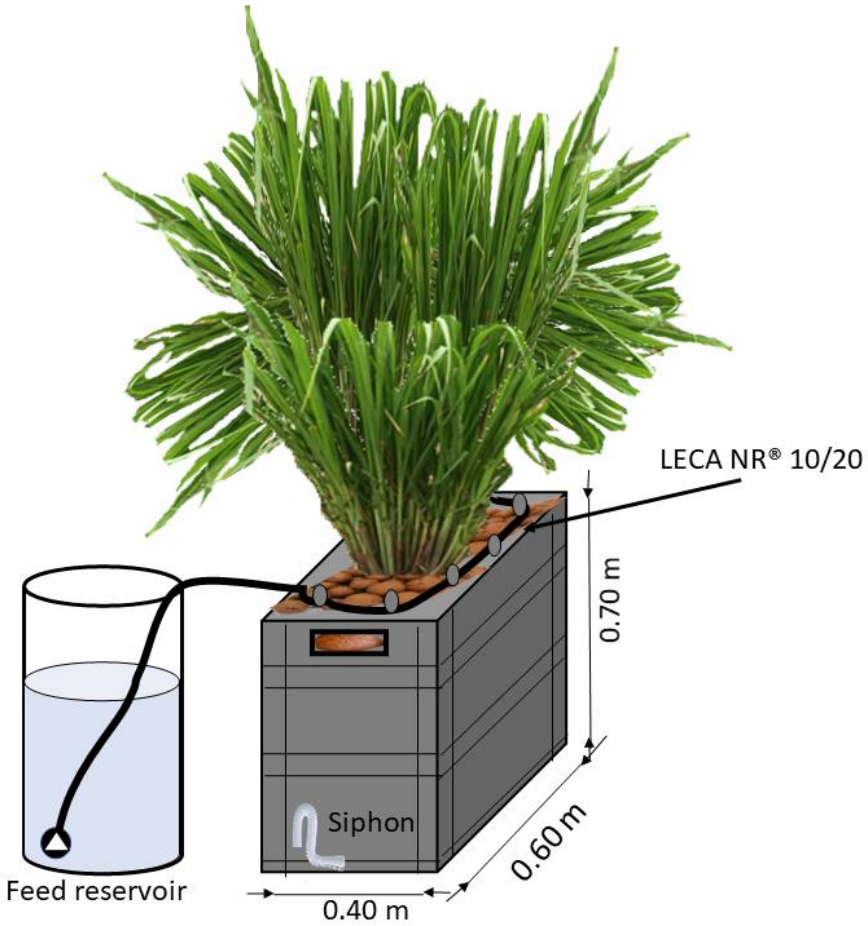

Figure 5.1 – Schematic representation (not at scale) of the vertical flow constructed wetland (VFCW) planted with *Vetiveria zizanioides*.

5.2.2. Experimental conditions

Explosives wastewater was collected from an international industry of ANFO and emulsion explosives, in Portugal. Then, EW was pretreated using a combined immediate one-step lime precipitation (IOSLM) and atmospheric CO_2 carbonation (AC) processes as presented in Madeira et al. (2020) (chapter 2). The IOSLM process was used to remove COD and consisted of applying an optimal hydrated lime dose (7.76 g L^{-1}) to the EW, under vigorous agitation for 1 minute. After the IOSLM process and sedimentation step, the obtained supernatant was pretreated by the AC process to reduce the supernatant pH to 9. Pretreated explosives wastewater (PEW) characteristics were: pH (9±1.4), DO

(6.8±0.3 mg L^{-1}), conductivity (8.9±0.1 mS cm^{-1}), COD (1226±287 mg L^{-1}), BOD (<5 mg L^{-1}), NH_4^+-N (494±464 mg L^{-1}), TKN (494±464 mg L^{-1}), NO_3^--N (2302±372 mg L^{-1}), and NO_2^--N (16±3.2 mg L^{-1}). PEW was then used in VCFW experiments, after PEW dilution to desirable concentrations, as it is pointed out by some researchers that high nitrogen concentrations are toxic to plants (Almeida, 2012; Britto and Kronzucker, 2002).

The experimental trials were conducted in two phases (Table 5.1). In the first phase (phase I), the concentrations studied were 45±3 mg L^{-1} for ammonium (NH_4^+-N), 107±1 mg L^{-1} for nitrate nitrogen (NO_3^--N), 0.6±0.0 mg L^{-1} for nitrite nitrogen (NO_2^--N), and BOD/TKN <<1 (since in PEW BOD <5 mg L^{-1} and TKN 494±464 mg L^{-1}), under constant H_L (50±3 L m^{-2} d^{-1}) without flooding level. In the second phase (phase II), the concentrations varied between 3 to 32 mg L^{-1} for ammonium nitrogen (NH_4^+-N), 56 to 160 mg L^{-1} for nitric nitrogen (NO_3^--N), 0.3 to 1.1 mg L^{-1} nitrite nitrogen (NO_2^--N), 170 to 965 mg L^{-1} for COD, and H_L was kept again constant but at a higher value (83±5 L m^{-2} d^{-1}) than phase I was used. In these trials (phase II) an external carbon source (sucrose) was added and the VFCW was operated with a flooding level of 25% to decrease DO into the bed (according to results obtained by Almeida et al. (2010) and Almeida (2012)). Throughout the experiments, the plants were assessed visually by identifying signs of toxicity (such as leaf curling, chlorosis, or death of the plant).

Table 5.1 – Inlet experimental conditions in Phases I and II (n ≥ 11).

		Chemical composition								Applied Operations	
		pH	EC (mS cm^{-1})	Eh (mV)	DO (mg L^{-1})	NH_4^+-N (mg L^{-1})	NO_3^--N (mg L^{-1})	NO_2^--N (mg L^{-1})	COD (mg L^{-1})	H_L (L m^{-2} d^{-1})	Flooding level (%)
Phase I	Minimum	8.2	1.2	88	5.0	42	106	0.6		47	
	Maximum	8.3	1.3	165	6.5	48	108	0.6	*	53	-
	SD	0.0	0.1	54	1.0	4	1	0.0		4	
Phase II	Minimum	7.7	1.0	96	4.9	3	56	0.3	170	77	
	Maximum	8.3	1.6	246	10.2	32	160	1.1	965	89	25
	SD	0.2	0.2	52	1.5	14	44	0.3	232	5	

* < 25 mg O_2 L^{-1} (detection limit).

5.2.3. Sampling collection and analysis

The VFCW was monitored every weekday at 10:00 a.m., between April and September, until sample number >11. The flow rate at the inlet and outlet was measured during all experimental period. Samples were collected in the inlet (feed tank) and outlet of the VFCW, and the following parameters were characterized: pH, electrical conductivity (EC), redox potential (Eh), dissolved oxygen (DO), ammonium (NH_4^+-N), nitrite (NO_2^--N), nitrate (NO_3^--N), and chemical oxygen demand (COD). The samples were stored at 5 ºC if it was not possible to analyze them immediately.

pH and Eh measurements were performed in a WTW InoLab level 1, using the electrodes SenTix 41 and WTW SenTix ORP, respectively. EC was evaluated in a Jenway 4510 meter, using an electrode VWR CO 11. DO was determined by a modification of the Winkler method (APHA, 2012). Ammonium nitrogen was determined by the distillation method in BUCHI Distillation Unit B-316 and then by titration (APHA, 2012). Nitrite was determined by a colorimetric method (APHA, 2012) at 543 nm using a Pharmacia Biotech Ultrospec 2000 UV/Visible spectrophotometer model 80-2106-00. Nitrate was measured by the sodium salicylate method (Rodier, 1989) at 420 nm using a Pharmacia Biotech Ultrospec 2000 UV/Visible spectrophotometer model 80-2106-00. COD was determined by standard dichromate closed reflux method, using a digester WPA HC 6016 and quantified by Pharmacia Biotech Ultrospec 2000 UV/Visible spectrophotometer model 80-2106-00 at 600 nm (APHA, 2012). COD was used to indirectly quantify carbon content (Metcalf and Eddy, 2014).

5.2.4. Data processing and statistical analysis

The results obtained in each phase were statistically treated. Agglomerative Hierarchical Clustering (AHC) was determined by SPSS 20 (SPSS Inc.) software and performed by Euclidean distance, Ward's method, and standardization of variables. Cluster analysis was performed for phase II, applied to the affluent parameters (pH, Eh EC, DO, NO_2^--N, NO_3^--N, NH_4^+-N), and to the hydraulic load. The outliers were eliminated whenever they existed. According to AHC, it was identified two groups (A and B) in phase II (see Figure 5.2), both under H_L constant (83±5 L m^{-2} d^{-1}). Organic matter loads from 10 to 80 g m^{-2} d^{-1} (COD) under constant loads of ammonium nitrogen (0.40±0.1 g m^{-2} d^{-1} NH_4^+-N),

nitrate (12±2 g m^{-2} d^{-1} NO_3^--N) and nitrite (0.08±0.01 g m^{-2} d^{-1} NO_2^--N) were grouped in group A, and organic loads of 30 to 50 g $m^{-2}d^{-1}$ under constant loads of ammonium nitrogen (2.4±0.4 g m^{-2} d^{-1} NH_4^+-N), nitrate (5±1 g m^{-2} d^{-1} NO_3^--N and nitrite (0.04±0.01 g m^{-2} d^{-1} NO_2^--N) were grouped in group B.

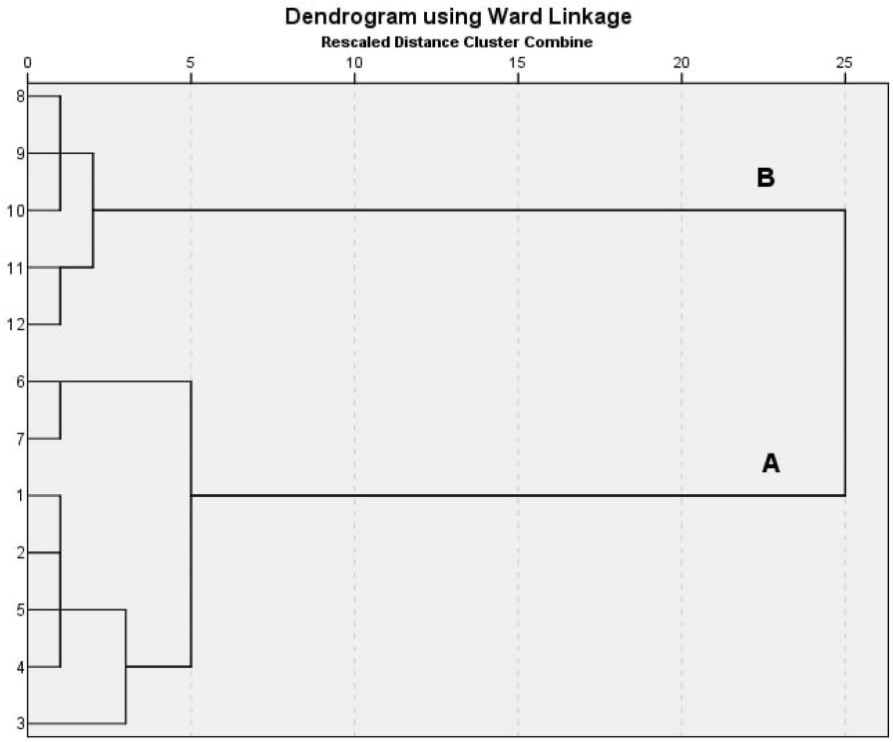

Figure 5.2 – Groups identified in Phase II according to the Dendrogram of hierarchical cluster analysis.

For the comparison between influent and effluent quality, ANOVA was used at a 95% confidence level. Two hypotheses were tested against each other (in which the null hypothesis H_0: "influent and effluent quality are identical", and the alternative hypothesis H1: "influent and effluent quality are different"). Post-hoc (a posteriori) Turkey's test was used to determine differences between means of specific variables.

5.3. Results and Discussion

5.3.1. Nitrogen removal in phase I

Ammonium (NH_4^+-N) and nitrate (NO_3^--N) results under unsaturated conditions (without flooding level) (Table 5.1) are presented in Figure 5.3. The ammonium nitrogen load in the VFCW outlet decreased significantly ($p<0.05$) and ammonium nitrogen removal was 30±16% (corresponding to 0.70±0.5 g m^{-2} d^{-1}) (Figure 5.3a). These results were not expected since the decrease in ammonium nitrogen observed in this work was lower than the data reported by Almeida et al. (2018), whose ammonia nitrogen removal efficiencies were around 60% using a synthetic effluent and a hydraulic retention time of 10 h identical that was used in this work (10 h±0.9). According to Cervantes et al. (2015) and Kadlec and Wallace (2009), NH_4^+-N transformation to NO_3^--N consumes alkalinity, H^+ ions are released, and dissolved oxygen is consumed too. These transformations can be observed by the pH decrease (Figure 5.3f) and the DO consumption (Figure 5.3e), both variations statistically significant ($p<0.05$). However, it was observed that pH effluent showed values between 4.0 and 5.6, which can contribute to remove the ammonium efficiently, since according to Lee et al. (2009) when pH values decrease lower than 7.0 nitrification rate decrease too. In this study, the nitrification process was not inhibited by organic matter because PEW had a low concentration of organic matter (≤ 25 mg O_2 L^{-1}) and the effluent contained 4±0.1 mg O_2 L^{-1}. Moreover, the BOD/TKN ratio was less than 1, which was favorable for successful nitrification, as mentioned by Kadlec and Wallace (2009). The nitrification process had the ideal initial conditions (pH, redox, nitrogen, oxygen) to occur successfully, which did not happen, probably due to the presence of nitrate (106 to 108 mg L^{-1} NO_3^-) in the influent, together with pH drop in the effluent, which inhibit nitrification, although a nitrate removal (0.40±0.1 g m^{-2} d^{-1}) (not significant, $p>0.05$) with a removal efficiency of 7±0.5% has been observed (Figure 5.3b). Nitrate production and its removal are processes that can occur in a sequential mode in CW since low H_L values can provide a greater removal of nitrate than formed.

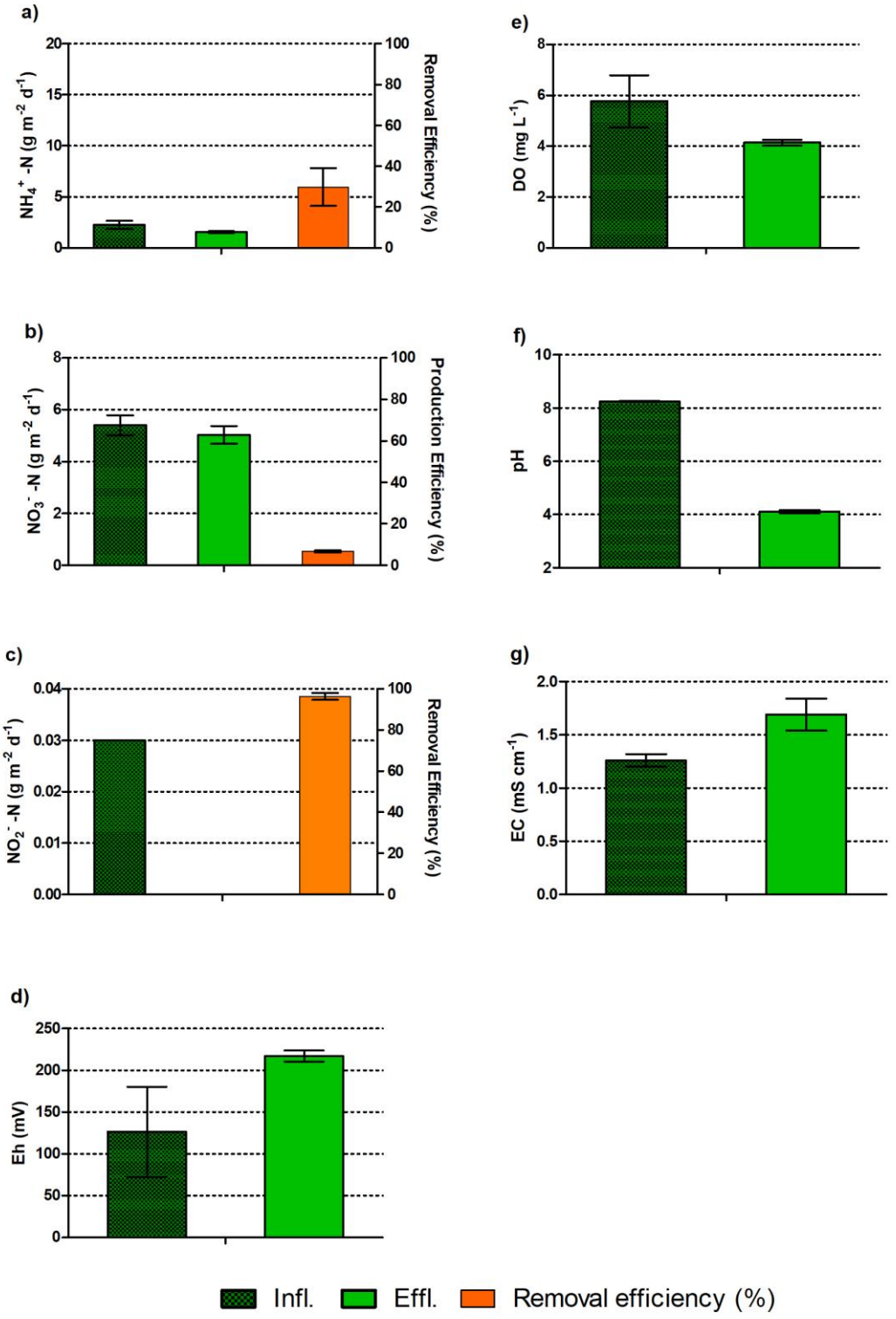

Figure 5.3 – Water quality in the inlet (Infl.) and outlet (Effl.) of the VFCW for **a)** ammonium applied load, **b)** nitrate applied load, **c)** nitrite applied load, **d)** redox potential, **e)** dissolved oxygen, **f)** pH and **g)** electrical conductivity. Removal efficiency for **a)** ammonium, **b)** nitrate, and **c)** nitrite. The hydraulic load was kept constant (50±3 L m^{-2} d^{-1}) and without flooding level. Bars represent the standard deviation of the mean (n≥11).

Nitrite was not found in the effluent (Figure 5.3c), so considering the method detection limit a removal efficiency of 96±2% was calculated. Usually, in biological treatment systems under stable operation, there is no accumulation of nitrites because the growth rate of *Nitrobacter* bacteria is significantly higher than the *Nitrosomonas* bacteria. As a result, the growth rate of the latter generally controls the overall nitrification rate (WEF et al., 2005).

An increase in the values of redox potential (from 126±54 to 217±7 mV) (Figure 5.3d) in the effluent was observed. According to Reddy and DeLaune (2008), more oxidized substances raise the electric potential as in the case of ammonium nitrogen transformation in nitrates. However, it did not happen in this work because there was no nitrate production in the effluent (Figure 5.3b). Moreover, any eventual nitrate production from nitrification would be too little for that. This increase in the redox potential may be related to the decrease in the pH of the effluent (DeLaune and Reddy, 2005), caused by the interaction between PEW and CO_2 present inside the bed, releasing H^+ ions (Madeira et al., 2020).

Electrical conductivity showed a significant increase ($p<0.05$) (Figure 5.3g), attributed to evapotranspiration. The electrical conductivity values in the effluent (about 1.5 dS m^{-1}) were always below the value (8 dS m^{-1}) from which plant *Vetiveria zizanioides* productivity decreases (Danh et al., 2009).

5.3.2. Nitrogen removal in phase II

Ammonium nitrogen and nitrate removals in presence of organic matter were studied (Figure 5.4). As PEW diluted had a low C/N ratio, it was necessary to add sucrose as an external source of carbon to ensure that all necessary conditions for denitrification were ensured.

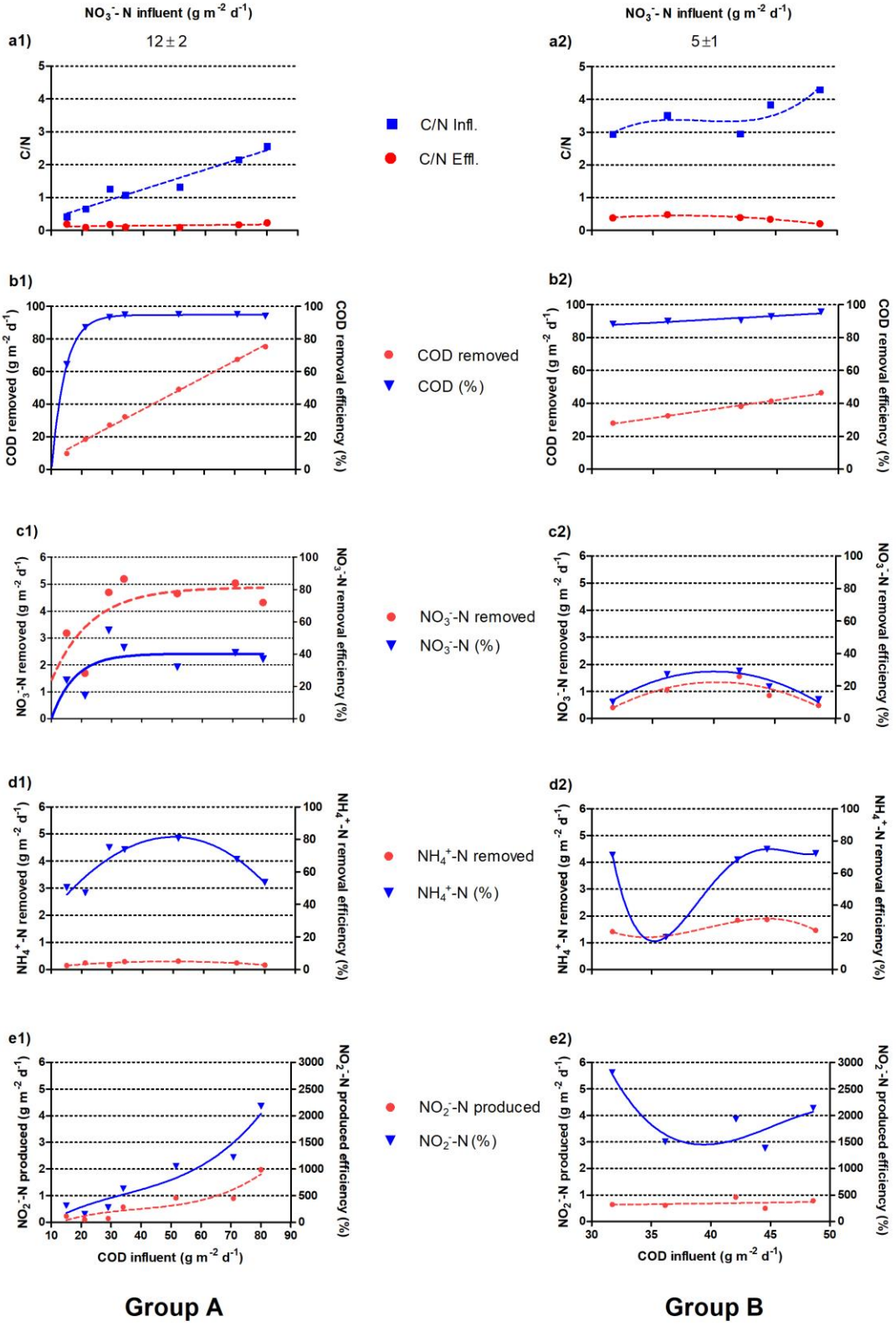

Figure 5.4 – Variation of the: C/N ratio in influent (Infl.) and effluent (Effl.) (**a1** and **a2)**; and removal load and removal efficiency for COD **(b1** and **b2)**, nitrate **(c1** and **c2)**, ammonium **(d1** and **d2)** and nitrite **(e1** and **e2)**, as a function of the applied organic matter load. Items **a1**) to **e1**) belong to group A (loads applied: 12±2 g m^{-2} d^{-1} NO_3^--N, 0.40±0.1 g m^{-2} d^{-1} NH_4^+-N and 0.08±0.01 g m^{-2} d^{-1} NO_2^--N) while items **a2**) to **e2**) belong to group B (loads applied: 5±1 g m^{-2}

d^{-1} NO_3^--N, 2.4±0.4 g m^{-2} d^{-1} NH_4^+-N and 0.04±0.01 g m^{-2} d^{-1} NO_2^--N). The hydraulic load was kept constant (83±5 L m^{-2} d^{-1}) and with a flooding level of 25%.

Figures 5.4a1 and 5.4a2 show the influence of the organic load applied in the C/N ratio in the influent and effluent. The C/N ratio in influent varied between 0.4 to 2.5 and 2.9 to 4.3 for groups A and B, respectively. For both groups, the input C/N ratios reduced significantly to values around 0.2±0.06 (Figure 5.4a1) and 0.4±0.08 (Figure 5.4a2), for all applied organic loads. These reductions were due to the greatest removal of applied organic matter (COD) than nitrogen. Organic matter removal efficiencies remained above 90%, for organic matter loads applied above 30 g $m^{-2}d^{-1}$ (Figures 5.4b1 and 5.4b2).

Although the nitrate removal was observed along with the applied organic load range (Figures 5.4c1 and 5.4c2), heterotrophic denitrification was not the main mechanism for organic matter removal in both groups because it was observed greater organic matter removal than would be expected by denitrification process. Schneider et al. (2008) referred that the degradation of 1 g of sucrose consumed only approximately 1.74 g of nitrate. Moreover, the organic matter removal was not proportional to the nitrate removal. So, most of the organic matter was due to aerobic biodegradation.

According to Figure 5.4c1, a maximum nitrate removal from about 4.5 g m^{-2} d^{-1} (corresponding to a maximum nitrate removal efficiency of about 55%) at 30 g m^{-2} d^{-1} COD was achieved, remaining constant for higher added organic loads. This maximum nitrate removal happened to C/N of 1.3 which is quite close to 1.25 where the denitrification process should be performed (Metcalf & Eddy, 2014). Xinshan et al. (2010) results showed that the excessive C/N ratio did not mean an increase in nitrogen removal efficiency. So, up to 30 g m^{-2} d^{-1} COD applied, the organic matter was the limiting agent in the denitrification process. From 30 g m^{-2} d^{-1} COD, the nitrate removal efficiency tended to decrease for values around 40%, which was possibly due to the increase in the dissolved oxygen concentration in the effluent (Figure 5.5b1).

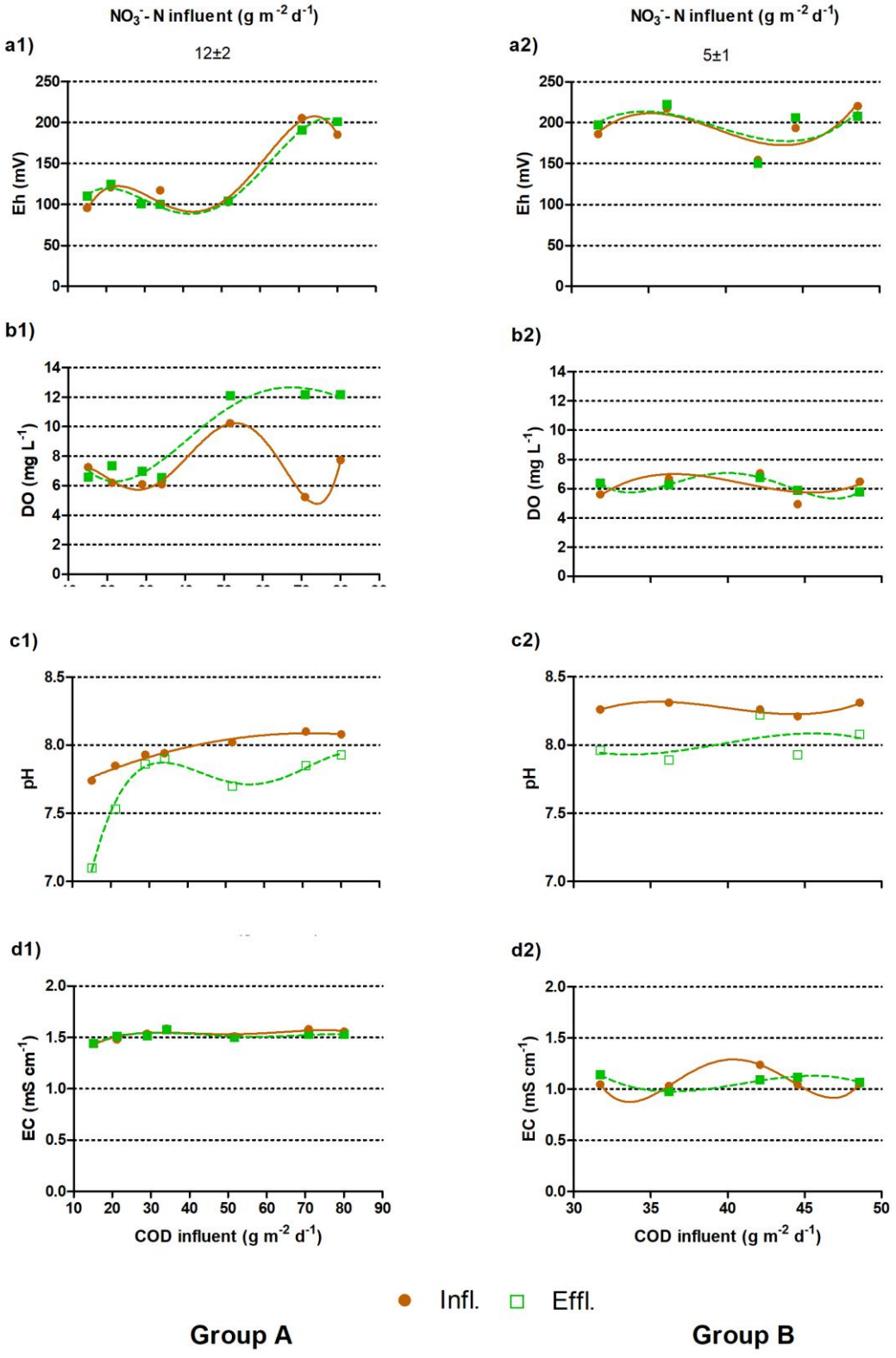

Figure 5.5 – Variation of the: redox potential **(a1** and **a2)**; dissolved oxygen **(b1** and **b2)**; pH **(c1** and **c2)**; electrical conductivity **(d1** and **d2)**; in influent (Infl.); and effluent (Effl.), as a function of the applied organic matter load. Items **a1)** to **d1)** belong to group A (loads applied: 12±2 g m^{-2} d^{-1} NO_3^--N, 0.40±0.1 g m^{-2} d^{-1} NH_4^+-N and 0.08±0.01 g m^{-2} d^{-1} NO_2^--N) while items **a2)** to **d2)** belong to group B (loads applied: 5±1 g m^{-2} d^{-1} NO_3^--N, 2.4±0.4 g m^{-2} d^{-1} NH_4^+-N and 0.04±0.01 g m^{-2} d^{-1} NO_2^--N). The hydraulic load was kept constant (83±5 L m^{-2} d^{-1}) and with a flooding level of 25%.

Nitrate removal efficiencies were lower in group B than in group A, for the same range of organic load applied. This difference can be due to the greater conversion of ammonium nitrogen into nitrate in group B (whose ammonium nitrogen removal ranged from 1.2 to 1.9 g $m^{-2}d^{-1}$ NH_4^+-N) than in group A (whose ammonium nitrogen removal ranged from 0.2 to 0.3 g $m^{-2}d^{-1}$ NH_4^+-N) (Figures 5.4d1 and 5.4d2), although the ammonium nitrogen removal efficiencies were the same (approximately 75% and 81%, for organic matter load range studied in both groups).

Nitrate removal happened in the presence of high concentrations of dissolved oxygen (about 5 to 12 mg O_2 L^{-1}) in both groups (Figures 5.5b1 and 5.5b2) and without significative differences in redox potential between influent and effluent (Figures 5.5a1 and 5.5a2). Although not expected, because the presence of oxygen suppresses the enzyme required for denitrification (Cooper et al., 1996), the denitrification process was observed in CWs in the presence of considerable concentrations of dissolved oxygen: 6±2 mg O_2 L^{-1} by Kadlec (2010) and of 4.7 ± 2.1 mg O_2 L^{-1} by Almeida et al. (2017). Kadlec (2010) referred that in the CWs there were alternating zones with different oxygenation states depending on the proximity to plant roots, which allowed nitrification and denitrification processes to occur simultaneously. In addition, the flooding level could determine aerobic/anaerobic activity (Moshiri, 1993).

An increase in oxygen concentration in the effluent (Figure 5.5b1) was observed for organic matter loads above 50 g $m^{-2}d^{-1}$ COD. Moreover, it would be expected a decrease in oxygen concentration, essentially due to the consumption of organic matter by aerobic biodegradation and the nitrification process. H_L was kept constant throughout the groups, so it is not responsible for the variation of oxygen in CW. The same behavior was observed by Bezbaruah and Zhang (2004). According to Bezbaruah and Zhang (2004), an increase in the concentration of organic matter in CW could promote the creation of areas with deficiencies of oxygen near the root, causing the plant to develop defense mechanisms, namely the formation of aerenchyma in the roots (large cavities in the interior of the plant filled with air). There are also other factors affecting oxygen released by the roots of macrophytes in the rhizosphere, namely, some factors that affect photosynthesis and oxygen transport through plants (Brix, 1994; Rehman et al., 2017).

Effluent pH decreased in the effluent in both groups (Figures 5.5c1 and 5.5c2). The pH drop was the result of all the mechanisms that occurred in the VFCW. As noted above, aerobic biodegradation of organic matter and nitrification process occurred in both groups and they were responsible for the pH drop due to the release of CO_2 and ions H^+ to the matrix, respectively. The denitrification process also occurred in CW and it is responsible for an increase in pH, but this process did not prove to be predominant over the other processes to counteract the drop in pH.

Nitrite accumulation was observed throughout the organic load range applied (Figures 5.4e1 and 5.4e2). Lu et al. (2009) also verified an increase of nitrite in the effluent when they supplemented the system with carbon. The accumulation of nitrite indicates that there were adverse conditions that inhibit the activity of *Nitrobacter* and consequently the nitrite removal. However, nitrification was not the only mechanism that contributed to the production of nitrites (mainly for group A), since the removal of ammonium nitrogen was less than the nitrite produced. Thus, the accumulation of nitrite may be essentially due to the interruption of the denitrification process caused by the high levels of oxygen in the effluent (Figures 5.5b1 and 5.5b2).

No significative oscillations of EC were found in both groups. The EC was around 1.5 dS m^{-1} (Figure 5.5d1) and 1.0 dS m^{-1} (Figure 5.5d2), throughout the organic load range applied. This means that the balance among evapotranspiration, salt precipitation, or nitrate reduction allowed maintain the EC. In both experiments, the EC values were below 8 dS m^{-1}, indicating that the productivity of *Veteriveria zizanioides* was not affected by this parameter (Danh et al., 2009). No signs of toxicity and no symptoms of micronutrient deficiency (e.g., yellowing of the leaves) were detected in the plant by visual inspection.

5.4. Conclusion

In this work, a VFCW planted with *Vetiveria zizanioides* in LECA was used to remove nitrogen (ammonium and nitrate) from a PEW.

The experimental trials were conducted in two phases: in the first phase, the ammonium nitrogen removal was evaluated under ammonium and nitrate nitrogen constant

concentrations, constant H_L (50±3 L m^{-2} d^{-1}), and without the presence of organic matter and flooding level. About 30±9 and 7±1% of ammonium and nitrate nitrogen removal were reached, respectively. According to the operational conditions applied (traces of organic matter and low hydraulic retention time), greater removal of ammonium nitrogen would be expected. High nitrate concentration in the affluent and the drop in pH to very low values in the effluent (between 4.0 and 5.6) would have been the main reasons for the inhibition of the nitrification process.

In the second phase, 55% of nitrate nitrogen removal was reached with the addition of organic matter, constant H_L (83±5 L m^{-2} d^{-1}), and a flooding level of 25%. Results showed that nitrate nitrogen removal was not dependent on the ratio C/N to values higher than 1.3±0.19. The denitrification process occurred in aerobic conditions. However, nitrite was produced which was probably due to partial inhibition of the denitrification process.

The results obtained show that it will be necessary to continue research related to ammonium and nitrate nitrogen removal, using the VFCW in series and other flooding levels.

5.5. References

Ahn, Y. H., 2006. Sustainable nitrogen elimination biotechnologies: A review. Process Biochem. 41, 1709–1721. https://doi.org/10.1016/j.procbio.2006.03.033

Almeida, A., Carvalho, F., Imaginário, M.J., Castanheira, I., Prazeres, A.R., Ribeiro, C., 2017. Nitrate removal in vertical flow constructed wetland planted with Vetiveria zizanioides: Effect of hydraulic load. Ecol. Eng. 99, 535–542. https://doi.org/10.1016/j.ecoleng.2016.11.069

Almeida, A., Jóźwiakowski, K., Kowalczyk-Juśko, A., Bugajski, P., Kurek, K., Carvalho, F., Durao, A., Ribeiro, C., Gajewska, M., 2018. Nitrogen removal in vertical flow constructed wetlands: influence of bed depth and high nitrogen loadings. Environ. Technol. (United Kingdom) 41 (17), 2196-2209. https://doi.org/10.1080/09593330.2018.1557749

Almeida, A., Ribeiro, C., Carvalho, F., Durao, A., Bugajski, P., Kurek, K., Pochwatka, P., Jóźwiakowski, K., 2019. Phytoremediation potential of Vetiveria zizanioides and Oryza sativa to nitrate and organic substance removal in vertical flow constructed wetland systems. Ecol. Eng. 138, 19–27. https://doi.org/10.1016/j.ecoleng.2019.06.020

Almeida, M.A.A., 2012. Remoção de compostos de azoto em efluente de suinicultura por recurso à fitoremediação. Technical University of Lisbon, Ph.D Thesis.

Almeida, A., Novais, J. M., Martins-Dias, S., 2010. Nitrate removal from synthetic wastewater in a VFCW planted with Vetiveria zizanioides. 12th International Conference on Wetland Systems for Water Pollution Control, Venice, Italia.

APHA, 2012. AWWA, WEF - Standard Methods for the Examination of Water and Wastewater, 22nd ed. American Public Health Association, Washington.

Badejo, A.A., Omole, D.O., Ndambuki, J.M., 2018. Municipal wastewater management using Vetiveria zizanioides planted in vertical flow constructed wetland. Appl. Water Sci. 8, 110. https://doi.org/10.1007/s13201-018-0756-0

Bezbaruah, A.N., Zhang, T.C., 2004. pH, redox, and oxygen microprofiles in rhizosphere of bulrush (Scirpus validus) in a constructed wetland treating municipal wastewater. Biotechnol. Bioeng. 88, 60–70. https://doi.org/10.1002/bit.20208

Britto, D. T., Kronzucker, H. J., 2002. NH_4^+ toxicity in higher plants: a critical review. J. Plant Physiol., 159 (6), 567 – 584.

Brix, H., 1994. Functions of macrophytes in constructed wetlands. Water Sci. Technol. 29, 71–78. https://doi.org/10.2166/wst.1994.0160

Cervantes, F., Pavlostathis, S., van Haandel, A., 2015. Advanced Biological Treatment Processes for Industrial Wastewaters - Principles & Applications. IWA Publishing. https://doi.org/10.2166/9781780402345

Cooper, P., 2005. The performance of vertical flow constructed wetland systems with special reference to the significance of oxygen transfer and hydraulic loading rates. Water Sci. Technol. 51, 81–90. https://doi.org/10.2166/wst.2005.0293

Cooper, P.F., Job, G.D., Green, M.B., Shutes, R.B.E., 1996. Reed beds and constructed wetlands for wastewater treatment. WRc Publications, Medmenham, Marlow, UK.

Danh, L.T., Truong, P., Mammucari, R., Tran, T., Foster, N., 2009. Vetiver grass, Vetiveria zizanioides: A choice plant for phytoremediation of heavy metals and organic wastes. Int. J. Phytoremediation 11, 664–691. https://doi.org/10.1080/15226510902787302

De Boer, H.C., 2017. Nitrate leaching from liquid cattle manure compared to synthetic fertilizer applied to grassland or silage maize in the Netherlands. Wageningen Livestock Research, Report 1055. https://doi.org/10.18174/425920

DeLaune, R.D., Reddy, K.R., 2005. Redox Potential, in: Encyclopedia of Soils in the Environment. Elsevier Inc., 366–371. https://doi.org/10.1016/B0-12-348530-4/00212-5

EU, 2013. Science for Environment Policy IN-DEPTH REPORT Nitrogen Pollution and the European Environment Implications for Air Quality Policy. Available: https://ec.europa.eu/environment/integration/research/newsalert/pdf/IR6_en.pdf [Accessed: 11th December 2020]

Holmes, D.E., Dang, Y., Smith, J.A., 2019. Nitrogen cycling during wastewater treatment, in: Advances in Applied Microbiology. Academic Press, 113–192. https://doi.org/10.1016/bs.aambs.2018.10.003

Hussain, M.Z., Robertson, G.P., Basso, B., Hamilton, S.K., 2020. Leaching losses of dissolved organic carbon and nitrogen from agricultural soils in the upper US Midwest. Sci. Total Environ. 734, 139379. https://doi.org/10.1016/j.scitotenv.2020.139379

IFPRI, Veolia, 2015. The murky future of global water quality: New global study projects rapid deterioration in water quality. International Food Policy Research Institute (IFPRI), Washington, D.C. and Veolia Water North America, Chicago, IL.

Kadlec, R.H., 2010. Nitrate dynamics in event-driven wetlands. Ecol. Eng. 36, 503–516. https://doi.org/10.1016/j.ecoleng.2009.11.020

Kadlec, R.H., Wallace, S.D., 2009. Treatment Wetlands, 2nd ed. CRC Press/Taylor & Francis Group, Boca Raton, FL.

Lee, C.G., Fletcher, T.D., Sun, G., 2009. Nitrogen removal in constructed wetland systems. Eng. Life Sci. 9, 11–22. https://doi.org/10.1002/elsc.200800049

Liu, G., She, Z., Gao, M., Liang, J., Jin, C., Guo, L., Zhao, Y., 2018. Influence of saturated zone depth and vegetation on the performance of vertical flow-constructed wetland with continuous feeding. Environ. Sci. Pollut. Res. 25, 33286–33297. https://doi.org/10.1007/s11356-018-3288-0

Lu, S., Hu, H., Sun, Y., Yang, J., 2009. Effect of carbon source on the denitrification in constructed wetlands. J. Environ. Sci. 21, 1036–1043. https://doi.org/10.1016/S1001-0742(08)62379-7

Madeira, L., Almeida, A., Ribau Teixeira, M., Prazeres, A., Chaves, H., Carvalho, F., 2020. Immediate one-step lime precipitation and atmospheric carbonation as pre-treatment for low biodegradable and high nitrogen wastewaters: A case study of explosives industry. J. Environ. Chem. Eng. 8, 103808. https://doi.org/10.1016/j.jece.2020.103808

Metcalf & Eddy, 2014. Wastewater Engineering: Treatment and Resource Recovery, 5th. ed. McGraw-Hill, Inc., New York.

Moshiri, G.A., 1993. Constructed Wetlands for Water Quality Improvement. Lewis Publishers, Boca Raton, FL.

OECD, 2017. Diffuse Pollution, Degraded Waters: Emerging Policy Solutions. https://doi.org/10.1787/9789264269064-en

Rajan, R.J., Sudarsan, J.S., Nithiyanantham, S., 2019. Microbial population dynamics in constructed wetlands: Review of recent advancements for wastewater treatment. Environ. Eng. Res. 24, 181–190. https://doi.org/10.4491/eer.2018.127

Reddy, K.R., DeLaune, R.D., 2008. Biogeochemistry of Wetlands: science and applications, Biogeochemistry of Wetlands. CRC Press, Taylor & Francis Group, Boca Raton, New York. https://doi.org/10.1201/9780203491454

Rehman, F., Pervez, A., Khattak, B.N., Ahmad, R., 2017. Constructed Wetlands: Perspectives of the Oxygen Released in the Rhizosphere of Macrophytes. Clean - Soil, Air, Water. https://doi.org/10.1002/clen.201600054

Rodier, J., 1989. Análisis de las aguas, aguas naturales, aguas residuales, aguas de mar. Ediciones Omega.

Saeed, T., Sun, G., 2012. A review on nitrogen and organics removal mechanisms in subsurface flow constructed wetlands: Dependency on environmental parameters, operating conditions and supporting media. J. Environ. Manage. 112, 429-448. https://doi.org/10.1016/j.jenvman.2012.08.011

Schneider, A.C., Corseuil, H.X., Costa, A.H.R., 2008. Remoção de nitrato de águas subterrâneas após biorremediação de gasolina com etanol., in: XV Congresso Brasileiro de Águas Subterrâneas. Natal.

Stefanakis, A.I., 2019. The Role of Constructed Wetlands as Green Infrastructure for Sustainable Urban Water Management. Sustainability 11, 6981. https://doi.org/10.3390/su11246981

Sutton, M.A. and Billen, G., 2010. European Nitrogen Assessment: Technical Summary. In: Sutton, M.A., Howard, C.M., Erisman, J.W., Billen, G., Bleeker, A., Grennfelt, P. and Hansen, J., eds. (2011) The European Nitrogen Assessment. Cambridge: Cambridge University Press.

Tjelldén, A.K.E., Kristiansen, S.M., Matthiesen, H., Pedersen, O., 2015. Impact of roots and rhizomes on wetland archaeology: A review. Conserv. Manag. Archaeol. Sites. 17 (4), 370-391. https://doi.org/10.1080/13505033.2016.1175909

Vymazal, J., 2013. The use of hybrid constructed wetlands for wastewater treatment with special attention to nitrogen removal: A review of a recent development. Water Res. 47 (14), 4795-4811. https://doi.org/10.1016/j.watres.2013.05.029

Vymazal, J., 2005. Horizontal sub-surface flow and hybrid constructed wetlands systems for wastewater treatment. Ecol. Eng. 25, 478–490. https://doi.org/10.1016/j.ecoleng.2005.07.010

Wang, X., Han, B. Ping, Shi, Y. Zheng, Pang, Z. Qiang, 2009. Advanced wastewater treatment by integrated vertical flow constructed wetland with vetiveria zizanioides in north China. Procedia Earth Planet. Sci. 1, 1258–1262. https://doi.org/10.1016/j.proeps.2009.09.194

Wang, X., Tian, Y., Liu, H., Zhao, X., Wu, Q., 2019. Effects of influent COD/TN ratio on nitrogen removal in integrated constructed wetland–microbial fuel cell systems. Bioresour. Technol. 271, 492–495. https://doi.org/10.1016/j.biortech.2018.09.039

WEF, ASCE, EWRI, 2005. Biological nutrient removal (BNR) operation in wastewater treatment plants. Manual of Practice nº 29 of WEF and Manuals and Reports on Engineering Practice nº 109 of WEF, ASCE, EWRI, WEF Press, McGraw-Hill, New York.

World Resources Institute, 2013. Sources of Nutrient Pollution. Available: http://www.wri.org/project/eutrophication/ about/sources [Accessed: April 2013].

Xinshan, S., Qin, L., Denghua, Y., 2010. Nutrient removal by hybrid subsurface flow constructed wetlands for high concentration ammonia nitrogen wastewater. Procedia Environ. Sci. 2, 1461–1468. https://doi.org/10.1016/j.proenv.2010.10.159

Zhou, Y., Ma, J., Zhang, Y., Qin, B., Jeppesen, E., Shi, K., Brookes, J.D., Spencer, R.G.M., Zhu, G., Gao, G., 2017. Improving water quality in China: Environmental investment pays dividends. Water Res. 118, 152–159. https://doi.org/10.1016/j.watres.2017.04.

Chapter 6

Tunning processes for organic matter removal from slaughterhouse wastewater pretreated by immediate one-step lime precipitation and atmospheric carbonation

This Chapter was submitted to:

Madeira, L., Almeida, A., Rosa da Costa, A. M., Mestre, A. S., Carvalho, F., Ribau Teixeira, M. Tunning processes for organic matter removal from slaughterhouse wastewater pretreated by immediate one-step lime precipitation and atmospheric carbonation**.** Submitted to Journal of Environmental Chemical Engineering in April 2023.

ABSTRACT

Adsorption using unmodified/modified commercial activated carbons and constructed wetlands (CW) planted with *Vetiveria zizanioides* were evaluated as tuning processes for lowering chemical oxygen demand (COD) from slaughterhouse wastewater pretreated by the integrated process of immediate one-step lime precipitation and atmospheric carbonation. Powdered and granular activated carbons (PAC and GAC), and PAC and GAC incorporated with iron oxide nanoparticles (PACMAG and GACMAG) were used. COD removal using different adsorbent separation methods (i.e., sedimentation, filtration, or magnetic separation) was also evaluated. The adsorption results indicated that the best adsorbent doses and contact times of the studied adsorbents were 70 g L^{-1} and 5 min for PAC and PACMAG, and 60 g L^{-1} and 60 min for GAC and GACMAG. Under optimized conditions, GAC (75.7±1.0%) and GACMAG (73.5±2.1%) were more efficient than PAC (59.7±1.0%) and PACMAG (59.0±0.0%) in removing COD. The incorporation of iron oxide nanoparticles in GAC and PAC did not affect the adsorption of COD. The Temkin model was the best isotherm model found for PAC and PACMAG, while for GAC and GACMAG was the BET model. Pseudo-order n kinetic model was the best kinetic model found for all the adsorbents tested. There were no significant differences in the removal of COD between filtration and magnetic separations. Phytoremediation results indicated that increased COD removal efficiency occurred when the applied COD mass load decreased or when the bed depth was increased. Maximum COD removals of around 89.9 to 95.0% were achieved. *Vetiveria zizanioides* showed no signs of toxicity throughout the trials.

6.1. Introduction

Slaughterhouse wastewater (SWW) is a complex effluent characterized by a high content of organic matter, nutrients (nitrogen and phosphorus), oils and fats, total suspended solids (TSS), and microorganisms (Bustillo-Lecompte and Mehrvar, 2015). Therefore, it is a challenge to find efficient, economic, low-energy, ecological, and simple treatment processes. Different SWW treatment processes have been investigated, namely: i) physical-chemical treatments (e.g., coagulation and flocculation, dissolved air flotation, electrocoagulation, adsorption, membranes, and acid precipitation (Prazeres et al., 2019)); ii) biological treatments (e.g., activated sludge (AS), anaerobic filters and constructed wetlands (CW)); iii) chemical oxidation processes (e.g., ozonation); iv) advanced oxidation processes (AOP) (e.g., UV-H_2O_2, gamma radiation, Fenton, photo-Fenton and electro-Fenton); and v) combined processes (e.g., coagulation/adsorption, AS/reverse osmosis, anaerobic baffled reactor (ABR)/UV/H_2O_2, ABR/aerobic AS/UV/H_2O_2, anaerobic lagoon/CW, anaerobic digestion/CW and coagulation/electro-Fenton (Bazrafshan et al., 2022)). Combined processes have shown better performance than individual treatments since the last ones complement each other to remove contaminants (Bustillo-Lecompte et al., 2014). Recently, Madeira et al. (2023) (chapter 3) developed a low-cost and easy-to-apply pretreatment for SWW, using a combined immediate one-step lime precipitation (IOSLM) and atmospheric carbonation (AC) process. These authors obtained removals higher than 80% for chemical oxygen demand (COD) and biochemical oxygen demand (BOD) (chapter 3). To fulfill discharge requirements, this combined process needs to be complemented with a refining process. Reverse osmosis and AOP are highly effective in removing organic matter, but they have high capital and operating/maintenance costs (Al-Marri et al., 2021; Foster et al., 2017). Biological treatments are low-cost and simple, but they are not suitable for removing some poorly biodegradable contaminants (Bracamontes-Ruelas et al., 2022; Bustillo-Lecompte and Mehrvar, 2015). So, adsorption and phytoremediation are treatment processes that could be a solution, however, their effectiveness for safe discharge into water bodies is still questioned (Keerthana and Thivyatharsan, 2018).

Adsorption is a low-cost, high-performance, and easy operational design process that has been used to remove a wide range of organic (e.g., dyes, pesticides, herbicides, drugs, and other emerging contaminants) and inorganic (e.g., heavy metals, radionuclides, etc.)

(Sahoo and Prelot, 2020). Different adsorbents have been used in adsorption, like activated carbons (powdered activated carbon (PAC) and granular activated carbon (GAC)), improved biochars, nano adsorbents, metal oxide adsorbents, magnetic adsorbents, hybrid adsorbents, and others (Rathi and Kumar, 2021). Some COD and BOD removal studies from SWW by adsorption processes using activated carbon and improved biochars have been reported. Agarry and Owabor (2012) achieved high COD (92-95%) and BOD (68-69%) removal efficiencies from a poorly biodegradable SWW, using rubber seed pericarp activated carbon and commercially supplied activated carbon. Djonga et al. (2021) obtained organic matter removals of 40.7% from SWW when they applied an adsorbent based on Ayous sawdust. About 64% of COD was removed from SWW by del Real-Olvera et al. (2016) using 7 g L^{-1} of powdered *Moringa oleifera* seeds. Affam (2020) observed that greater COD removals from SWW were obtained with iron oxide-coated GAC (ca. 70.7%) than with GAC alone (ca. 27.6%) at 3.5 g L^{-1} of adsorbent and pH 3-7. The modification of activated carbon by iron oxide or iron oxide nanoparticles (NPs) has also been recently investigated to remove organic matter. However, no studies on the application of iron oxide NPs incorporated in activated carbon (PAC or GAC) to remove COD from SWW were found in the literature. Lompe et al. (2017) found that the adsorption capacity of iron oxide/activated carbon nanoparticle composite to remove dissolved organic carbon (DOC) from a synthetic solution is reduced proportionally to the mass fraction of PAC in the composite due to the relatively low adsorption capacity of iron oxide NPs for DOC compared to PAC. In fact, unlike mesopores volume (which increased), a decrease in surface area and micropores volume was observed with increasing iron oxide NPs mass fraction incorporated in PAC (Lompe et al., 2017). Thus, these authors recommend the use of highly mesoporous PAC and small fractions of iron oxide NPs during the synthesis of iron oxide/activated carbon nanoparticle composite. Anyway, the incorporation of iron oxide NPs in PAC is still not very clear, as positive effects on the adsorption capacity of natural organic matter have been found in the literature (Park et al., 2015). The advantage of using iron oxide or iron oxide nanoparticles incorporated in activated carbon is the easy separation of the adsorbent from water using a magnetic field since this composite presents magnetic characteristics, simplicity, high efficiency, and low costs compared to the filtration process (Aragaw et al., 2021). Moreover, some conventional processes of adsorbent separation such as centrifugation, precipitation, filtration, and chromatography are not very economical and require labor (Ali et al., 2020).

Phytoremediation in constructed wetlands (CW) has also been applied to the SWW (Keerthana and Thivyatharsan, 2018; Soroko, 2007) and pretreated SWW (e.g., from anaerobic-aerobic SBRs (Odong et al., 2013), septic tank (Carreau et al., 2012) and biodigester (Manh et al., 2014)). High COD (61.3 to 97.4%) and BOD (52.4 to 99.9%) removals from raw/pretreated SWW using different plant species (such as *Phragmites australis* (Soroko, 2007), *Typha latifólia* (Carreau et al., 2012; Keerthana and Thivyatharsan, 2018), *Cyperus papyrus*, *Miscanthidium violaceum*, *Phragmites mauritianus*, and *Typha domingensis* (Odong et al., 2013)) has been obtained. The plant *Vetiveria zizanioides* has also been highlighted in the phytoremediation of synthetic and real effluents (Ramos-Arcos et al., 2022), although there are few reported cases of its use in the treatment of SWW. Manh et al. (2014) obtained COD and BOD removals of 60 and 59.8%, respectively, using CW planted with *Vetiveria zizanioides* to treat the biodegradable pretreated SWW from a biodigester. However, no information on the effect of some operative variables (e.g., bed depth and applied mass load), on the tuning of poorly biodegradable and alkaline pretreated SWW by CW planted with *Vetiveria zizanioides*, has been found in the literature. Although some authors, such as Madeira et al. (2021) (chapter 5) and Ramalho et al. (2022) have shown that it is possible to use CW planted with *Vetiveria zizanioides* to treat poorly biodegradable and alkaline pretreated wastewaters (e.g., explosives wastewater and landfill leachate) from IOSLM and AC integrated process, the effect of the variables mentioned has not been studied. Since the plant *Vetiveria zizanioides* tolerates wide pH ranges (3-10.5) (Danh et al., 2009), the application of alkaline effluents in CW could also be an advantage in reducing the carbonation time. Almeida et al. (2020) observed that the bed depth and applied mass load can influence the nitrogen removal from synthetic wastewater (at pH 7.5±0.2) in constructed wetlands planted with *Vetiveria zizanioides*. More information on organic matter removal under these conditions is needed.

This work aims to evaluate the tuning of poorly biodegradable and alkaline pretreated SWW from the IOSLM and AC integrated process, using two processes, adsorption, and phytoremediation, for wastewater discharge or reuse. In the adsorption process, the effect of operative variables such as time and concentration, as well as the effect of iron oxide NPs incorporation into adsorbents (PAC and GAC) and the adsorbent separation methods (filtration, magnetic, and settling) on the COD removal, were studied. For the phytoremediation process, the effect of bed depth and organic matter mass load applied

in CW planted with *Vetiveria zizanioides*, were studied, under high pH (close to the tolerance limit of the plant).

6.2. Materials and methods

6.2.1. Slaughterhouse wastewater sampling

Raw SWW was collected at the output of the rotary drum screen filter in a slaughterhouse located in Portugal. The samples were immediately transferred to the laboratory and were then pretreated by the IOSLM process at pH 12 followed by the AC process, according to Madeira et al. (2023) (chapter 3). If not immediately analyzed, the pretreated samples were stored at 4ºC until use. Parameters such as pH, conductivity, COD, soluble chemical oxygen demand (SCOD), BOD, total suspended solids (TSS), ammoniacal nitrogen, and turbidity were determined (see section 6.2.4). Table 6.1 shows the SWW characteristics pretreated by IOSLM+AC processes for the adsorption and phytoremediation tests.

Table 6.1 – Physicochemical characterization of pretreated SWW by IOSLM+AC process.

Parameters	Unit	Range
pH	Sorensen	7.89 – 11.10
Conductivity	mS cm^{-1}	579 – 3.270
COD	mg O_2 L^{-1}	385 – 507
SCOD	mg O_2 L^{-1}	372 – 498
BOD_5	mg O_2 L^{-1}	80 –90
BOD_5/COD	-	0.18 – 0.21
NH_4^+	mg N L^{-1}	8.4 – 56.4
TSS	mg L^{-1}	4 – 8
Turbidity	NTU	0.8 – 0.9

Note: COD - chemical oxygen demand; SCOD - soluble chemical oxygen demand; BOD - biological oxygen demand; TSS - total suspended solids.

6.2.2. Magnetite nanoparticles and adsorbent preparation

Magnetite NPs were obtained as described by Vargues et al. (2021). In general, ferric chloride hexahydrate was first dissolved in HCl (2 M) and then mixed with the sodium sulfite solution, under stirring for 30 minutes, until the initial color of the ferric chloride solution was reached. Then, the above mixture was added to the ammonia solution and kept under strong stirring for 30 minutes, occurring an immediate precipitation of a black solid. Subsequently, the supernatant was decanted by applying a neodymium magnet to

the black precipitate, which was washed once with HCl (0.1 M) and then several times with deionized water until reaching neutral pH. The precipitate was air-dried for 2 days and then macerated for incorporation in activated carbon.

Two commercial activated carbons, one in powdered form (SORBOPOR® MV 118/P and hereinafter referred to as PAC), and another in granular form (NORIT® GAC 830 and hereinafter referred to as GAC), were previously washed with deionized water to remove some soluble impurities. After washing, they were air-dried for 2 days and then stored in a desiccator until use.

Magnetite NPs were incorporated into PAC according to Vargues et al. (2021). For this, the magnetite NPs were sonicated in deionized water for 15 minutes. Then, the PAC was added to the sonicated NPs (in a proportion of 0.150 g of magnetite NPs per 0.500 g PAC), under agitation at 1200 rpm. After 15 minutes, the agitation was interrupted and the sedimentation was started for 10 minutes, under the action of the neodymium magnet (40x15x5 mm). Subsequently, the PAC with the magnetite NPs (called PACMAG) was washed 10 times with deionized water under the action of a neodymium magnet. Finally, the PACMAG was air-dried for 2 days and then stored in a desiccator until use. The incorporation of magnetite NPs into GAC followed the same procedure was like used for PAC, resulting in GACMAG.

6.2.3. Experimental set-up

An experimental setup for the adsorption process and phytoremediation process is shown in Figure 6.1.

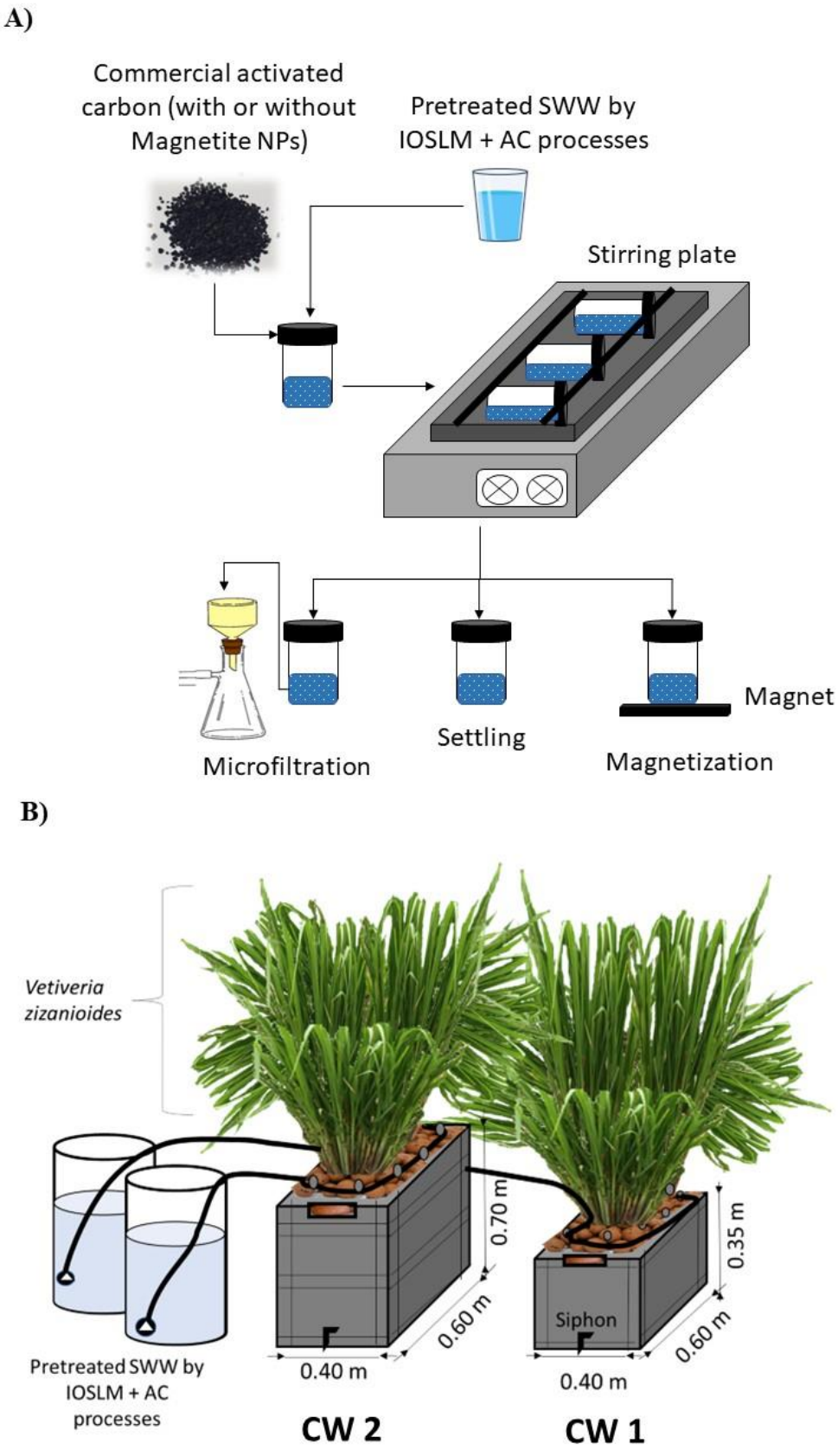

Figure 6.1 – Experimental scheme of tuning tests, using a) adsorption, and b) constructed wetlands.

6.2.3.1. Adsorption tests

Three batch adsorption assays were made (Table 6.2, Figure 6.1a). The type of adsorbent, dosage, time, and separation method were tested (Table 6.2). In general, in the adsorption assays, about 5 mL of pretreated SWW by IOSLM+AC process (Table 6.1) were placed in a sample vial with a predetermined dose of the adsorbent (PAC, PACMAG, GAC, or GACMAG), and then the mixture was shaken in an orbital shaker (Edmund Bühler KS-15) at 250 rpm and room temperature. After the defined contact time, the adsorbents were separated from the effluent using one of the separation methods (Table 6.2). In the first and second experiments (trials A and B, Table 6.2) adsorption equilibrium isotherms (dosage at 10 to 100 g/L) and adsorption kinetics (0 to 60 min. for PAC and PACMAG and 0 to 300 min for GAC and GACMAG) were made. Then, the samples were filtered by dead-end microfiltration (using Whatman^{TM} membrane filters with a 0.45 μm pore size) and analyzed for COD. Finally, in the third experiment (trial C, Table 6.2), the adsorbents (PAC, GAC, PACMAG, and GACMAG) were applied to treat 5 mL of pretreated SWW, in an orbital shaker, using the best adsorption operating conditions (dose and contact time) from first and second experiments. After adsorption, different effluent separation methods were individually applied, namely: gravitational sedimentation, magnetic separation using neodymium magnet (40 x 15 x 5 mm), and dead-end microfiltration. During the sedimentation and magnetic step, the effluent samples were collected over time and analyzed for COD and turbidity.

Table 6.2 – Operating conditions applied to the adsorption process.

	Operating conditions						Physical-chemical characteristics of pretreated SWW			
Trials	**Type of Adsorbent**	**Dosage** ($g\ L^{-1}$)	**Time** (h)	**Stirring speed** (rpm)	**Temp.** (ºC)	**Separation method**	**pH**	**COD** ($mg\ L^{-1}$)	**Turbidity** (NTU)	**NH_4^+** ($mg\ N\ L^{-1}$)
A	PAC, PACMAG, GAC, and GACMAG	10 to 100	13	250	17.6±0.1	Filtration	7.91±0.02	458±5	-	-
B	PAC, PACMAG, GAC, and GACMAG	60[a] and 70[b]	0-5[a] and 0-1[b]	250	17.6±0.1	Filtration	7.91±0.02	458±5	-	-
C	PAC, PACMAG, GAC and GACMAG	60[a] and 70[b]	0.083[b] and 1[a]	250	18.9±1.1	Filtration / settling (0-60 min.) / magnetic separation (0-60 min.)	8.02±0.01	467±9	0.9±0.1	8.9±0.7

Note: a) for GAC and GACMAG; b) for PAC and PACMAG.

6.2.3.2. Phytoremediation tests

Two pilot-scale CWs planted with *Vetiveria zizanioides* (>120 plants m^{-2}) in light-expanded clay aggregates (Leca®NR 10/20) were used in the phytoremediation tests (Figure 6.1b). Both beds had a surface area of 0.24 m^2 (0.40x0.60 m) but different bed heights, 0.35 m for CW1 and 0.70 m for CW2. The effect of bed height and COD and ammonium nitrogen (NH_4^+) applied mass load on COD and NH_4^+ removal efficiency was evaluated. The tests took place between February and April, and according to the operating conditions applied to the beds shown in Table 6.3. Both beds were fed in vertical flow, continuous mode, and constant applied hydraulic load around 80 L m^{-2} d^{-1}, using submersible pumps and a network of equidistant sprinklers. Hydraulic retention times were 3.6±0.5 and 7.1±0.9 h, for CW1 and CW2, respectively. Air and soil temperatures varied on average from 16 to 23 ºC and from 13 to 18 ºC, respectively (Table 6.3). To achieve COD mass loads of 3.2 to 9.5 g m^{-2} d^{-1} (trials A and B, Table 6.3), the pretreated SWW by IOSLM+AC process (Table 6.1) was diluted with tap water and only then fed to both beds. To evaluate the high COD loadings and the importance of SWW pretreatment by the IOSLM+AC process, both CWs were fed with raw SWW (pH 7.85±0.45, conductivity 3.1±0.3 mS cm^{-1}, COD 2648±329 mg O_2 L^{-1}, and NH_4^+ 48±7 mg N-NH_4^+ L^{-1}, see Table 6.3, trials C). Daily, at 10:00 am, wastewater samples were collected at the inlet and outlet of the bed, and the flow rates were measured. The samples were immediately characterized in terms of pH, redox potential, electrical conductivity, and dissolved oxygen (DO). For NH_4^+ and COD, when it was not possible to measure immediately, the samples were refrigerated at 4ºC until further analysis. Signs of *Vetiveria zizanioides* toxicity were evaluated weekly by visual inspection. Plant growth and biomass composition (for calcium, magnesium, sodium, potassium, total Kjeldahl nitrogen, and phosphorus) were evaluated at the beginning and end of the phytoremediation test. For this, twenty plants were randomly selected from each CW. In periods of rain, the beds were covered with thin transparent plastic.

Table 6.3 – Operating conditions applied to CW1 and CW2.

Type of CW	Trials	Parameters						
		pH	COD ($g\ m^{-2}\ d^{-1}$)	NH_4^+-N load ($g\ m^{-2}\ d^{-1}$)	Hydraulic load ($L\ m^{-2}\ d^{-1}$)	HRT (h)	Air temp. (ºC)	Soil temp. (ºC)
CW1	A1	9.48±0.77	4.1±0.5	0.3±0.1	81±10	3.6±0.5	16±1	13±1
	B1	10.25±1.03	9.5±2.2	0.5±0.05			21±3	16±3
	C1	7.85±0.45	211.8±26.4	3.9±0.5			23±5	18±2
CW2	A2	9.48±0.77	3.2±1.1	0.3±0.1	80±10	7.1±0.9	16±1	13±1
	B2	10.25±1.03	9.4±2.5	0.5±0.06			21±3	16±3
	C2	7.85±0.45	211.8±26.4	3.9±0.5			23±5	18±2

Note: Mean ± Standard Deviation, calculated for a 95% confidence level; number of determinations (n≥10).

6.2.4. Analytical methods

The wastewater samples were analyzed according to the standard methods of analysis (Baird et al., 2017). pH was measured by the potentiometric method using a WTW pocket pH meter kit (model pH 340). Conductivity was determined by the electrometric method using a Crison GLP32 conductimeter. COD and soluble COD (SCOD) were determined by closed reflux colorimetric method using MACHEREY-NAGEL Thermoblock NANOCOLOR VARIO C2, Thermo scientific Genesys 10S UV-VIS spectrophotometer, and Whatman™ membrane filters with a 0.45 μm pore size for soluble COD. BOD_5 was determined by the respirometric method using the WTP OxiTop® IS 12 system. NH_4^+ was obtained by distillation method using BUCHI B-316 distillation unit. TSS were quantified by the gravimetric method using glass microfiber filters (VWR) with a pore size of 1.0 μm and a diameter of 47 mm. Turbidity was determined by the nephelometric method or estimated by absorption of light at 750 nm. Redox potential was measured by the potentiometric method using WTW Inolab apparatus and WTW SenTix ORP electrode. Dissolved oxygen was quantified by modifications of the Winkler method.

The physicochemical characteristics of the *Vetiveria zizanioides* leaves were quantified according to Tabatabai (1998). First, the leaves were cut into small pieces and placed in an oven (Memmert UL40 Oven) at 70°C for 48 hours for the determination of the dry matter by the gravimetric method. Subsequently, the samples were placed in a muffle furnace at 550°C for 4 hours. The ash obtained was dissolved with hydrochloric acid (3 M), followed by filtration with a Whatman™ 1001 filter, and then diluted with deionized water (for calcium, magnesium, total phosphorus, sodium, and potassium determination). Calcium and magnesium were determined by the flame atomic absorption spectrometry

method using Varian SpectrAA 220FS equipment. Sodium and potassium were quantified by the flame photometric method using the Corning Model 410 Flame Photometer. Phosphorus was determined by the colorimetric method using muffle P SELECTA-HORN 186331 and UV/Vis spectrophotometer Pharmacia Biotech Ultrospec 2000. TKN was analyzed by the Kjeldahl method using Bloc Digest 6 P-Selecta digester and BUCHI B-316 distillation unit.

The activated carbon materials were characterized by their morphology, texture, surface chemistry, and physicochemical properties. Morphology was analyzed by scanning electron microscopy (SEM, FEI Quanta 200), using Everhart–Thornley detector. For the visualization of particles present in activated carbon, the samples were analyzed by SEM, using the solid-state detector. The texture was assessed by N_2 adsorption at -196 °C in an Automatic apparatus Micromeritics ASAP 2010. Before data acquisition, ≈75 mg of the materials were outgassed overnight at 120 °C. The apparent surface area, A_{BET}, was estimated through the Brunauer-Emmett-Teller (BET) method following the recommended practices for microporous solids (ISO9277, 2010; Rouquerol et al., 2006; Thommes et al., 2015). The total pore volume, V_{total}, was determined through the Gurvich rule at p/p^0 =0.975) (Rouquerol et al., 2013), and the micropore volume, V_{micro}, was assessed by applying the α_s method taking as reference the isotherm reported by Rodriguez-Reinoso et al. (1987), and the mesopore volume, V_{meso}, was obtained from the difference between the total pore volume, V_{total}, and the micropore volume, V_{micro}. The reverse mass titration method (Noh and Schwarz, 1989) was used to determine the pH at the point of zero charge (pH_{PZC}). Briefly, the measurements were made with ≈100 mg of previously dried material with decarbonized deionized water following the methodology described by Mestre et al. (2009) and the pH was assessed with a Symphony SP70P pH meter. The moisture content was assessed following the oven drying method (ASTM D2867-04). Each sample was dried at 110 °C in a ventilated oven (Heraeus Instrument) until constant weight. The ash content was determined according to ASTM D2866-99 with correction for the moisture content (Mestre et al., 2022). Briefly, the samples were heated at 815 °C in air (Select-Horn from Selecta, Omron E5Cx controller), until constant mass. The particle size distribution of the powdered and granular materials was assessed by dry sieving considering the percentage of weight collected in sieves with dimensions between 850 and 20 μm and assuring a total weight loss lower than 10% to guarantee a valid distribution (AWWA, 1996; CEFIC, 1986). The apparent density of the powdered

activated carbon materials was determined by the tapping method using a graduated cylinder according to the procedure described by Viegas et al. (2020). For granular materials, the sample was added to the graduated cylinder by a vibratory feeder and the cylinder was selected assuring its inner diameter was at least 10 times the mean particle diameter (ASTM2854-2000).

6.2.5. Statistical analysis

Results were presented as means ± standard deviation, using n=3 for the adsorption tests and n≥10 for the phytoremediation tests. All samples were analyzed in triplicate. IBM SPSS Statistics for Windows was used for statistical purposes. One-way ANOVA with Tukey's test at a 95% confidence level was used for comparison between averages. Two-Way ANOVA with Least Significance Difference (LSD) test at a 95% confidence level, was used for the analysis of variance with two factors. Graphs were created using GraphPad Prism for Windows (version 8.0.1, GraphPad Software, Inc.).

In the adsorption tests, different non-linear equations relative to the isotherm adsorption and kinetic adsorption were used to find the best one that portrays the experiments. For that, the sum of squared residuals was minimized using Microsoft Excel Solver and the generalized reduced gradient nonlinear solving method. Langmuir, Freundlich, Redlich-Peterson, Two-site Langmuir, Generalized Freundlich, Langmuir-Freundlich, Toth, Temkin, and BET were the adsorption isotherms used (Table 6.4). On the other hand, Pseudo-first order, Pseudo-second order, Pseudo-order n (n≠1), Weber and Morris intra-particle diffusion, Elovich, and Bangham were the adsorption kinetics models used (Table 6.5). For all adsorption isotherms and adsorption kinetics, the average absolute relative deviation percent (AARD) (Eq. 1), the root-mean-square error (E) (Eq. 2), and the coefficient of determination (R^2) (Eq. 3) were calculated. The adsorption capacity of absorbate (q) and the percentage of removal of the absorbate (%R) were determined according to Eqs. 4 and 5, respectively.

Table 6.4 – Equations used in adsorption isotherms.

Isotherm model	Equations	
Langmuir	$q_e = q_m \frac{K_a C_e}{1 + K_a C_e}$	
Freundlich	$q_e = K_F C_e^{1/n}$	1/n < 1
Redlich-Peterson	$q_e = q_m \frac{K_a C_e}{1 + (K_a C_e)^n}$	n > 0
Two-site Langmuir	$q_e = q_{m,1} \frac{K_{a,1} C_e}{1 + K_{a,1} C_e} + q_{m,2} \frac{K_{a,2} C_e}{1 + K_{a,2} C_e}$	
Generalized Freundlich	$q_e = q_m \left(\frac{K_a C_e}{1 + K_a C_e} \right)^n$	0 < n < 1
Langmuir-Freundlich	$q_e = q_m \frac{K_a C_e{}^n}{1 + K_a C_e{}^n}$	0 < n < 1
Toth	$q_e = q_m \frac{K_T C_e}{(1 + (K_T C_e)^n)^{1/n}}$	0 < n < 1
Temkin	$q_e = \frac{RT}{b_T} \ln(K_T C_e)$	
BET	$q_e = q_m \frac{K_a C_e}{(1 - K_L C_e)(1 - K_L C_e + K_a C_e)}$	n = 1

Note: C_e - Concentration of adsorbate in solution at equilibrium (mg L^{-1}); q_e – the amount of substance adsorbed per mass of adsorbent at equilibrium (mg g^{-1}); K_a – Langmuir model isotherm constant (L mg^{-1}); q_m – maximum adsorption capacity (mg g^{-1}); K_F – Freundlich model isotherm constant ($mg^{1-1/n}$ $L^{1/n}$ g^{-1}); n – heterogeneity factor; K_T – Toch or Temkin model isotherm constant (L mg^{-1}); b_T - Temkin constant (J mol^{-1}); R - universal gas constant (8.314 J/mole k); T – absolute temperature (K); K_L - Equilibrium constant of adsorption for upper layers in BET isotherm (L mg^{-1}).

Table 6.5 – Equations used in adsorption kinetics.

Kinetic model	Equations
Pseudo-first order	$q_t = q_e (1 - e^{-k_1 t})$
Pseudo-second order	$q_t = \frac{k_2 q_e^2 t}{1 + k_2 q_e t}$
Pseudo-order n (n≠1)	$q_t = q_e - q_e \left(1 + k_2 (n-1) q_e^{(n-1)} t\right)^{1/(1-n)}$
Intra-particle diffusion (Weber and Morris)	$q_t = k_{ip} t^{1/2} + C_i$
Elovich	$q_t = \frac{1}{\beta} \ln(1 + \alpha\beta t)$
Bangham	$q_t = k t^{v}$

Note: q_e - the amount of substance adsorbed per mass of adsorbent at equilibrium (mg g^{-1}); q_t - the amount of substance adsorbed per mass of adsorbent at time t (mg g^{-1}); t - time (min); k_1 - rate constant of the pseudo-first-order kinetics (min^{-1}); k_2 - rate constant of the pseudo-second-order kinetics or pseudo-order n kinetics (g mg^{-1} min^{-1}); n - order of reaction to the adsorbent in the pseudo order n model; k_{ip} - intra-particle rate constant (mg g^{-1} $min^{-1/2}$); C_i – intercept to the y axis (mg g^{-1}); α – Elovich constant (mg g^{-1} min^{-1}); β – Elovich exponent (g mg^{-1}); v – parameter in the Bangham model; k – Bangham constant (mg g^{-1} min^{-v}).

$$AARD = \frac{1}{N} \sum_{i=1}^{N} \left(\left| \frac{q_{e.i} - q_{cal.i}}{q_{e.i}} \right| \right) \times 100 \quad (1)$$

$$E = \sqrt{\frac{\sum_{i=1}^{N} (q_{cal.i} - q_{e.i})^2}{N}} \quad (2)$$

$$R^2 = 1 - \frac{\sum_{i=1}^{N} (q_{e.i} - q_{cal.i})^2}{\sum_{i=1}^{N} (q_{e.i} - q_{mean})^2} \quad (3)$$

$$q = \frac{(C_0 - C)}{m} \times V \quad (4)$$

$$\%R = \frac{(C_0 - C)}{C_0} \times 100 \quad (5)$$

where: $q_{e.i}$ and $q_{cal.i}$ are the adsorption capacity of the absorbate obtained by the experimental method and by calculation, respectively; N is the number of experiments; q_{mean} is the average of the $q_{e.}$ values; C_0 and C are the initial and the final concentrations of absorbate (mg L^{-1}), respectively; m is the adsorbent mass (g), and V is the solution volume (L).

In phytoremediation tests, the removal efficiency of each parameter (η) (%) and the hydraulic retention time (HRT) (d) were determined according to equations 6 and 7, respectively.

$$\eta = \frac{(H_{Li} \times C_i - H_{Le} \times C_e)}{H_{Li} \times C_i} \times 100 \quad (6)$$

$$HRT = \frac{V}{Q_i} = \frac{A \times y \times p}{Q_i} \quad (7)$$

where: H_{Li} and H_{Le} are the hydraulic loads at the inlet and outlet of the bed (L m^{-2} d^{-1}), respectively; C_i and C_e are the concentrations of a parameter at the inlet and outlet of the bed (mg L^{-1}), respectively; V is the volume of the bed (m^3); Q_i is the influent flow rate (L d^{-1}); A is the surface area of the bed (m^2); y is the depth of the bed (m); p is the porosity of the bed.

6.3. Results and discussion

6.3.1 Characterization of pretreated SWW

The pretreated SWW shows a wide range of pH (7.89 to 11.10), conductivity (579 to 3270 mS cm^{-1}), and ammonium nitrogen (8.4 to 56.4 mg N L^{-1}) (Table 6.1). These values are due to sampling at different stages in the atmospheric carbonation process, in which high and low values were associated with the beginning and end of atmospheric carbonation,

respectively (Madeira et al., 2023 (chapter 3)). The pretreated SWW still has some organic matter (385 to 507 mg O_2 L^{-1} for COD and 80 to 90 mg O_2 L^{-1} for BOD_5) that was not removed by the IOSLM+AC process (Table 6.1). Most of the organic matter is soluble (SCOD at 372 to 498 mg O_2 L^{-1}, Table 6.1). SWW is a low biodegradable wastewater as it has a BOD_5/COD ratio of 0.18 to 0.21 (Table 6.1), so it would not be possible to be treated by conventional biological treatment processes. Low biodegradable wastewater from the slaughterhouse has also been found in the literature, with BOD_5/COD ratios of 0.30 (Affam, 2020), 0.09, and 0.14 (Agarry and Owabor, 2012), for example. Some SWWs may present low biodegradability due to cleaning activities at the facilities, as mentioned by Ng et al. (2022). In this case, the biodegradability of wastewater was reduced by the IOSLM+AC process (Madeira et al., 2023 (chapter 3), 2020 (chapter 2)). Low values of TSS (4 to 8 mg L^{-1}) and turbidity (0.8 to 0.9 NTU) were observed (Table 6.1).

6.3.2. Adsorption

6.3.2.1. Characterization of adsorbents

Figure 6.2 shows the morphology of PAC, PACMAG, GAC, and GACMAG obtained by scanning electron microscope (SEM), at different magnifications. According to Figure 6.2, PAC and PACMAG present irregular laminar structures. GAC and GACMAG have very rough surfaces and irregular cavities of different shapes. Compared to PAC and GAC, the SEM image of PACMAG (Figures 6.2d, 6.2e, and 6.2f) and GACMAG (Figures 6.2j, 6.2k, and 6.2l) show several clusters of bright particles of different dimensions. These clusters appear to be more evenly distributed over the activated carbon on GACMAG (Figures 6.2j, 6.2k, and 6.2l) than on PACMAG (Figures 6.2d, 6.2e, and 6.2f). It is expected that these clusters of bright particles are clusters of iron oxide NPs that have been incorporated into the surface of the activated carbon. It is not expected that these agglomerates of particles are activated carbon particles since they were still detected by the solid-state detector, which would not be possible if it was activated carbon (Figure 6.3).

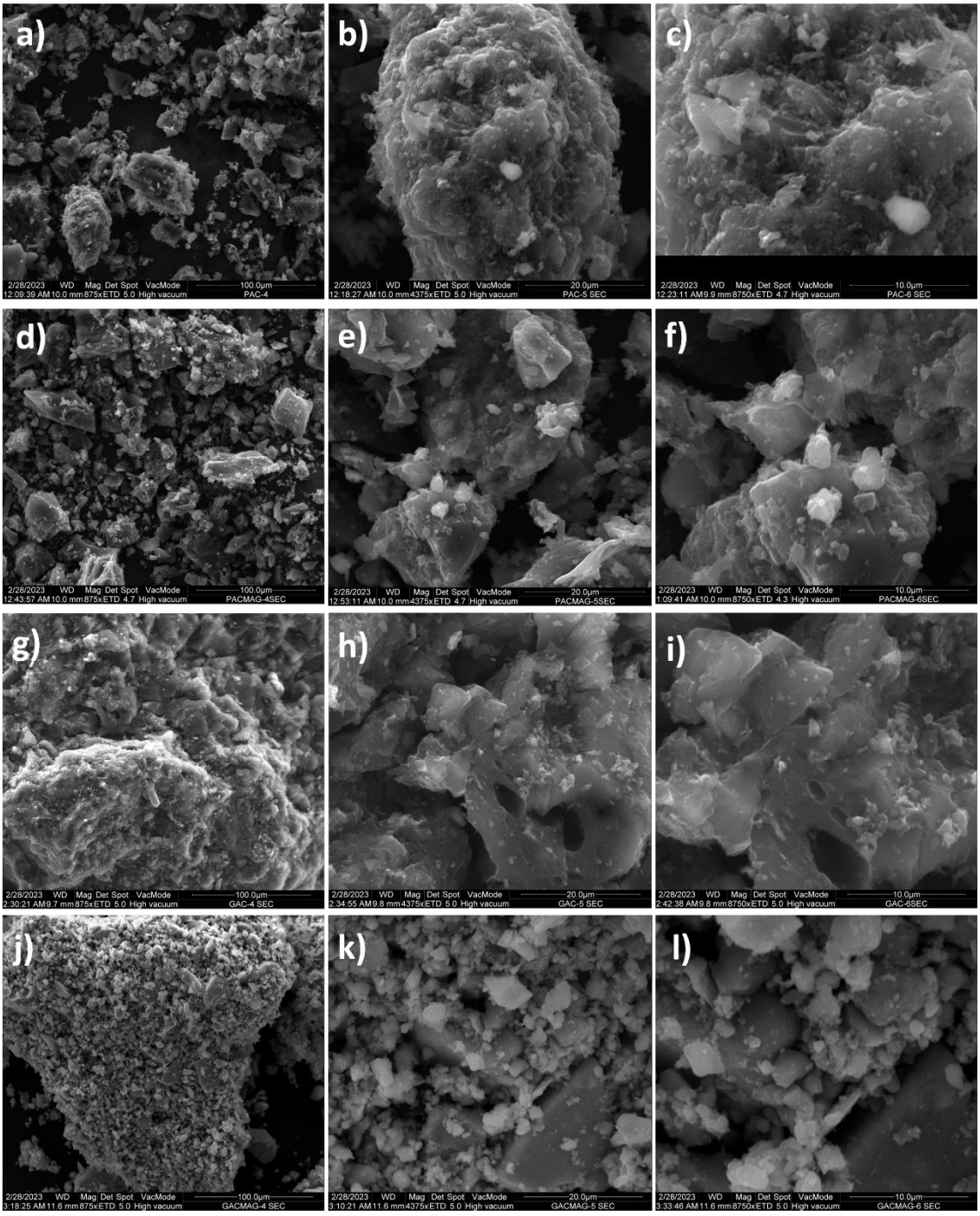

Figure 6.2 - SEM images of PAC (a, b, and c), PACMAG (d, e, and f), GAC (g, h, and i), and GACMAG (j, k, and l), at different magnifications (875X, 4375X, and 8750X), using the Everhart–Thornley detector.

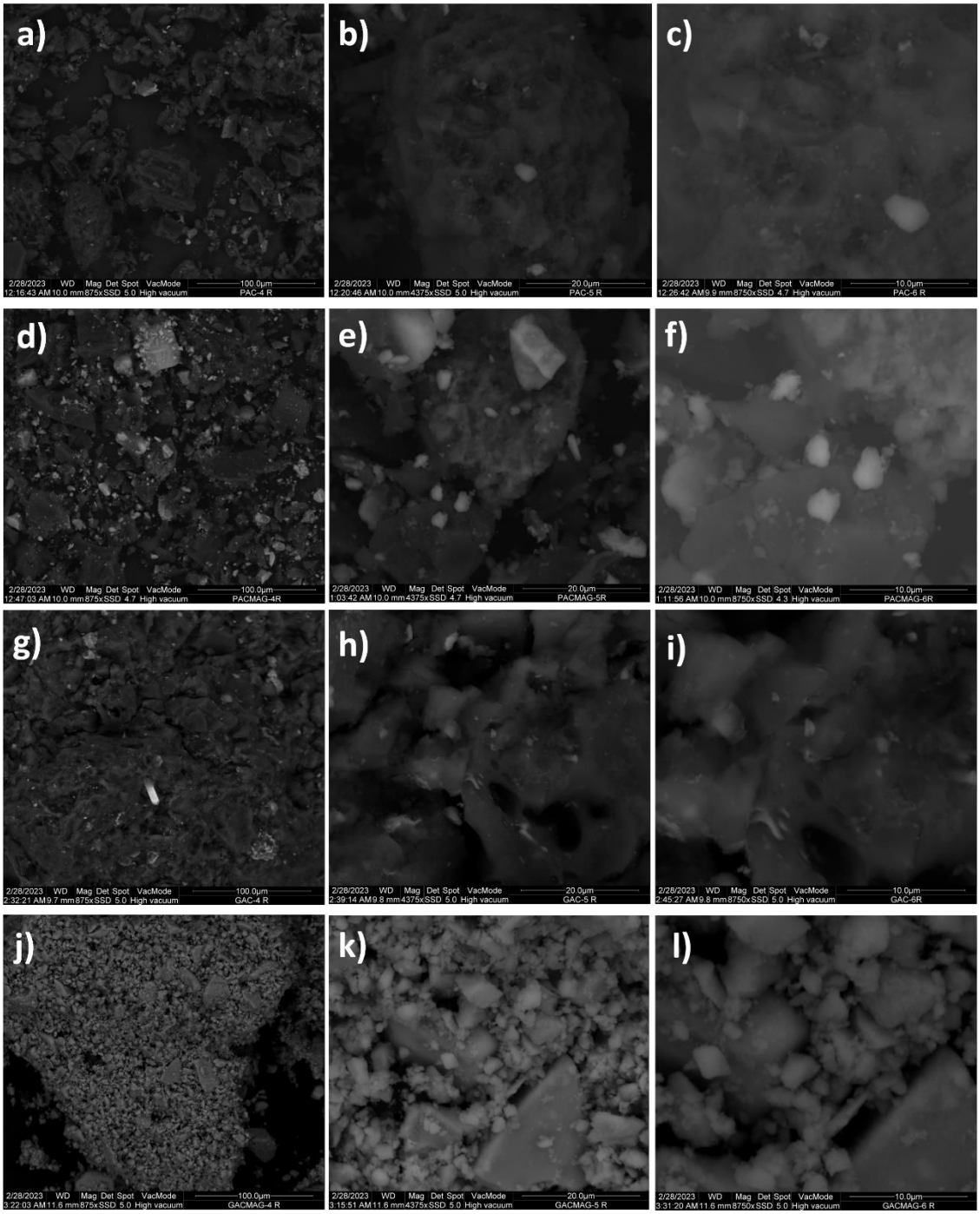

Figure 6.3 - SEM images of PAC (a, b, and c), PACMAG (d, e, f), GAC (g, h, i), and GACMAG (j, k, and l), at different magnifications (875X, 4375X, and 8750X), using the solid-state detector.

Table 6.6 gathers the A_{BET}, V_{total}, V_{meso}, V_{micro}, pH_{PZC}, moisture content, total ash content, and apparent density values, for the adsorbents used in this work.

Table 6.6 – Textural parameters, pH at the point of zero charge, moisture, and ash content for the listed activated carbon materials.

	A_{BET} ($m^2\ g^{-1}$)	V_{total}[a] ($cm^3\ g^{-1}$)	V_{meso}[b] ($cm^3\ g^{-1}$)	V_{micro}[c] ($cm^3\ g^{-1}$)	pH_{PZC}	Moisture (%)	Ash (%)	Apparent density ($kg\ m^{-3}$)
PAC	650	0.39	0.14	0.25	8.1	7.3	13.2	560
PACMAG	548	0.36	0.18	0.18	7.3	6.0	35.0	639
GAC	906	0.50	0.18	0.32	6.8	12.7	8.0	491
GACMAG	655	0.43	0.22	0.21	6.3	6.9	31.1	580

Note:
[a] V_{total} evaluated at $p/p^0 = 0.975$ in the N_2 adsorption isotherms at − 196 °C
[b] V_{meso} – mesopore volume (2 < width < 50 nm), given by $V_{total} - V_{micro}$
[c] V_{micro} – total micropore volume (width < 2 nm)

From the N_2 adsorption isotherm (Figure 6.4) it is possible to verify that the incorporation of the magnetic NPs reflects in the decrease of the adsorption capacity, more pronounced for the GAC material. GAC presents higher apparent surface area and pore volumes than PAC (Table 6.6).

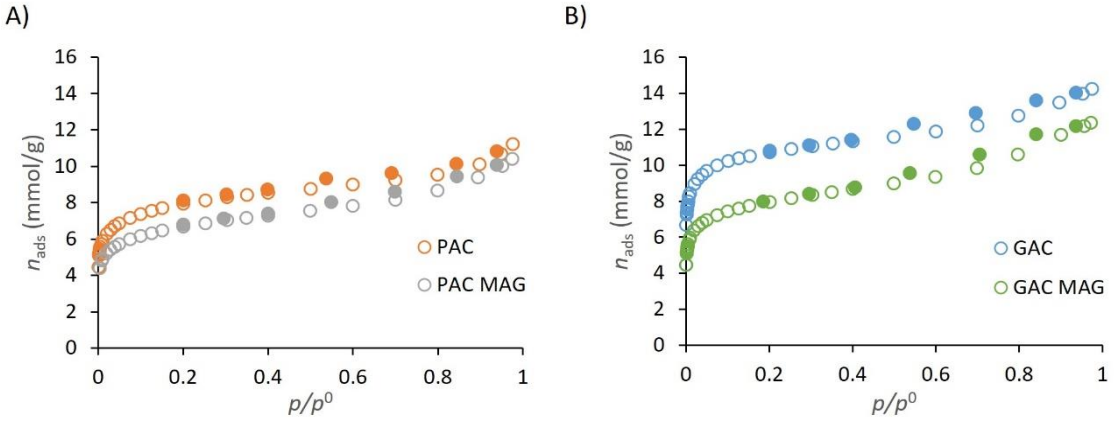

Figure 6.4 - N_2 adsorption isotherms at -196 °C for a) PAC and PACMAG, and b) GAC and GACMAG. Empty and full symbols correspond, respectively, to adsorption and desorption data.

In line with the analysis of the isotherms, the apparent surface area decreased from 650 to 548 $m^2\ g^{-1}$ and from 906 to 655 $m^2\ g^{-1}$ with the incorporation of iron oxide NPs in PAC and GAC, respectively. The same behavior was observed for the total pore volume. The values corroborate that in terms of percentage reduction in surface area or pore volume, these were greater for the incorporation of iron oxide NPs in GAC than for PAC. The reduction of the textural parameters after magnetization of the activated carbon materials results from a mass effect (the NPs are heavy particles and are less porous than the

activated carbons) and possibly also some pore blocking (deposition of iron oxide NPs in the entrance of the activated carbon nanopores). However, the incorporation of iron oxide NPs in activated carbon contributed to the increase in the mesopores volumes (Table 6.6), which was also observed in literature studies (Labuto et al., 2022; Lompe et al., 2017). The work by Labuto et al. (2022) reports the mesoporous nature of the magnetic NPs and the consequent increase of the mesopore volume of the PAC after magnetization. Lompe et al. (2017) observe the increase of the mesopore volume with the increase of the Fe_2O_3 mass fraction incorporated in PAC. For PACMAG or GACMAG, the volume of mesopores and micropores was similar while the PAC and GAC have a higher volume of micropores in line with their higher surface areas compared to the magnetic counterparts. The apparent surface areas and total pore volumes obtained for PACMAG or GACMAG in this work were slightly higher than the values that have been reported in the literature. For example, Shahrashoub and Bakhtiari (2021) obtained an apparent surface area of 406 and 587 $m^2\ g^{-1}$, and total pore volumes of 0.34 and 0.29 $cm^3\ g^{-1}$ for magnetite/PAC and GAC composites, respectively. Regarding the pH_{PZC} of the adsorbents, it was observed that these values were slightly acidic for the granular materials (*i.e.*, pH 6.8 for GAC and pH 6.3 for GACMAG) and slightly basic for the powdered counterparts (*i.e.*, pH 8.1 for PAC and pH 7.3 for PACMAG). Since the pH values of the effluent to be treated are above the mentioned pH_{PZC} values the surface will be negatively charged and thus more prone to the adsorption of cationic compounds. On the other hand, for effluent pH values below pH_{PZC} the adsorbent surface will be positively charged favoring the adsorption of anionic compounds. In both activated carbons the incorporation of iron oxide NPs nanoparticles in activated carbon also contributed to a slight decrease in pH_{PZC} effect not always observed in the literature (Labuto et al., 2022). Regarding the particle size distribution for the adsorbents used, higher percentages of weight were observed in the range of 53 to 74 μm for PAC (Figure 6.5) (corresponding to 42.4%) and in the range of 20 to 36 μm for PACMAG (Figure 6.5) (corresponding to 34.0%). For GAC and GACMAG (Figure 6.6) the highest weight percentage occurred for particle sizes >850 μm (corresponding to 91.9 and 74.5% for GAC and GACMAG, respectively). The incorporation of iron oxide NPs in activated carbon contributed to the increase in the weight percentage of particles with smaller particle sizes (Figures 6.5 and 6.6).

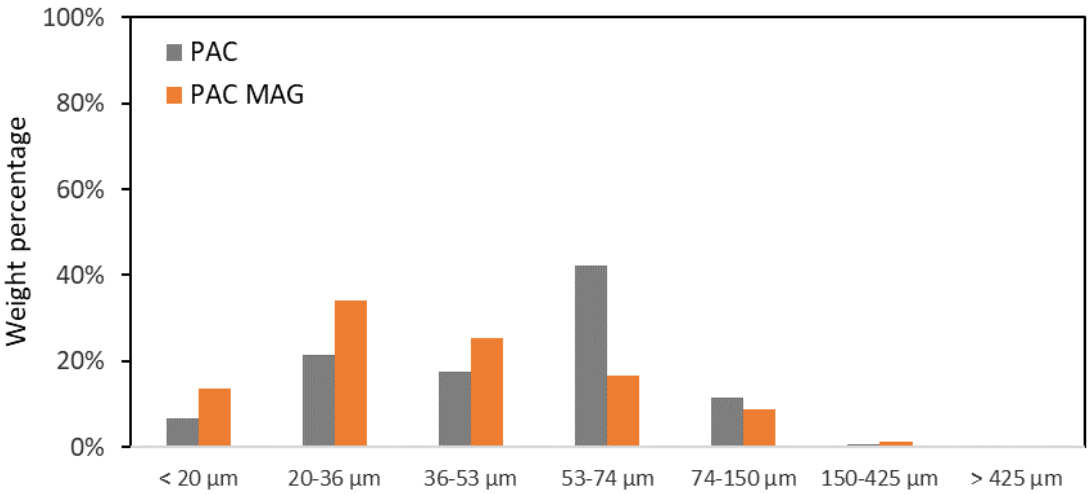

Figure 6.5 - Particle size distribution of PAC and PACMAG.

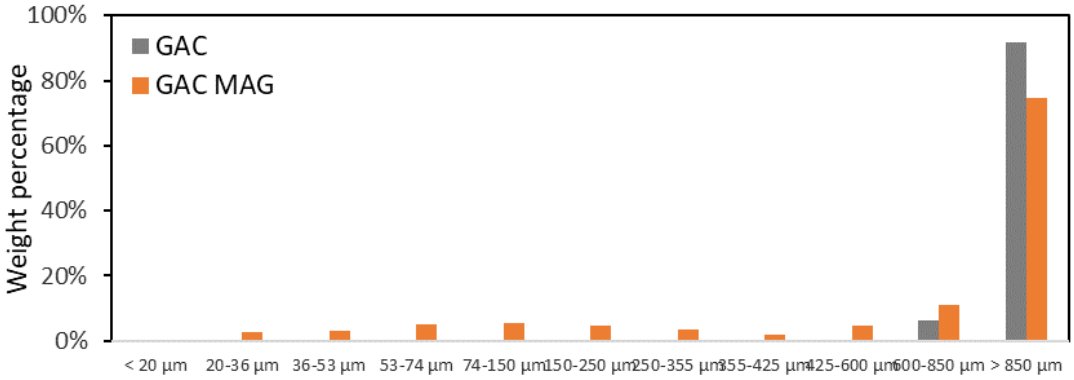

Figure 6.6 - Particle size distribution of GAC and GACMAG.

6.3.2.2. Effect of adsorbent concentration on COD removal and adsorption isothermal models

The influence of PAC, PACMAG, GAC, and GACMAG dosages on COD removal was studied (Figure 6.7). COD removals increased with the increase in the applied adsorbent dose, with COD removals varying between 38.6 and 59.7% for PAC (Figure 6.7a), 39.3 and 61.9% for PACMAG (Figure 6.7a), 59.0 and 83.0% for GAC (Figure 6.7b), and 57.5 and 80.1% for GACMAG (Figure 6.7b), in the dosage range of adsorbents studied. GAC and GACMAG were more efficient than PAC and PACMAG in removing COD.

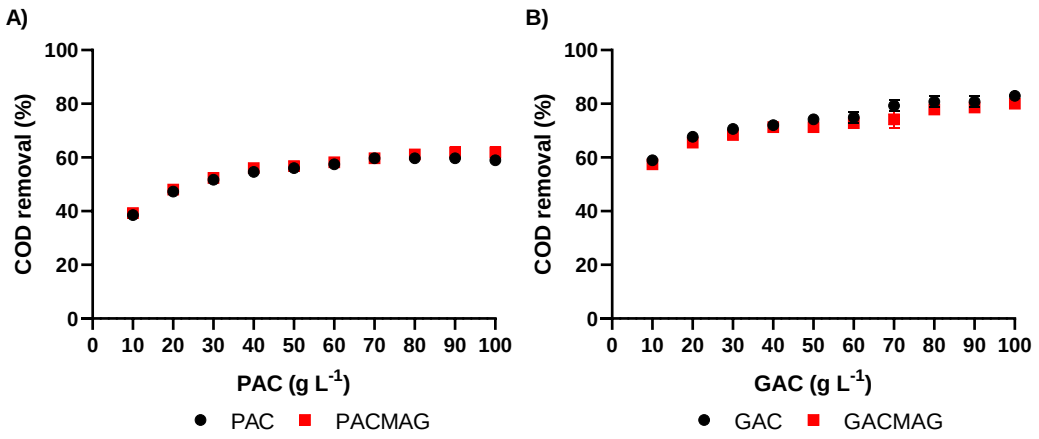

Figure 6.7 – Effect of adsorbent dosage on the COD removal using a) PAC and PACMAG, and b) GAC and GACMAG (mixing time = 13 h, stirring speed = 250 rpm, temperature = 17.6±0.1 ºC, adsorbent dosage = 10–100 g L^{-1}, COD = 458±5 mg O_2 L^{-1}, pH = 7.91±0.02).

For PAC and PACMAG above the dosage of 70 g L^{-1} added, there was no significant change in the removal of COD. These results show that there is some organic matter that cannot be adsorbed by PAC and PACMAG. These differences in COD adsorption efficiency between PAC and GAC or between PACMAG and GACMAG may be due to the nature of the adsorbent (e.g., surface area, porosity, and pore size) and to the polarity and charge of the organic compounds (Lawtae and Tangsathitkulchai, 2021). In fact, GAC/GACMAG showed higher apparent surface area and total pore volume than PAC/PACMAG (Table 6.6). High values of apparent surface area and the presence of mesopores pores indicate a good potential for the removal of pollutants by adsorption (Vinayagam et al., 2022). As can be observed in Figure 6.7a, the COD removal with or without incorporation of iron oxide NPs in PAC was similar. However, for GACMAG (Figure 6.7b) a slight decrease (not significant, $p<0.05$) in COD removal was observed when compared to GAC most probably because there was a greater reduction in the apparent surface area and volume of pores with the incorporation of iron oxide NPs in the GAC than in the PAC (Table 6.6).

Considering the COD requirements for discharge (COD < 125 mg L^{-1}) and/or the maximum COD adsorption using the minimum adsorbent dosage, the doses 70 g L^{-1} for PACMAG and 60 g L^{-1} for GACMAG were chosen for the next experiments. Although under these dosages, the BOD values obtained, 115±7 mg O_2 L^{-1} and 90±0 mg O_2 L^{-1} for PAC and GAC, respectively, are above the allowed value for discharge (25 mg O_2 L^{-1}).

In this way, for comparison purposes, PAC and GAC were used under the same doses of PACMAG and GACMAG. Using these doses, COD removals were 59.7±1.0%, 59.7±1.0%, 75.0±2.1%, and 72.8±1.0%, respectively, for PAC, PACMAG, GAC, and GACMAG. Thus, considering that the pairs of adsorbents (i.e., PAC/PACMAG and GAC/GACMAG) were applied at the same dosage, these results show that the COD adsorption capacity by PACMAG or GACMAC was not influenced by the 23% substitution of activated carbon weight (PAC or GAC) by iron oxide NPs, despite the reduction in apparent surface area and total pore volume with the incorporation of NPs (Table 6.6). Therefore, this seems to point out that there was a synergistic effect between activated carbon (PAC or GAC) and the incorporated iron oxide NPs. Incidentally, an isolated experiment (results not yet disclosed) resulted in a COD removal of 41.2% of pretreated SWW by IOSLM+AC process (COD = 458±5 mg O_2 L^{-1}), applying a dose of 60 g L^{-1} of iron oxide NPs and contact time of 1 h. Jain et al. (2018) refer that iron oxide NPs can be a great adsorbent. The synergistic effect between activated carbon (PAC or GAC) and iron oxide NPs has been observed by some authors but there are also reports stating lower performance for the magnetic activated carbons. Affam (2020) evaluated the COD removal from SWW by the adsorption process, using GAC and iron oxide-coated GAC at 3.5 g L^{-1}. The author observed that greater COD removals were obtained for iron oxide-coated GAC (ca. 70.7%) than for GAC (ca. 27.6%). Regarding PACMAG, Vargues et al. (2021) observed that the adsorption capacity of ibuprofen by PACMAG was not compromised with the incorporation of iron oxide NPs into PAC. However, for amoxicillin, these authors observed a slight decrease in the performance of PACMAG in relation to PAC, indicating that the iron oxide NPs were distributed in macro and mesopores of the adsorbent, making it difficult for the large molecules (such as amoxicillin) to access some available active adsorption sites. Labuto et al. (2022) also verified a decrease in the adsorption capacity of a PACMAG compared with the parent PAC being more pronounced for ibuprofen (negatively charged specie) than for caffeine a neutral specie. The authors propose the lower adsorption capacity of PACMAG to ibuprofen is due to the dominant mass effect of the NPs while for caffeine, smaller than ibuprofen, the more efficient packing in the micropore structure allows overcoming the mass effect. Kim et al. (2013) also observed that PACMAG provided a lower removal of natural organic matter compared to PAC, derived from the reduction of micropore volume and surface area. On the other hand, Lompe et al. (2017) state that a decrease in the removal of adsorbates with the incorporation of iron oxide NPs in PAC is not expected if

small fractions of iron oxide NPs are used during the synthesis of iron oxide/activated carbon nanoparticle composite, or if PAC is highly mesoporous.

A set of isothermal models (Table 6.4) was studied to find the model that best fits the experimental data. Figures 6.8a and 6.8b show the amount of COD adsorbed by PAC and PACMAG, and GAC and GACMAG, respectively, as a function of the final COD concentration.

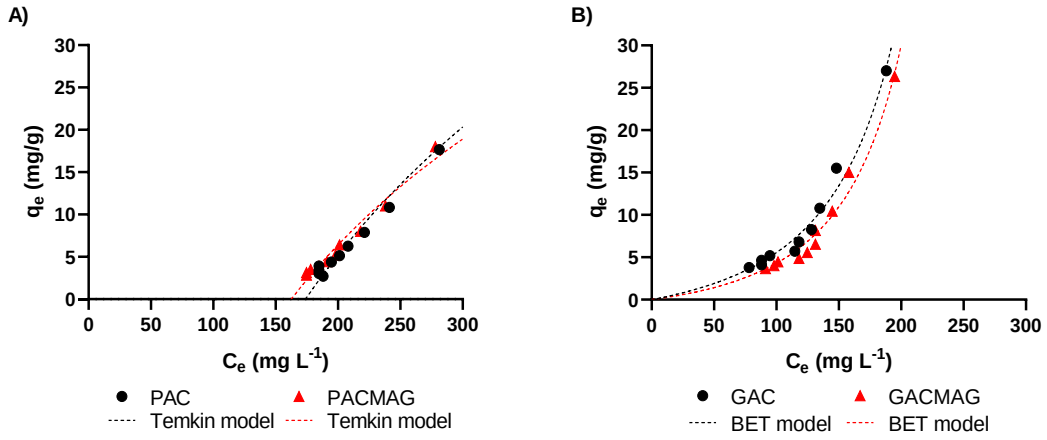

Figure 6.8 – Adsorption capacity (q_e) versus equilibrium concentration (C_e) for the adsorption of COD onto a) PAC and PACMAG, and b) GAC and GACMAG (mixing time = 13 h, stirring speed = 250 rpm, temperature = 17.6±0.1 ºC, adsorbent dosage = 10–100 g L^{-1}, COD = 458±5 mg O_2 L^{-1}, pH = 7.91±0.02).

Using the Giles classification of adsorption isotherms from solute solutions (Giles et al., 1960), the adsorption isotherms shown in Figures 6.8a and 6.8b are of types L1 and S1, respectively. The curvature presented by the type L1 shows that as more sites in the substrate are filled, it becomes increasingly difficult for a solute molecule to find an available vacant site (Giles et al., 1960). On the other hand, the form S1 of isotherm indicates that the initial adsorption is low and increases as the number of adsorbed species increases. This means that there was an association between the adsorbed species, called cooperative adsorption, *i.e.*, the adsorbed adsorbate affected the adsorption of other adsorbate molecules (Liu, 2015). Considering the isotherm models studied (Table 6.7), it was observed that the model that would best fit the experimental data adequately were the Temkin model for PAC and PACMAG, and the BET model for GAC and GACMAG, achieving high correlation coefficients (R^2 of 0.9568, 0.9668, 0.9771, and 0.9769 for PAC, PACMAG, GAC, and GACMAG, respectively).

Table 6.7 – Isotherm models used to fit the COD adsorption data for PAC, PACMAG, GAC, and GACMAG.

Type of AC	Model	R^2	AARD (%)	E	Isotherm parameters
PAC	Langmuir	0.3868	54.65	3.45	q_m = 4204.73 mg g^{-1}; K_a = 7.98E-06 L mg^{-1}
	Freundlich	0.3874	54.64	3.45	K_F = 0.034 $mg^{0.0001}$ $L^{0.9999}$ g^{-1}; n = 1.0001
	Redlich-Peterson	0.3875	54.64	3.45	q_m = 0.227 mg g^{-1}; K_a = 0.295 L mg^{-1}; n =0.0001
	Two-site Langmuir	0.3870	54.65	3.45	q_{m1} = 6432.69 mg g^{-1}; K_{a1} = 5.22E-06 L mg^{-1} q_{m2} = 3.98E-12 mg g^{-1}; K_{a2} = 1256.81 L mg^{-1}
	Generalized Freundlich	0.3849	54.68	3.46	q_m = 1122.27 mg g^{-1}; K_a = 3.00E-05 L mg^{-1}; n = 0.9999
	Langmuir-Freundlich	0.3851	54.24	3.46	q_m = 1240.69 mg g^{-1}; K_a = 2.70E-05 L mg^{-1}; n = 0.9999
	Toth	0.3853	54.66	3.46	q_m = 2298.95 mg g^{-1}; K_a = 1.47E-05 L mg^{-1}; n = 0.9000
	Temkin	0.9568	15.68	0.92	b_T = 64.67 J mol^{-1}; K_T = 0.0058 L mg^{-1}
	BET	-0.4601	60.64	5.33	q_m = 59.14 mg g^{-1}; K_a = 0.023 L mg^{-1}; K_L = 0.054 L mg^{-1}
PACMAG	Langmuir	0.4135	52.62	3.43	q_m = 3855.95 mg g^{-1}; K_a = 9.13E-06 L mg^{-1}
	Freundlich	0.4142	52.62	3.43	K_F = 0.035 $mg^{0.0001}$ $L^{0.9999}$ g^{-1}; n = 1.0001
	Redlich-Peterson	0.4142	52.62	3.43	q_m = 6.999 mg g^{-1}; K_a = 0.010 L mg^{-1}; n =0.0001
	Two-site Langmuir	0.4135	52.62	3.43	q_{m1} = 3946.77 mg g^{-1}; K_{a1} = 8.92E-06 L mg^{-1} q_{m2} = 8.15E-07 mg g^{-1}; K_{a2} = 1256.81 L mg^{-1}
	Generalized Freundlich	0.4072	52.68	3.45	q_m = 446.30 mg g^{-1}; K_a = 7.99E-05 L mg^{-1}; n = 0.9999
	Langmuir-Freundlich	0.4125	52.64	3.44	q_m = 1794.45 mg g^{-1}; K_a = 1.97E-05 L mg^{-1}; n = 0.9999
	Toth	0.4128	52.63	3.43	q_m = 3913.00 mg g^{-1}; K_a = 9.02E-06 L mg^{-1}; n = 0.9000
	Temkin	0.9668	13.31	0.82	b_T = 78.24 J mol^{-1}; K_T = 0.0062 L mg^{-1}
	BET	-0.5091	63.00	5.51	q_m = 42.74 mg g^{-1}; K_a = 0.027 L mg^{-1}; K_L = 0.054 L mg^{-1}
GAC	Langmuir	0.5743	50.58	4.47	q_m = 4204.73 mg g^{-1}; K_a = 2.06E-05 L mg^{-1}
	Freundlich	0.5757	50.55	4.47	K_F = 0.086 $mg^{0.0001}$ $L^{0.9999}$ g^{-1}; n = 1.0001
	Redlich-Peterson	0.5757	50.54	4.47	q_m = 52.102 mg g^{-1}; K_a = 0.002 L mg^{-1}; n =13.41
	Two-site Langmuir	0.5748	50.57	4.47	q_{m1} = 6432.69 mg g^{-1}; K_{a1} = 1.34E-05 L mg^{-1} q_{m2} = 0 mg g^{-1}; K_{a2} = 1256.81 L mg^{-1}
	Generalized Freundlich	0.3051	60.30	5.71	q_m = 272.92 mg g^{-1}; K_a = 1.15E-05 L mg^{-1}; n = 0.5016
	Langmuir-Freundlich	0.5735	50.78	4.48	q_m = 2714.03 mg g^{-1}; K_a = 3.20E-05 L mg^{-1}; n = 0.9999
	Toth	0.5714	50.65	4.49	q_m = 2298.95 mg g^{-1}; K_a = 3.78E-05 L mg^{-1}; n = 0.9000
	Temkin	0.7986	36.02	3.08	b_T = 102.19 J mol^{-1}; K_T = 0.0129 L mg^{-1}
	BET	0.9771	9.19	1.04	q_m = 18.66 mg g^{-1}; K_a = 0.001 L mg^{-1}; K_L = 0.004 L mg^{-1}
GACMAG	Langmuir	0.5013	54.84	4.73	q_m = 3855.95 mg g^{-1}; K_a = 1.98E-05 L mg^{-1}
	Freundlich	0.5026	54.82	4.72	K_F = 0.076 $mg^{0.0001}$ $L^{0.9999}$ g^{-1}; n = 1.0001
	Redlich-Peterson	0.5026	54.82	4.72	q_m = 4.962 mg g^{-1}; K_a = 0.031 L mg^{-1}; n =0.0001
	Two-site Langmuir	0.5014	54.84	4.73	q_{m1} = 3946.77 mg g^{-1}; K_{a1} = 1.93E-05 L mg^{-1} q_{m2} = 8.15E-07 mg g^{-1}; K_{a2} = 1256.81 L mg^{-1}
	Generalized Freundlich	0.2639	62.38	5.75	q_m = 333.04 mg g^{-1}; K_a = 7.03E-06 L mg^{-1}; n = 0.5072
	Langmuir-Freundlich	0.5007	54.66	4.73	q_m = 2729.34 mg g^{-1}; K_a = 2.79E-05 L mg^{-1}; n = 0.9999
	Toth	0.5014	54.84	4.73	q_m = 3913.00 mg g^{-1}; K_a = 1.95E-05 L mg^{-1}; n = 0.9999
	Temkin	0.8112	40.39	2.91	b_T = 87.78 J mol^{-1}; K_T = 0.0110 L mg^{-1}
	BET	0.9769	9.85	1.02	q_m = 39.40 mg g^{-1}; K_a = 0.001 L mg^{-1}; K_L = 0.034 L mg^{-1}

A different result was observed by Vargues et al. (2021). These authors obtained different isothermal models between PAC and PACMAG, either in the adsorption of ibuprofen or amoxicillin, indicating that the structural changes introduced by magnetite seem to have an impact on the adsorption mechanism. This was not observed in this work, perhaps because the effluent used is very complex. The Temkin isotherm model, which presumes a multilayer adsorption process, postulates the following: i) as surface coverage increases, the heat of adsorption of all molecules in the layer decreases linearly rather than logarithmically, ii) the adsorption process is characterized by a uniform distribution of binding energies at the adsorbent surface, and iii) considers interactions between the adsorbent and the adsorbate (Amin et al., 2015; Kalam et al., 2021). The BET isotherm is based on the assumption that adsorption is multilayer (Ebadi et al., 2009). GAC and GACMAG had a higher affinity with the organic matter than the PAC and PACMAG. This can be seen in Figures 6.8a and 6.8b, where the experimental adsorption capacity of COD for the GAC (q_e = 27.0 mg/g) and GACMAG (q_e = 26.3 mg/g) were greater than that for the PAC (q_e = 5.1 mg/g) and PACMAG (q_e = 5.2 mg/g) at 200 mg L^{-1} of equilibrium concentration. The COD adsorption capacity values for GAC (q_e =70.97 mg/g) and iron oxide-coated GAC (q_e = 181.67 mg/g) obtained by Affam (2020) were much higher than the values obtained in this work, since the initial COD concentration, the adsorbent dosage and the effluent volume were different. Other factors such as pH, temperature, type of adsorbents, type of adsorbates, presence of several pollutants, contact time, surface functional group, and other experimental conditions can affect the adsorption process (Ali et al., 2020). Low R^2 values were obtained for other models (*e.g.*, Langmuir isotherm, Redlich-Peterson, and others) (Table 6.7), which may be justified by the complexity of the effluent to be analyzed. By the way, Vargues et al. (2021) obtained high coefficients of determination in several isothermal models also used in this work, probably due to the solutions prepared with only one contaminant, thus minimizing interference between adsorbates and between these and the adsorbent.

6.3.2.3. Effect of adsorption time on COD removal and the kinetics adsorption models

The effect of adsorption time on COD removal was studied (Figure 6.9).

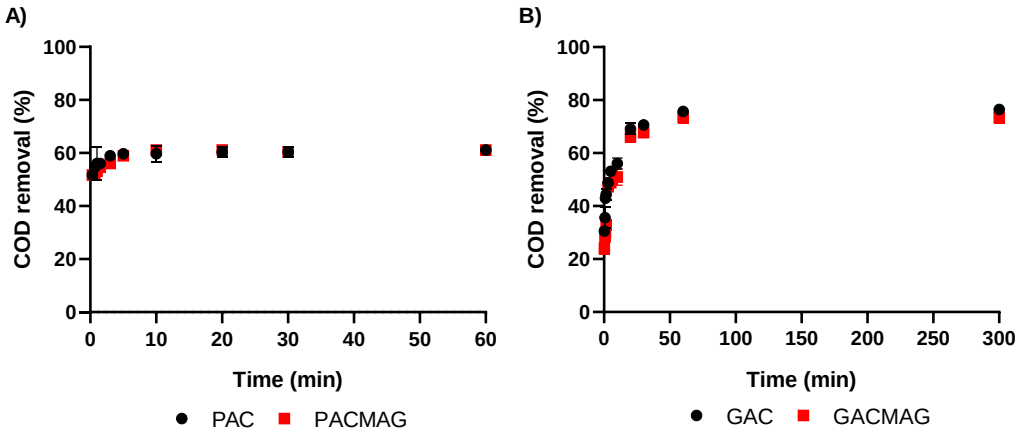

Figure 6.9 - Effect of contact time on the COD removal using a) PAC and PACMAG, and b) GAC and GACMAG (stirring speed = 250 rpm, temperature = 17.6±0.1 ºC, COD = 458±5 mg O_2 L^{-1}, pH = 7.91±0.02, PAC and PACMAG dosages = 70 g L^{-1}, GAC, and GACMAG dosages = 60 g L^{-1}).

The maximum COD removal efficiency occurred at 5 minutes of contact time for PAC (ca. 59.7±1.0%) and PACMAG (ca. 59.0±0.0%), and at 60 minutes for GAC (ca. 75.7±1.0%) and GACMAG (ca. 73.5±2.1%). After this time, the system reaches equilibrium and the removal remains practically constant. In the first few minutes, the rapid increase in COD removal is due to the large empty adsorption sites and the high concentration gradient between the solution and the adsorbent. As the contact time increases, this gradient and the amount of available adsorption sites decrease, making the adsorption rates slower until the process reaches equilibrium and the removal rate remains constant (Konggidinata et al., 2017). The adsorption kinetics of PAC and PACMAG were much faster than those of GAC and GACMAG since PAC and PACMAG present larger external areas and thus the active adsorption centers are more accessible to organic matter than GAC and GACMAG.

Adsorption kinetics is important in a wastewater treatment plant as it controls the efficiency of the process. Therefore, kinetic analysis was performed for PAC, PACMAG, GAC, and GACMAG using the kinetic adsorption models shown in Table 6.5, and the parameters calculated from the studied models are presented in Table 6.8.

Table 6.8 - Kinetic models used to fit the COD adsorption data for PAC, PACMAG, GAC, and GACMAG.

Type of AC	Model	R^2	AARD (%)	E	Isotherm parameters
PAC	Pseudo-first order	0.5742	2.95	0.13	q_e= 3.85 mg g^{-1}; k_1 = 5.933 min^{-1}
	Pseudo-second order	0.9317	1.04	0.05	q_e = 3.94 mg g^{-1}; k_2 = 4.063 g mg^{-1} min^{-1}
	Pseudo-order n (n≠1)	0.9810	0.51	0.03	q_e = 4.04 mg g^{-1}; k_2 = 3.326 g mg^{-1} min^{-1}; n= 2.97
	Weber and Morris intra-particle diffusion	0.6165	2.51	0.12	k_{ip} = 0.067 mg g^{-1} $min^{-1/2}$; C_i = 3.594 mg g^{-1}
	Elovich	0.8701	1.45	0.07	α = 2.86E+13 mg g^{-1} min^{-1}; β = 9.15 g mg^{-1}
	Bangham	0.8575	1.51	0.07	ν = 0.028; k = 3.624 mg g^{-1} $min^{-0.028}$
PACMAG	Pseudo-first order	0.2846	5.31	0.21	q_e= 3.79 mg g^{-1}; k_1 = 5.982 min^{-1}
	Pseudo-second order	0.7405	3.18	0.13	q_e= 3.91 mg g^{-1}; k_2 = 3.338 g mg^{-1} min^{-1}
	Pseudo-order n (n≠1)	0.9283	1.68	0.07	q_e = 4.47 mg g^{-1}; k_2 = 0.273 g mg^{-1} min^{-1}; n= 5.97
	Weber and Morris intra-particle diffusion	0.6881	3.14	0.14	k_{ip} = 0.092 mg g^{-1} $min^{-1/2}$; C_i = 3.467 mg g^{-1}
	Elovich	0.9039	1.66	0.08	α = 6.33E+09 mg g^{-1} min^{-1}; β = 6.96 g mg^{-1}
	Bangham	0.8938	1.68	0.08	ν = 0.038; k = 3.523 mg g^{-1} $min^{-0.038}$
GAC	Pseudo-first order	0.6633	15.73	0.68	q_e= 4.95 mg g^{-1}; k_1 = 1.036 min^{-1}
	Pseudo-second order	0.8498	10.53	0.45	q_e= 5.32 mg g^{-1}; k_2 = 0.261 g mg^{-1} min^{-1}
	Pseudo-order n (n≠1)	0.9673	4.48	0.21	q_e = 7.71 mg g^{-1}; k_2 = 3.70E-05 g mg^{-1} min^{-1}; n= 6.53
	Weber and Morris intra-particle diffusion	0.6131	15.99	0.73	k_{ip} = 0.196 mg g^{-1} $min^{-1/2}$; C_i = 3.370 mg g^{-1}
	Elovich	0.9468	4.86	0.27	α = 136.43 mg g^{-1} min^{-1}; β = 1.74 g mg^{-1}
	Bangham	0.8929	7.17	0.38	ν = 0.123; k = 3.252 mg g^{-1} $min^{-0.123}$
GACMAG	Pseudo-first order	0.7801	17.87	0.64	q_e = 4.91 mg g^{-1}; k_1 = 0.551 min^{-1}
	Pseudo-second order	0.9030	11.36	0.43	q_e = 5.30 mg g^{-1}; k_2 = 0.140 g mg^{-1} min^{-1}
	Pseudo-order n (n≠1)	0.9600	7.61	0.27	q_e = 7.30 mg g^{-1}; k_2 = 1.69E-04 g mg^{-1} min^{-1}; n= 5.46
	Weber and Morris intra-particle diffusion	0.5913	24.84	0.87	k_{ip} = 0.225 mg g^{-1} $min^{-1/2}$; C_i = 2.833 mg g^{-1}
	Elovich	0.9319	7.76	0.36	α = 30.37 mg g^{-1} min^{-1}; β = 1.50 g mg^{-1}
	Bangham	0.8578	13.62	0.52	ν = 0.152; k = 2.741 mg g^{-1} $min^{-0.152}$

A very strong correlation coefficient ($0.8 \leq R^2 \leq 1.00$) was observed for the pseudo-second-order (for PAC with R^2 of 0.9317, GAC with R^2 of 0.8498, and GACMAG with R^2 of 0.9030), Pseudo-order n (n≠1) (for PAC with R^2 of 0.9810, PACMAG with R^2 of 0.9283, GAC with R^2 of 0.9673, and GACMAG with R^2 of 0.9600), Elovich (for PAC with R^2 of 0.8701, PACMAG with R^2 of 0.9039, GAC with R^2 of 0.9468, and GACMAG with R^2 of 0.9319), and Bangham models (for PAC with R^2 of 0.8575, PACMAG with

R^2 of 0.8938, GAC with R^2 of 0.8929, and GACMAG with R^2 of 0.8578) (Table 6.8). According to Revellame et al. (2020), $R^2 \geq 0.8$ indicates a good fit between the data and the model, but it is not enough to validate the choice of model, so it must be combined with other parameters. For example, it is usual to compare the adsorption capacity of the adsorbate obtained experimentally with the calculated value, to justify the fit of a model. Thus, according to the results in Table 6.8, the pseudo-order n kinetic model best fits the experimental data, for the PAC, PACMAG, GAC, and GACMAG. This model showed higher values of correlation coefficients close to 1 ($R^2 = 0.9810$ for PAC, $R^2 = 0.9283$ for PACMAG, $R^2 = 0.9673$ for GAC, and $R^2 = 0.9600$ for GACMAG) than the other models (see Figure 6.10). On the other hand, this kinetic model also showed a calculated ($q_{cal.}$ = 4.04 mg g^{-1} for PAC, $q_{cal.}$ = 4.47 mg g^{-1} for PACMAG, $q_{cal.}$ = 7.71 mg g^{-1} for GAC, and $q_{cal.}$ = 7.30 mg g^{-1} for GACMAG) and experimental (q_e = 3.90±0.07 mg g^{-1} for PAC, q_e = 3.86±0.00 mg g^{-1} for the PACMAG, q_e = 5.78±0.08 mg g^{-1} for the GAG, and q_e = 5.61±0.16 mg g^{-1} for the GACMAG) adsorption capacity quite close.

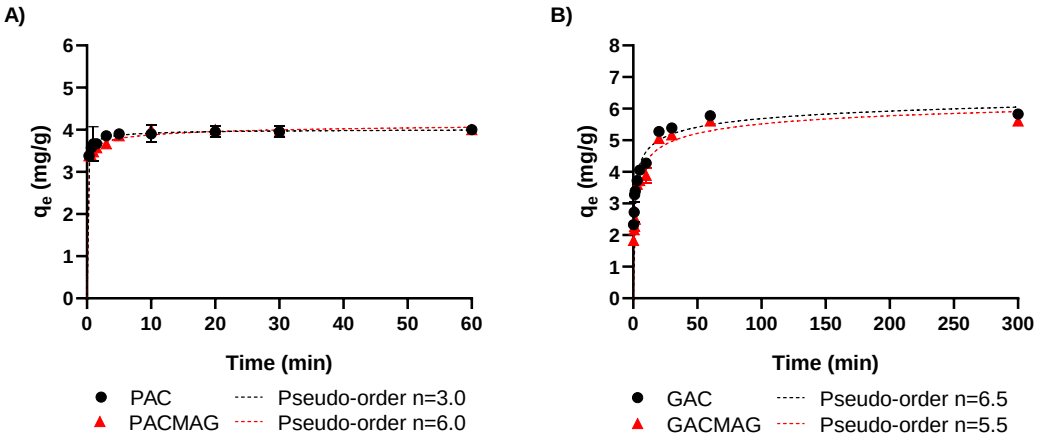

Figure 6.10 – Adsorption capacity (q_e) versus time (min) for the adsorption of COD onto a) PAC and PACMAG, and b) GAC and GACMAG (stirring speed = 250 rpm, temperature = 17.6±0.1 ºC, COD = 458±5 mg O_2 L^{-1}, pH = 7.91±0.02, PAC and PACMAG dosages = 70 g L^{-1}, GAC and GACMAG dosages = 60 g L^{-1}).

Vargues et al. (2021) also observed the adsorption of ibuprofen using PAC or PACMAG following the pseudo-order n kinetic model. The pseudo-order n kinetic model predicts that the adsorption process is dependent on the adsorption capacity (i.e., that the rate-limiting step is chemisorption) and not on the adsorbate concentration (Sahoo and Prelot, 2020). Furthermore, this mechanism of adsorption occurs in two phases, the first being related to the diffusion of the pollutants from the solution to the adsorbent, and the second

phase the fixation of the pollutants to the active sites available on the surface of the adsorbent (Djonga et al., 2021). In all kinetics models, lower AARD and E were found for PAC and PACMAG relative to GAC and GACMAG (Table 6.8).

6.3.2.4. Evaluation of different adsorbent separation methods

COD and turbidity removal by different adsorbent separation methods, namely, settling and magnetic separation over time (Figure 6.11), and filtration (Table 6.9), using PAC, PACMAG, GAC, and GACMAG, were evaluated and compared.

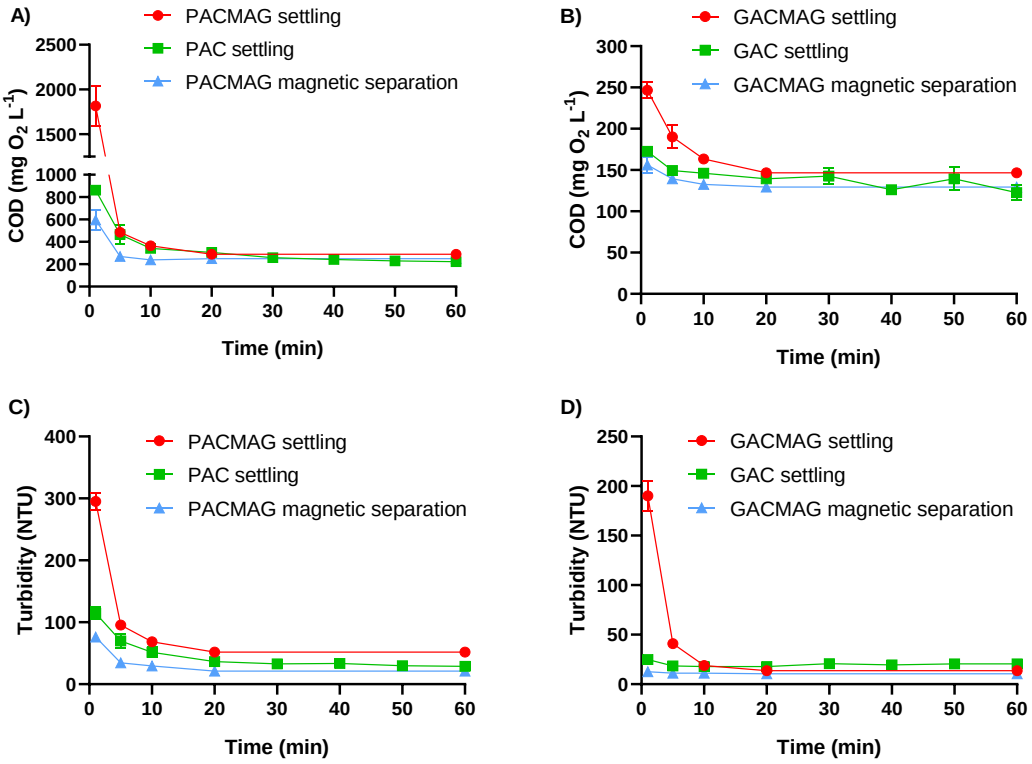

Figure 6.11 – Variation of the a) COD concentration and c) turbidity using PACMAG and PAC; and b) COD concentration and d) turbidity using GACMAG and GAC with the magnetic separation and settling time. Adsorption operating conditions: stirring speed = 250 rpm, temperature = 18.9±1.1 ºC, mixing time = 5 min (for PAC and PACMAG) and 60 min (for GAC and GACMAG), adsorbent dosage = 70 g L^{-1} (for PAC and PACMAG) and 60 g L^{-1} (for GAC and GACMAG), COD = 467±9 mg O_2 L^{-1}, and pH = 7.82±0.01.

Table 6.9 – COD, turbidity, and pH values obtained by adsorption-filtration process with PAC, PACMAG, GAC, and GACMAG, under operating conditions: stirring speed = 250 rpm, temperature = 18.9±1.1 ºC, mixing time = 5 min (for PAC and PACMAG) and 60 min (for GAC and GACMAG), adsorbent dosage = 70 g L^{-1} (for PAC and PACMAG) and 60 g L^{-1} (for GAC and GACMAG), COD = 467±9 mg O_2 L^{-1}, NH_4^+ = 8.9±0.7 mg N L^{-1}, and pH = 7.82±0.01.

Type of adsorbent	COD (mg O_2 L^{-1})	Turbidity (NTU)	NH_4^+ (mg N L^{-1})	pH
PAC	235±7.1	0.253±0.023	5.5±0.8	9.42±0.04
PACMAG	232±9.4	0.272±0.017	6.5±0.4	8.23±0.12
GAC	128±2.4	0.227±0.018	5.0±0.8	8.82±0.06
GACMAG	123±9.4	0.291±0.021	6.5±0.4	7.90±0.16

According to Figure 6.11a, high COD concentrations (well above the COD concentration of the pretreated SWW, 467±9 mg O_2 L^{-1}) were observed in the first minutes (between 0 and 5 min) of sedimentation (for PACMAG and PAC) or magnetic separation (for PACMAG), which indicates that the adsorbents used (PACMAG or PAC) were not yet completely separated from the effluent. For GACMAG or GAC, this did not occur as a faster separation of the adsorbent was observed (Figure 6.11b). A decrease and stabilization of COD concentrations and turbidity over time were observed for all separation methods and adsorbents used. The magnetic separation method for PACMAG or GACMAG showed lower COD and turbidity values in the first minutes (0 to 20 min.) than the settling separation method for PAC, PACMAG, GAC, or GACMAG. The minimum COD values reached in the magnetic separation method were 238±0 mg O_2 L^{-1} (for PACMAG at 10 min.) and 129±0 mg O_2 L^{-1} (for GACMAG at 20 min.). In the settling separation method, the following minimum COD values were 222±9 mg O_2 L^{-1} (for PAC at 60 min.), 288±5 mg O_2 L^{-1} (for PACMAG at 20 min.), 126±5 mg O_2 L^{-1} (for GAC at 40 min.), and 147±0 mg O_2 L^{-1} (for GACMAG at 20 min.). For PACMAG, no significant difference (p<0.05) was observed between the filtration (COD = 232±9 mg O_2 L^{-1}, Table 6.9) and the magnetic (COD = 238±0 mg O_2 L^{-1} at 10 min., Figure 6.11a) separation methods. Regarding GACMAG, no significant difference (p<0.05) was observed between the filtration (COD = 123±9 mg O_2 L^{-1}, Table 6.9) and the magnetic (COD = 129±0 mg O_2 L^{-1} at 20 min., Figure 6.11b) separation methods. The results also show that the settling separation method provides higher COD values than the filtration or magnetic separation methods when PACMAG and GACMAG are applied. This means that the effluent resulting from the settling separation method may have some easily non-settleable organic impurities, which affected the final COD concentration of the effluent. However, for PAC and GAC, there were no significant differences (p<0.05) between the filtration (COD = 235±7 mg O_2 L^{-1} and 128±2 mg O_2

L^{-1} for PAC and GAC, respectively, Table 6.9) and settling separation method (COD = 222±9 mg O_2 L^{-1} for PAC (at 60 min., Figure 6.11a) and 126±5 mg O_2 L^{-1} for GAC (at 40 min., Figure 6.11b)). In fact, PACMAG and GACMAG had a higher weight percentage of smaller particles than PAC and GAC (Figures 6.5 and 6.6), so a longer settling time for the former will be expected. Krahnstöver and Wintgens (2018) state that PAC settling velocities are around 1 m h^{-1} for a particle size of 45 μm or 0.5 m h^{-1} for a particle size of 30 μm and even lower for the fine particle fraction. Generally, the sedimentation operation is subsequently associated with other PAC separation processes, such as deep bed filtration, lamella separator, pile cloth filtration, hydrocyclone, flotation, and microsieve (Krahnstöver and Wintgens, 2018), to prevent activated carbon of leaving the wastewater treatment plant.

According to Table 6.9, an increase in effluent pH after adsorption was observed for all adsorbents used. The increase in effluent pH may indicate that there was a loss of protons from the solution to the adsorbent, making the adsorbent surfaces more positively charged (Čerović et al., 2007). The observed ammonium nitrogen removal (Table 6.9) could be a reason for this increase in effluent pH. In any case, all studied adsorbents generate an effluent that meets the discharge pH requirements (pH<9.5).

6.3.3. Phytoremediation

6.3.3.1. Effect of bed depth and COD mass load on COD and ammonium nitrogen removal

The effect of bed depth on COD and ammonium nitrogen removal was analyzed for pretreated SWW by IOSLM+AC integrated process (trials A1 and B1 for CW1, and trials A2 and B2 for CW2) and for raw SWW (trials C1 for CW1 and C2 for CW2), at constant hydraulic loads (about 80 L m^{-2} d^{-1}) (Figure 6.12).

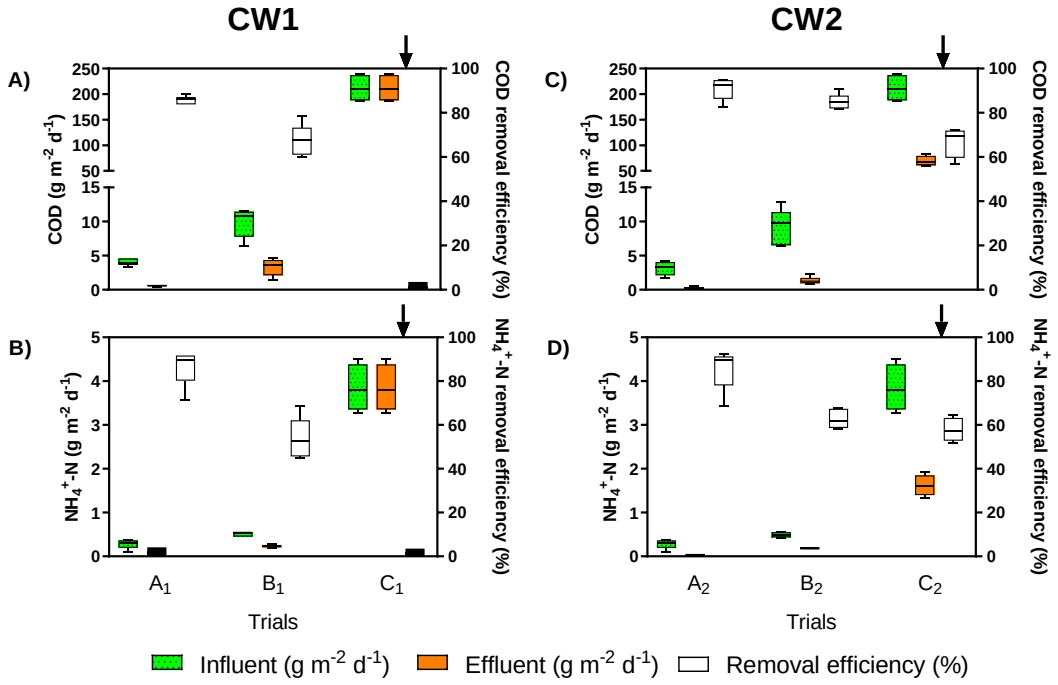

Figure 6.12 - Organic and ammonium load values in the inlet and outlet of CW1 (A and B, respectively) and CW2 (C and D, respectively), and the respective COD and ammonium removal efficiencies in different trials (A, B, and C). The average air and substrate temperature in the phytoremediation trials were 19.7±3.9 and 15.9±2.7 ºC, respectively.

According to Figure 6.12, it is observed that, for pretreated SWW, there are no significant differences (P<0.05) in the COD removal efficiencies between tests A1 (83.8 to 88.3%) and A2 (89.9 to 95.0%). The same result was observed for ammonium nitrogen removal efficiencies between tests A1 (71.2 to 91.7%) and A2 (68.6 to 92.3%) as well as between tests B1 (44.8 to 68. 6%) and B2 (58.3 to 67.6%), which indicates that shallow beds may be sufficient to support low ammonium nitrogen mass loads. However, between tests B1 (59.8 to 78.6%) and B2 (81.5 to 90.8%) there were significant differences (P<0.05) for COD removal efficiencies, indicating that the depth of the bed tested influenced the COD removal. For raw SWW, significant differences (P<0.05) were observed in COD and ammonium nitrogen removal efficiencies between CW1 and CW2 (Figure 6.12). In fact, no COD and ammonium nitrogen removal efficiencies were observed for CW1, but for CW2 these values ranged from 59.1 to 83.2% for COD and 51.9 to 64.5% for ammonium nitrogen (Figure 6.12). Deeper beds allow a greater distribution of roots and microorganisms in the substrate, as well as greater HRT that allows a longer contact time between the microbiological community and the effluent to be treated, favoring a more complete degradation and/or assimilation of pollutants. HRT of about 3.6±0.5 and 7.1±0.9

h were determined for CW1 and CW2, respectively. Almeida et al. (2018) also observed greater nitrogen removals in deeper beds planted with *Vetiveria zizanioides*, in the treatment of synthetic effluent (68±3 to 290±8 mg NH_4^+-N L^{-1}). These authors concluded that deeper root systems are more favorable to the creation of zones with different oxidation conditions that lead to nitrogen removal. Mburu et al. (2019) evaluated the effect of bed depth (from 0.65 to 0.8 m) and retention time (from 1 to 5 days) on the removal of COD, BOD_5, NH_4^+, and TSS from SWW, using vertical subsurface flow constructed wetland mesocosms without plants. These authors observed that, contrary to NH_4^+ and TSS removal, the effect of depth was insignificant in the removal of COD and BOD_5. However, an increase in retention time has a significant influence on the removal efficiency of organic matter, reaching removals of 50%, 55%, and 82% for BOD_5, COD, and TSS, respectively, on the 5th day of retention time.

According to Figure 6.12, significant differences (p<0.05) in the concentrations of COD and ammonium nitrogen were observed between the inlet and outlet effluents of the beds, for all tests (except for test C1). High COD (from 61 to 75%) and total nitrogen (from 47 to 62%) removals of poorly biodegradable SWW (BOD/COD ratio from 0.21 to 0.27) were also achieved by Odong et al. (2013) when the authors tested constructed wetland planted with *M. violaceum*, *C. papyrus*, *P. mauritianus*, and *T. domingensis*. For biodegradable pretreated SWW from a biodigester, Manh et al. (2014) obtained COD and BOD removals around 60%, using CW planted with *Vetiveria zizanioides*.

The effect of COD loading on COD and ammonium nitrogen removal for pretreated SWW was evaluated, for both beds studied (Figure 6.12). For CW1, an increase in COD load mass from 4.1±0.5 to 9.5±2.2 g m^{-2} d^{-1} had a significant effect (P<0.05) on COD (Figure 6.12a) and ammonium nitrogen (Figure 6.12b) removal efficiency. Higher COD and ammonium nitrogen removal efficiencies were obtained when smaller COD loads applied were applied. For CW2, increasing COD mass load contributed to a significant (P<0.05) decrease in the ammonium nitrogen removal efficiency but had no significant effect (P<0.05) on COD removal efficiency. Therefore, it appears that ammonium nitrogen removal occurred in the presence of organic matter and with low dissolved oxygen. When the COD mass load of the beds was increased to 211.8±26.4 g m^{-2} d^{-1}, a significant reduction in the removal efficiencies of COD and ammonium nitrogen was observed for both beds (except for ammonium nitrogen in the CW2) (Figure 6.12d).

Mburu et al. (2019) report that a wide variation in the physicochemical characteristics of the SWW at the CW input can influence pollutant removal efficiencies.

The results show that only trials A1 (91±11 mg O_2 L^{-1} for COD), A2 (41±15 mg O_2 L^{-1} for COD), and B2 (86±14 mg O_2 L^{-1} for COD) would be able to meet discharge requirements in terms of COD concentrations (COD ≤125 mg L^{-1}). On the other hand, the remaining tests, such as B1 (181±52 mg O_2 L^{-1} for COD), C1 (2504±321 mg O_2 L^{-1} for COD), and C2 (1111±24 mg O_2 L^{-1} for COD) resulted in effluents even with high concentrations of COD. The COD values in tests C1 and C2 show how important is the IOSLM+AC pretreatment before the phytoremediation process. The IOSLM+AC processes have emerged as a pretreatment solution for high removals of organic matter, ammonia, and other compounds present in the effluent (Madeira et al., 2023 (chapter 3), 2021 (chapter 5), 2020 (chapter 2)). Ramalho et al. (2022) also noted the need for pretreatment by IOSLM+AC processes in the removal of organic matter and nitrogen from landfill leachate before the phytoremediation process with wetlands constructed with *Vetiveria zizanioides*.

Organic matter and ammonium nitrogen removal in the beds is associated with the occurrence of certain removal mechanisms. There are several indicators (e.g., pH, DO, potential redox) that can indicate the type of removal mechanisms that occurred in the bed. The removal of ammonium nitrogen could be due to ammonia volatilization (VanderZaag et al., 2008) since the pH of the pretreated SWW (from tests A1, B1, A2, and B2) was still above 9.2 (that is, pH from which 50% of the ammoniacal nitrogen is available to be volatilized (Lin et al., 2009)). It is also expected that nitrogen removal may be associated with the nitrification process since the pH of the effluent decreased in all tests (Figures 6.13a and 6.13e). Nitrification is a biological process of converting NH_4^+ to NO_3^- in two sequential steps in the presence of oxygen and results in the release of protons. In the first step, the biological oxidation of NH_4^+ to NO_2^- occurs by the action of bacteria of the genus *Nitrosomonas*, while in the second step, the oxidation of NO_2^- to NO_3^- occurs by the action of bacteria of the genus *Nitrobacter* (Vymazal, 2007). On the other hand, the decrease in pH can also be due to carbonation reactions or microbial degradation of organic matter. The removal of ammonium nitrogen may also be associated with plant assimilation (Carreau et al., 2012).

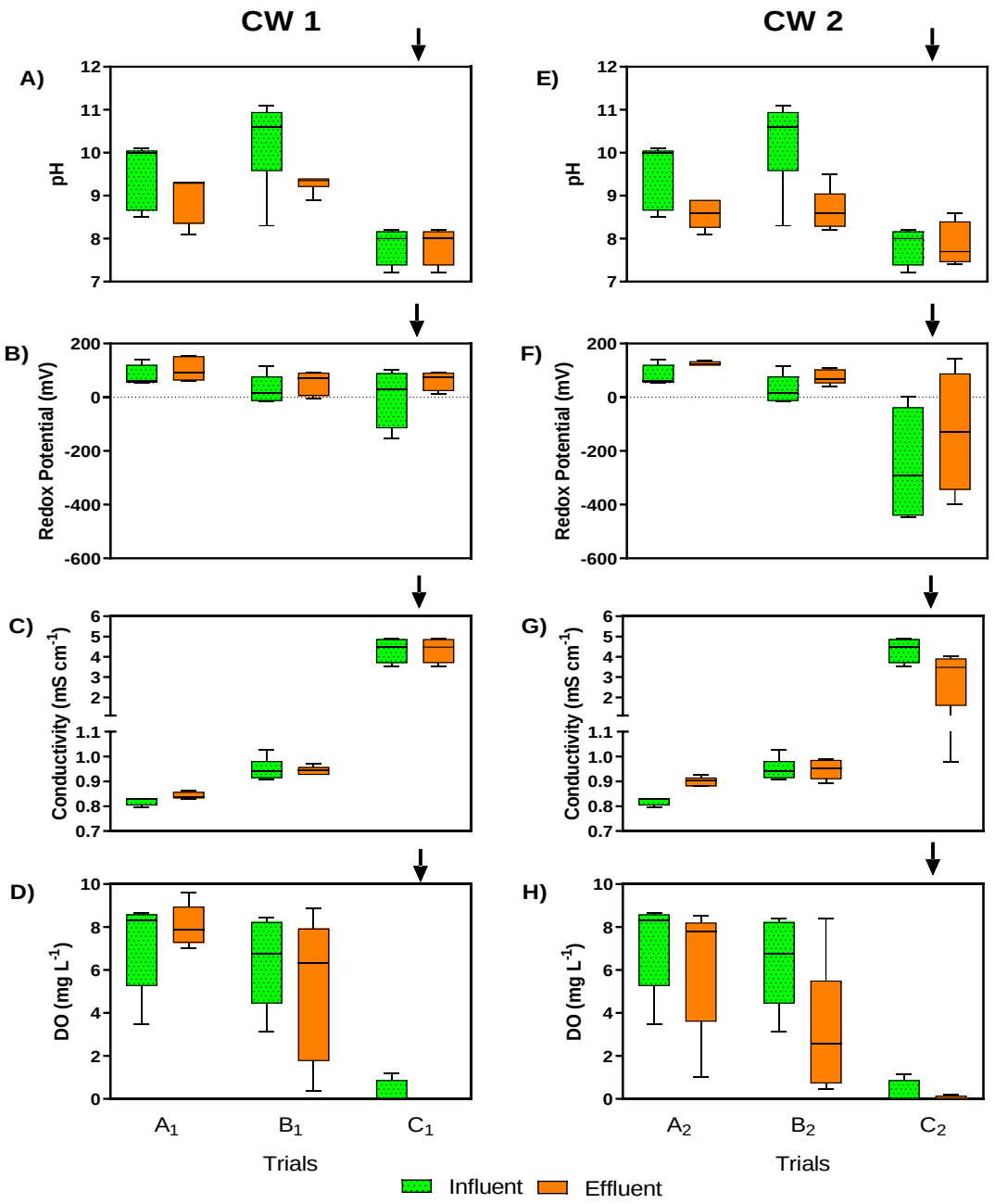

Figure 6.13 - pH, redox potential, conductivity, and DO values, in the inlet and outlet of CW 1 (A, B, C, and D, respectively) and CW 2 (E, F, G, and H, respectively), in different trials (A1, A2, B1, B2, C1, and C2).

Degradation of organic matter from poorly biodegradable wastewater in CW planted with *Vetiveria zizanioides* may be due to the release of plant enzymes. Enzymes released by plant roots can transform complex organic matter into simpler forms (Tjelldén et al., 2015). No significant difference (p<0.05) between the inlet and outlet was observed for redox potential (Figures 6.13b and 6.13f), conductivity (Figures 6.13c and 6.13g), and DO (Figures 6.13d and 6.13h) for both beds. As expected, significant oxygen

consumption (p<0.05) was observed in trials C1 and C2, due to the high concentrations of COD applied, reaching zero DO values in both beds (Figures 6.13d and 6.13h). Dissolved oxygen consumption should be due primarily to the aerobic degradation of organic matter and then to the nitrification process. According to Soroko (2007), beds fed in vertical flow are favorable for carrying out aerobic processes since they allow intensive aeration caused by diffusion and convection phenomena.

6.3.3.2. Composition of plant biomass

Table 6.10 shows the biomass composition of the leaves of *Vetiveria zizanioides*, before and after the phytoremediation tests, for both beds studied.

Table 6.10 - Leaves biomass composition for CW1 and CW2.

Parameter (mg g^{-1} DW)	**Leaves biomass composition**		
	Initial	Final	
		CW 1	CW 2
Ca^{2+}	1.20±0.05	2.00±0.09	2.30±0.01
Mg^{2+}	0.04±0.01	0.06±0.01	0.07±0.02
Na^{+}	0.45±0.01	0.30±0.01	0.36±0.02
K^{+}	0.47±0.02	3.14±0.02	4.0±0.02
TKN	10.50±0.50	15.90±0.20	17.60±0.20
P	1.02±0.01	0.20±0.03	0.44±0.03

Note: Mean ± Standard Deviation, calculated for a 95% confidence level; number of determinations (n=3). DW – dried weight.

According to Table 6.10, the bed with greater depth (CW2) contributed significantly (p<0.05) to greater accumulation of nutrients in the leaves (such as calcium, potassium, total nitrogen, and phosphorus) than the beds with less depth (CW1). The accumulation of nutrients in the leaves of the *Vetiveria zizanioides* plant in deeper beds can be explained by the better root distribution of the plants, which leads to greater alternation of aerobic, anoxic, and anaerobic conditions inside the bed, and consequently a better symbiosis between plants and microorganisms. During the phytoremediation tests, no signs of toxicity or chlorosis were detected in the leaves of *Vetiveria zizanioides*. The plants showed a very low growth rate (i.e., 0.4±0.1 cm d^{-1} for CW1 and 0.5 ± 0.2 cm d^{-1} for CW2), maybe due to the season of the year (February to April), with average air and substrate temperatures in the phytoremediation tests around 19.7±3.9 and 15.9±2.7 ºC, respectively. Even so, plant growth was not inhibited by the presence of high pH (around 10.25±1.03), which could contribute to reducing the long time of the carbonation process that has been observed in the literature. No significant differences (p<0.05) in plant

growth between beds were observed. However, Almeida et al. (2018) concluded that the bed depth influenced plant growth, with values around 1.5 ± 0.1 cm d^{-1} for the deepest bed and 1.1 ± 0.1 cm d^{-1} for the shallower bed, in summer. The reason may be the bed depth that may limit the increase of the plant's root growth (Vymazal, 2006), which seems not to have occurred in this work.

6.4. Conclusion

The present work aimed to evaluate the effectiveness of the adsorption and the phytoremediation processes as tuning processes in the removal of organic matter from a poorly biodegradable and alkaline pretreated SWW by the IOSLM and AC process. The following conclusions were drawn from this work:

- Under optimized conditions (dose and time), PAC and PACMAG were less effective than GAC and GACMAG in the removal of COD, being the COD adsorption capacity 3.90±0.07 mg g^{-1} for PAC, 3.86±0.00 mg g^{-1} for PACMAG, 5.78±0.08 mg g^{-1} for GAG, and 5.61±0.16 mg g^{-1} for GACMAG;
- Temkin (for PAC and PACMAG) and BET (for GAC and GACMAG) models were the best isotherm models found, indicating that probably adsorption occurred on the multilayer adsorption mechanism;
- Pseudo-order n kinetic model was the best kinetic model found for PAC, PACMAG, GAC, and GACMAG, indicating that the adsorption process is dependent on the adsorption capacity (i.e., that the rate-limiting step is chemisorption) and not on the adsorbate concentration;
- COD adsorption capacity by PACMAG or GACMAC was not influenced by the impregnation of iron oxide NPs on PAC and GAC;
- Magnetic separation of PACMAG and GACMAG may replace the filtration separation method without changing the quality of the treated effluent;
- Bed depth and applied mass load are two factors that influence organic matter removal in constructed wetlands planted with *Vetiveria zizanioides*. Deeper beds and low COD loads contribute to greater efficiency of organic matter removal; thus, if the availability of land is a restriction, the option for deeper beds can be advantageous;

- *Vetiveria zizanioides* grew and showed no signs of toxicity when it was fed with very alkaline pretreated SWW (pH ≈ 10). The use of highly alkaline pretreated SWW could substantially reduce the time of the carbonation process;
- The adsorption process and the phytoremediation process can be tuned processes in the removal of organic matter from a poorly biodegradable and alkaline pretreated SWW from the IOSLM and AC integrated process and fulfill the discharge requirements in terms of COD (<125 mg L^{-1}).

6.5. References

Affam, A.C., 2020. Modification of granular activated carbon by aluminum and iron oxides for decontamination of poultry slaughterhouse wastewater using central composite design. Desalin. Water Treat. 177, 48–59. https://doi.org/10.5004/DWT.2020.25030

Agarry, S.E., Owabor, C.N., 2012. Evaluation of the Adsorption Potential of Rubber (*Hevea brasiliensis*) Seed Pericarp-Activated Carbon in Abattoir Wastewater Treatment and in the Removal of Iron (iii) Ions from Aqueous Solution. Niger. J. Technol. 31, 346–358. https://doi.org/10.4314/njt.v31i3.

Al-Marri, S., Alquzweeni, S.S., Hashim, K.S., Matei, A., Racoviteanu, G., 2021. Review of the technologies for nitrates removal from water intended for human consumption. IOP Conf. Ser. Earth Environ. Sci. 664, 012024. https://doi.org/10.1088/1755-1315/664/1/012024

Ali, M.E., Hoque, M.E., Safdar Hossain, S.K., Biswas, M.C., 2020. Nanoadsorbents for wastewater treatment: next generation biotechnological solution. Int. J. Environ. Sci. Technol. 17, 4095–4132. https://doi.org/10.1007/S13762-020-02755-4/TABLES/5

Almeida, A., Jóźwiakowski, K., Kowalczyk-Juśko, A., Bugajski, P., Kurek, K., Carvalho, F., Durao, A., Ribeiro, C., Gajewska, M., 2020. Nitrogen removal in vertical flow constructed wetlands: influence of bed depth and high nitrogen loadings. Environ. Technol. (United Kingdom) 41, 2196–2209. https://doi.org/10.1080/09593330.2018.1557749

Amin, M.T., Alazba, A.A., Shafiq, M., 2015. Adsorptive removal of reactive black 5 from wastewater using bentonite clay: Isotherms, kinetics and thermodynamics. Sustainability 7, 15302–15318. https://doi.org/10.3390/su71115302

Aragaw, T.A., Bogale, F.M., Aragaw, B.A., 2021. Iron-based nanoparticles in wastewater treatment: A review on synthesis methods, applications, and removal mechanisms. J. Saudi Chem. Soc. 25, 101280. https://doi.org/10.1016/J.JSCS.2021.101280

AWWA, 1996. Standard for Powdered Activated Carbon, American Water Works Association, Denver, Colorado.

Baird, R., Eaton, A.D., Rice, E.W., Bridgewater, L., American Public Health Association, American Water Works Association, Water Environment Federation, 2017. Standard Methods for the Examination of Water and Wastewater, 23rd ed. American Public Health Association, American Water Works Association, Water Environment Federation.

Bazrafshan, E., Zakeri, H.R., Vieira, M.G.A., Derakhshan, Z., Mohammadi, L., Mohammadpour, A., Mousavi Khaneghah, A., 2022. Slaughterhouse Wastewater Treatment by Integrated Chemical Coagulation and Electro-Fenton Processes. Sustain. 14, 11407. https://doi.org/10.3390/SU141811407

Bracamontes-Ruelas, A.R., Ordaz-Díaz, L.A., Bailón-Salas, A.M., Ríos-Saucedo, J.C., Reyes-Vidal, Y., Reynoso-Cuevas, L., 2022. Emerging Pollutants in Wastewater, Advanced Oxidation Processes as an Alternative Treatment and Perspectives. Processes. 10, 1041. https://doi.org/10.3390/pr10051041

Bustillo-Lecompte, C.F., Mehrvar, M., 2015. Slaughterhouse wastewater characteristics, treatment, and management in the meat processing industry: A review on trends and advances. J. Environ. Manage. 161, 287–302 https://doi.org/10.1016/j.jenvman.2015.07.008

Bustillo-Lecompte, C.F., Mehrvar, M., Quiñones-Bolaños, E., 2014. Cost-effectiveness analysis of TOC removal from slaughterhouse wastewater using combined anaerobic-aerobic and UV/H2O2 processes. J. Environ. Manage. 134, 145–152. https://doi.org/10.1016/j.jenvman.2013.12.035

Cao, W., Mehrvar, M., 2011. Slaughterhouse wastewater treatment by combined anaerobic baffled reactor and UV/H_2O_2 processes. Chem. Eng. Res. Des. 89, 1136–1143. https://doi.org/10.1016/j.cherd.2010.12.001

Carreau, R., VanAcker, S., VanderZaag, A.C., Madani, A., Drizo, A., Jamieson, R., Gordon, R.J., 2012. Evaluation of a Surface Flow Constructed Wetland Treating Abattoir Wastewater. Appl. Eng. Agric. 28, 757–766. https://doi.org/10.13031/2013.42416

CEFIC, 1986. Test methods for activated carbon, Conseil Européen des Fédérations de l'Industrie Chimique (European Council of Chemical Manufacturers' Federation).

Čerović, L.S., Milonjić, S.K., Todorović, M.B., Trtanj, M.I., Pogozhev, Y.S., Blagoveschenskii, Y., Levashov, E.A., 2007. Point of zero charge of different carbides. Colloids Surfaces A Physicochem. Eng. Asp. 297, 1–6. https://doi.org/10.1016/J.COLSURFA.2006.10.012

Danh, L.T., Truong, P., Mammucari, R., Tran, T., Foster, N., 2009. Vetiver grass, *Vetiveria zizanioides*: A choice plant for phytoremediation of heavy metals and organic wastes. Int. J. Phytoremediation 11, 664–691. https://doi.org/10.1080/15226510902787302

del Real-Olvera, J., Rustrian-Portilla, E., Houbron, E., Landa-Huerta, F.J., 2016. Adsorption of organic pollutants from slaughterhouse wastewater using powder of *Moringa oleifera* seeds as a natural coagulant. Desalin. Water Treat. 57, 9971–9981. https://doi.org/10.1080/19443994.2015.1033479

Djonga, W.G., Noubissié, E., Noumi, G.B., 2021. Removal of nitrogen, phosphate and carbon loads from slaughterhouse effluent by adsorption on an adsorbent based on Ayous sawdust (Triplochyton scleroxylon). Case Stud. Chem. Environ. Eng. https://doi.org/10.1016/j.cscee.2021.100120

Ebadi, A., Soltan Mohammadzadeh, J.S., Khudiev, A., 2009. What is the correct form of BET isotherm for modeling liquid phase adsorption? Adsorption 15, 65–73. https://doi.org/10.1007/S10450-009-9151-3/METRICS

Foster, J.E., Mujovic, S., Krishnan, S., Rawindran, H., Sinnathambi, C.M., Lim, J.W., Mohan Sinnathambi, C., 2017. Comparison of various advanced oxidation processes used in remediation of industrial wastewater laden with recalcitrant pollutants. IOP Conf. Ser. Mater. Sci. Eng. 206, 012089. https://doi.org/10.1088/1757-899X/206/1/012089

Giles, C.H., MacEwan, T.H., Nakhwa, S.N., Smith, D., 1960. 786. Studies in adsorption. Part XI. A system of classification of solution adsorption isotherms, and its use in diagnosis of adsorption mechanisms and in measurement of specific surface areas of solids. J. Chem. Soc. 3973–3993. https://doi.org/10.1039/JR9600003973

ISO9277, 2010. Determination of Specific Surface Area of Solids by Gas Adsorption - BET Method, Second Ed., ISO. Switzerland.

Jain, M., Yadav, M., Kohout, T., Lahtinen, M., Garg, V.K., Sillanpää, M., 2018. Development of iron oxide/activated carbon nanoparticle composite for the removal of Cr(VI), Cu(II) and Cd(II) ions from aqueous solution. Water Resour. Ind. 20, 54–74. https://doi.org/10.1016/J.WRI.2018.10.001

Kalam, S., Abu-Khamsin, S.A., Kamal, M.S., Patil, S., 2021. Surfactant Adsorption Isotherms: A Review. ACS Omega 6, 32342. https://doi.org/10.1021/ACSOMEGA.1C04661

Keerthana, K., Thivyatharsan, R., 2018. Evaluation of the efficiency of constructed wetland and activated charcoal for the treatment of slaughterhouse wastewater. Earth, Energy Environ. 6, 12.

Kim, S., Kim, J., Seo, G., 2013. Iron oxide nanoparticle-impregnated powder-activated carbon (IPAC) for NOM removal in MF membrane water treatment system. New pub Balaban 51, 6392–6400. https://doi.org/10.1080/19443994.2013.781000

Konggidinata, M.I., Chao, B., Lian, Q., Subramaniam, R., Zappi, M., Gang, D.D., 2017. Equilibrium, kinetic and thermodynamic studies for adsorption of BTEX onto Ordered Mesoporous Carbon (OMC). J. Hazard. Mater. 336, 249–259. https://doi.org/10.1016/J.JHAZMAT.2017.04.073

Krahnstöver, T., Wintgens, T., 2018. Separating powdered activated carbon (PAC) from wastewater – Technical process options and assessment of removal efficiency. J. Environ. Chem. Eng. 6, 5744–5762. https://doi.org/10.1016/J.JECE.2018.09.001

Labuto, G., Carvalho, A.P., Mestre, A.S., dos Santos, M.S., Modesto, H.R., Martins, T.D., Lemos, S.G., da Silva, H.D.T., Carrilho, E.N.V.M., Carvalho, W.A., 2022. Individual and competitive adsorption of ibuprofen and caffeine from primary sewage effluent by yeast-based activated carbon and magnetic carbon nanocomposite. Sustain. Chem. Pharm. 28, 100703. https://doi.org/10.1016/j.scp.2022.100703

Lawtae, P., Tangsathitkulchai, C., 2021. The use of high surface area mesoporous-activated carbon from longan seed biomass for increasing capacity and kinetics of methylene blue adsorption from aqueous solution. Molecules 26(21), 6521. https://doi.org/10.3390/molecules26216521

Lin, L., Yuan, S., Lin, L., Yuan, S., Chen, J., Xu, Z., Lu, X., 2009. Removal of ammonia nitrogen in wastewater by microwave radiation. J. Hazard. Mater. 161, 1063–1068. https://doi.org/10.1016/j.jhazmat.2008.04.053

Liu, S., 2015. Cooperative adsorption on solid surfaces. J. Colloid Interface Sci. 450, 224–238. https://doi.org/10.1016/J.JCIS.2015.03.013

Lompe, K.M., Menard, D., Barbeau, B., 2017. The influence of iron oxide nanoparticles upon the adsorption of organic matter on magnetic powdered activated carbon. Water Res. 123, 30–39. https://doi.org/10.1016/J.WATRES.2017.06.045

Madeira, L., Almeida, A., Ribau Teixeira, M., Prazeres, A., Chaves, H., Carvalho, F., 2020. Immediate one-step lime precipitation and atmospheric carbonation as pre-treatment for low biodegradable and high nitrogen wastewaters: A case study of explosives industry. J. Environ. Chem. Eng. 8, 103808. https://doi.org/10.1016/j.jece.2020.103808

Madeira, L., Carvalho, F., Almeida, A., Ribau Teixeira, M., 2023. Optimization of atmospheric carbonation in the integrated treatment immediate one-step lime precipitation and atmospheric carbonation. The case study of slaughterhouse effluents. Results Eng. 17, 100807. https://doi.org/10.1016/J.RINENG.2022.100807

Madeira, L., Carvalho, F., Teixeira, M.R., Ribeiro, C., Almeida, A., 2021. Vertical flow constructed wetland as a green solution for low biodegradable and high nitrogen wastewater: A case study of explosives industry. Chemosphere 272, 129871. https://doi.org/10.1016/j.chemosphere.2021.129871

Manh, L.H., Dung, N.N.X., Van Am, L., Le Minh, B.T., 2014. Treatment of wastewater from slaughterhouse by biodigester and *Vetiveria zizanioides* L. L. Livest. Res. Rural Dev. 26.

Mburu, C., Kipkemboi, J., Kimwaga, R., 2019. Impact of substrate type, depth and retention time on organic matter removal in vertical subsurface flow constructed wetland mesocosms for treating slaughterhouse wastewater. Phys. Chem. Earth 114, 102792. https://doi.org/10.1016/j.pce.2019.07.005

Mestre, A.S., Pires, J., Nogueira, J.M.F., Parra, J.B., Carvalho, A.P., Ania, C.O., 2009. Waste-derived activated carbons for removal of ibuprofen from solution: Role of surface chemistry and pore structure. Bioresour. Technol. 100, 1720–1726. https://doi.org/10.1016/J.BIORTECH.2008.09.039

Mestre, A.S., Viegas, R.M.C., Mesquita, E., Rosa, M.J., Carvalho, A.P., 2022. Engineered pine nut shell derived activated carbons for improved removal of recalcitrant pharmaceuticals in urban wastewater treatment. J. Hazard. Mater. 437, 129319. https://doi.org/10.1016/J.JHAZMAT.2022.129319

Ng, M., Dalhatou, S., Wilson, J., Kamdem, B.P., Temitope, M.B., Paumo, H.K., Djelal, H., Assadi, A.A., Nguyen-tri, P., Kane, A., 2022. Characterization of Slaughterhouse Wastewater and Development of Treatment Techniques: A Review. Processes. 10(7), 1300. https://doi.org/10.3390/pr10071300

Noh, J.S., Schwarz, J.A., 1989. Estimation of the point of zero charge of simple oxides by mass titration. J. Colloid Interface Sci. 130, 157–164. https://doi.org/10.1016/0021-9797(89)90086-6

Odong, R., Kansiime, F., Omara, J., Kyambadde, J., 2013. The potential of four tropical wetland plants for the treatment of abattoir effluent. Int. J. Environ. Technol. Manag. 16, 203–222. https://doi.org/10.1504/IJETM.2013.053640

Park, H.S., Koduru, J.R., Choo, K.H., Lee, B., 2015. Activated carbons impregnated with iron oxide nanoparticles for enhanced removal of bisphenol A and natural organic matter. J. Hazard. Mater. 286, 315–324. https://doi.org/10.1016/J.JHAZMAT.2014.11.012

Prazeres, A.R., Fernandes, F., Madeira, L., Luz, S., Albuquerque, A., Simões, R., Beltrán, F., Jerónimo, E., Rivas, J., 2019. Treatment of slaughterhouse wastewater by acid precipitation (H_2SO_4, HCl and HNO_3) and oxidation ($Ca(ClO)_2$, H_2O_2 and CaO_2). J. Environ. Manage. 250, 109558. https://doi.org/10.1016/j.jenvman.2019.109558

Ramalho, M., Jovanović, T., Afonso, A., Baía, A., Lopes, A., Fernandes, A., Almeida, A., Carvalho, F., 2022. Landfill leachate treatment by immediate one-step lime precipitation, carbonation, and phytoremediation fine-tuning. Environ. Sci. Pollut. Res. 1, 1–10. https://doi.org/10.1007/S11356-022-18729-7/TABLES/3

Ramos-Arcos, S.A., G. González-Mondragón, E., S. López-Hernández, E., R. Rodríguez-Luna, A., M. Morales-Bautista, C., Lagunas-Rivera, S., López-Martínez, S., 2022. Phytoremediation Potential of *Chrysopogon zizanioides* for Toxic Elements in Contaminated Matrices, in: Biodegradation Technology of Organic and Inorganic Pollutants. IntechOpen. https://doi.org/10.5772/intechopen.98235

Rathi, B.S., Kumar, P.S., 2021. Application of adsorption process for effective removal of emerging contaminants from water and wastewater. Environ. Pollut. 280, 116995. https://doi.org/10.1016/J.ENVPOL.2021.116995

Revellame, E.D., Fortela, D.L., Sharp, W., Hernandez, R., Zappi, M.E., 2020. Adsorption kinetic modeling using pseudo-first order and pseudo-second order rate laws: A review. Clean. Eng. Technol. 1, 100032. https://doi.org/10.1016/J.CLET.2020.100032

Rodriguez-Reinoso, F., Martin-Martinez, J.M., Prado-Burguete, C., McEnaney, B., 1987. A standard adsorption isotherm for the characterization of activated carbons. J. Phys. Chem. 91, 515–516. https://doi.org/10.1021/J100287A006/ASSET/J100287A006.FP.PNG_V03

Rouquerol, J., Llewellyn, P., Rouquerol, F., 2006. Is the BET equation applicable to microporous adsorbents?, in: P.L. Llewellyn, F. Rodriquez Reinoso, J. Rouqerol, N.S. (Ed.), Characterization of Porous Solids Vii - Proceedings of the 7th International Symposium on the Characterization of Porous Solids. pp. 49–56.

Rouquerol, J., Rouquerol, F., Llewellyn, P., Maurin, G., Sing, K.S., 2013. Adsorption by powders and porous solids: principles, methodology and applications, Academic press.

Sahoo, T.R., Prelot, B., 2020. Chapter 7 - Adsorption processes for the removal of contaminants from wastewater: The perspective role of nanomaterials and nanotechnology, in: Nanomaterials for the Detection and Removal of Wastewater Pollutants. Elsevier, pp. 161–222. https://doi.org/10.1016/B978-0-12-818489-9.00007-4

Shahrashoub, M., Bakhtiari, S., 2021. The efficiency of activated carbon/magnetite nanoparticles composites in copper removal: Industrial waste recovery, green synthesis, characterization, and adsorption-desorption studies. Microporous Mesoporous Mater. 311, 110692. https://doi.org/10.1016/J.MICROMESO.2020.110692

Soroko, M., 2007. Treatment of wastewater from small slaughterhouse in hybrid constructed wetlands systems, in: Ecohydrology and Hydrobiology. Polish Academy of Sciences, pp. 339–343. https://doi.org/10.1016/S1642-3593(07)70117-9

Tabatabai, M.A., 1998. Handbook of Reference Methods for Plant Analysis. Crop Sci. 38, 1710–1711. https://doi.org/10.2135/cropsci1998.0011183x003800060050x

Thommes, M., Kaneko, K., Neimark, A. V., Olivier, J.P., Rodriguez-Reinoso, F., Rouquerol, J., Sing, K.S.W., 2015. Physisorption of gases, with special reference to the evaluation of surface area and pore size distribution (IUPAC Technical Report). Pure Appl. Chem. 87, 1051–1069. https://doi.org/10.1515/PAC-2014-1117/MACHINEREADABLECITATION/RIS

Tjelldén, A.K.E., Kristiansen, S.M., Matthiesen, H., Pedersen, O., 2015. Impact of roots and rhizomes on wetland archaeology: A review. Conserv. Manag. Archaeol. Sites, 17(4), 370-391. https://doi.org/10.1080/13505033.2016.1175909

VanderZaag, A.C., Gordon, R.J., Burton, D.L., Jamieson, R.C., Stratton, G.W., 2008. Ammonia Emissions from Surface Flow and Subsurface Flow Constructed Wetlands Treating Dairy Wastewater. J. Environ. Qual. 37, 2028–2036. https://doi.org/10.2134/JEQ2008.0021

Vargues, F., Brion, M.A., Rosa da Costa, A.M., Moreira, J.A., Ribau Teixeira, M., 2021. Development of a magnetic activated carbon adsorbent for the removal of common pharmaceuticals in wastewater treatment. Int. J. Environ. Sci. Technol. 18, 2805–2818. https://doi.org/10.1007/S13762-020-03029-9/FIGURES/9

Viegas, R.M.C., Mestre, A.S., Mesquita, E., Campinas, M., Andrade, M.A., Carvalho, A.P., Rosa, M.J., 2020. Assessing the applicability of a new carob waste-derived powdered activated carbon to control pharmaceutical compounds in wastewater treatment. Sci. Total Environ. 743, 140791. https://doi.org/10.1016/J.SCITOTENV.2020.140791

Vinayagam, R., Pai, S., Murugesan, G., Varadavenkatesan, T., Narayanasamy, S., Selvaraj, R., 2022. Magnetic activated charcoal/Fe_2O_3 nanocomposite for the adsorptive removal of 2,4-Dichlorophenoxyacetic acid (2,4-D) from aqueous solutions: Synthesis, characterization, optimization, kinetic and isotherm studies. Chemosphere 286. https://doi.org/10.1016/j.chemosphere.2021.131938

Vymazal, J., 2007. Removal of nutrients in various types of constructed wetlands. Sci. Total Environ. 380, 48–65. https://doi.org/10.1016/J.SCITOTENV.2006.09.014

Vymazal, J., 2006. Constructed wetland with emergent macrophytes: from experiments to a high quality treatment technology., in: 10th International Conference on Wetland Systems for Water Pollution Control, Lisbon, Portugal. pp. 1611–1621.

Chapter 7

Reuse of lime sludge from immediate one-step lime precipitation process as a coagulant (aid) in slaughterhouse wastewater treatment

This Chapter was submitted and is under review as:

Madeira, L., Ribau Teixeira, M., Almeida, A., Santos, T., Carvalho, F. Reuse of lime sludge from immediate one-step lime precipitation process as a coagulant (aid) in slaughterhouse wastewater treatment. Submitted to Journal of Environmental Management in March 2023.

ABSTRACT

The circularity of wastewater treatment subproducts is on the worldwide agenda. In this way, this work aims to evaluate alternatives for the reuse of sludge from slaughterhouse wastewater treatment. Wetted sludges produced in the immediate one-step lime precipitation process were applied directly or first calcinated, as a coagulant or coagulant aid, in the absence or presence of $Ca(OH)_2$, to slaughterhouse wastewaters with different characteristics. For the best sludge reuse, successive reuses of the sludge were carried out and the characteristics of treated slaughterhouse wastewater were evaluated after each reuse. Results showed a great similarity between slaughterhouse and treated slaughterhouse wastewaters using wetted and calcined sludges as a coagulant for highly contaminated slaughterhouse wastewater. In addition, a great similarity was also observed between the calcined and the wetted sludges, both as a coagulant aid, for all the slaughterhouse wastewaters tested. However, the latter consumed more hydrated lime, more volume of sludge sedimented, and higher concentrations of phosphorus and organic matter in the treated wastewater. Calcined sludge as a coagulant aid guaranteed the best slaughterhouse wastewater quality for most of the tested parameters (≥ 94% for absorbances at 254 nm and 410 nm, *E. coli*, turbidity, and phosphorus, chemical oxygen demand between 3-91%, and total Kjeldahl nitrogen between 3-62%) independently of the wastewater characteristics. Calcined sludge as a coagulant aid can be three times reused for the tested parameters and slaughterhouse wastewater characteristics without significantly decreasing the quality. The successive sludge reused saves the hydrated lime dose applied (up to 28.4%) and the sedimented sludge volume (up to 24.7%), and can be a solution to stabilize sludge due to the pH increase (sludge pH=12).

7.1. Introduction

Slaughterhouses produce large amounts of wastewater and global meat production will grow until 2031, according to OECD/FAO (2022). Thus, an increase in sludge production resulting from the slaughterhouse wastewater (SWW) treatment processes (*e.g.*, flotation, coagulation-flocculation, and activated sludge processes) is expected. These sludges are characterized by a high content of organic matter, nutrients, and pathogens among other contaminants, which could have an impact on the environment if they are not properly disposed of (Ávila-Pozo et al., 2021).

Sludge from the activated sludge process at slaughterhouses have been investigated regarding their recovery as a nutrient source for energy crop (Ozdemir et al., 2020) and walnut plantation (Ozdemir et al., 2019), or for the production of biogas (Agabo-García et al., 2022; Erden, 2013), tiles (Ferreira et al., 2018) and stabilized compounds for agriculture (Martins et al., 2022). Other applications of sludge from the dissolved air flotation process have been studied, such as crop growth (De Oliveira et al., 2018) and biodiesel production (Pirmoradi et al., 2021). However, the valorization of the sludge from the coagulation-flocculation process (that uses metallic coagulants such as ferric sulfate, ferric chloride, aluminum sulfate, or aluminum chloride, Bustillo-Lecompte & Mehrvar, 2015), is practically non-existent. Metallic coagulants can be recovered by acidifying the sludge, but this process is complex and expensive in heavily contaminated sludge (Chakraborty et al., 2020; Shewa and Dagnew, 2020), so less attractive (Basibuyuk and Kalat, 2004; Foroughi et al., 2018; Jangkorn et al., 2011; Mazari et al., 2018; Scalize et al., 2019; Taheriyoun et al., 2020). In this way, slaughterhouse sludges are usually dehydrated, stabilized, and sent to landfill (Alvarenga et al., 2015). Nevertheless, this solution is not environmentally sustainable, so new valorization processes must be studied to increase the sustainability and circularity of these wastewaters (de Oliveira et al., 2018; Gherghel et al., 2019; Guerra-Rodríguez et al., 2020). Lime precipitation has been studied as an alternative to the coagulation-flocculation process in wastewater treatment, since i) hydrated lime is a low-cost reagent, ii) high chemical oxygen demand (≥87%) and phosphorus (≥94-99%) removals have been observed in the treatment of various types of wastewater (*e.g.*, cheese whey wastewaters (Prazeres et al., 2016), landfill leachate (Ramalho et al., 2022), and slaughterhouse (Hossaini et al. 2013)), and iii) the high

reaction's pH produced stabilized sludge (Luz et al., 2021). However, the disadvantage of lime precipitation compared to coagulation-flocculation is the production of larger amounts of sludge (Satyanarayan et al., 2005). Thus, solutions for sludges reuse must be found. Prazeres et al. (2016) and Ramalho et al. (2022) demonstrated the possibility of using the sludge as an acidity corrector in acidic and/or calcium-deficient soils for lime sludge with high pH values (≥12.4). Martínez-Cruz et al. (2021) concluded that the sludge from leachate chemical precipitation can be applied as sanitary landfill coverage. However, to the best of our knowledge, no study on the reuse of lime sludge resulting from wastewater treatment by lime precipitation as a reagent in wastewater treatment has been found. Although lime sludges have considerable amounts of contaminants (e.g., organic matter, phosphorus, etc.) (Prazeres et al., 2016), the interest in reusing these sludges as a reagent lies in the presence of calcium carbonate, which has the potential to remediate the inorganic and organic pollutants from the environment by the adsorption process (Yadav et al., 2021). Some studies have evaluated the use of lime sludge resulting from the softening process of water treatment plants (WTP) as a reagent, either directly or indirectly (*e.g.,* using a previous heat treatment), in the treatment of industrial wastewater. For example, Van Leeuwen et al. (2010) evaluated the use of lime sludge to neutralize acidic industrial wastewater in food processing. These authors observed that these lime sludges effectively adjusted the pH of the wastewater to the desired value without increasing salinity, but also contributed to better sedimentation of the sludge flocs and savings in pH adjustment reagents. On the other hand, Bal Krishna et al. (2017) observed that the calcined lime sludge resulting from WTP can be effective in removing phosphorus from aqueous solutions. In fact, when lime sludges are subjected to heat treatment, there is a change in their texture, which provides a greater capacity for adsorbing contaminants (Yan et al., 2014). Temperature is a determining factor in the calcination process of lime sludge since it can determine the presence/absence of organic matter and the fractions of $CaCO_3$, CaO, and MgO in the calcined sludge, and consequently the adsorption capacity of contaminants (Köse and Kivanç, 2011; Wajima and Rakovan, 2013). Bal Krishna et al. (2017) observed a significant improvement in phosphorus removal efficiency from aqueous solution using calcined lime sludge obtained at high temperatures (i.e., 700°C, with 96 to 99% of phosphorus removal), rather than when calcined at 400 ºC (9% of phosphorus removal) and oven dried at 105 ºC (5% of phosphorus removal). However, the ability of lime sludges calcined at high temperatures, from industrial wastewater treatment to treat wastewaters is unknown. The

adsorption capacity of pollutants by lime sludge from WTP is likely greater than that of lime sludge from wastewater treatment since the latter has a higher concentration of pollutants in their composition. However, it is not known to what extent the reuse of the lime sludge from wastewater treatment would be effective in the treatment of industrial effluents or would need to be supplemented with the addition of hydrated lime.

Thus, the purpose of this work is to evaluate the reuse of lime sludge resulting from the immediate one-step lime precipitation (IOSLM) process as a coagulant and coagulant aid in the SWW treatment, with and without heat treatment, as well as the possibility of sludge successive reuse. Given the recognized variability of slaughterhouse wastewater characteristics, it is important to obtain a sludge reuse method that is universally suitable for all types of slaughterhouse water characteristics. In this way, different slaughterhouse wastewater characteristics were tested.

7.2. Materials and Methods

7.2.1. Slaughterhouse wastewater collection

SWW was collected in three different places from a full-operation slaughterhouse wastewater treatment plant, in Portugal: SWW was collected in the aeration and homogenization tank (pre-aerated SWW), at the exit of the sieve (sieved SWW), and after coagulation-flocculation/dissolved air flotation (CF/DAF SWW). Samples were stored in containers and kept at 4ºC until the IOSLM tests started. The characterization of the three SWWs is provided in Table 7.1.

Table 7.1 – Physicochemical and microbiological characterization of pre-aerated SWW, sieved SWW, and CF/DAF SWW.

Parameters	Unit	Pre-aerated SWW	Sieved SWW	CF/DAF SWW
pH	Sorensen	7.1±0.0	7.2±0.2	7.4±0.1
Conductivity	mS cm^{-1}	3.0±0.1	2.9±0.1	3.0±0.1
COD	mg O_2 L^{-1}	6981±476	1524±84	219±4
SCOD	mg O_2 L^{-1}	183±47	461±38	190±5
TKN	mg N-Kj. L^{-1}	213±2	96±2	62±0
NH_4^+	mg N-NH_4^+ L^{-1}	89±1	69±1	51±1
Total phosphorus	mg L^{-1}	554.9±29.9	329.6±39.8	156.0±20.1
Abs. at 254 nm	cm^{-1}	1.679±0.139	0.970±0.028	0.205±0.040
Abs. at 410 nm	cm^{-1}	2.197±0.217	1.641±0.029	0.325±0.087
Turbidity	NTU	1234±28	467±7	13±0
TSS	mg L^{-1}	3696±12	860±20	66±5
Nitrate	mg N L^{-1}	< 2	< 2	< 2
Nitrites	mg N L^{-1}	< 0.05	< 0.05	< 0.05
Calcium	mg L^{-1}	190.5±0.0	156.7±3.4	192.4±3.4
Magnesium	mg L^{-1}	60.2±4.2	77.0±4.2	59.0±2.1
Chlorides	mg L^{-1}	961.9±32.1	621.6±32.1	803.1±32.1
Sodium	mg L^{-1}	602.4±16.9	331.0±16.9	319.1±0.0
Potassium	mg L^{-1}	25.3±0.3	24.5±0.3	13.5±0.9
Iron	mg L^{-1}	6.924±0.090	3.192±0.076	0.234±0.006
Manganese	mg L^{-1}	0.456±0.005	0.348±0.009	0.176±0.017
Copper	mg L^{-1}	0.404±0.062	0.378±0.055	0.352±0.020
Lead	mg L^{-1}	<DL	<DL	<DL
Nickel	mg L^{-1}	<DL	<DL	<DL
Zinc	mg L^{-1}	0.672±0.024	0.364±0.008	0.183±0.066
Cadmium	mg L^{-1}	<DL	<DL	<DL
E. coli	CFU/100 ml	17500	900	20

Note: DL – Detection limit.

7.2.2. Experimental set-up

First, experiments were performed to produce the sludges using the immediate one-step lime precipitation (IOSLM) process. This process was already described by Madeira et al. (2020) (chapter 2) and Madeira et al. (2023) (chapter 3). Briefly, the IOSLM process uses hydrated lime solution (at 200 g L^{-1}), drop by drop, under vigorous agitation until pH 12 is reached. After 1 minute the stirring stopped, and the sedimentation took place for 1 hour. Then, the sedimented sludges were used in the reuse tests started. In this experiment, about 1.31±0.08, 1.10±0.14, and 1.00±0.20 g L^{-1} of hydrated lime were used to treat pre-aerated SWW, sieved SWW, and CF/DAF SWW, respectively. A scheme of the experimental setup used is shown in Figure 7.1.

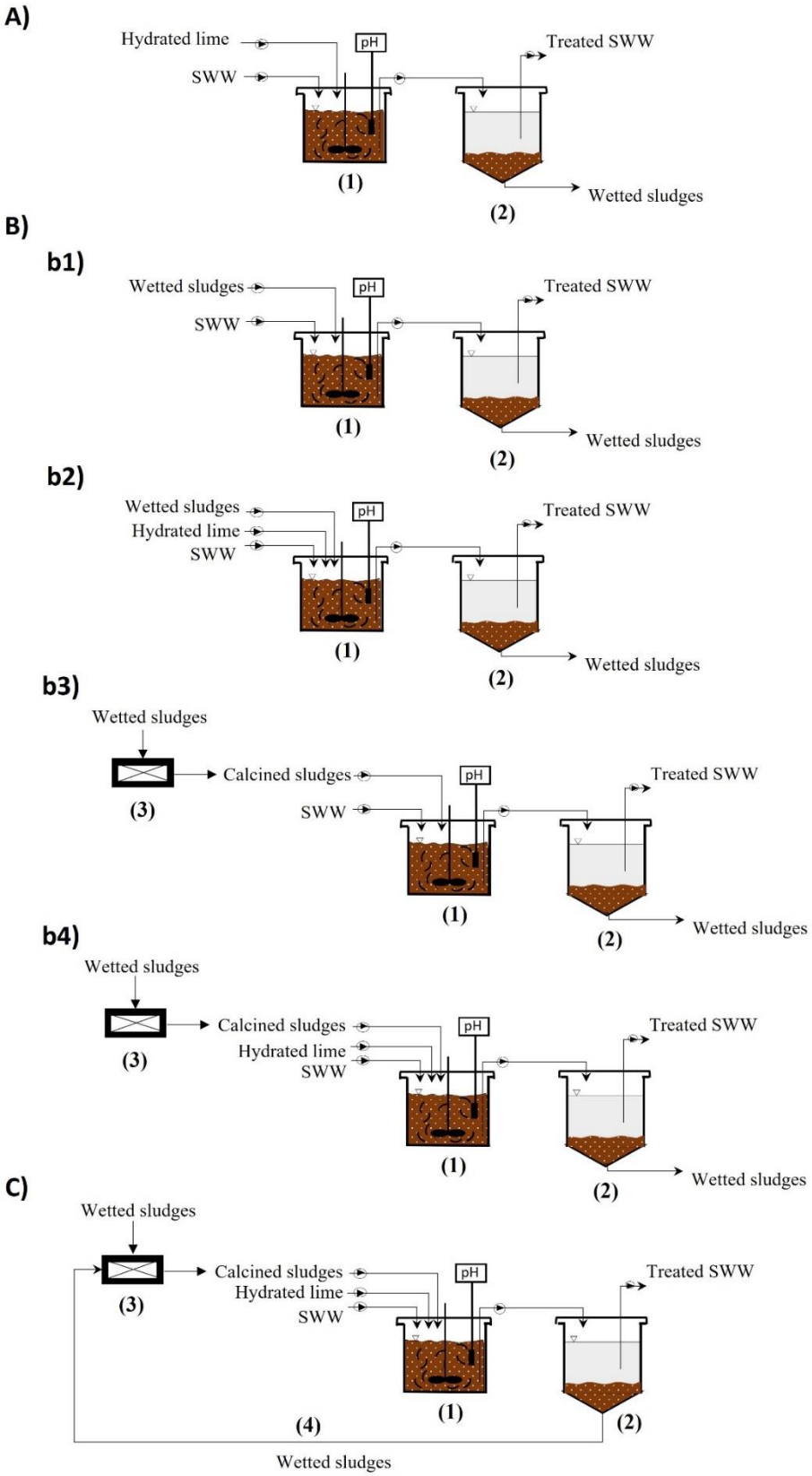

Figure 7.1 – Schematic diagram relating to A) wetter sludge production test by IOSLM process; B) sludge reuse test, using: b1) wetted sludge as coagulant, b2) wetted sludge as coagulant aid, b3) calcined sludge as coagulant, and b4) calcined sludge as coagulant aid; C) successive sludge reuse test. Numbers 1, 2, 3, and 4 refer to the IOSLM process, sedimentation operation, calcination process, and successive sludge recirculation as reagent for the IOSLM process, respectively.

7.2.2.1. Sludge reuse tests

Table 7.2 presents the characteristics of the sludges produced in the IOSLM process using pre-aerated SWW, sieved SWW, and CF/DAF SWW.

Table 7.2 – Characteristics of the sludge obtained by the IOSLM process at pH 12, using Pre-aerated SWW, sieved SWW, and CF/DAF SWW.

Parameters	Unit	Pre-aerated SWW	Sieved SWW	CF/DAF SWW
Sedimented sludge volume	mL L^{-1}	148±11	85±2	56±7
Centrifuged sludge volume	mL L^{-1}	56±11	14±3	5±1
Centrifuged sludge weight	mg L^{-1}	29.6±5.5	9.3±1.5	3.3±0.2
Dry matter	%	18.9±1.2	26.1±0.2	43.1±2.0
Organic matter (dry sample)	%	66.8±1.3	39.6±8.8	11.3±2.7
Organic matter (wet sample)	%	12.6±0.6	10.3±2.2	4.9±1.3
pH	Sorensen	10.4±0.2	11.0±0.0	11.9±0.1
Conductivity	mS cm^{-1}	0.4±0.1	0.3±0.0	0.5±0.1
Calcium	g kg^{-1}	145.1±9.6	265.2±22.3	414.2±13.8
Magnesium	g kg^{-1}	28.8±6.6	32.4±14.9	28.6±16.0
Chlorides	g kg^{-1}	2.2±0.1	2.3±1.2	1.2±0.2
TKN	g kg^{-1}	15.8±0.4	6.6±0.1	1.6±0.1
Sodium	g kg^{-1}	4.4±0.2	2.7±0.3	3.0±0.6
Potassium	g kg^{-1}	0.2±0.0	0.1±0.0	0.4±0.2
Iron	g kg^{-1}	1.5±0.3	1.2±0.1	0.4±0.1
Manganese	mg kg^{-1}	116.8±9.1	170.2±16.2	269.8±6.9
Copper	mg kg^{-1}	26.4±12.4	20.3±1.3	11.6±1.8
Zinc	mg kg^{-1}	153.2±21.6	118.2±22.4	30.4±14.3
Cadmium	mg kg^{-1}	1.0±0.0	1.5±0.0	1.4±0.3
Total phosphorus	g kg^{-1}	1.3±0.4	3.0±0.7	0.8±0.4

Two sets of experiments were conducted using the sludges from these three SWW. In the first set, about 37 mL (for pre-aerated SWW), 21 mL (for sieved SWW), and 14 mL (for CF/DAF SWW) of the sedimented sludge were used in the following ways: wetted sludges as coagulant (WSC) (Figure 7.1b1), wetted sludges as coagulant aid (WSCA) (Figure 7.1b2), calcined sludge as coagulant (CSC) (Figure 7.1b3), and calcined sludge as coagulant aid (CSCA) (Figure 7.1b4). Experiments with wetted or calcined sludge as a coagulant (Figures 7.1b1 and 7.1b3) included the application of the sludges directed to the jar without hydrated lime. When wetted or calcinated sludges were used as a coagulant aid, first the sludges were added to the SWW, and then the hydrated lime (about 1.26±0.22, 1.13±0.00 and 1.21±0.08 g L^{-1} for WSCA and 1.20±0.00, 0.80±0.12 and 0.73±0.06 g L^{-1} for CSCA were used in pre-aerated SWW, sieved SWW, and CF/DAF SWW, respectively) to adjust the pH at 12 (Figures 7.1b2 and 7.1b4). Calcined sludges

were prepared using wetted sludges heated at 100ºC in an oven and at 700ºC in an electric muffle furnace (Select-Horn, P Selecta) for 2 hours under an air atmosphere, followed by the maceration. The sludges (wetted or calcinated) were applied to 250 mL of SWWs, and precipitation and sedimentation processes took place as described by Madeira et al. (2020) (chapter 2). The treated SWW was separated from the sludge after the sedimentation, and then both samples were analyzed according to section 7.2.3.

In the second set of experiments, the sludges were successively reused (up to three times) (Figure 7.1c). Thus, the sludges resulting from the first set of experiments were calcined and then added as a coagulant aid to 1 L of SWW along with hydrated lime to adjust pH to 12, under the same operating conditions mentioned in the first set of experiments. The physicochemical characteristics of treated SWW were evaluated after each reuse (section 7.2.3). The sludges obtained after the first and third reuse were analyzed (section 7.2.3).

7.2.3. Analytical methods

All wastewater and sludge samples were analyzed according to Standard Methods for the examination of water and wastewater and EN standards, respectively (Table 7.3). The effluents samples were characterized in terms of pH, conductivity, total Kjeldahl nitrogen (TKN), total phosphorus (TP), calcium, magnesium, chlorides, sodium, potassium, heavy metals (Fe, Mn, Cu, Pb, Ni, Zn, and Cd), chemical oxygen demand (COD), soluble chemical oxygen demand (SCOD), ammonium nitrogen (NH_4^+), turbidity, total suspended solids (TSS), nitrites, and *E. coli* using standardized methods (Baird et al., 2017), absorbances at 254 and 410 nm using Rivas et al. (2010) method, and nitrate using Monteiro et al. (2003) method. Absorbance at 254 nm was determined because it indicates the presence of high molecular weight organic compounds with a high degree of aromaticity, a high number of double and triple bonds, and phenolic groups. Absorbance at 410 nm was quantified because it indicates the presence of compounds responsible for color (Rivas et al., 2010).

Table 7.3 – The parameters and analytical methods used.

Sample	Parameters	Equipment	Method
Effluent and sludge	pH	WTW InoLab pH Level 1 apparatus; pH electrode SenTix® 4; P Selecta Unitronic 320 OR for sludge agitation	Potentiometric method (Baird et al., 2017)[1] (EN 12176, 1998)[2]
	Conductivity	Jenway 4510 conductivity meter; conductivity sensor VWR phenomenal CO 11	Electrometric method (Baird et al., 2017)[1] (CEN/BT/Task Force 151, 2005)[2]
	Total Kjeldahl nitrogen	Bloc Digest 6 P-Selecta digester; distillation unit BUCHI B-316	Kjeldahl method (Baird et al., 2017)[1] (EN 13342, 2000)[2]
	Total phosphorus	Muffle P SELECTA-HORN 186331; UV/Vis spectrophotometer Pharmacia Biotech Ultrospec 2000	Colorimetric method (Baird et al., 2017)[1] (Kitson and Mellon, 1944)[2]
	Calcium	-	Volumetric complexation with EDTA (Baird et al., 2017)
	Magnesium	-	Difference between total hardness and calcium hardness (Baird et al., 2017)
	Chlorides	-	Mohr method (Baird et al., 2017)
	Sodium and Potassium	Corning Model 410 Flame Photometer	Flame photometric method (Baird et al., 2017)
	Fe, Mn, Cu, Pb, Ni, Zn and Cd	Varian SpectrAA 220FS equipment	Flame atomic absorption spectrometry method (Baird et al., 2017)[1] (EN 13346, 2000)[2]
Effluent	COD and SCOD	COD digester WPA Hydrocheck HC 6016, UV/Vis spectrophotometer Pharmacia Biotech Ultrospec 2000; 0.45-µm pore-size filter for soluble COD.	Closed reflux colorimetric method (Baird et al., 2017)
	NH_4^+	Distillation unit BUCHI B-316	Distillation method (Baird et al., 2017)
	Turbidity	HACH 2100N turbidimeter; 0.45-µm pore-size filter for soluble turbidity.	Nephelometric method (Baird et al., 2017)
	Total suspended solids	Whatman® glass microfiber filters (Grade 934-AH®)	Gravimetric method (Baird et al., 2017)
	Abs. at 254 and 410 nm	UV/Vis spectrophotometer Pharmacia Biotech Ultrospec 2000	Spectroscopic method (Rivas et al., 2010)
	Nitrate	-	Sodium salicylate method (Monteiro et al., 2003)
	Nitrites	-	Colorimetric method (Baird et al., 2017)
	E. coli	-	Membrane filter (MF) technique and most probable number method (Baird et al., 2017)
Sludge	Dry matter	Memmert UL40 Oven	Gravimetric method (EN 12880, 2000)
	Organic matter (dry or wet sample)	Muffle P Select-Horn 186331	Calcination method (EN 12879, 2000)

Note: 1 – Standard Methods for effluent; 2 – Standard Methods for sludge.

Wetted sludge was quantified in terms of volume (before and after centrifugation at 3500 rpm for 10 minutes using the Hermle Z300 Micro Centrifuge) and dry matter (EN 12880, 2000). pH (EN 12176, 1998), conductivity (CEN/BT/Task Force 151, 2005), chlorides (Baird et al., 2017) and TKN (EN 13342, 2000) were immediately measured after experiments. After weighing the centrifuged sludge, the calcination process started at 550°C and the organic matter content (dry and wet sample) was determined (EN 12879, 2000). The calcined sludges obtained were digested with hydrochloric acid (3N), followed by filtration with a WhatmanTM 1001 filter, and then diluted with deionized water (for total phosphorus (Kitson and Mellon, 1944), calcium, magnesium, sodium, and potassium determination (Baird et al., 2017)) or with aqua regia (for metals such as Fe, Mn, Cu, Pb, Ni, Zn and Cd determination (EN 13346, 2000)).

7.2.4. Statistical analysis

Statistical analysis of data was performed. The average and standard deviation were determined based on the analysis of samples and treatments in triplicate. One-way ANOVA (pairwise comparison of means with Tukey´s test at 95% confidence level) was applied to experimental data using GraphPad Prism (version 9.0.0 for Windows, GraphPad Software, San Diego, California USA). Cluster analysis was performed by Agglomerative Hierarchical Clustering (AHC), using the complete linkage method. Cluster analysis was determined by XLSTAT 2022 software.

7.3. Results and discussion

7.3.1. Sludge characterization

Table 7.2 presents the characteristics of the sludge obtained by the IOSLM process at pH 12 for all SWWs. The sludge characteristics varied with the characteristics of the SWWs (Table 7.1). As expected, the sludge from pre-aerated SWW and sieved SWW showed a higher percentage of organic matter and TKN than CF/DAF SWW, due to the initial characteristics of these effluents, pre-aerated SWW with a high concentration of COD and TKN (6981±476 mg O_2 L^{-1} and 213±2 mg N-Kj. L^{-1}), followed by sieved SWW (1524±84 mg O_2 L^{-1} and 96±2 mg N-Kj. L^{-1}) and CF/DAF SWW (219±4 mg O_2 L^{-1} and

62±0 mg N-Kj. L^{-1}). The sludge had low concentrations of heavy metals (Mn, Cu, Zn, and Cd). As a result of the IOSLM treatment, calcium was the most abundant inorganic element in the sludge. High calcium and phosphorus ratios (about 112:1, 88:1, and 518:1, for pre-aerated SWW, sieved SWW, and CF/DAF SWW, respectively) indicate that most of the calcium may be in the form of calcium carbonate. The decrease in the sludge volume after centrifugation indicates that most of the sedimented sludge was composed of water. After centrifugation, the sludge still had a low percentage of dry matter (about 19, 26, and 43% for pre-aerated SWW, sieved SWW, and CF/DAF SWW, respectively). All sludges had alkaline characteristics (pH ≥ 10.4) and a low conductivity value (0.3 to 0.5 mS cm^{-1}).

7.3.2. Sludge reuse as a coagulant and coagulant aid

Figures 7.2 and 7.3 show the characteristics of the raw SWWs, treated SWW by the IOSLM process, and treated SWWs using WSC, CSC, WSCA, and CSCA for the three wastewaters studied.

According to Figure 7.2a, WSC and CSC produced treated SWWs with pH values around 7.7 to 8.8 and 9.4 to 10.1, respectively, depending on the wastewater tested. Even so, these values were above the pH of the raw SWWs (between 7.1 and 7.4, Table 7.1). For WSC, this difference in water pH can be related to the pH of the sludge interstitial water, and/or to the dissolution of hydroxide precipitates (e.g., magnesium hydroxide). In fact, an increase in magnesium concentrations was observed for sieved SWW and CF/DAF SWW, when compared to raw SWWs (Figure 7.3b). Calcium hydroxide was completely dissociated in Ca^{2+} and OH^- ions in the IOSLM process since the maximum solubility of calcium hydroxide added in SWW was not achieved (i.e. 0.160 g/100 g water at 20ºC, Lide et al., 2003). Thus, it is not expected that there will be a contribution from the increase in pH by the eventual dissolution of calcium hydroxide.

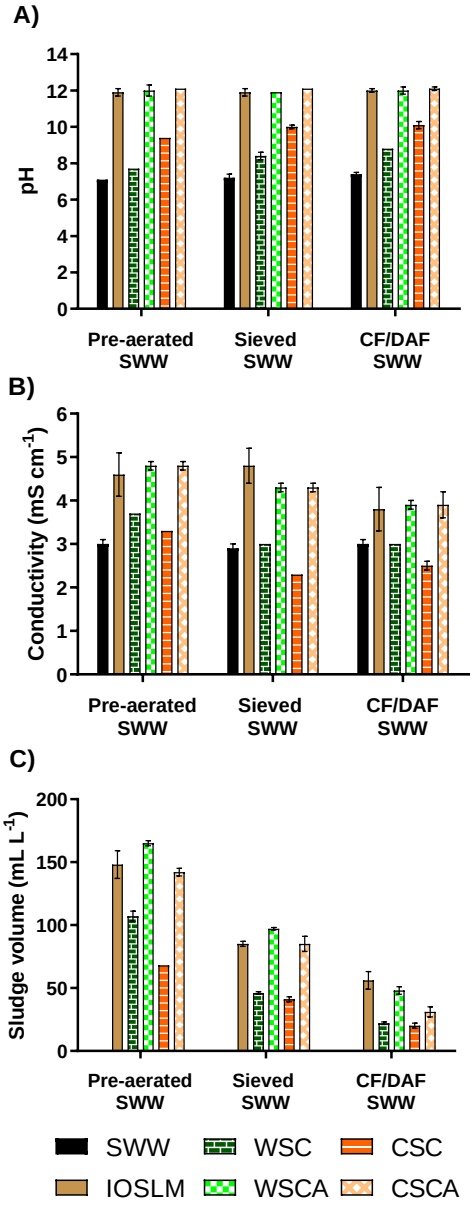

Figure 7.2 – Characteristics of raw SWWs, treated SWW by IOSLM process, and treated SWW by sludge reuse (wetted sludge as coagulant (WSC), wetted sludge as coagulant aid (WSCA), calcined sludge as coagulant (CSC), and calcined sludge as coagulant aid (CSCA)), for a) pH; b) conductivity, and c) sedimented sludge volume and pre-aerated SWW, sieved SWW, and CF/DAF SWW. Bars represent the standard deviation of the mean.

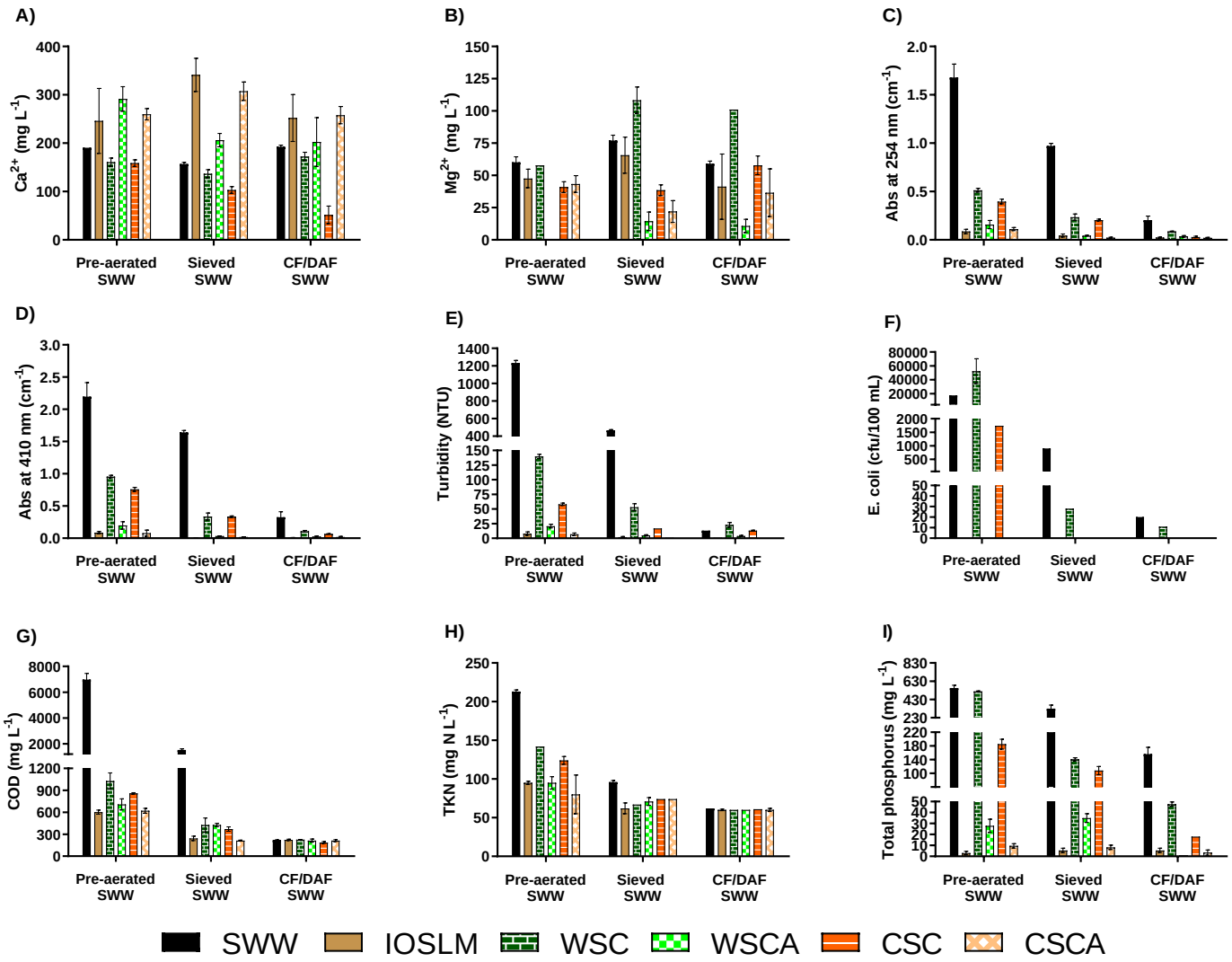

Figure 7.3 – Characteristics of the raw SWWs, treated SWW by IOSLM process, and treated SWW by sludge reuse (wetted sludge as coagulant (WSC), wetted sludge as coagulant aid (WSCA), calcined sludge as coagulant (CSC), and calcined sludge as coagulant aid (CSCA)), for a) calcium concentration; b) magnesium concentration; c) absorbance at 254 nm; d) absorbance at 410 nm; e) turbidity; f) *E. coli*; g) COD concentration; h) TKN concentration; and i) total phosphorus concentration, and pre-aerated SWW, sieved SWW and CF/DAF SWW. Bars represent the standard deviation of the mean.

For CSC sludges, the increase in pH was due to the dissolution of calcium oxide in the SWW. CSC sludges came from the calcination process, where calcium carbonate precipitates formed during the IOSLM process were subjected to high temperatures (e.g., 700 ºC), and were converted into calcium oxide (Eq. 1). Then, calcium oxide in water is dissociated into calcium ions and hydroxide ions (Eq. 2), raising the pH of the effluent. In addition, calcium oxide can also react with carbonic acid (Eq. 3), calcium bicarbonate (Eq. 4), magnesium bicarbonate (Eq. 5), or magnesium carbonate (Eq. 6) present in raw SWW, forming precipitates (calcium carbonate, magnesium carbonate, and magnesium hydroxides). Moreover, Krishna et al. (2017) observed that the temperature of the lime sludge calcination process may influence the pH of the effluent to be treated. These authors verified that for temperatures 400 and 700 ºC, there was a change in the effluent pH value from 7 to 8.77 and from 7 to 10.24, respectively.

$$CaCO_3 \rightarrow CaO + CO_2 \quad (1)$$

$$CaO + H_2O \rightarrow Ca^{2+} + 2OH^- \quad (2)$$

$$CaO + H_2CO_3 \rightarrow CaCO_3 + H_2O \quad (3)$$

$$CaO + Ca(HCO_3)_2 \rightarrow 2CaCO_3 + H_2O \quad (4)$$

$$CaO + Mg(HCO_3)_2 \rightarrow MgCO_3 + CaCO_3 + H_2O \quad (5)$$

$$CaO + MgCO_3 + H_2O \rightarrow CaCO_3 + Mg(OH)_2 \quad (6)$$

For CSCA and WSCA processes, treated SWWs had a pH around 12, due to the addition of hydrated lime to adjust pH to 12 (0.73 to 1.20 g L^{-1} and 1.13 to 1.26 g L^{-1}, respectively, depending on SWW tested). The consumption of hydrated lime in CSCA was lower than its consumption using WSCA. In fact, calcined sludges contain CaO which contributes to the pH increase and consequently, there was no need to apply high hydrated lime doses. On the other hand, the addition of hydrated lime resulted in the dissociation of calcium ions and hydroxide ions (Eq. 7), raising the pH, and in the production of precipitates (calcium carbonate, magnesium carbonate, or magnesium hydroxide), when reacting with carbonic acid (Eq. 8), calcium bicarbonate (Eq. 9), magnesium bicarbonate (Eq. 10) or magnesium carbonate (Eq. 11).

$$Ca(OH)_2 \rightarrow Ca^{2+} + 2OH^- \quad (7)$$

$$Ca(OH)_2 + H_2CO_3 \rightarrow CaCO_3 + 2H_2O \quad (8)$$

$$Ca(OH)_2 + Ca(HCO_3)_2 \rightarrow 2CaCO_3 + 2H_2O \quad (9)$$

$$Ca(OH)_2 + Mg(HCO_3)_2 \rightarrow MgCO_3 + CaCO_3 + 2H_2O \quad (10)$$

$$Ca(OH)_2 + MgCO_3 \rightarrow Mg(OH)_2 + CaCO_3 \quad (11)$$

For conductivity, there were no significant differences (P<0.05) for treated SWWs by CSCA and WSCA, with conductivity values around 3.9 to 4.6 mS cm^{-1} according to SWW tested (Figure 7.2b). These conductivity values were higher than the values found for WSC (3.0 to 3.7 mS cm^{-1}) or CSC (2.3 to 3.3 mS cm^{-1}), possibly due to a higher concentration of calcium in the solution, as shown in Figure 7.3a.

The sedimentation sludge volume was smaller using WSC (about 107, 41, and 20 mL L^{-1}, for pre-aerated SWW, sieved SWW, and CF/DAF SWW, respectively) and CSC (about 68, 46, and 22 mL L^{-1}, for pre-aerated SWW, sieved SWW, and CF/DAF SWW, respectively) (Figure 7.2c). This may indicate a lower production of precipitates (and consequently lower organic matter, nitrogen organic matter, and total phosphorus removals), possibly due to the low pH of the waters treated by WSC and CSC (Figure 7.2a). As expected, WSCA had a higher sedimented sludge volume (about 165, 97, and 48 mL L^{-1}, for pre-aerated SWW, sieved SWW, and CF/DAF SWW, respectively) than the other types of sludge reused, since sedimented sludge included the precipitates of the sludge and the precipitates formed in the meantime. The calcination process reduced the sedimented sludge volume (Figure 7.2c).

Comparing the raw SWWs quality and treated SWWs using sludge reuse, WSC, and CSC were the processes that resulted in high absorbances at 254 nm and 410 nm (Figures 7.3c and 7.3d, respectively) and turbidity (Figure 7.3e) in treated SWWs. For WSCA and CSCA, a higher decrease of absorbances at 254 nm and 410 nm, and turbidity was observed, for the different SWWs tested.

In CSCA and WSCA processes, 100% of *E. coli* were removed in all the SWWs tested (Figure 7.3f). Similar results were obtained with CSC but only for sieved SWW and CF/DAF SWW, due to the less initial quantity of *E. coli* present in these waters. In fact, pH was responsible for the removal of *E. coli*, as *E. coli* is a neutrophilic bacterium (grows optimally at pH between 5 and 8) so an increase in pH outside this range favors its inactivation (Paruch, 2015). The use of WSC as pre-aerated SWW treatment resulted in an increase in the amount of *E. coli*, from 17500 to 52500 cfu/100 mL, indicating that

these sludges were not chemically stabilized. These sludges had a pH of 10.4 (Table 7.2) and the pH of the treated pre-aerated SWW was 7.7 (Figure 7.2a), still within the *E. coli* growth range. Substantial removal of *E. coli* was observed with WSC as sieved SWW and CF/DAF SWW treatment, justified by the high pH (≥11) of their sludges (Table 7.2) and the high pH of the treated SWW (around 8.4 and 8.8, respectively, Figure 7.2a). Compared to WSC, CSC was more effective in removing *E. coli* since it was eliminated at high temperatures by the calcination process.

For COD and TKN concentrations (Figures 7.3g and 7.3h), all types of sludge reuse showed a significant (P<0.05) decrease in COD and TKN when compared with raw SWWs, reaching COD concentrations between 621 to 1029 mg O_2 L^{-1} for pre-aerated SWW and 213 to 426 mg O_2 L^{-1} for sieved SWW, and TKN concentrations between 80 to 142 mg N L^{-1} for pre-aerated SWW and 67 to 74 mg N L^{-1} for sieved SWW. However, for CF/DAF SWW there were no significant differences (P<0.05) in the COD and TKN concentrations between raw SWW and treated CF/DAF SWW from all types of sludge reuse, remaining the COD and TKN concentrations around 188 to 225 mg O_2 L^{-1} and 60 mg N L^{-1}, respectively. These results indicate that the organic matter present in CF/DAF SWW is not easily precipitable. Moreover, in this SWW the removal of NH_4^+ was not possible (even though the pH was above 9.2 for possible volatilization) since the stirring times were small (Madeira et al. (2020), chapter 2). The COD and organic nitrogen removals are related to the aggregation of colloidal SWW particles with precipitates (e.g., calcium carbonate, magnesium carbonate, or magnesium hydroxide) formed by the addition of hydrated lime (Eqs. 8 to 11) and/or CaO (from calcined sludge) (Eqs. 3 to 6). It is also possible, that part of the organic matter removal (including organic nitrogen) was due to the sedimentation of easily sedimentable solids, regardless of the form of sludge used. In fact, according to Satyanarayan et al. (2005), previous sedimentation of SWW (COD = 10226 mg O_2 L^{-1}) can result in a removal of 32% of COD and 75% of TSS.

All forms of sludge reuse decreased phosphorus concentrations for all SWW (except for pre-aerated SWW when the WSC was used) (Figure 7.3i). The SWWs treated by sludges supplemented with hydrated lime doses (CSCA and WSCA) presented a greater phosphorus decrease than the SWWs treated by sludge without hydrated lime addition (WSC and CSC). This means that the conversion of $CaCO_3$ to CaO during the calcination

process of the sludge is not sufficient to react with the phosphorus present in the effluent, and therefore, the addition of hydrated lime is still necessary. Bal Krishna et al. (2017) observed that phosphorus removal depends on the concentration of phosphorus in the solution and the amount of sludge reused. Phosphorus removals may be related to the formation of hydroxyapatite (Eq. 12), calcium phosphate (Eq. 13), and octacalcium phosphate (Eq. 14) precipitates (Dai et al., 2018).

$$5Ca^{2+} + 3PO_4^{3-} + OH^- \rightarrow Ca_5H(PO_4)_3OH \downarrow \quad (12)$$

$$3Ca(OH)_2 + 2PO_4^{3-} \rightarrow Ca_3(PO_4)_2 \downarrow + 6\ OH^- \quad (13)$$

$$4Ca(OH)_2 + 3PO_4^{3-} + H_2O \rightarrow Ca_4H(PO_4)_3 \downarrow + 9\ OH^- \quad (14)$$

Figure 7.4 shows the dendrogram of similarity between raw SWW and treated SWW by the studied sludge reuses (WSC, CSC, CSCA, and WSCA), based on their respective physicochemical characteristics (absorbance at 254 nm, absorbance at 410 nm, turbidity, *E. coli*, COD, TKN, and TP), for the three SWWs studied. Raw SWW is presented for comparison. According to Figure 7.4, there is a great similarity between CSCA and WSCA sludge reuses, and between WSC and CSC sludge reuses for all the studied SWWs. This indicates that the way the sludge is applied (i.e. as a coagulant or coagulant aid) had a higher impact on the results than how the sludge is treated (i.e. wetted or calcined). CSCA and WSCA provide a treated SWW with higher pH and greater removal of the tested parameters. Figure 7.4a shows a great similarity between pre-aerated SWW and treated waters using WSC and CSC sludge reuses, indicating that these types of sludge reuse were not effective in the treatment of SWW with high concentrations of contaminants as was the case of pre-aerated SWW. For sieved SWW (Figure 7.4b) and CF/DAF SWW (Figure 7.4c), the similarity is higher between treated waters using WSCA and CSCA, and WSC and CSC, indicating that these types of sludges reuse may be more advantageous for less contaminated wastewaters.

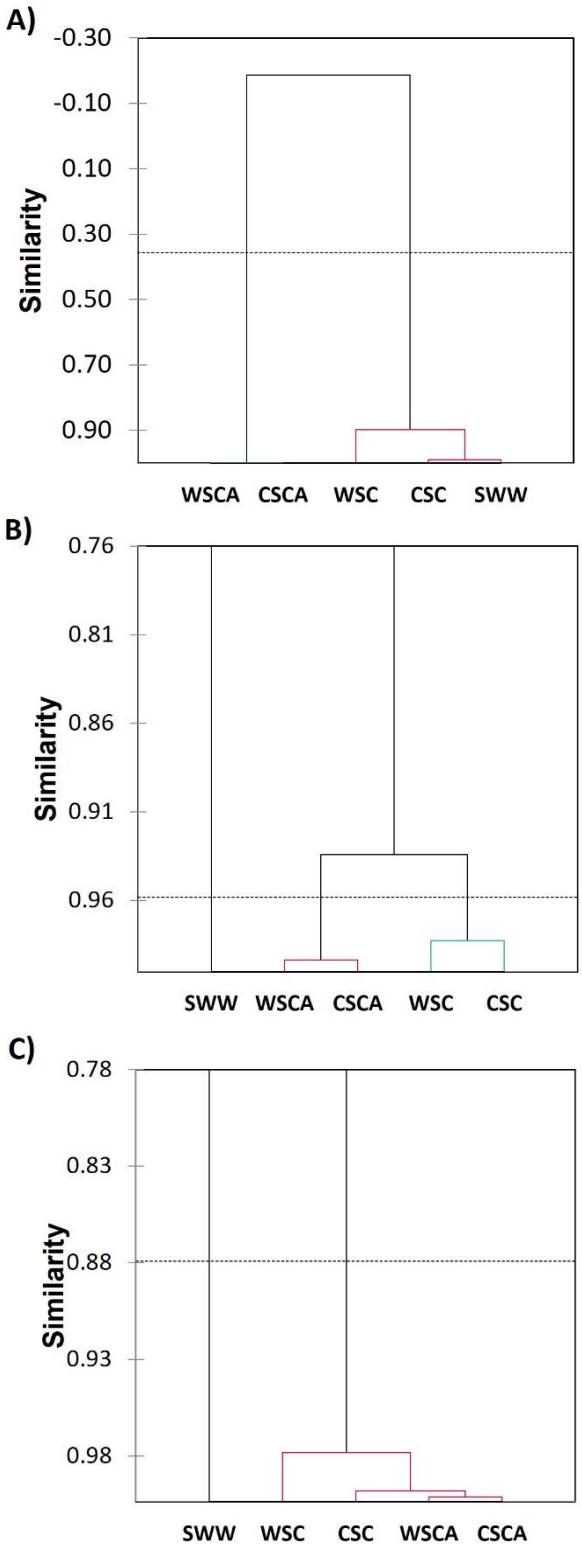

Figure 7.4 – Cluster analysis dendrogram based on physicochemical characteristics of raw SWW (SWW), and treated SWWs using wetted sludge as coagulant (WSC), wetted sludge as coagulant aid (WSCA), calcined sludge as coagulant (CSC), and calcined sludge as coagulant aid (CSCA) reuse processes and A) Pre-aerated SWW; B) Sieved SWW, and C) CF/DAF SWW.

Overall, the results presented in Figure 7.3 reveal that the quality of the treated SWW by the sludge reuse was not better than the treated SWW by the IOSLM process. However, there are some sludge reuse options, such as CSCA, that were better than others and that can guarantee a similar quality to the treated SWW by the IOSLM process. CSCA removals were quite high for most of the parameters analyzed (Table 7.4). Therefore, an analysis of successive reuse was performed using CSCA.

Table 7.4 – Parameters removals for CSCA, using pre-aerated SWW, sieved SWW, and CF/DAF SWW.

Parameters	Pre-aerated SWW	Sieved SWW	CF/DAF SWW
COD (%)	91	86	3
TP (%)	98	98	98
Absorbance at 254 nm (%)	93	98	90
Absorbance at 410 nm (%)	96	99	94
Turbidity (%)	99	100	100
E. coli (%)	100	100	100
TKN (%)	62	23	3

7.3.3. Sludge successive reuse

7.3.3.1. Treated SWW characteristics

Figures 7.5 and 7.6 show the physicochemical characteristics of the treated SWW at each stage of the successive sludge reuse process using CSCA, for the three raw SWWs tested. No significant difference (P<0.05) in pH was observed between the number of sludge reuses for the three SWWs (Figure 7.5a), maintaining treated SWW at pH 12. However, a reduction of the applied hydrated lime doses was observed from the beginning to 3rd sludge reuse phase (Figure 7.5b). CaO resulting from the calcination process (Eq. 1) can react with some chemical species of the effluent (such as carbonic acid, calcium bicarbonate, and others) (Eqs. 3 to 6) increasing the pH of the effluent. Figure 7.7a shows the savings of the hydrated lime at each stage of the successive sludge reuse process. According to this figure, at the 3rd sludge reuse stage, hydrated lime savings were about 21.6, 28.4, and 21.8% for pre-aerated SWW, sieved SWW, and CF/DAF SWW, respectively.

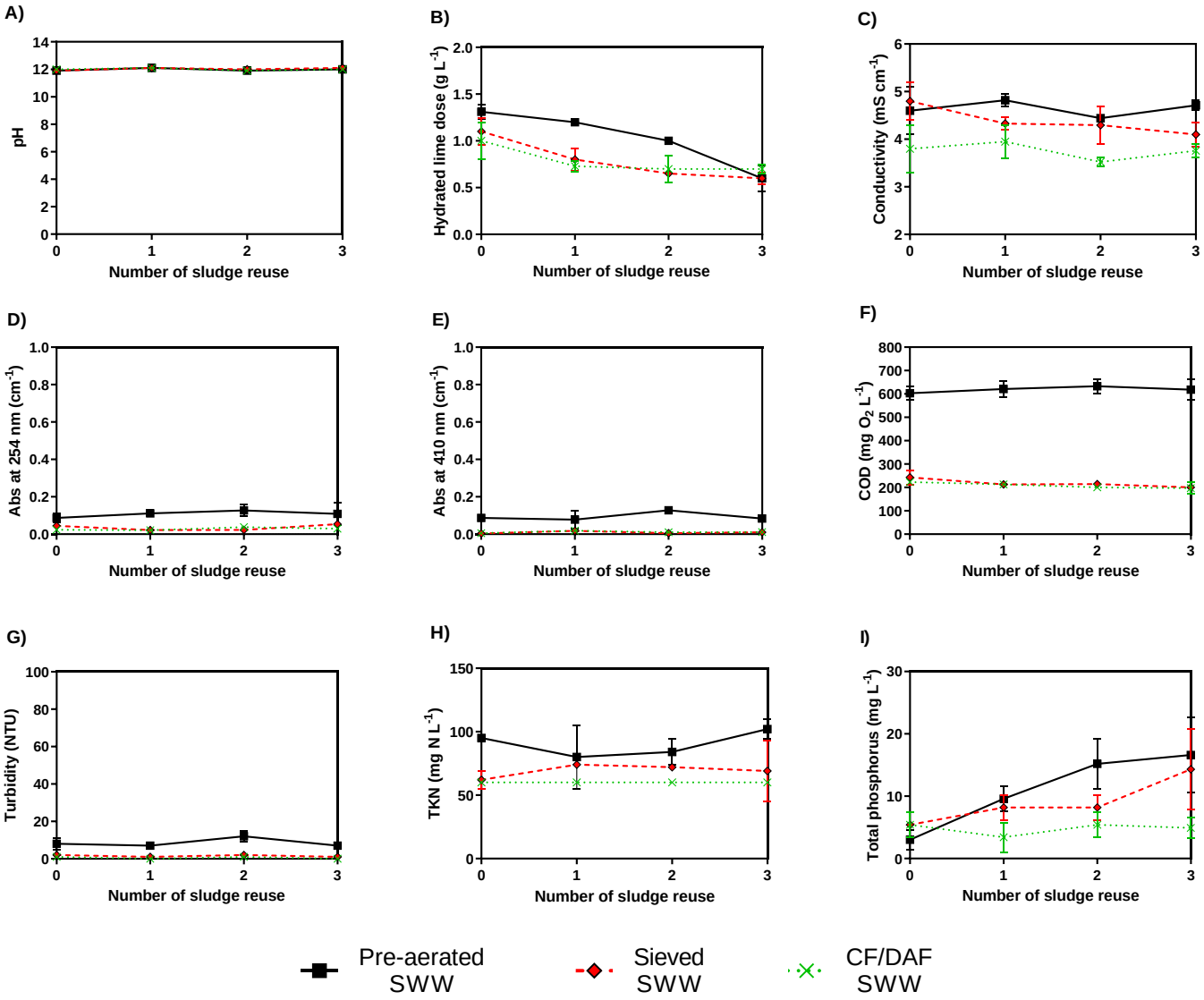

Figure 7.5 – Characteristics of the treated SWW for a) pH; b) hydrated lime dose consumption; c) conductivity; d) absorbance at 254 nm; e) absorbance at 410 nm; f) COD; g) turbidity; h) TKN; and i) total phosphorus, using calcined sludge as coagulant aid in a sludge successive reuse, for different SWWs tested. Bars represent the standard deviation of the mean.

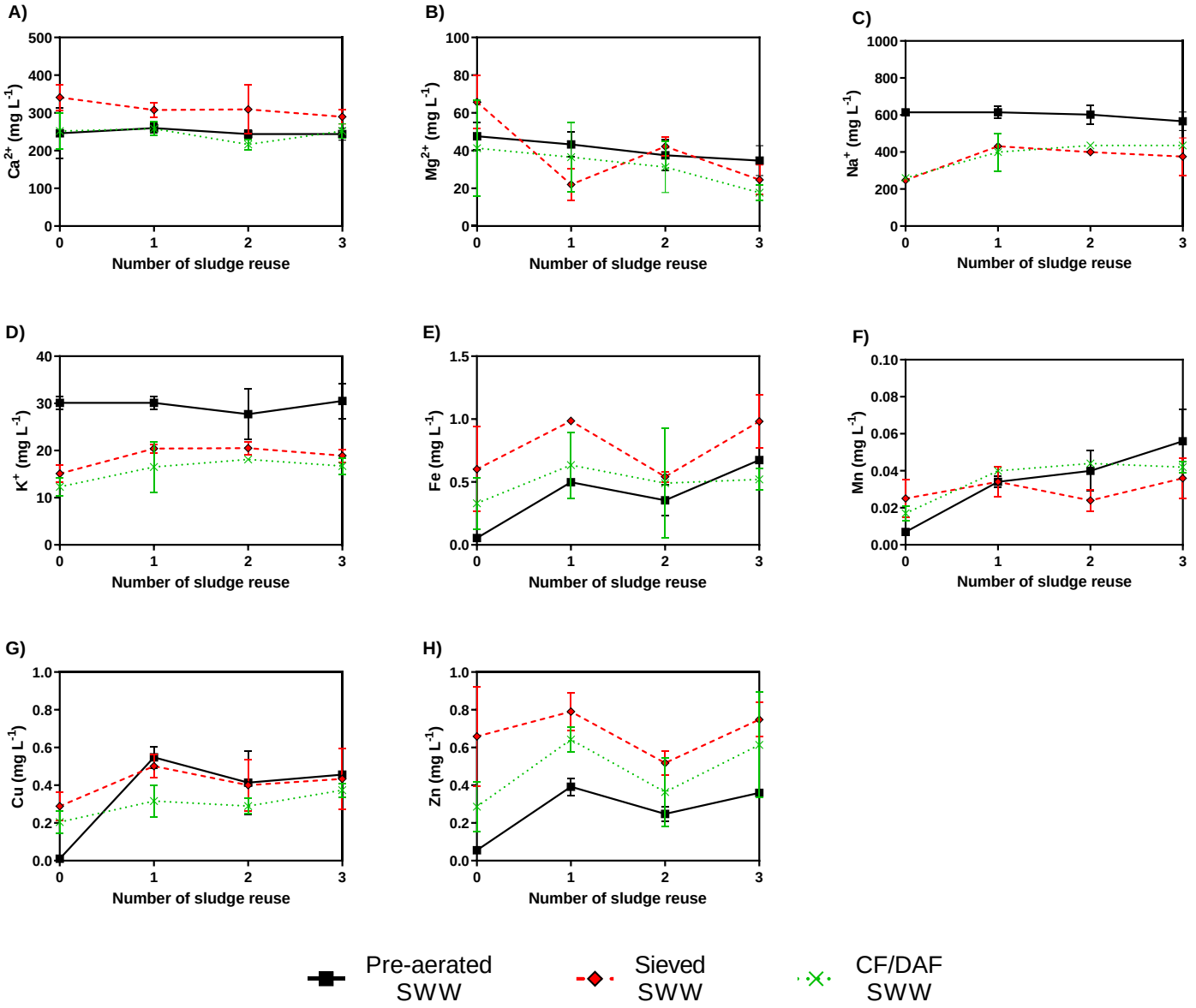

Figure 7.6 – Characteristics of the treated SWW for a) calcium; b) magnesium; c) sodium; d) potassium; e) iron; f) manganese; g) copper; and h) zinc, using calcined sludge as coagulant aid in a sludge successive reuse, for different SWWs tested. Bars represent the standard deviation of the mean.

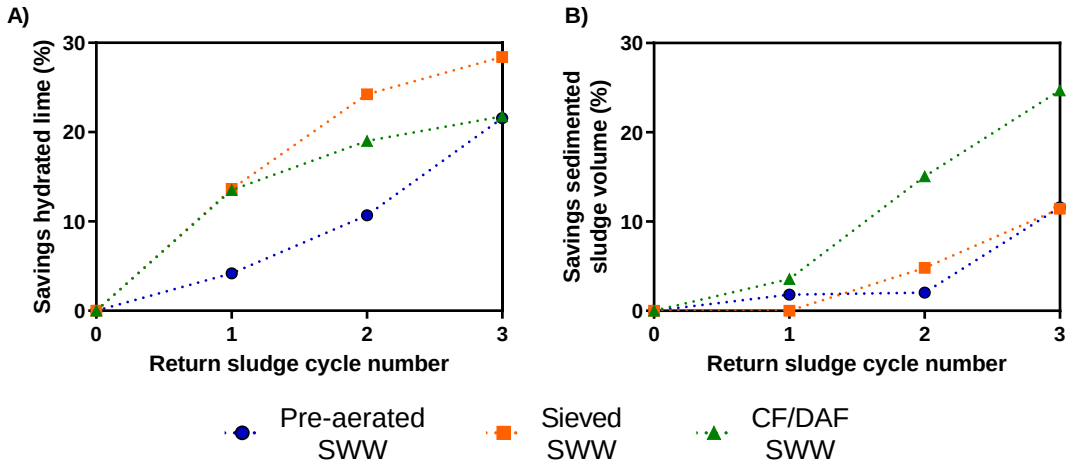

Figure 7.7 - Savings of a) hydrated lime dose and b) sedimented sludge volume per return sludge cycle number, for all SWWs tested. Bars represent the standard deviation of the mean.

No significant differences (P<0.05) were observed for the following parameters during the successive reuse of sludge: conductivity, absorbance at 254 nm, absorbance at 410 nm, COD, turbidity, and TKN, for all SWWs tested (Figures 7.5c to 7.5h). For total phosphorus (Figure 7.5i), the concentration increased with the sludge successive reuse, for pre-aerated SWW and sieved SWW, becoming significantly different (P<0.05) between the beginning and the end of the successive reuses of the sludge. Pre-aerated SWW and sieved SWW had high concentrations of TSS (*ca.* 3696 and 860 mg L^{-1}, respectively, Table 7.1) that sediment by gravity, so after the sludge calcination process there will be a greater amount of phosphorus available to precipitate and consequently a lower removal efficiency. Bal Krishna et al. (2017) investigated the calcined lime sludge reuse resulting from the water softening process to remove phosphorus from an aqueous solution. These authors observed that, for a fixed amount of sludge, the phosphorus removal efficiency decreased with an increase in the phosphorus concentration in the solution. These authors also observed that the greater the amount of calcined sludge used, the greater the efficiency of removing phosphorus from the solution.

E. coli was not detected at different sludge reuse stages, for all SWWs tested since high pH was reached (about 12), so 100% was removed.

Regarding the calcium ions (Figure 7.6a), magnesium (Figure 7.6b), sodium (Figure 7.6c), and potassium (Figure 7.6d), no significant difference (P<0.05) was observed for

each of these between the different sludge reuse stages, for the three SWWs tested. Metals such as lead, cadmium, and nickel were not detected for the SWWs tested after the successive sludge reuse phases since they were not detected in raw SWWs (Table 7.1). However, the metals that were present in raw SWWs, such as iron, manganese, copper, and zinc (Figures 7.6e to 7.6h) were not removed efficiently, sometimes reaching concentrations higher than the SWWs. Metal removals may be due to precipitation in the form of hydroxides or the ability to adsorb to calcium carbonate. Ahmad et al. (2012) investigated the adsorption capacity of calcium carbonate of heavy metals ions (Fe^{3+}, Cr^{3+}, Cu^{2+}, Zn^{2+}, Pb^{2+}, and Cd^{2+}) from aqueous solutions, and observed a significant decrease in the concentration of all metal ions after treatment.

7.3.3.2. Sludge characteristics

Table 7.5 shows the characteristics of the sludge obtained after the first and third stages of successive sludge reuse using CSCA, for the studied SWWs. According to Table 7.5, a significant reduction in the volume of sludge was observed from the first to the third stage of sludge reuse, for all SWWs tested. However, this reduction is not reflected in the volume of the centrifuge sludge, which remained at the same values (no significant differences, $P<0.05$). These results indicate that the sludge's successive reuse led to high sludge compaction and consequently a reduction in the volume of sludge. The savings of sedimented sludge volume were about 11.6, 11.4 and 24.7% for pre-aerated SWW, sieved SWW, and CF/DAF SWW tested, respectively (Figure 7.7b). A sludge volume reduction with the iron sludge successive reuse was also observed by Taheriyoun et al. (2020), when these authors used iron sludge from steel mill wastewater treatment as a coagulant aid, in combination with a coagulant (ferric chloride) and flocculant (polyelectrolyte) for turbidity removal.

From the IOSLM process (Table 7.2) to the third sludge reuse (Table 7.5), an increase in sludge pH was observed for pre-aerated SWW (from 10.4 to 11.5) and sieved SWW (from 11.0 to 12.0), and CF/DAF SWW's pH maintained at 12. The stabilization of the pH of the sludge at 12 is due to the adjustment of the pH of the SWW to 12 with hydrated lime. On the other hand, these increases in sludge pH may be due to the poor solubility of CaO in water. Rapid precipitation of magnesium hydroxide onto the surface of the CaO may

have hindered the progress of the hydration reaction of CaO (Justnes et al., 2020). The contact time between CaO and the effluent can also be an interfering factor in the dissolution of CaO. Justnes et al. (2020) mixed 1% fine CaO with seawater at 5ºC, and the authors observed that bulk composition (%) of solids from the reaction varied over time, that is, in the first minute there was 30.1% of CaO and 50.4% of $Ca(OH)_2$, but after 1 hour there was 12.3% of CaO and 61.3% of $Ca(OH)_2$.

Table 7.5 – Characterization of the sludge obtained by CSCA in different sludge successive reuse stages, for pre-aerated SWW, sieved SWW, and CF/DAF SWW. Pb and Ni were not detectable in the sludge successive reuse, for different SWW.

Parameters	Unit	SWW	Sludge successive reuse	
			1st sludge reuse	3rd sludge reuse
Sedimented sludge volume	mL L^{-1}	1	142±3	87±6
		2	85±6	59±3
		3	52±0	26±2
Centrifuged sludge volume	mL L^{-1}	1	57±12	60±10
		2	27±6	25±9
		3	20±1	20±1
Centrifuged sludge weight	mg L^{-1}	1	28.2±0.7	29.0±3.0
		2	12.5±1.3	17.4±2.6
		3	4.3±0.3	8.7±0.7
pH	Sorensen	1	11.1±0.1	11.5±0.1
		2	12.1±0.1	12.0±0.2
		3	11.9±0.1	12.1±0.0
Conductivity	mS cm^{-1}	1	0.5±0.0	0.4±0.0
		2	0.8±0.1	1.1±0.2
		3	0.6±0.2	1.3±0.5
Dry matter	%	1	21.2±0.7	22.1±1.0
		2	21.6±1.2	28.5±0.8
		3	34.2±2.0	34.3±3.8
Organic matter (dry sample)	%	1	68.5±5.5	57.7±3.8
		2	33.5±2.1	24.3±3.6
		3	30.3±3.5	9.9±1.2
Organic matter (wet sample)	%	1	14.5±1.5	12.7±0.6
		2	7.2±1.1	6.9±0.9
		3	10.3±0.6	3.4±0.2
Calcium	g kg^{-1}	1	181.0±30.6	173.0±2.9
		2	296.9±2.2	335.0±31.5
		3	399.9±9.6	466.2±27.6
Magnesium	g kg^{-1}	1	21.4±6.0	21.3±7.9
		2	53.4±25.3	43.7±5.0
		3	85.1±0.8	67.4±19.4
Chlorides	g kg^{-1}	1	1.8±0.5	1.1±0.5
		2	5.9±1.5	4.6±0.4
		3	3.7±0.1	2.2±0.3
TKN	g kg^{-1}	1	12.5±0.3	11.9±0.1
		2	5.5±0.0	3.3±0.6
		3	1.8±0.1	0.7±0.2

Note: 1 – Pre-aerated SWW; 2 – Sieved SWW; 3 – CF/DAF SWW.

Table 7.5 – (continued) Characterization of the sludge obtained by CSCA in different sludge successive reuse stages, for pre-aerated SWW, sieved SWW, and CF/DAF SWW. Pb and Ni were not detectable in the sludge successive reuse, for different SWW.

Parameters	Unit	SWW	Sludge successive reuse	
			1st sludge reuse	3rd sludge reuse
Sodium	g kg^{-1}	1	5.0±0.3	4.5±0.5
		2	4.5±2.2	2.9±0.1
		3	4.5±0.4	4.3±1.1
Potassium	g kg^{-1}	1	0.4±0.2	0.2±0.1
		2	0.2±0.0	0.2±0.1
		3	0.0±0.0	0.0±0.0
Iron	g kg^{-1}	1	2.6±0.1	3.2±0.5
		2	1.9±0.3	2.6±0.4
		3	0.5±0.0	0.5±0.1
Manganese	mg kg^{-1}	1	177.0±7.0	240.6±35.8
		2	309.4±48.1	384.3±63.0
		3	351.1±15.2	371.4±46.8
Copper	mg kg^{-1}	1	34.8±6.5	66.6±11.8
		2	36.5±7.3	78.6±23.9
		3	59.2±11.9	91.7±15.2
Zinc	mg kg^{-1}	1	224.1±12.1	248.5±15.8
		2	155.4±33.5	319.9±31.9
		3	75.8±19.6	67.1±17.0
Cadmium	mg kg^{-1}	1	1.0±0.1	1.0±0.3
		2	2.7±0.1	2.9±0.7
		3	1.7±0.2	4.3±0.1
Total phosphorus	g kg^{-1}	1	4.5±0.6	8.5±2.1
		2	7.4±1.3	9.0±1.7
		3	3.3±0.1	4.5±1.2

Note: 1 – Pre-aerated SWW; 2 – Sieved SWW; 3 – CF/DAF SWW.

E. coli of the sludge was not determined, but low levels (in the case of pre-aerated SWW) or even its absence (especially for sieved SWW and CF/DAF SWW) are expected, due to the high pH value of the sludge at the third sludge reuse (pH ≥11.5, Table 7.5). According to Bina et al. (2004), adding lime to increase the pH of sewage sludge from 6.6 to 11 or 12, can remove up to 99% of fecal coliform.

A decrease in the concentration of TKN in the sludge was observed from the IOSLM process (Table 7.2) to the third sludge reuse (Table 7.5), for all SWW studied. This decrease in TKN may be possible due to the combustion of nitrogenous organic matter with the release of nitrogen oxides during the calcination process, or to the volatilization of ammonia since, as previously mentioned, the pH of the sludge increased with the sludge successive reuse.

Conductivity, total phosphorus, and metals (such as iron, manganese, copper, zinc, and cadmium) increased in the sludge successive reuse stages, for all SWW studied (Table

7.5). The increase in conductivity was due to the increase in calcium concentration in the sludge. In fact, calcium is the element with the highest weight per kg of sludge compared to other ions responsible for conductivity (such as magnesium, sodium, chloride, and potassium) (Table 7.5). Lead and nickel were not detected in the sludge throughout the sludge successive reuse.

7.4. Conclusion

In this work, the feasibility of reusing sludge from the IOSLM process at pH 12 to treat slaughterhouse wastewater with different characteristics was evaluated. For that, four different methods of sludge reuse, such as coagulant – wetted (WSC) and calcinated (CSC) – and coagulant aid – wetted (WSCA) and calcinated (CSCA) – were used.

All forms of sludge reuse contributed to removals of absorbance at 245 nm, absorbance at 410 nm, turbidity, COD, and TKN, although WSC and CSC were the least efficient. WSC was not effective in removing *E. coli* and TP. WSCA had a higher sedimented sludge volume. Given the variability of slaughterhouse wastewater characteristics in a wastewater treatment system, choosing a single sludge reuse method is critical. In this case, CSCA was the only method that best provided high COD (3 to 91%), TP (98%), absorbance at 254 nm (90 to 98%), absorbance at 410 nm (94 to 99%), turbidity (99 to 100%), *E. coli* (100%), and TKN (3 to 62%) removals for the three effluents studied.

Using CSCA, the sludge successive reuse in the treatment of SWW had some advantages in all SWWs tested, namely:

- Similar treated wastewater characteristics after each sludge reuse (except for the total phosphorus parameter which increased with the reuse of sludges),
- Savings in the dose of hydrated lime applied, which means a reduction in costs associated with the purchase of reagent,
- High sludge compaction, which means a reduction in transportation costs and storage volume,
- High sludge's pH, so no need for further chemical sludge stabilization.

The increase in phosphorus levels in the treated SWW may indicate that there will be a limit to the successive reuse of the sludge. After reaching a certain established phosphorus level, new sludge reuse will have to be started.

7.5. References

Agabo-García, C., Solera, R., Perez, M., 2022. Anaerobic sequential batch reactor for CO-DIGESTION of slaughterhouse residues: Wastewater and activated sludge. Energy 255, 124575. https://doi.org/10.1016/J.ENERGY.2022.124575

Ahmad, K., Bhatti, I.A., Muneer, M., Iqbal, M., Iqbal, Z., 2012. Removal of heavy metals (Zn, Cr, Pb, Cd, Cu and Fe) in aqueous media by calcium carbonate as an adsorbent. Int. J. Chem. Biochem. Sci. 2, 48–53.

Alvarenga, P., Mourinha, C., Farto, M., Santos, T., Palma, P., Sengo, J., Morais, M.C., Cunha-Queda, C., 2015. Sewage sludge, compost and other representative organic wastes as agricultural soil amendments: Benefits versus limiting factors. Waste Manag. 40, 44–52. https://doi.org/10.1016/j.wasman.2015.01.027

Ávila-Pozo, P., Parrado, J., Caballero, P., Díaz-López, M., Bastida, F., Tejada, M., 2021. Use of Slaughterhouse Sludge in the Bioremediation of an Oxyfluorfen-Polluted Soil. Int. J. Environ. Res. 15, 723–731. https://doi.org/10.1007/S41742-021-00351-Z/TABLES/5

Baird, R., Eaton, A.D., Rice, E.W., Bridgewater, L., 2017. American Public Health Association, American Water Works Association, Water Environment Federation. Standard Methods for the Examination of Water and Wastewater, 23rd ed. American Public Health Association, American Water Works Association, Water Environment Federation.

Bal Krishna, K.C., Niaz, M.R., Sarker, D.C., Jansen, T., 2017. Phosphorous removal from aqueous solution can be enhanced through the calcination of lime sludge. J. Environ. Manage. 200, 359–365. https://doi.org/10.1016/j.jenvman.2017.06.003

Basibuyuk, M., Kalat, D.G., 2004. The use of waterworks sludge for the treatment of vegetable oil refinery industry wastewater. Environ. Technol. (United Kingdom) 25, 373–380. https://doi.org/10.1080/09593330409355471

Bina, B., Movahedian, H., Kord, I., 2004. The Effect of Lime Stabilization on the Microbiological Quality of Sewage Sludge. Iranian J. Environ. Health Sci. Eng. 1, 38–42.

CEN/BT/Task Force 151, 2005. EN 0000:2003. Determination of electrical conductivity in soil, sewage sludge and biowaste.

Chakraborty, T., Balusani, D., Smith, S., Santoro, D., Walton, J., Nakhla, G., Ray, M.B., 2020. Reusability of recovered iron coagulant from primary municipal sludge and its impact on chemically enhanced primary treatment. Sep. Purif. Technol. 231. https://doi.org/10.1016/J.SEPPUR.2019.115894

Dai, H., Tan, X., Zhu, H., Sun, T., Wang, X., 2018. Effects of Commonly Occurring Metal Ions on Hydroxyapatite Crystallization for Phosphorus Recovery from Wastewater. Water 10, 1619. https://doi.org/10.3390/w10111619

de Oliveira, J.J., Dalmazo, G.O., Morselli, T.B.G.A., de Oliveira, V.F. da S., Corrêa, L.B., Nora, L., Corrêa, É.K., 2018. Composted slaughterhouse sludge as a substitute for chemical fertilizers in the cultures of lettuce (*Lactuca sativa* L.) and radish (*Raphanus sativus* L.). Food Sci. Technol. 38, 91–97. https://doi.org/10.1590/1678-457x.00717

EN 12176, 1998. Characterization of sludge - Determination of pH-value.

EN 12879, 2000. Characterization of sludges - Determination of the loss on ignition of dry mass.

EN 12880, 2000. Characterization of sludges. Determination of dry residue and water content.

EN 13342, 2000. Characterization of Sludges - Determination of Kjeldahl Nitrogen.

EN 13346, 2000. Characterization of sludges. Determination of trace elements and phosphorous. Aqua regia extraction methods.

Erden, G., 2013. Combination of alkaline and microwave pretreatment for disintegration of meat processing wastewater sludge. Environ. Technol. 34, 711–718. https://doi.org/10.1080/09593330.2012.715678

Ferreira, A., Fagnani, K.C., Alves, H.J., Colpini, L.M.S., Kunh, S.S., Nastri, S., Conserva, L.R.S., Melchiades, F.G., 2018. Effect of incorporating sludge from poultry slaughterhouse wastewater treatment system in ceramic mass for tile production. Environ. Technol. Innov. 9, 294–302. https://doi.org/10.1016/J.ETI.2017.11.010

Foroughi, M., Chavoshi, S., Bagheri, M., Yetilmezsoy, K., Samadi, M.T., 2018. Alum-based sludge (AbS) recycling for turbidity removal in drinking water treatment: an insight into statistical, technical, and health-related standpoints. J. Mater. Cycles Waste Manag. 20, 1999–2017. https://doi.org/10.1007/s10163-018-0746-1

Gherghel, A., Teodosiu, C., De Gisi, S., 2019. A review on wastewater sludge valorisation and its challenges in the context of circular economy. J. Clean. Prod. 228, 244-263. https://doi.org/10.1016/j.jclepro.2019.04.240

Guerra-Rodríguez, S., Oulego, P., Rodríguez, E., Singh, D.N., Rodríguez-Chueca, J., 2020. Towards the Implementation of Circular Economy in the Wastewater Sector: Challenges and Opportunities. Water 12, 1431. https://doi.org/10.3390/w12051431

Hossaini, H.., Fatehizadeh, A.., Yousefi, N.., Reshadat, S.., Gilan, N.R.., Ghasemi, S., Ahmadian, M., 2013. Application of enhanced softening process in slaughterhouse. Indian J. Chem. Technol. 20, 217–221.

Jangkorn, S., Kuhakaew, S., Theantanoo, S., Klinla-or, H., Sriwiriyarat, T., 2011. Evaluation of reusing alum sludge for the coagulation of industrial wastewater containing mixed anionic surfactants. J. Environ. Sci. 23, 587–594. https://doi.org/10.1016/S1001-0742(10)60451-2

Justnes, H., Escudero-Oñate, C., Garmo, Ø.A., Mengede, M., 2020. Transformation kinetics of burnt lime in freshwater and seawater. Materials (Basel). 13, 1–24. https://doi.org/10.3390/ma13214926

Kitson, R.E., Mellon, M.G., 1944. Colorimetric Determination of Phosphorus as Molyloclivanaclophosphoric Acid. Ind. Eng. Chem. - Anal. Ed. 16, 379–383. https://doi.org/10.1021/i560130a017

Köse, T.E., Kivanç, B., 2011. Adsorption of phosphate from aqueous solutions using calcined waste eggshell. Chem. Eng. J. 178, 34–39. https://doi.org/10.1016/J.CEJ.2011.09.129

Lide, D.R., 2003. Handbook of Chemistry and Physics, 84th ed. CRC Press, Boca Raton.

Luz, S., Rivas, J., Afonso, A., Carvalho, F., 2021. Immediate one-step lime precipitation process for the valorization of winery wastewater to agricultural purposes. Environ. Sci. Pollut. Res. 1–10. https://doi.org/10.1007/s11356-020-11933-3

Madeira, L., Almeida, A., Ribau Teixeira, M., Prazeres, A., Chaves, H., Carvalho, F., 2020. Immediate one-step lime precipitation and atmospheric carbonation as pre-treatment for low biodegradable and high nitrogen wastewaters: A case study of explosives industry. J. Environ. Chem. Eng. 8, 103808. https://doi.org/10.1016/j.jece.2020.103808

Madeira, L., Carvalho, F., Almeida, A., Ribau Teixeira, M., 2023. Optimization of atmospheric carbonation in the integrated treatment immediate one-step lime precipitation and atmospheric carbonation. The case study of slaughterhouse effluents. Results Eng. 17, 100807. https://doi.org/10.1016/j.rineng.2022.100807

Martínez-Cruz, A., Fernandes, A., Ramos, F., Soares, S., Correia, P., Baía, A., Lopes, A., Carvalho, F., 2021. An Eco-Innovative Solution for Reuse of Leachate Chemical Precipitation Sludge: Application to Sanitary Landfill Coverage. Ecol. Eng. Environ. Technol. 22, 52–58. https://doi.org/10.12912/27197050/133329

Martins, G.A., Corrêa, L.B., Guidoni, L.L.C., Lucia, T., Gerber, M.D., Silva, F.M.R., Corrêa, E.K., 2022. Toxicity and physicochemical parameters of composts including distinct residues from agribusiness and slaughterhouse sludge. Waste Manag. 138, 75–82. https://doi.org/10.1016/J.WASMAN.2021.11.032

Mazari, L., Abdessemed, D., Szymczyk, A., 2018. Evaluating Reuse of Alum Sludge as Coagulant for Tertiary Wastewater Treatment. J. Environ. Eng. 144, 04018119. https://doi.org/10.1061/(asce)ee.1943-7870.0001462

Monteiro, M.I.C., Ferreira, F.N., De Oliveira, N.M.M., Ávila, A.K., 2003. Simplified version of the sodium salicylate method for analysis of nitrate in drinking waters. Anal. Chim. Acta 477, 125–129. https://doi.org/10.1016/S0003-2670(02)01395-8

OECD/FAO, 2022. OECD-FAO Agricultural Outlook 2022-2031, OECD Publishing. Paris. https://doi.org/https://doi.org/10.1787/f1b0b29c-en.

Ozdemir, S., Yetilmezsoy, K., Nuhoglu, N.N., Dede, O.H., Turp, S.M., 2020. Effects of poultry abattoir sludge amendment on feedstock composition, energy content, and combustion emissions of giant reed (Arundo donax L.). J. King Saud Univ. - Sci. 32, 149–155. https://doi.org/10.1016/J.JKSUS.2018.04.002

Ozdemir, Saim, Ozdemir, Serkan, Yetilmezsoy, K., 2019. Agro-economic and ecological assessment of poultry abattoir sludge as bio-nutrient source for walnut plantation in low-fertility soil. Environ. Prog. Sustain. Energy 38. https://doi.org/10.1002/EP.13225

Paruch, A.M., 2015. Effects of temperature, storage time and pH on survival of Escherichia coli in source-separated yellow water. Water Environ. J. 29, 98–104. https://doi.org/10.1111/wej.12105

Pirmoradi, N., Ghaneian, M.T., Ehrampoush, M.H., Salmani, M.H., Hatami, B., 2021. The conversion of poultry slaughterhouse wastewater sludge into biodiesel: Process modeling and optimization. Renew. Energy 178, 1236–1249. https://doi.org/10.1016/J.RENENE.2021.07.016

Prazeres, A.R., Rivas, J., Paulo, Ú., Ruas, F., Carvalho, F., 2016. Sustainable treatment of different high-strength cheese whey wastewaters: an innovative approach for atmospheric CO_2 mitigation and fertilizer production. Environ. Sci. Pollut. Res. 23, 13062–13075. https://doi.org/10.1007/s11356-016-6429-3

Ramalho, M., Jovanović, T., Afonso, A., Baía, A., Lopes, A., Fernandes, A., Almeida, A., Carvalho, F., 2022. Landfill leachate treatment by immediate one-step lime precipitation, carbonation, and phytoremediation fine-tuning. Environ. Sci. Pollut. Res. 1, 1–10. https://doi.org/10.1007/S11356-022-18729-7/TABLES/3

Rivas, J., Prazeres, A.R., Carvalho, F., Beltrán, F., 2010. Treatment of cheese whey wastewater: Combined Coagulation - Flocculation and aerobic biodegradation. J. Agric. Food Chem. 58, 7871–7877. https://doi.org/10.1021/jf100602j

Satyanarayan, S., Ramakant, Vanerkar, A.P., 2005. Conventional approach for abattoir wastewater treatment. Environ. Technol. 26, 441–448. https://doi.org/10.1080/09593332608618554

Scalize, P.S., Souza, L.M.D., Albuquerque, A., 2019. REUSE OF ALUM SLUDGE FOR REDUCING FLOCCULANT ADDITION IN WATER TREATMENT PLANTS. Environ. Prot. Eng. 45. https://doi.org/10.37190/epe190105

Shewa, W.A., Dagnew, M., 2020. Revisiting Chemically Enhanced Primary Treatment of Wastewater: A Review. Sustainability 12, 5928. https://doi.org/10.3390/SU12155928

Taheriyoun, M., Memaripour, A., Nazari-Sharabian, M., 2020. Using recycled chemical sludge as a coagulant aid in chemical wastewater treatment in Mobarakeh Steel Complex. J. Mater. Cycles Waste Manag. 22, 745–756. https://doi.org/10.1007/s10163-019-00966-7

Van Leeuwen, J., White, D.J., Baker, R.J., Jones, C., 2010. Reuse of water treatment residuals from lime softening, Part I: Applications for the reuse of lime sludge from water softening. L. Contam. Reclam. 18, 393–415. https://doi.org/10.2462/09670513.1012

Wajima, T., Rakovan, J.F., 2013. Removal behavior of phosphate from aqueous solution by calcined paper sludge. Colloids Surfaces A Physicochem. Eng. Asp. 435, 132–138. https://doi.org/10.1016/J.COLSURFA.2012.12.054

Yan, Y., Sun, X., Ma, F., Li, J., Shen, J., Han, W., Liu, X., Wang, L., 2014. Removal of phosphate from etching wastewater by calcined alkaline residue: Batch and column studies. J. Taiwan Inst. Chem. Eng. 45, 1709–1716. https://doi.org/10.1016/J.JTICE.2013.12.023

Chapter 8

Conclusions

ABSTRACT

This chapter presents the main conclusions of the processes studied in the treatment of poorly biodegradable effluents with low C/N and biodegradable effluents with a high C/N ratio, as well as in the valorization of sludge produced as a coagulant (aid). Finally, some proposals for future work on this topic are presented.

8.1. Conclusions

In this work, a circular treatment sequence was developed, consisting of immediate one-step lime precipitation and atmospheric carbonation followed by constructed wetland or adsorption, to treat poorly biodegradable effluents with low C/N ratio (as is the case of effluent from explosives industry) and biodegradable effluents with a high C/N ratio (as is the case of effluent from slaughterhouse industry). The reuse of IOSLM sludge as a coagulant (aid) was also considered as an integral part of the treatment system. The main conclusions obtained in this work are presented and discussed below, for both effluents.

8.1.1. Immediate one-step lime precipitation and atmospheric carbonation

This work started with the study of the integrated sequence composed of immediate one-step lime precipitation and atmospheric carbonation as pretreatment to treat wastewaters with different characteristics using both case studies - wastewaters from explosives and from slaughterhouse.

The effect of dose or reaction pH on removing several compounds from both wastewaters were evaluated in the IOSLM process. The results showed that the pH and the dose of hydrated lime have a significant effect on the removal some compounds, in both wastewaters, and thus the optimal pH must always be found. Additionally, for slaughterhouse wastewater it was found that only at a reaction pH of 12, final characteristics of the slaughterhouse wastewater are more similar and at this pH high removals were obtained.

In open systems, atmosferic carbonatation applied to both wastewaters was influenced by several factors, such as the presence or absence of IOSLM precipitates, the reactor A/V ratios, and the reaction pH. The presence of IOSLM sludge contributes to increase the carbonation time, since the sludge slows down the effluent pH drop. This brings advantages that include the use of one less sludge/effluent separation step since during atmospheric carbonation precipitates of calcium carbonate are formed, as well as the great removal of ammonia since high pH values will remain longer for ammonia volatilize. The application of higher reactor A/V ratios contributes to greater contact of the effluent with

the atmospheric air, thus allowing a greater transfer of atmospheric CO_2 to the effluent, and consequently a rapid pH reduction of the effluent. Despite the rapid decrease in pH, ammonia removal is not diminished by increasing the A/V ratio. Increasing the A/V ratio of the reactor contributes to the need for larger areas of site, which may be a disadvantage for sites limited in area. For the reaction pH applied during the carbonation process, it was observed that regardless of the reaction pH chosen from the range 9.5 to 12, the same carbonation time would be necessary to reach pH 8.

For wastewater from the explosives industry and under optimal conditions of dose of hydrated lime (at 7.76 g L^{-1}, corresponding to a reaction pH of 10) and a carbonation for 10 days in the presence of IOSLM sludge, the pretreatment achieved removals of 92% for organic matter, 98% for oils and fats, 63% for ammonium nitrogen, and 100% for organic nitrogen, and a pH around 8. As expected, the removal of nitrates and ammonia were not effective, resulting in high concentrations of these compounds in wastewater. The wastewater now produced by pretreatment has the quality (at least in terms of BOD_5 = 3 mg L^{-1}) to be used as irrigation in accordance with Portuguese legislation.

Regarding slaughterhouse wastewater and under optimal conditions of reaction pH of 12 and carbonation time between 10 to 15 days in the absence of IOSLM sludge, IOSLM+AC integrated process contributed to removals of 7 to 91% of COD, 71 to 97% of TKN, 80 to 86% of BOD_5, 52 to 88% of ammonium nitrogen, 98 to 99 % of TP, 52 to 99% of TSS, 62 to 97% of turbidity, 47 to 92% oils and fats, and a pH around 7.8, according to the characteristics of the slaughterhouse wastewater studied. Despite the high removals, these effluents still have considerable concentrations of COD (> 125 mg L^{-1}). Thus, the use of refining processes to reduce the concentration of COD is evident. However, one of the effluents studied from the slaughterhouse (the most treated at the slaughterhouse), now has a low value of BOD_5 (i.e., 8 mg L^{-1}) where a greater coverage in crop irrigation is already possible, according to Portuguese legislation.

The advantages of the integrated IOSLM+AC process are evident. IOSLM is a simple process, and the reagent used is low cost and easily available. Atmospheric carbonation does not require chemicals or specialized maintenance, has low energy consumption and contributes to the mitigation of atmospheric CO_2. On the other hand, the ammonia removal during the carbonation process is advantageous in downstream processes,

namely in biological systems and mainly in wastewater with a low C/N ratio, since it contributes to a lower need of add external organic matter in the denitrification process.

The disadvantage encountered with atmospheric carbonation in open systems is the release of ammonia into the atmosphere. Therefore, it is advisable to use these systems in alkaline wastewater with low concentrations of ammonia, otherwise the use of closed systems is needed.

Atmospheric carbonation in closed systems was also investigated, using a lab-scale stirrer bubble column (SBC) and a lab-scale stepped continuous flow capillary column (SCFCR) to reduce the pH of the pretreated slaughterhouse effluent by integrated IOSLM+AC process, as well as to capture volatilized ammonia in acidic solution. The results demonstrated that the carbonation process occurred in both columns and the carbonation time was substantially shorter than the atmospheric carbonation in open systems. Furthermore, about 99% of the volatilized ammonia was captured in acidic solution. Aeration time, agitation speed, and SWW volume used in the SBC were the factors that had a significant effect on pH, conductivity, calcium, total alkalinity, and ammonium nitrogen. The increase in aeration time and agitation speed, and the decrease in the SWW volume in the SBC are important for the occurrence of the atmospheric carbonation process. Regarding SCFCR, SWW flow rate and capillary area were the variables that had a significant effect on pH, conductivity, calcium, total alkalinity, and ammonium nitrogen. Decreasing the effluent flow rate and increasing the capillary area have a positive effect on the atmospheric carbonation process. The air flow rate was not a variable with a significant effect on most of the studied parameters, for both columns. Both columns have been optimized according to the response surface methodology using central composite design. For SBC, the optimized conditions (time at 21 h, air flow rate at 65 L h^{-1}, stirring speed at 52 rpm, and SWW volume at 178 mL) allowed reaching pH 8 and removals of 76% of calcium and 66% of ammonium nitrogen. On the other hand, for SCFCR and under optimized conditions (effluent flow rate at 1.2 mL min^{-1}, air flow rate at 90 L h^{-1}, and capillary area at 700 cm^2) it was possible to obtain a pH of 8.2 and removals of 81% of calcium and 58% ammonium nitrogen. The carbonation process using SCFCR was more efficient than SBC, contributing to a faster pH reduction and SCFCR does not require an additional precipitates/effluent separation step like SBC. Furthermore,

one of the great advantages of the SCFCR is that during its operation, the effluent is immediately available at a pH around neutrality and there is no change in quality.

8.1.2. Constructed wetlands

Vertical flow constructed wetland planted with *Vetiveria zizanioides* were used as a refining process to remove nitrogen from poorly biodegradable effluent and low C/N ratios (as is the case with wastewater from the explosives industry), as well as to remove organic matter from poorly biodegradable effluent and high C/N ratios (as is the case with slaughterhouse wastewater), resulting from IOSLM + AC pretreatment.

For nitrogen removal from explosive wastewater, the effect of flooding level, C/N ratio, and nitrogen load were studied. As expected, the removal of nitrates without flooding level (unsaturated) was low, of around 7%. However, an increase in nitrate removal was observed when a flooding level of 25% was applied with the addition of an external carbon source (C/N ratio of 1.3), nitrate load 12 g m^{-2} d^{-1}, and hydraulic load at 83 L m^{-2} d^{-1}. Under these conditions, the maximum removal of nitrates was 55%, and removals above 90% of COD and 75% of ammonium nitrogen were also observed. Flooding level contributed to the occurrence of the denitrification process. Increasing the C/N ratio to values above 1.3 has no influence on nitrate removal. Decreasing the nitrate load did not favor the efficiency of nitrate removal since the effluent initially contained more ammoniacal nitrogen which was meanwhile converted into nitrates.

For wastewater from the slaughterhouse, it was observed that the efficiency of removal of organic matter can be reduced with an increase in the organic load of the effluent or with a decrease in the depth of the bed. The maximum observed COD removal efficiencies were around 89.9 to 95.0% when deeper beds and lower organic loads are used.

No signs of toxicity and no symptoms of micronutrient deficiency were detected in the plant *Vetiveria zizanioides*, for both effluents studied.

The treatment system composed of IOSLM and AC followed by constructed wetland was not sufficient in the removal of nitrogen from explosives wastewater to discharge of

according to EU rules. However, for slaughterhouse wastewater, this treatment solution meets the requirements for water reuse for irrigation and for discharge into water.

8.1.3. Adsorption

Adsorption was used as a refinement process in the removal of organic matter present in the slaughterhouse effluent after IOSLM and AC. PAC, GAC, PACMAG, and GACMAG were the unmodified/modified activated carbons applied. The effect of dosage and contact time of these carbons on the removal of organic matter was evaluated.

The results showed that, under optimized conditions, removals of 76% and 74% of COD removals were obtained, corresponding to a COD adsorption capacity of 5.78 mg g^{-1} and 5.61 mg g^{-1} for GAC and GACMAG, respectively, using a dose of 60 g L^{-1} and a contact time of 60 min. For PAC and PACMAG, smaller removals were obtained, that is, 60 and 59%, corresponding to an adsorption capacity of 3.90 mg g^{-1} and 3.86 mg g^{-1} respectively, and applying a dosage of 70 g L^{-1} and a contact time of 5 min. It has been demonstrated that the incorporation of iron oxide nanoparticles into the PAC or the GAC does not affect the adsorption of COD. Therefore, the incorporation of iron oxide nanoparticles and sequent magnetic separation of the adsorbent seems to be advantageous in terms of time, since no significant differences in COD concentrations were observed when adsorbent separation occurs by filtration or magnetic separation.

Compared to constructed wetlands, the adsorption process is less efficient in removing COD and does not allow its discharge into the water environment and agricultural reuse since it still has BOD values above the limits.

8.1.4. Lime sludge reuse

It is recognized that the production of lime sludge is one of the disadvantages of the IOSLM process, and therefore it is fundamental, in terms of environmental sustainability, to guarantee its recovery.

Thus, in this work, the viability of reusing lime sludge from the IOSLM process to treat slaughterhouse wastewater with different characteristics was studied. Lime sludge was

reused as a coagulant or coagulant aid in the IOSLM treatment, and before or after the heat treatment.

The results showed that the use of lime sludge as a coagulant aid and with heat treatment contribute to greater removals of COD from 3 to 91%, TP 98%, turbidity from 99 to 100%, *E. coli* 100%, and TKN from 3 to 62%, depending on the characteristics of the wastewater of the slaughterhouse treated.

Subsequently, reusing lime sludge as a coagulant aid and with heat treatment, the successive reuse of sludge was carried out. The results showed that the quality of the effluent did not change after each reuse (except for phosphorus which increased). In addition, after each reuse there were savings in terms of the dose of hydrated lime applied in the IOSLM process, and the sludge was more compacted and stabilized with a high pH value after three sludge reuses. The sludge obtained is rich in nutrients and may have a potential application in nutrient-poor and acidic soils.

Finally, it can be concluded that the circular treatment sequences proposed to treat poorly biodegradable effluents with low C/N and biodegradable effluents with a high C/N ratio, as well as the sludge recovery processes, contribute to producing by-products, such as effluents with potential agricultural reuse, and sludge with potential reuse as a coagulant (aid). So, the change the linear paradigm to the circular one, is possible using simple, eco-innovative, and low-cost strategies in the treatment of industrial effluents, especially in effluents from explosives and slaughterhouses.

8.2. Next works

Despite the advances of the present work, there are still aspects to consider in future research, in each of the processes used or sequence of processes, such as:

- Immediate one-step lime precipitation and atmospheric carbonation:
    - Evaluate the effect of temperature and CO_2-laden environments on alkaline wastewater neutralization,

- Evaluate the effectiveness of other materials (*e.g.*, fabrics) in conducting wastewater to be neutralized in a stepped continuous flow capillary column,
- Evaluate the removal of ammonia and neutralization of alkaline wastewater if the stepped continuous flow capillary column is exposed to solar radiation,
- Evaluate the effect of using an intermittent air flow in the neutralization of alkaline effluents in a stepped continuous flow capillary column, to reduce electricity consumption,
- Focus on the recovery of calcium carbonate present in the capillary material, given that this is a product with potential value in several industries;

- Constructed wetlands:
  - Evaluate the use of VFCW in series and other flooding levels, to promote greater removal of ammonium and nitrate from effluents with low C/N ratio,
  - Evaluate the use of organic substrates in the treatment of effluents with low C/N ratio, to replace the addition of external carbon,
  - Evaluate the treatability of low C/N ratio effluents through mixing with high C/N ratio effluents as an external carbon source,
  - Evaluate the use of construction materials as a substrate in constructed wetland, in the treatment of effluents with high C/N ratios, to contribute to environmental sustainability,
  - Evaluate phosphorus removal in constructed wetlands from effluents obtained by successive reuse of sludge;

- Adsorption:
  - Test the adsorption of organic matter by GAC and GACMAG in adsorption columns, as well as its regeneration,
  - Evaluate the effect of temperature on the adsorption process,

- Evaluate the effect of higher ratios PAC/iron oxide NPs and GAC/iron oxide NPs in the removal of organic matter,
- Evaluate the COD removal with previous treatment with iron oxide NPs, before adsorption with PACMAG or GACMAG, to reduce the dosage of activated carbon,
- Test other natural adsorbents that are more efficient, inexpensive, and recoverable.

- Lime sludge reuse:
    - Evaluate the use of sludge (which are rich in organic matter, nutrients, and calcium) as an acidity corrector in acidic and/ or calcium-deficient soils;

- IOLSM + AC + Constructed wetlands/adsorption
    - Evaluate the effectiveness of the full-scale treatment sequence, continuously and at different times of the year,
    - Carry out economic analysis,
    - Carry out a life cycle analysis,
    - Test in other types of industrial wastewater.